DYNAMIC MODELING AND MONITORING

OF BRIDGE DECKS

JAMES P.A. BURNS B.Sc.

DEPARTMENT OF CIVIL ENGINEERING

UNIVERSITY OF GLASGOW

THESIS SUBMITTED FOR THE DEGREE

OF

DOCTOR OF PHILOSOPHY

DECEMBER 1986

To Mum and Dad

ACKNOWLEDGEMENTS

The writer is grateful for the facilities made available by Professors H.B. Sutherland and A. Coull of the Department of Civil Engineering of Glasgow University. My thanks are also due to supervisor Dr D R Green and to Mr W Watson for the help during my experimental studies. Their valuable help will not be forgotten.

In addition I am indebted to the following:

- The Staff of the University Computer Services
- The Staff of WALDER and Partners, Bern
- The Staff of the Civil Engineering Workshop
- Mrs G Preedy for Typing my Thesis
- To the S.E.R.C for Support during my Studies.

TABLE OF CONTENTS

SUMMARY

In this research a very expensive method of monitoring the structural integrity of offshore platforms has been partially adapted for application to bridge decks. The method is based on measuring the response of the structure through its natural frequencies over a period of time. If there has been any change in these frequencies, the frequencies are compared to a data bank of computer finite element models in order to predict what structural changes have occurred. Hence in this thesis the research can be divided into two parts : the main part, computer (numerical) research and the second part experimental research.

The computer research was designed to produce a simple, accurate and cheap method of calculating the response of bridge decks to a number of structural changes to produce the required data bank of natural frequencies, i.e. Dynamic re-analysis. The method developed was based on subspace iteration, and the rate of change of the generalized eigenproblem. The method proved to be successful in predicting the response of bridge structures to a number of changes, and it was concluded that structural changes of less than 40% produce changes of less than 5% in the structural natural frequencies.

The experimental research designed to investigate how the response of bridge decks could be measured using simple techniques; this research sought to determine if these simple techniques could be used to measure the response of a structure brought about by a number of small changes in structural form. The method proved to be successful in measuring the response of a model bridge, but the results of measuring the response of the model bridge due to a number of small changes proved less successful since the changes induced in the model proved to be too small.

CONTENTS OF CHAPTER 1

CHAPTER 1 INTRODUCTION

1.1 Introduction

In this research a very expensive method of monitoring the structural integrity of offshore platforms has been partially adopted for application to bridge decks. The proposed method is based on the hypothesis that a structure will always display the same frequency response to any exciting forces unless the stiffness or mass changes. Isolated changes in stiffness or mass affect some natural frequencies more than others.

By measuring these changes in frequency response it may be possible to predict what changes in stiffness and mass have caused them.

The steps taken in monitoring the integrity of a structure by this approach are as follows:

a) The natural frequencies of the structure are measured insitu.

b) A computer model is constructed to calculate the natural frequencies of the structure.

c) The computer model is "tuned" so that, as far as possible the measured frequencies match the calculated frequencies. If it is an old structure and the differences between the two sets of frequencies are large, then it is possible that structural damage has already occurred. This is checked by a visual inspection of the structure before the method is applied.

d) A large number of computer models are constructed with a number of different structural faults to produce a "data bank" of natural frequencies associated with different structural defects.

e) At frequent intervals (e.g. six months) the structure's natural frequencies are monitored. If there has been any change in the measured natural frequencies, these changed frequencies are compared with the "data bank" of computer model frequencies to identify the change in structural configuration causing them.

1.2 Bridge Defects and Inspection

At present, the structural integrity of bridge decks is monitored by visual inspection, and defects are likely to be hidden until they becomes severe. These defects fall into two categories: stiffness defects and mass defects. Some examples of defects are:

Stiffness defects: cracking of concrete in a reinforced concrete deck

loss of shear connection betweem the slab and stiffening beams in a composite construction

buckling of structural members

faulty bridge bearings

delamination of the "black top"

Mass defects: bits of the structure falling off

drainage pipes filling up with silt and water

The visual technique is very dependent on access and this may not be easy or cheap or even possible in the case of a large bridge. Any visual method must infer soundness from a lack of evidence of damage, and such evidence being taken only from surfaces and indeed from only a sample set of surfaces, there must always be some doubt associated with visual inspection.

Since the vibration method described measures the structural stiffness and mass, so it can be used to detect stiffness and mass defects. Also since it measures structural stiffness, the application of the method can provide positive evidence of structural soundness. This is very important, since recent legislation in the UK has permitted a higher axle loading than that which the structures were originally designed for.

1.3 Review of Previous Research

A brief review of previous work is presented in three sections under the following headings:

a) Methods of vibration monitoring in offshore platforms

b) Methods of measuring natural frequencies of bridges

c) Methods of calculating natural frequencies of bridges

1.3.1 Methods of Vibration Monitoring in Offshore Platforms

An offshore platform vibrates continuously under the action of wind and waves. Apart from the response to the periodic wave loading vibrations peaks occur mainly at specific frequencies, the natural frequencies of the structure. These frequencies are measured by using accelerometers above the waterline on the platform. These natural frequencies of the structure depend on the mass, stiffness and geometry, but are generally independent of the method of excitation.

If the platform is damaged or deteriorates so that there is a measurable change in stiffness or mass then some of the natural frequencies will be changed. The nature of damage can be deduced from the patterns of changes of the frequencies and the associated mode shapes.

The first application of the method outlined in section 1.1 was on a model oil rig in the Mechanical Engineering department at Glasgow University (Ref 19). This research led to the first practical application on a gas production platform in the southern sector of the North Sea. This study was carried out before the platform was removed in 1978, (see Figure 1.11 (Ref 17)), by Structural Monitoring Limited.

The objectives of the study were to demonstrate the damage detection techniques as outlined in section 1.1, and to assess the possibility of using changes in natural frequencies to detect changes in structural integrity. Specifically, one member was deliberately damaged in three different ways as follows:

a) A hole was cut to allow it to be flooded with water

b) The member was half-severed by a through-thickness cut half way around the circumference, close to a node.

c) The cut was to be extended to produce a complete severance of the member.

(Figure 1.11 shows the location of the damaged member).

In 1975, in another study, the natural frequencies of the platform were recorded. Between that date and 1985 non-structural equipment was removed, thus providing an opportunity to assess the application of the method to changes in platform mass.

The natural frequencies of the platform are given in Table 1.1; also given are the damage frequencies for complete severance of the member given in Figure 1.11.

At the same time as the damage study was being carried out, a computer study of frequency response was carried out using MSC/NASTRAN. The results of this study are given in Table 1.2 for the baseline measurements, and for complete severance.

In this study the authors concluded that:

a) The overall vibration monitoring technique can reliably detect damage.

b) Structural Monitoring techniques can assist in providing assurance of the integrity of a structure. The second conclusion is derived by comparing the undamaged measured natural frequencies with the computed natural frequencies.

Over the years Structural Monitoring Limited have carried out a number of studies as discussed above and they conclude that at least a 5% change in structural stiffness or structural mass must occur before the method can be used to detect damage through the use of natural frequencies (Ref 11).

1.3.2 Measurement of Bridge Natural Frequencies

There are four main methods which have been used to excite bridge structures, as follows:

i). Pull and Release Method

ii) Energy Input Method

iii) Special Vehicles Method

iv) Ordinary Vehicles Method

A number of different devices can be used to measure the response of the bridges, from which structural natural frequencies can be calculated.

1.3.2.1 Pull and Release Method

This method is based on loading the structure, then quick-releasing the load thus causing the structure to vibrate. Different modes of vibration can be excited by symmetrical and unsymmetrical loading of the bridge.

Douglas and Reid (Ref 10) applied loads to a bridge deck through loading cables by two D-8 crawler tractors, and then simultaneously quick-releasing the loading cables with electrical solenoid triggers thus causing the structure to vibrate. These tractors applied loads of 11 tonnes. Symmetrical and antisymmetrical modes were excited by pulling on the bridge structure in a number of different directions. The responses of the structures were measured by the use of accelerometers, and the natural frequencies were obtained by using Fourier Transform techniques (see Appendix). In total six natural frequencies were recorded in the range of 2.72Hz to 14.2Hz.

Eyre (Ref 13) loaded the Cleddon Bridge, Milford Haven, with loading cables attached to a dead weight (327 tonnes). The load was jacked to a

height of 2-3m above the water level and then it was released to excite the bridge. The aim of this study was to measure the damping of the bridge, and to determine the first longitudinal bending mode, which was found, through the use of accelerometers, to be at a frequency of 0.52Hz.

1.3.2.2 Energy_Input_Method

This method is based on a vibrator system placed on the bridge deck and used to vibrate the deck randomly. It can be placed anywhere on the deck to excite symmetrical and unsymmetrical modes. An example of an energy input device is given in Figure 1.2. This device was developed by the Transport and Road Research Laboratory. It is an inertia excitation system consisting of four masses, each driven simusoidally at variable frequencies by electro-hydraulic actuators. These masses are mounted on a mobile axle system fitted with solid rubber tyres, so that the device can be easily towed (Ref 18).

1.3.2.3 Special_Vehicles_Method

There are a number of forms of this method of excitation, but they all have one thing in common; they involve running vehicles over the bridge to excite symmetrical and unsymmetrical modes. Two examples of this method are:

i Using the energy input device developed by the Transport and Road Research Laboratory.

ii Using very heavy vehicles. An example is a logging truck and trailer loaded with heavy steel piles, Figure 1.3 (Ref 12).

An example of this special vehicle method was used in measuring the response of two bridges in Oregon USA i.e. North Delland Bridge and Troutdale Bridge. The bridge was excited by the heavy vehicle given in Figure 1.3. These bridges were excited by running the vehicle at different speeds and along different longitudinal axes. In this case

the authors were not interested in the structure's natural frequencies, but in the induced structural stresses due to vibration. These stresses were measured by magnetic strain gauges and were recorded on an oscillogram and digitised every 0.5 second.

1.3.2.4 Ordinary Vehicles Method

This method measures the vibration response of the bridge structure excited by normal traffic flow, and this method has been used in a number of studies (Ref 24, 25, 26, 27).

Rainer and Permina (Ref 24) found that a full set of natural frequencies could be obtained from normal traffic flow. They came to this conclusion by measuring the response of the Ottowa River Parkway Service Road Bridge, Canada, by using an energy input method and ordinary traffic vehicles.

The energy input method used was an electrohydraulic inertia shaker, with the shaker driven sinusoidally. The structure's natural frequencies were recorded by carrying out frequency sweeps to find points of resonance. The corresponding modes of vibration were deduced by comparing the phases of the seven seismometers used to detect resonance.

The traffic flow method recorded the response of the structure using seven seismometers, and the structural natural frequencies were deduced by carrying out fourier analyses of the seismometers signals. Again the modes of vibration were deduced from the phases of the seismometers.

The natural frequencies of both methods are given in Table (1.3) and it can be seen that very good comparison was found between the two methods. The difference in the higher modes could be attributed to the slight increase in the modal masses owing to the mass of the traffic flow.

1.3.2.5 Instrumentation

There are a number of instruments used in conjunction with the methods mentioned above to measure different forms of response of the structure. These instruments are:

a) Static measurements

i) Strain gauges (strain)

ii) Cantilever deflection gauges (static deflection) (Figure 1.4).

b) Dynamic Measurement (or continuous measurements)

i) Deflectometer (displacement) (Figure 1.5)

ii) Seismometers (Velocity) (Figure 1.6)

iii) Accelerometers (acceleration) (Figures 1.7)

The methods by which dynamic measurements are digitised and processed to find the natural frequencies are described in the Appendix.

1.3.3 Vibration Monitoring in Bridge Decks

Under a contract to T.R.R.L, Structural Monitoring Limited carried out a study over a 18 month period from 1978 on a number of bridge structures using the procedure described om Section 1.1 (Ref 26, 27) by using ordinary vehicles to excite the bridge structure. Part of the programme was to study the effects of different air temperatures on the natural frequencies of the bridge. They found that the surface temperatures of the "black top" affects the bridge natural frequencies. They therefore concluded that this factor should be eliminated by taking all measurements in "hot" weather (10^{o}C).

1.3.4 Calculation of Bridge Natural Freguencies

The development of techniques for calculating natural frequencies in structures are linked closely with development in digital computing.

The first method to calculate the natural frequencies of bridge decks was to use very simple beam elements which have bending and torsional stiffness constants, corresponding to those of the bridge cross section. For example a simple supported bridge was modelled using 3 equally spaced lumped masses connected by beam elements, see Figure 1.8 (Ref 29).

Continuous spanned bridges were modelled with more lumped masses connected by beam elements, spaced at equal intervals within each span, see Figure 1.9 (Ref 31). (In the above two examples the number of dynamic degrees of freedom equals the number of lumped masses).

As computers increased in power more and more beam elements were used. Then the bridge idealization was changed from beam elements to two dimensional plate elements for simple supported bridges (Ref 31).

Then different elements of the bridge were represented by different types of elements, for example, the deck being modelled by plate elements, and the girders by beam elements Figure 1.10 (Ref 8).

The final stage of computer modelling was to change the mass representation of bridge structures, from lumped mass theory (mass of the structure is concentrated at the nodes) to consistent mass theory (mass representation is formed in the same way as the stiffness matrix). The consistent mass theory has the advantage that it permits the calculation of the bridge higher mode shapes and frequencies more accurately,

1.4 Conclusion

As described above the proposed method for determining the structural integrity of bridge decks can be used with advantage, since it is quick to carry out, and does not involve any disturbance to traffic flow of the bridge (Ref 23). The method has, however, the major disadvantage of high cost, and no previous studies like the offshore platform case have been carried out. The high cost is associated with two major areas.

i) Computer modelling; the cost is involved in calculating a data bank of natural frequencies associated with a number of structural changes

ii) Equipment; the cost is involved in using complex and advanced methods of frequency extraction

The aim therefore of this thesis is to study these disadvantages of monitoring bridges and to see if they can be overcome. The project can be split into two sections.

Section one : Computer Research (Chapters 2-5).

A method is presented which will allow the calculation of changed natural frequencies very efficiently at lower reduced cost than before.

Section two : Expermental Research (Chapters 6-7)

Since no study similar to the offshore platform has been carried out before to test the procedure, a similer study to the oil rig was carried out on a model bridge and is presented in this section.

MODE	BASELINE 1978	BEFORE MASS WAS REMOVED 1975	MEMBER SEVERED 1978
1	1.365	1.375	1.325
2	1.44	1.375	1.375
3	2.07	2.025	1.76
4	2.91	2.875	2.89
5	3.5	3.5	2.62
6	3.95	4.0	3.85

TABLE 1.1 COMPARISON BETWEEN BASELINE MEASUREMENT OF NATURAL FREQUENCIES AND DAMAGED NATURAL FREQUENCIES (HZ)

MODE	BASELINE	MEMBER SEVERED
1	1.351	1.32
2	1.368	1.33
3	1.76	1.58
4	2.908	2.78
5	2.597	1.955
6	3.85	3.696

TABLE 1.2 NATURAL FREQUENCIES OF THE COMPUTER MODEL (HZ)

MODE	FORCED	TRAFFIC
1	5.7	5.7
2	6.3	6.3
3	8.7	8.7
4	12.0	11.8
5	17.4	16.8

TABLE 1.3 OTTAWA RIVER BRIGDE NATURAL FREQUENCIES (HZ)
DUE TO FORCED VIBRATION AND TRAFFIC FLOW

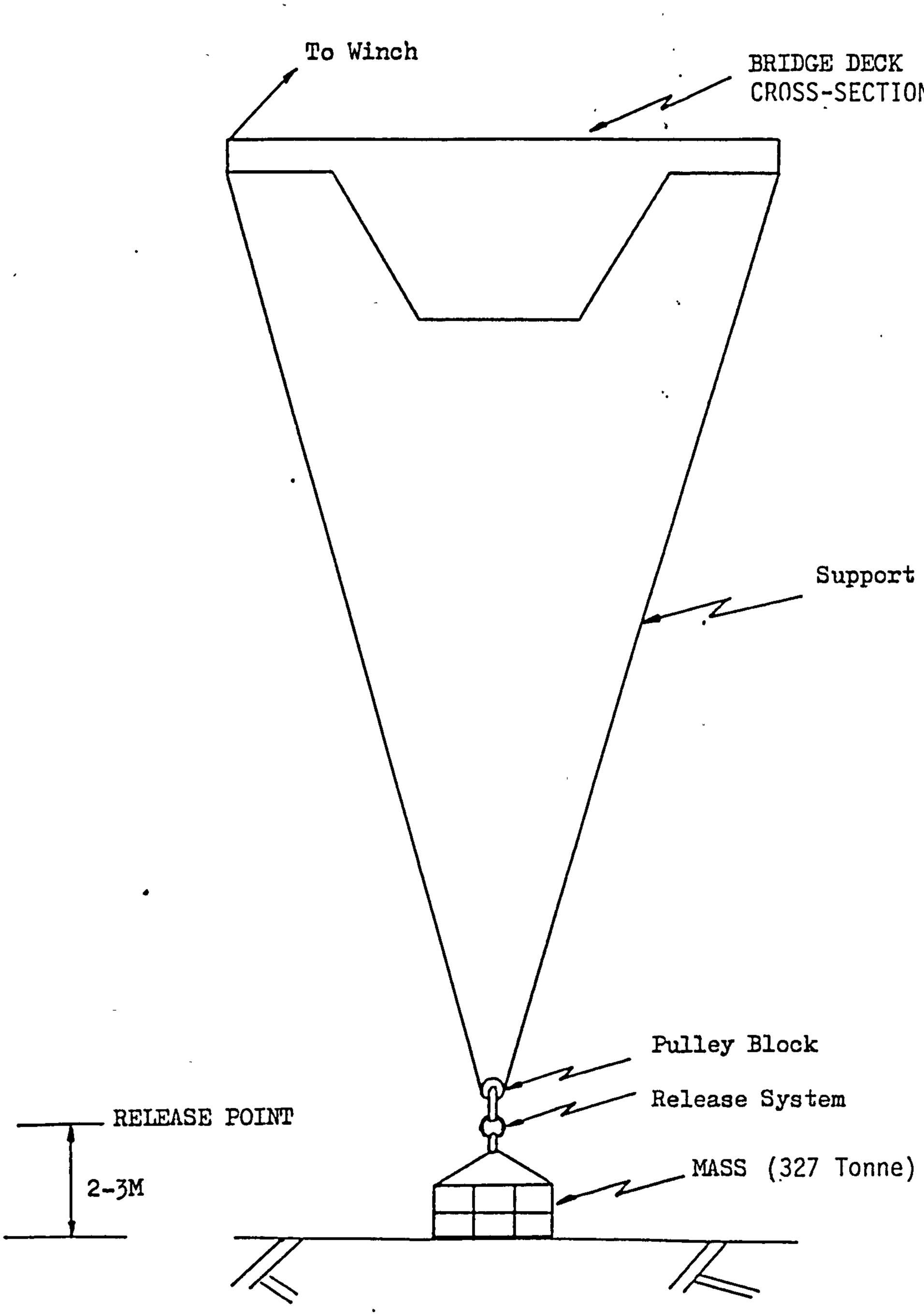

Figure 1.1 MASS RELEASE SYSTEM

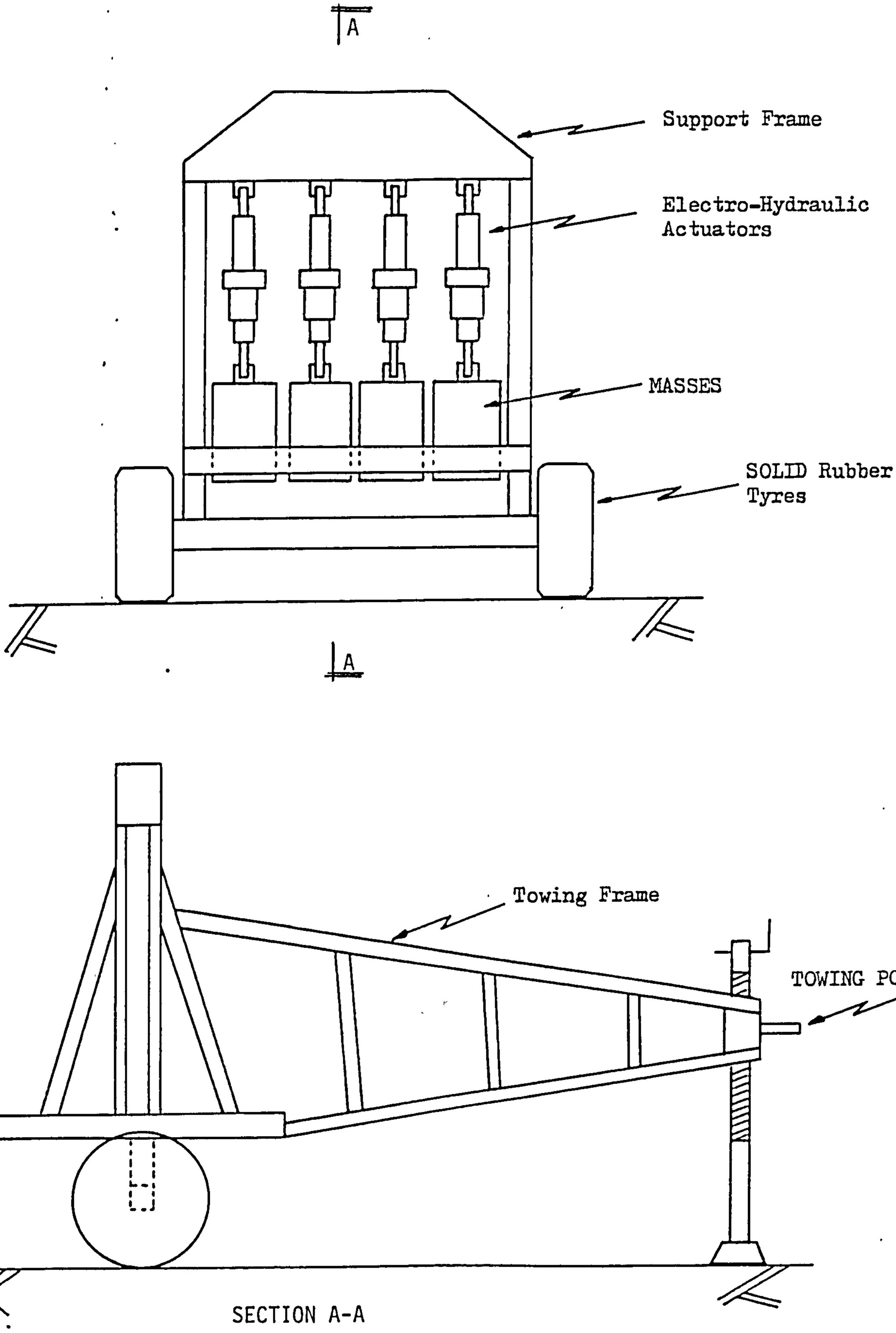

SECTION A-A

Figure 1.2 ENERGY INPUT DEVICE

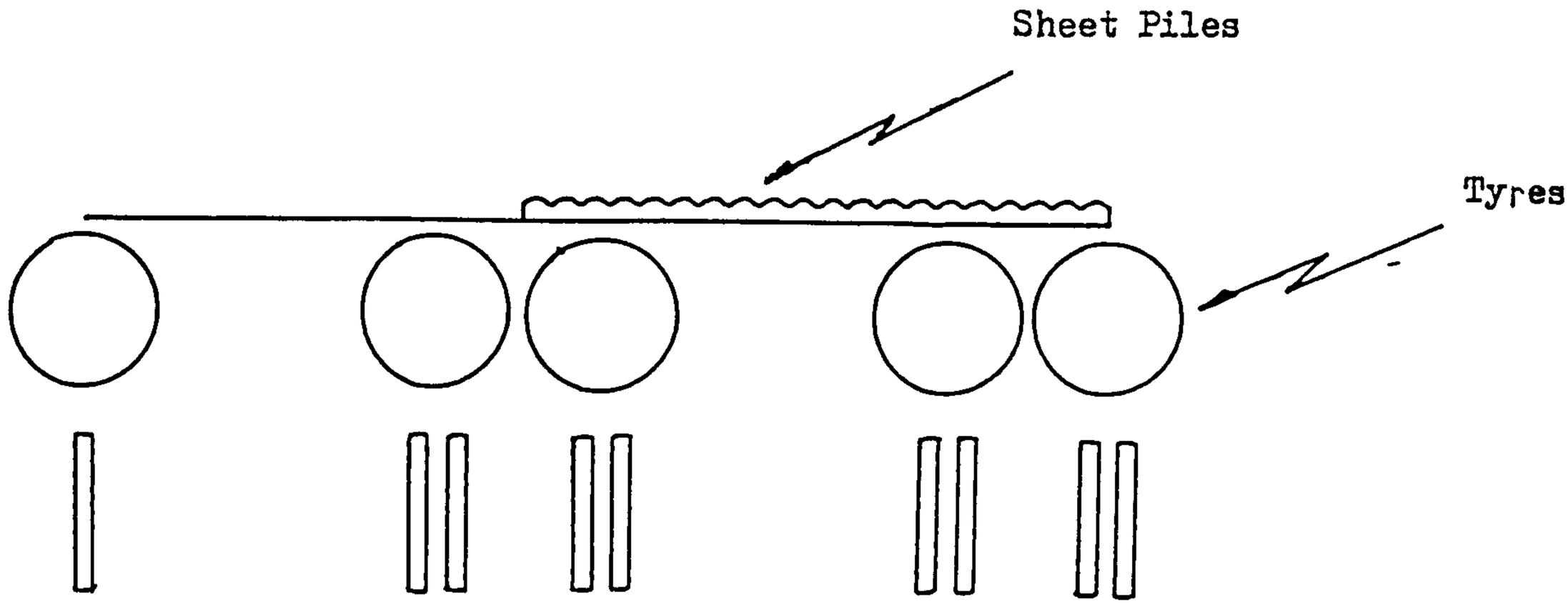

Figure 1.3 Typical Special Vehicle
Line Diagram

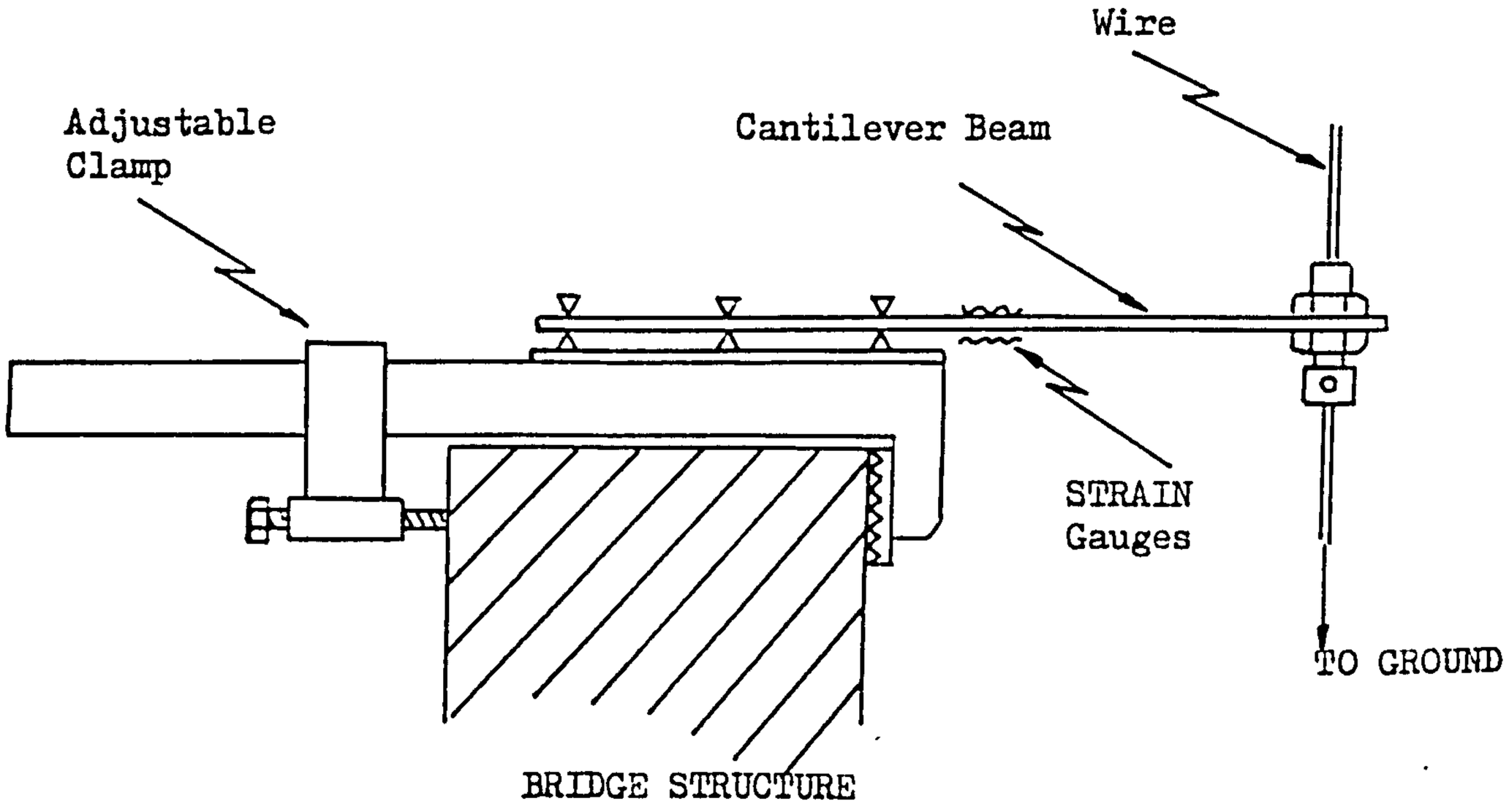

Figure 1.4 Typical Deflection Gauge

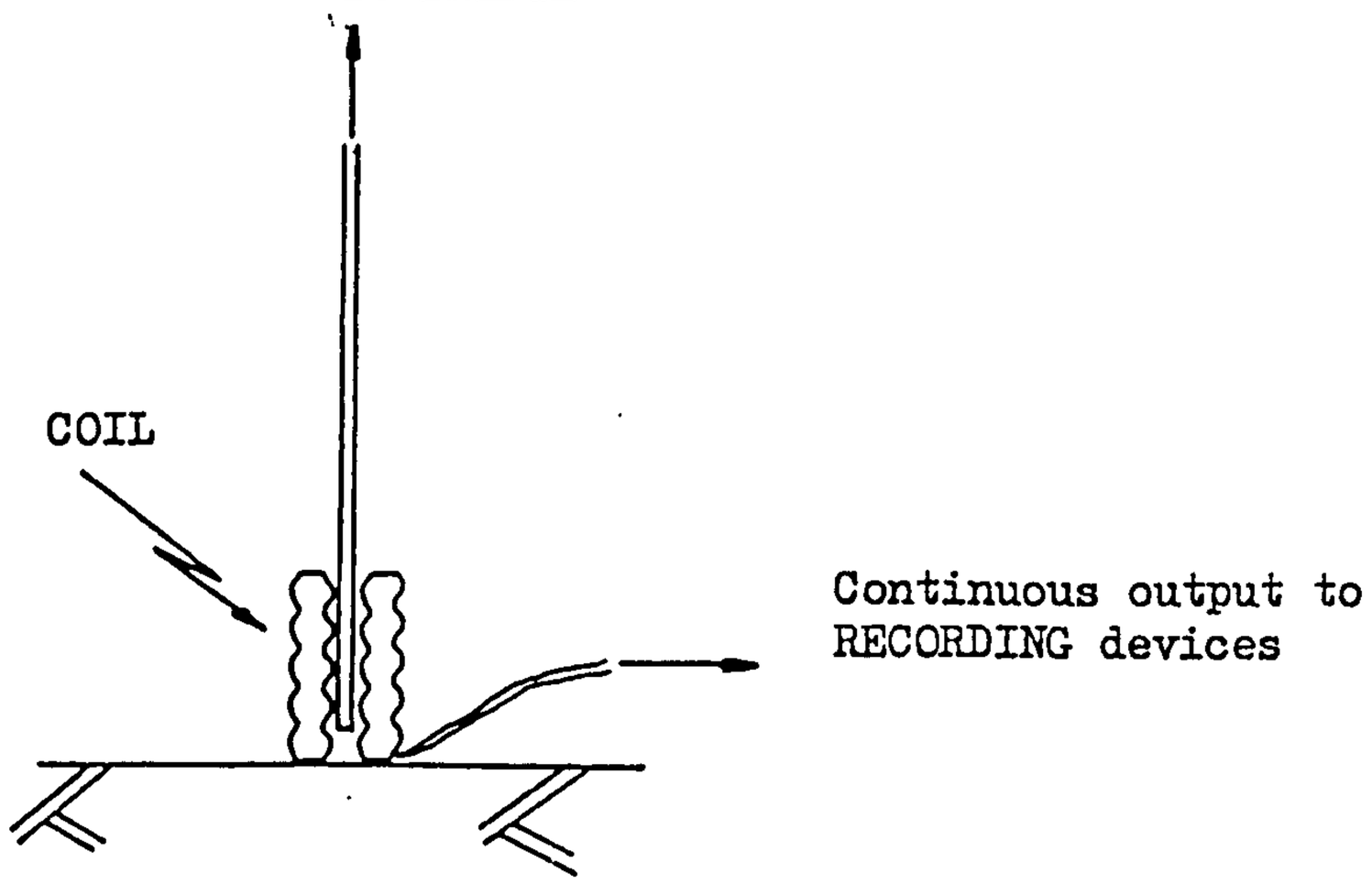

Figure 1.5 Typical Deflectometer

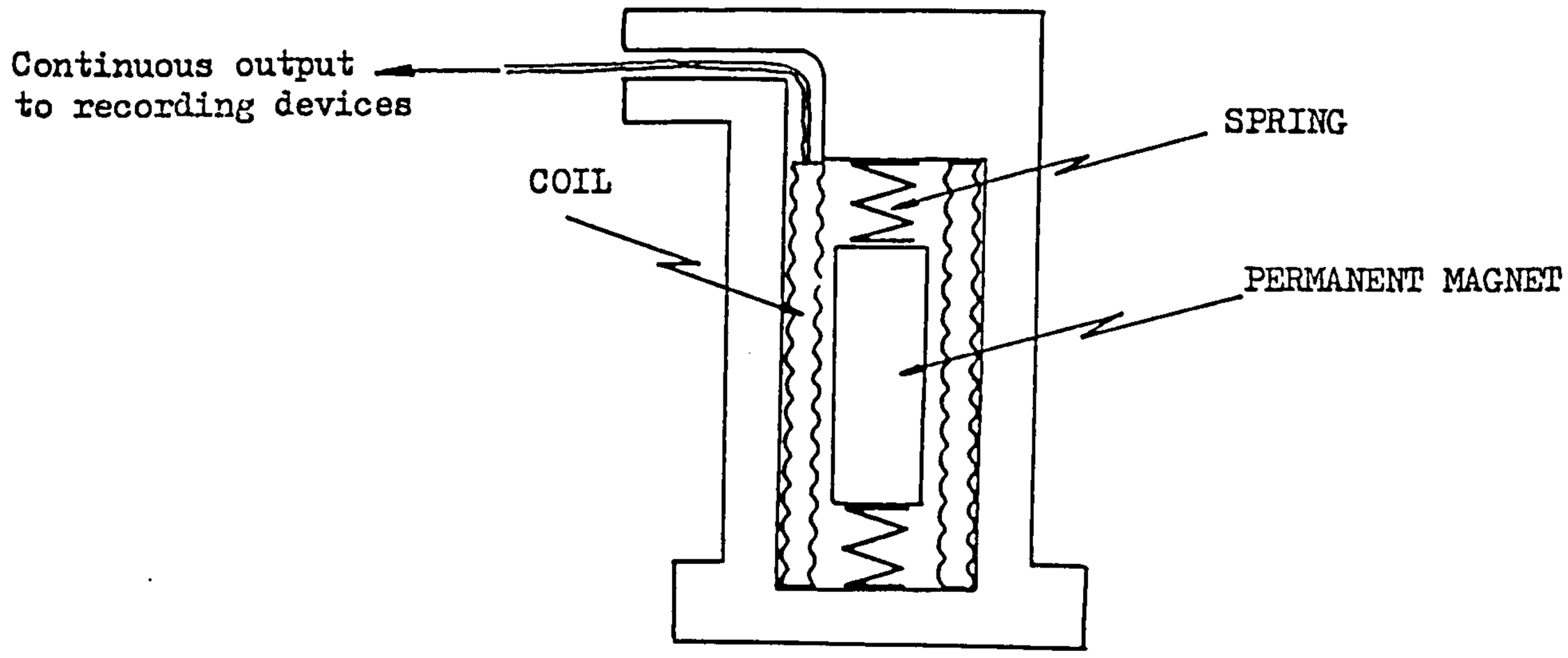

Figure 1.6 TYPICAL SEISMOMETER

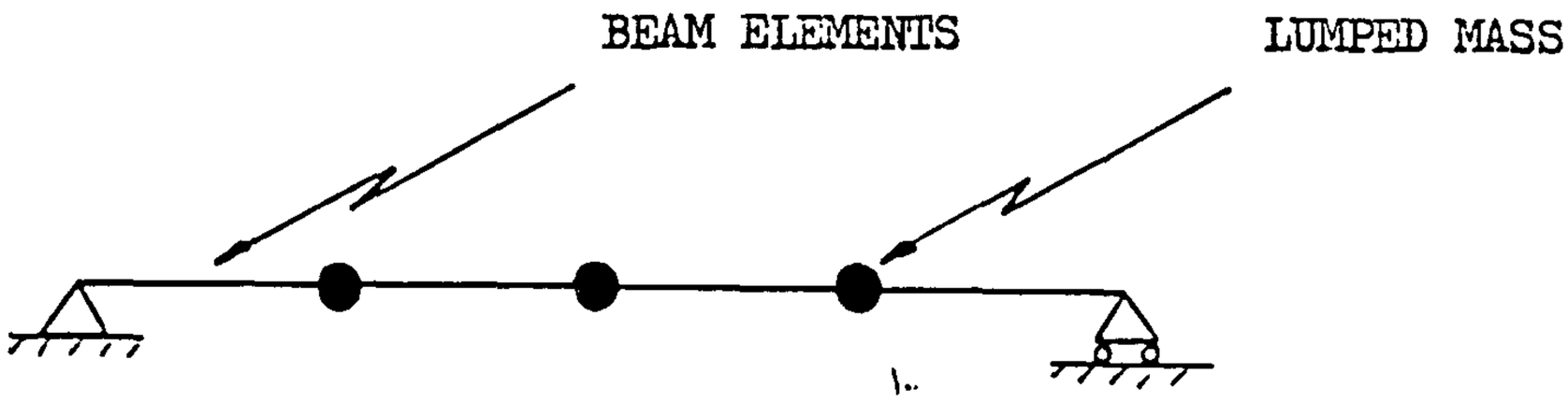

Figure 1.8 SIMPLE SUPPORTED MODEL

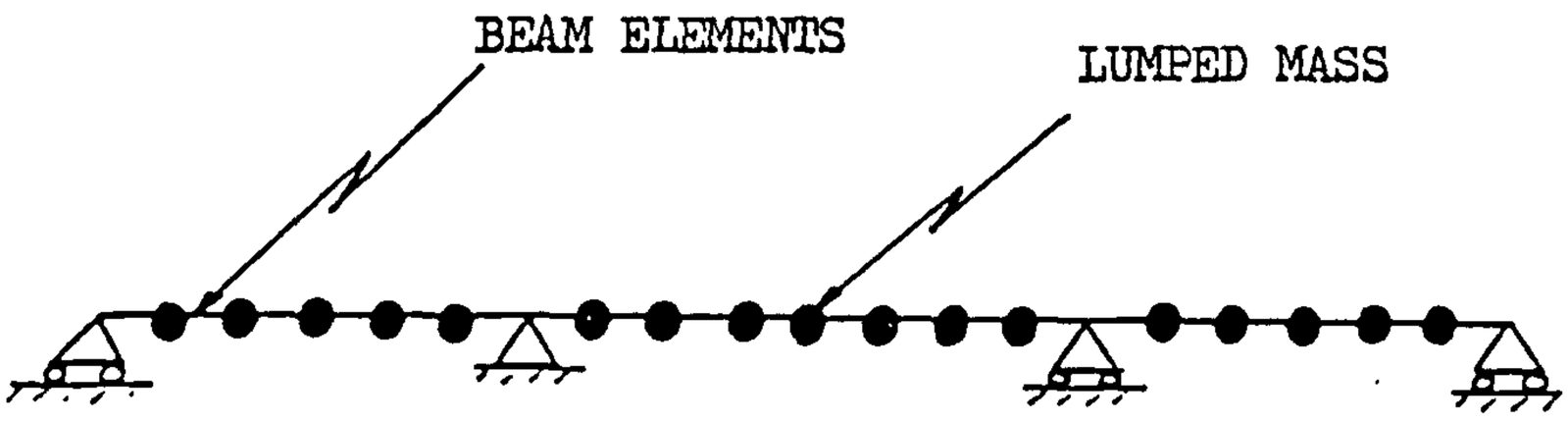

Figure 1.9 CONTINUOUS SPANNED MODEL

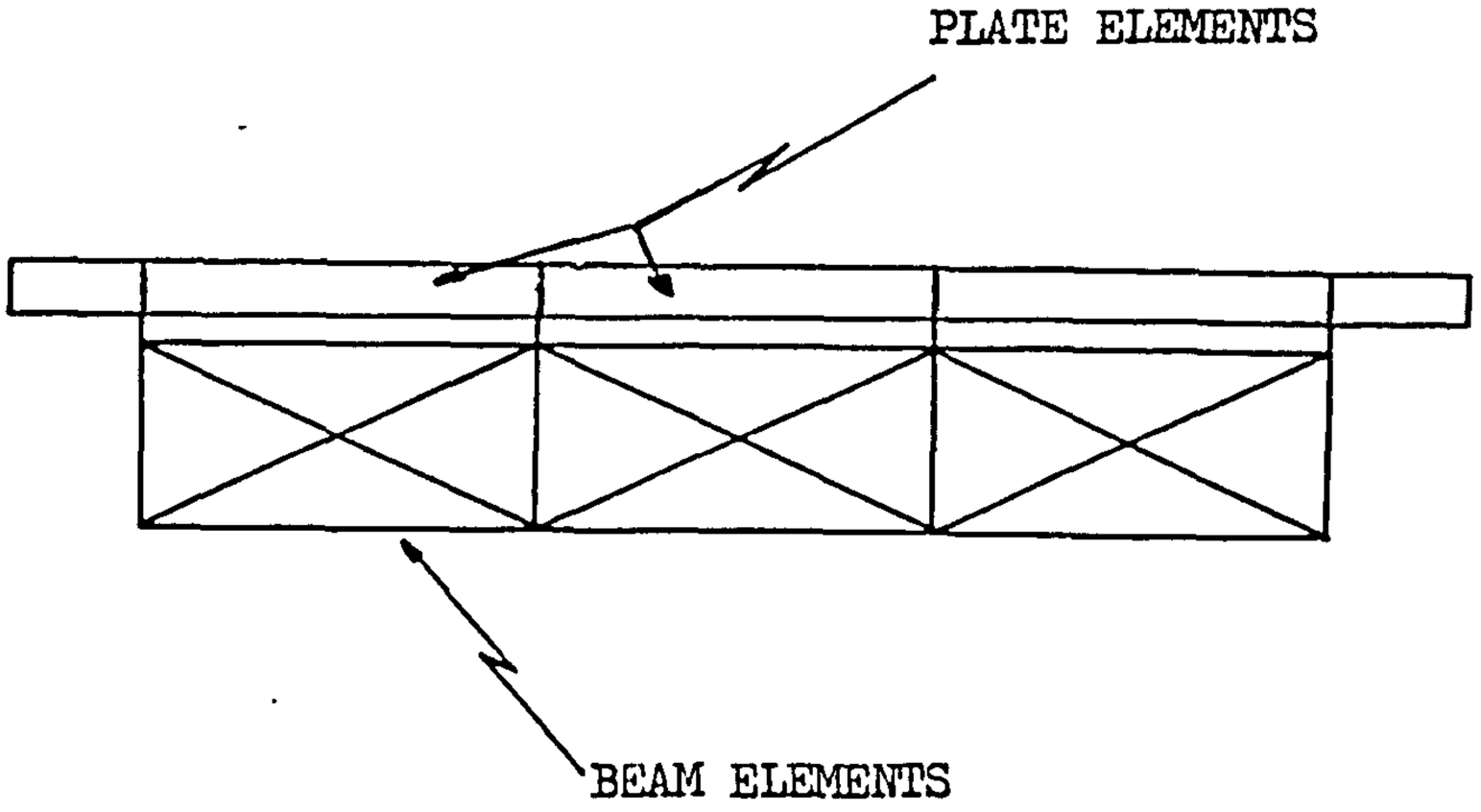

Figure 1.10 TYPICAL CROSS SECTION OF A COMPUTER MODEL

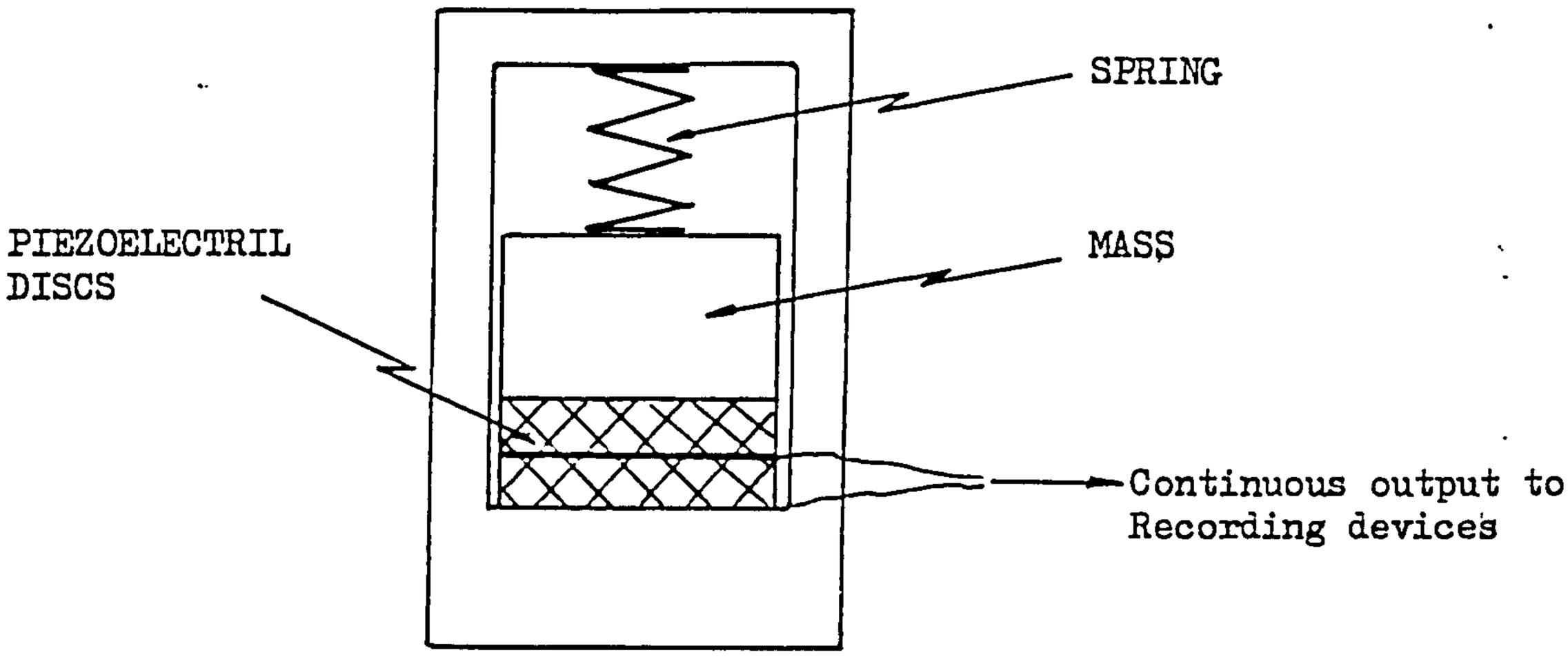

Figure 1.8 TYPICAL ACCELEROMETER

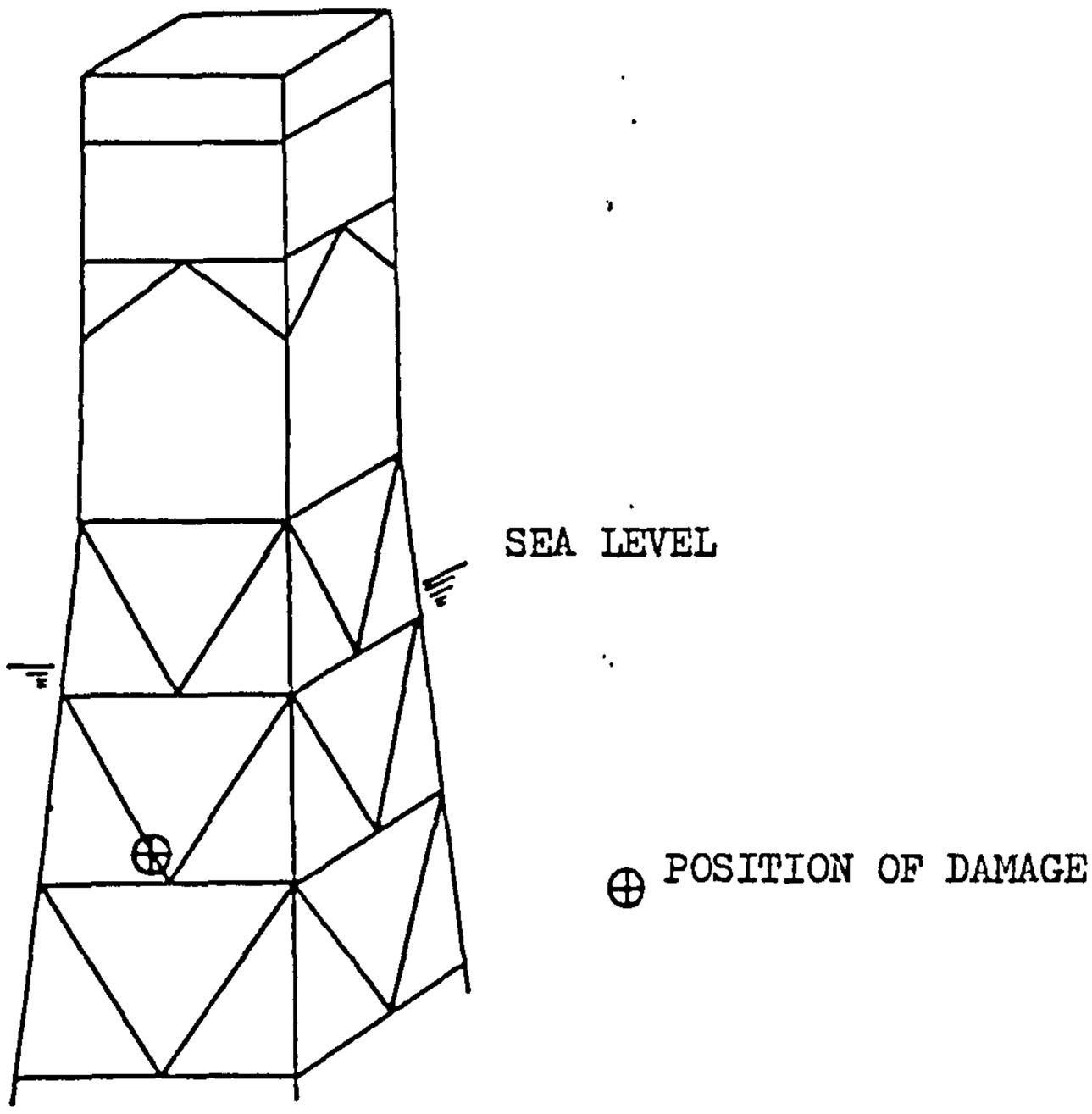

Figure 1.11 OFFSHORE PLATFORM

SECTION ONE

CONTENTS OF CHAPTER 2

CHAPTER 2 VERIFICATION OF FLASH

2.1 Introduction

In this research work it was planned to incorporate the techniques developed in a general purpose, civil engineering computer program, FLASH (Ref 14). The first stage was to check the usefulness and the accuracy of FLASH by comparison with published work of similar nature based on analysis using MSC/NASTRAN (Ref 20).

Under Transport and Road Research Laboratory and Fife Regional Council Contracts, Structural Monitoring Limited carried out dynamic monitoring of four bridges in Scotland (Ref 25, 26, 27). Part of their work was to construct computer models of these bridges using MSC/NASTRAN (Ref 20). This Chapter gives the results of the dynamic finite element analysis of three of the four bridges. These three bridges are:

a) Southfield Bridge (Fife)

b) Westerhouse Bridge (Glasgow)

c) Baillieston Interchange (Glasgow)

The dynamic models using FLASH after tuning are described and the results compared with the measured values and the computed values calculated by Structural Monitoring Limited using MSC/NASTRAN.

2.2 General Description of the Bridges and the Finite Element Models Used

As far as possible the finite element idealisations used follows the models of Structural Monitoring Limited using MSC/NASTRAN and using the same number of elements and where possible the same element types.

In all three bridges the road bitumen surface and pavements were modelled as non-structural mass. These masses were represented by point masses at all the joints except the support joints. Any contribution to the structural stiffness of these layers was neglected.

2.2.1 Southfield Bridge

Southfield Bridge Figure 2.1 is part of the southern freeway of Glenrothes new town, Fife. The bridge is, a four span continuous, reinforced concrete slab structure. The five supports are a combination of concrete cross beams and columns, with the two abutments encased in earth embankments.

The bridge was modelled as a plate with the element mesh as shown in Figure 2.4. A typical cross section of the element mesh is shown in Figure 2.5. In the computer model the following material properties were used:

Density of concrete = 2400 kg/m^3

Density of road surface = 2100 kg/m^3

Poisson's Ratio = 0.15

Young's Modulus = 32E9 N/m^2

The bridge supports were represented by springs which allowed no rotation about the x-axis, free rotation about the Y-axis, and a vertical movement. To include a contribution to the structure stiffness from the earth embankment, the vertical springs stiffness of the outer spring was increased by a factor; by tuning, this factor was found to be approximately 20.

2.2.2 Westerhouse Bridge

Westerhouse Bridge, Figure 2.2, carries traffic on Westerhouse Road over the M8 motorway in the Easterhouse district of Glasgow. The traffic flow in each direction is supported in two separate, simply-supported sections over four spans. The bridge deck is of composite construction, with seven steel I-beams running along the length of the deck and supporting a concrete slab and the bitumen pavement. The steel I-beams are supported on a concrete beam which in turn is supported on two concrete columns. These supports are common to two spans. Running the full length of both decks are two pipe ducts.

Access to these is through a concrete slab which in turn is supported at approximatly 6.25m centres by 500 x 400 mm reinforcement concrete beams.

For this dynamic finite element analysis deck BC of bridge No. 2 was only used. See Figure 2.2.

The bridge was idealised as a plate model, with the element mesh as shown in Figure 2.6. A typical cross section of the element mesh is shown in Figure 2.7.

The main steel beams were represented by beam elements eccentrically connected to the concrete deck (plate elements). The transverse beams in the pipe access duct were also represented by beam elements, and were connected to the concrete deck. The stiffness of this non-structural slab was neglected with the mass of the slab being represented as a number of point masses along the edge of the duct, hence producing "holes" in the element mesh see Figure 2.6. In the computer model the following material properties were used.

Density of concrete = 2400 kg/m^3

Density of road surface = 2100 kg/m^3

Density of steel = 7700 kg/m^3

Young's Modulus of concrete = 28E9 N/m^2

Young's Modulus of steel = 200E9 N/m^2

Poissons ratio = 0.15

Since the supports are made up of two columns and a cross beam, so the supports were represented by two types of springs. The stiff vertical springs represented the columns, and the weak vertical spring represented the cross beam, see Figure 2.7. All the supports allowed no rotation about the x-axis. See Figure 2.6.

2.2.3 Bailliston Interchange

The analysis was carried out on Bridge No 18 of Bailliston Interchange, Figure 2.3, which is just East of Glasgow. It carries westbound traffic on the slip road from the A89 Airdrie - Glasgow road to the M8 Glasgow-Edinburgh motorway. It passes over the M8 and also over the eastbound carriageway of the A89.

The bridge is a continuous reinforced concrete deck over seven spans with the spans varying in length between 20m and 30m. In plan the bridge forms a circular arc of 278.65m radius. It is supported on six concrete columns, five of which lie normal to the centre line of the bridge, while the sixth lies at an angle, and also there are two concrete wall abutments at each end of the bridge.

The element types used by Structural Monitoring Limited consisted of eight noded solid elements which only have three translational degrees of freedom per node. This type of element is not available on the FLASH program, so the bridge was idealised by a shell element model with the element mesh as shown in Figure 2.8. Since the shell elements used were four noded, the element joints were taken as the centre line of the deck cross section. See Figure 2.9. In the computer model the following material properties were used:

Density of concrete = 2400 kg/m^3

Density of road surface = 2100 kg/m^3

Poisson's ratio = 0.15

Young's modulus = 28.7E9 N/m^3

The bridge supports were represented by two different spring arrangements, two vertical springs which represented each of the six concrete columns and nine vertical springs which represented each of the concete abutments. The other five degrees of freedom were all fixed apart from the rotation about the local Y-axis which was free. This was carried out because the Structural Monitoring Limited computer model constrained all the translations at the supports.

2.3 Results

For each of the examples the number of actual frequencies calculated were varied to match the number of frequencies produced by Structural Monitoring Limited under these two contracts. For Southfield Bridge, the first five frequencies were calculated; for Westerhouse Bridge, ten frequencies were calculated, and Bailliston Interchange seven frequencies were calculated.

Tables 2.1, 2.2 and 2.3 compare the results of the FLASH computer models and MSC/NASTRAN models by Structural Monitoring Limited. Also given in these tables are the measured natural frequencies by Structural Monitoring Limited. For each of the FLASH and the MSC/NASTRAN (excluding Southfield) models the corresponding mode shapes for the natural frequencies were calculated and are given in Figures 2.10 - 2.14.

During this verification of FLASH a number of different types of analyses of the bridges using FLASH were carried out. For Southfield Bridge, since the deck has a thickness of 0.89m a thick plate and shell analyses were carried out using the same material properties as the plate analysis, and the results are given in Table 2.4. For Bailliston Interchange, a thick plate model was carried out since in the case the problem is two-dimensional. The elements were taken to act along the top surface instead of the centroid of the element's axis-section, but the same material properties were used as the shell analysis, and the results are given in Table 2.5.

2.4 Conclusion

2.4.1 Southfield Bridge

The results from the Southfield Bridge FLASH analysis compare well with the natural frequencies found by Structural Monitoring Limited.

The differences in the results between the plate, thick plate, and shell analysis could be due to the fact that the measured frequencies only include degrees of freedom which affect vertical motion. In the

case of the thick plate, shear stiffness is included, hence changing overall stiffness and mass, and hence changing the natural frequencies and in the shell case the analysis has both a translational and rotational degrees of freedom in other directions of motion, hence making the model more flexible.

2.4.2 Westerhouse Bridge

The results from Westerhouse Bridge FLASH analysis do compare well with the lower frequencies found by Structural Monitoring Limited

The differences are shown by the different mode shapes. The reasons could be twofold.

i) MSC/NASTRAN uses a dynamic reduction technique so that only those degrees of freedom representing vertical motion are retained for the analysis. This dynamic reduction technique is not availabe in the FLASH program.

ii) The method of solution of the finite element equation, the method used in FLASH is Subspace iteration and MSC/NASTRAN used a determinant search method, and in both analysis eigenvalues (natural frequencies) may have been missed.

2.4.3 Bailliston Interchange

The results from Bailliston Interchange FLASH analysis do not compare so well with the frequencies found by Structural Monitoring Limited.

In this case Structural Monitoring Limited did not use dynamic reduction techniques. The number of degrees of freedom is very large, over 2000, so it is very plausible that eigenvalues (natural frequencies) are missed by MSC/NASTRAN or FLASH, because the models do not compare.

The difference in the results between the thick plate and shell analysis could be due to the fact that the measured frequencies only include degrees of freedom which affect vertical motion. In the case of the thick plate the model has less degrees of freedom hence making the model more stiff.

In conclusion the dynamic finite element analysis of the three bridges have shown in FLASH an excellent program for the dynamic analysis of bridges. Even so, great care has to be used in choosing the type of computer analysis (plate, thick plate, shell) to be used when comparing measured and monitored values of natural frequencies.

MODE	MEASURED FREQUENCIES	CALCULATED MSC/NASTRAN	CALCULATED FLASH
1	4.8	4.8	4.67
2	6.6	6.7	6.39
3	6.9	7.2	6.93
4	8.4	8.7	8.86
5	11.6	11.5	12.08

TABLE 2.1 SOUTHFIELD BRIDGE
--------- NATURAL FREQUENCIES
(HZ)

MODE	MEASURED FREQUENCIES	CALCULATED MSC/NASTRAN	CALCULATED FLASH
1	3.55	3.58	3.55
2	4.00	3.94	4.04
3	6.35	6.73	6.34
4	----	11.63	9.68
5	13.05	12.54	10.89
6	----	13.43	11.57
7	16.0	14.31	13.03
8	19.6	20.03	15.86
9	----	22.36	16.87
10	24.05	23.56	18.42

TABLE 2.2 WESTERHOUSE BRIDGE
--------- NATURAL FREQUENCIES
(HZ)

MODE	MEASURED FREQUENCIES	CALCULATED MSC/NASTRAN	CALCULATED FLASH
1	3.075	3.35	3.08
2	3.975	3.97	4.99
3	5.10	5.14	6.09
4	----	6.76	6.21
5	6.95	6.86	7.74
6	----	7.27	8.27
7	8.0	7.99	8.80

TABLE 2.3 BAILLIESTON INTERCHANGE BRIDGE
--------- NATURAL FREQUENCIES
(HZ)

MODE	CALCULATED THIN PLATE	CALCULATED THICK PLATE	CALCULATED SHELL
1	4.67	5.65	2.10
2	6.89	8.19	7.81
3	6.93	13.40	9.39
4	8.86	13.82	9.39
5	12.08	14.69	10.68

TABLE 2.4 SOUTHFIELD BRIDGE
--------- COMPARISON BETWEEN DIFFERENT TYPES OF COMPUTER MODELS
(HZ)

MODE	CALCULATED SHELL	CALCULATED THICK PLATE
1	3.08	5.23
2	4.99	7.98
3	6.09	8.62
4	6.21	9.25
5	7.74	9.33
6	8.27	10.73
7	8.80	10.95

TABLE 2.5 BAILLIESTON INTERCHANGE BRIDGE
--------- COMPARISON BETWEEN DIFFERENT TYPES OF COMPUTER MODELS
(HZ)

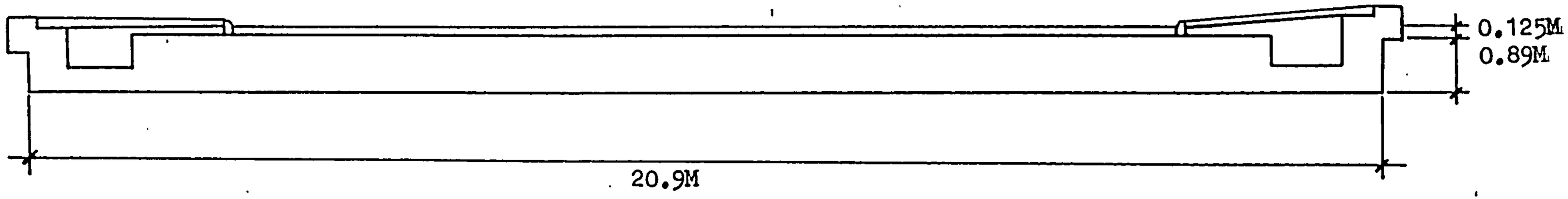

GERERAL SECTION

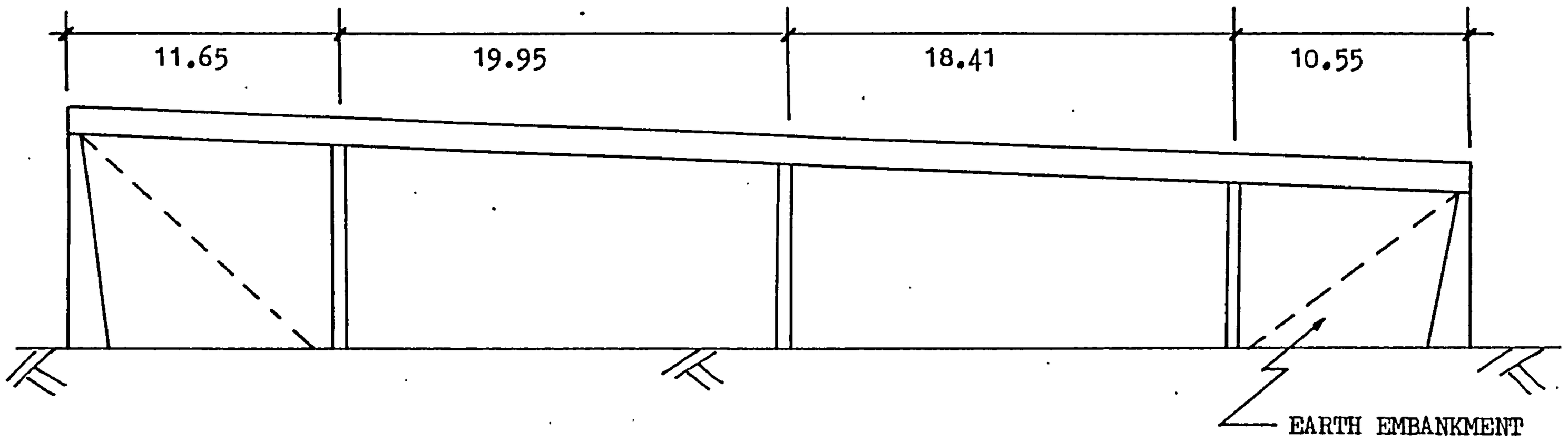

ELEVATION

Figure 2.1 SOUTHFIELD BRIDGE

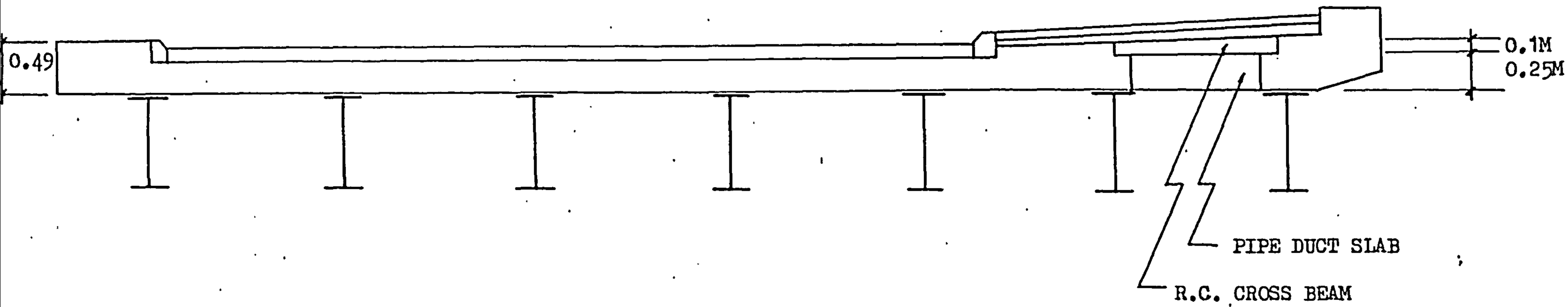

GENERAL SECTION

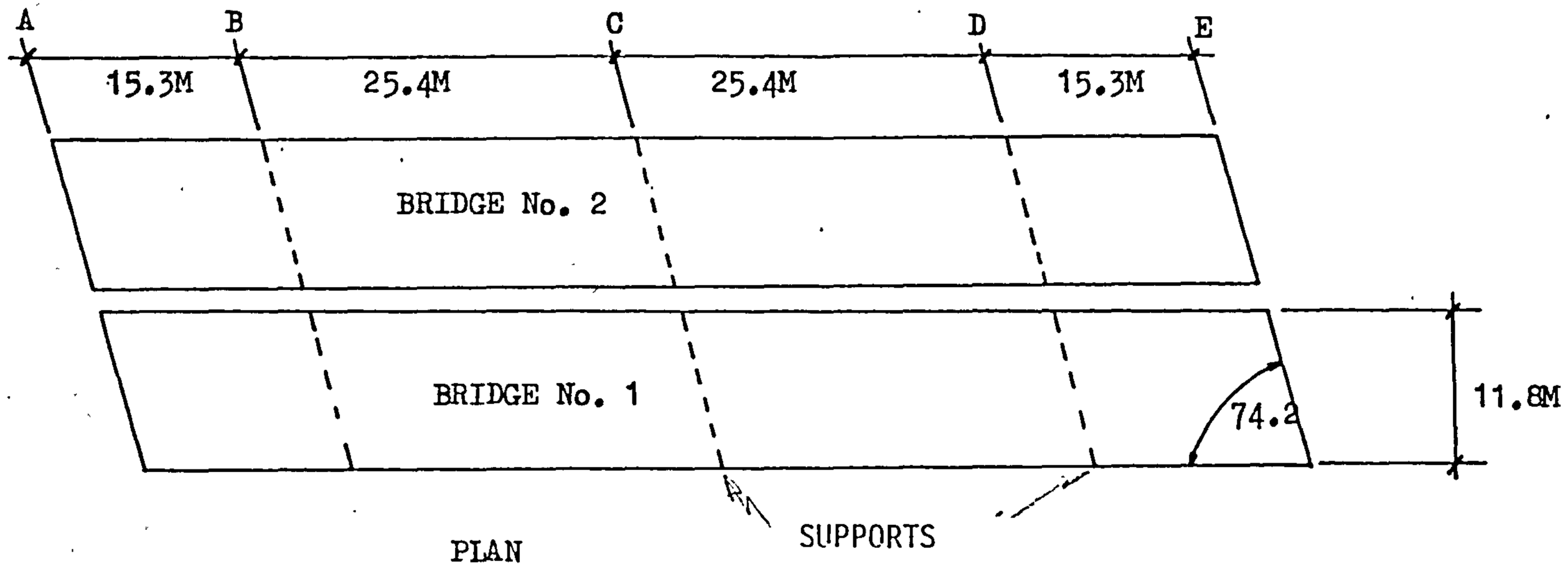

PLAN

Figure 2.2 WESTERHOUSE BRIDGE

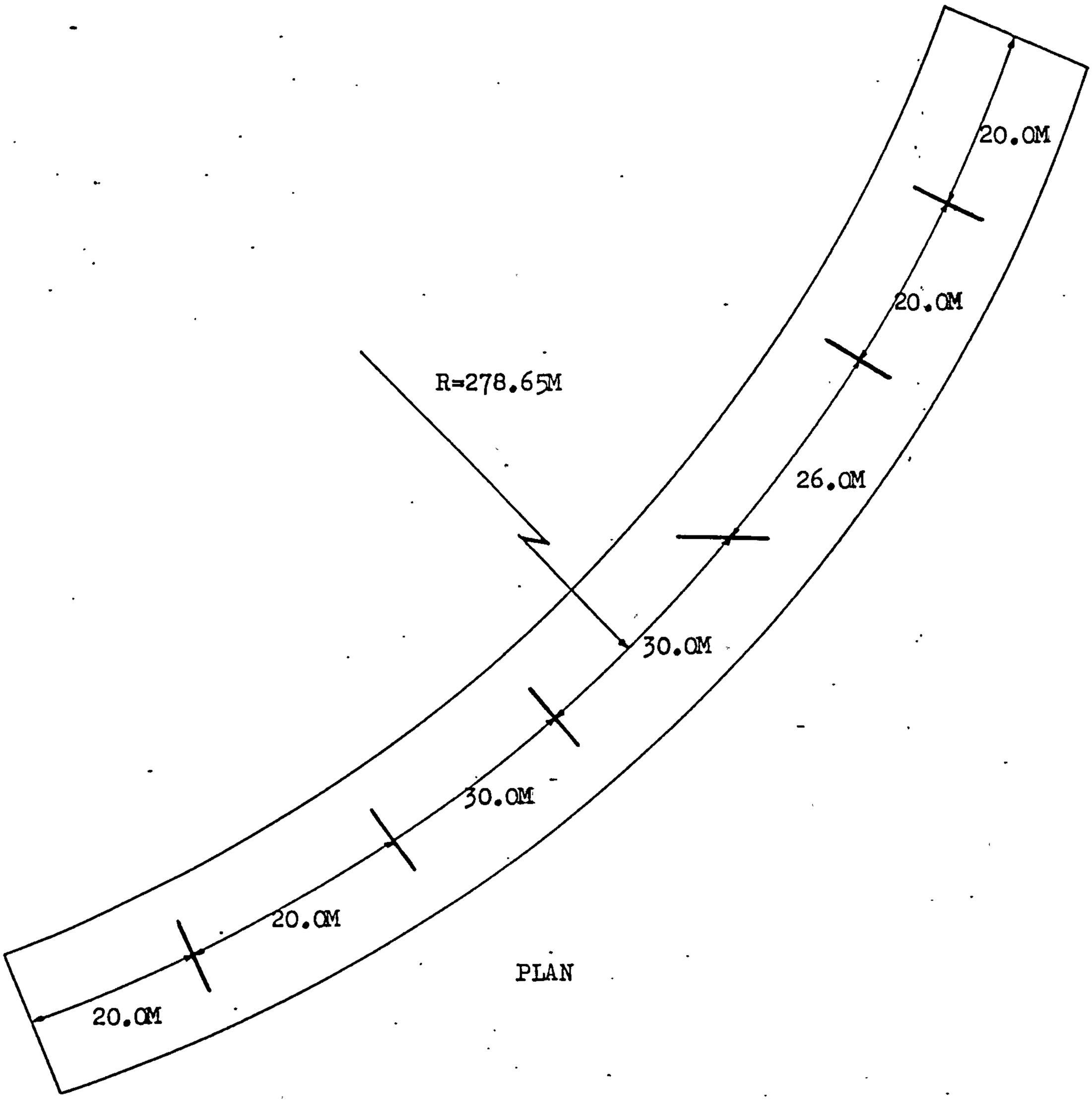

PLAN

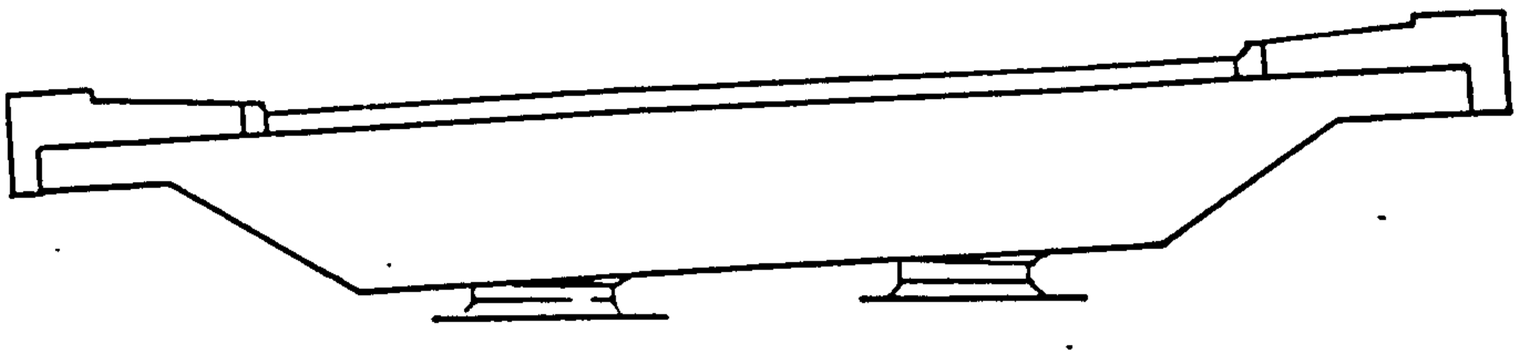

SECTION

Figure 2.3 BAILLIESTON INTERCHANGE - GENERAL ARRANGEMENT

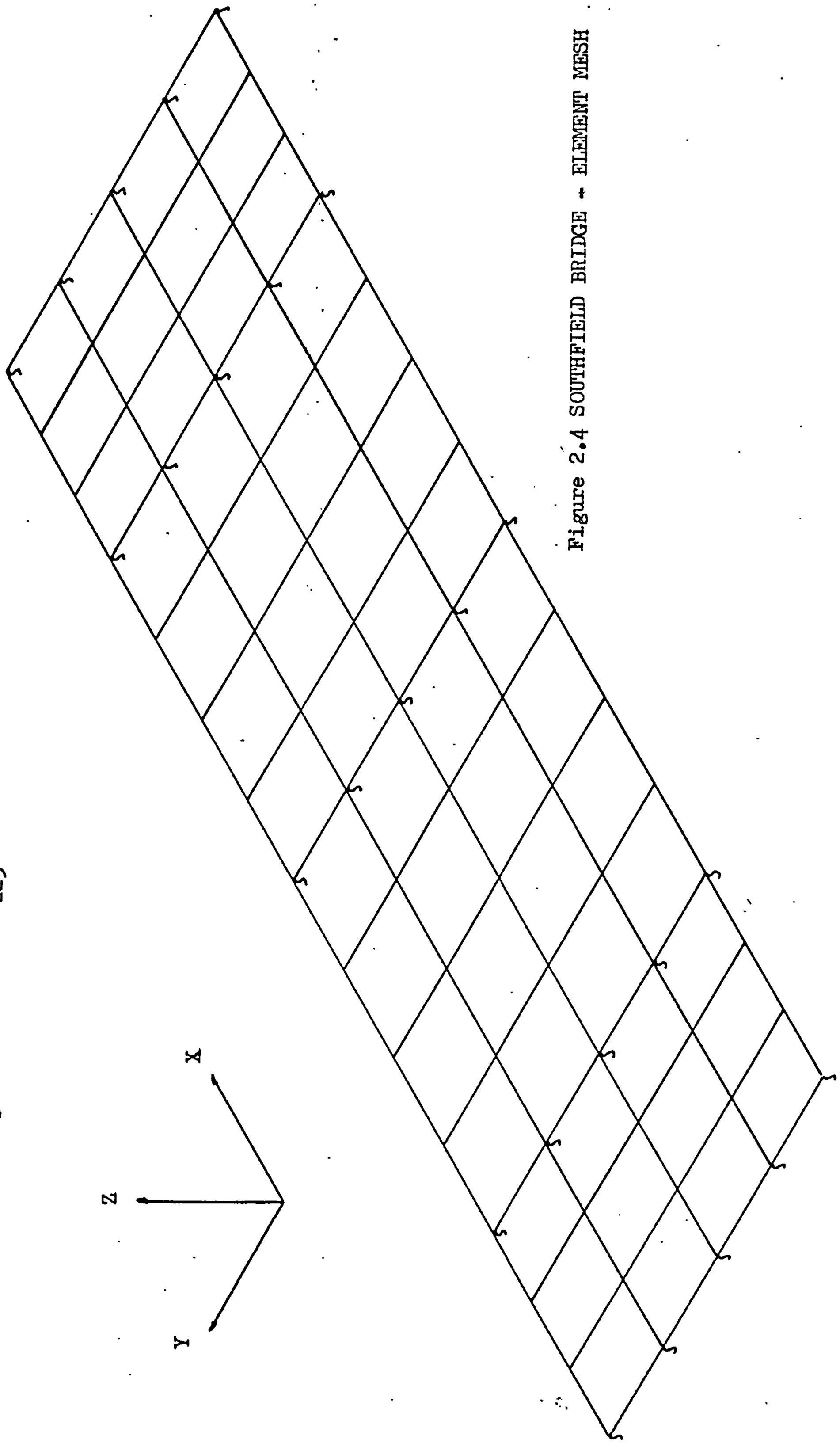

Figure 2.4 SOUTHFIELD BRIDGE - ELEMENT MESH

Number of Node =75
Total Number of Degrees of Freedom =225

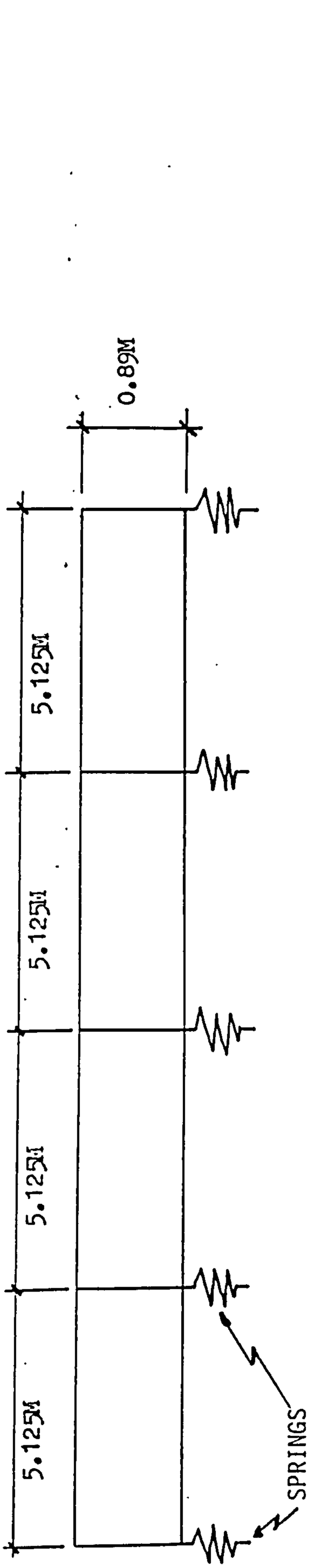

Figure 2.5 SOUTHFIELD BRIGDE
FINITE ELEMENT - CROSS SECTION

Number of Nodes = 90
Total Number of Degrees of Freedom = 270

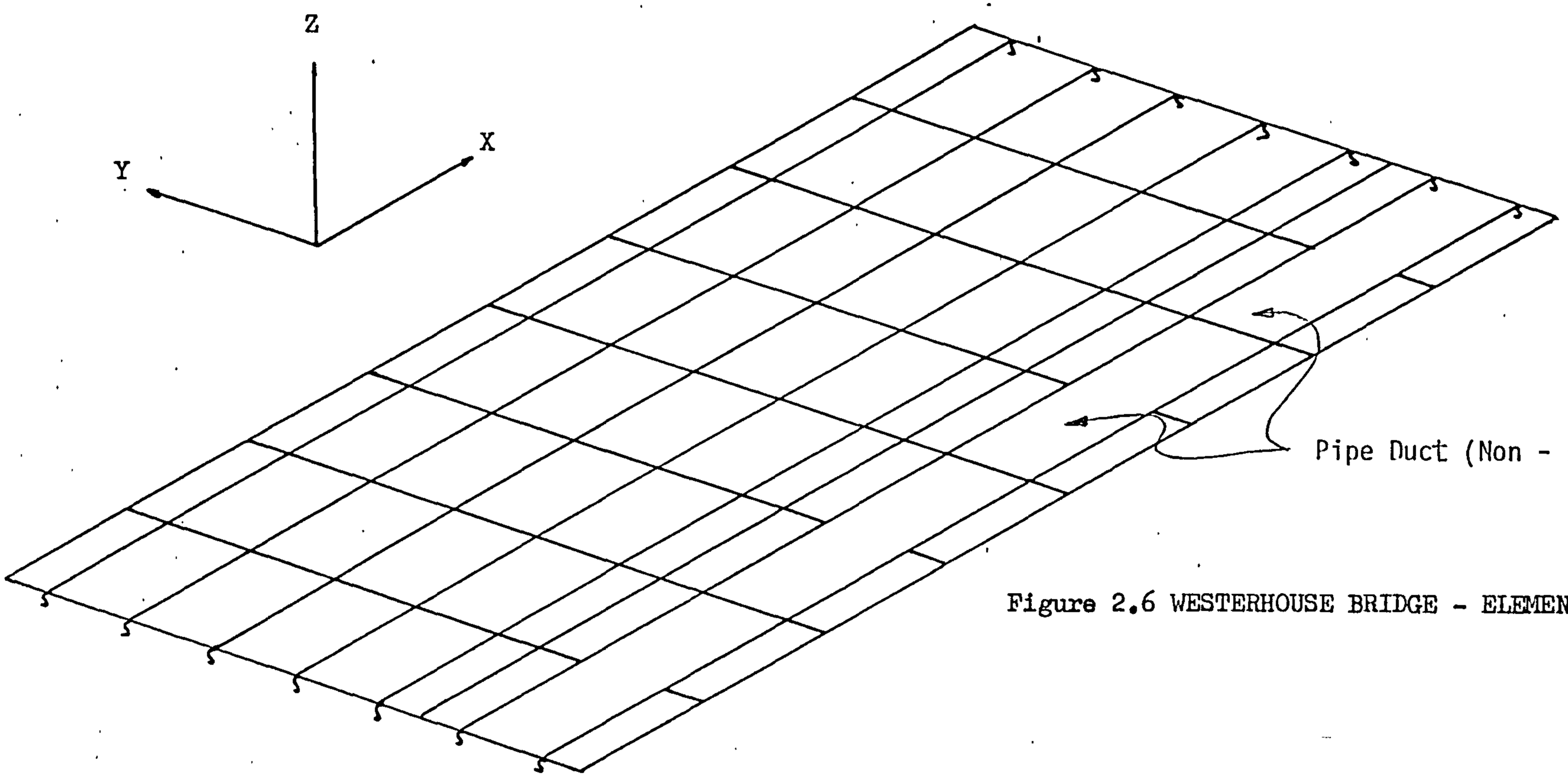

Figure 2.6 WESTERHOUSE BRIDGE - ELEMENT MESH

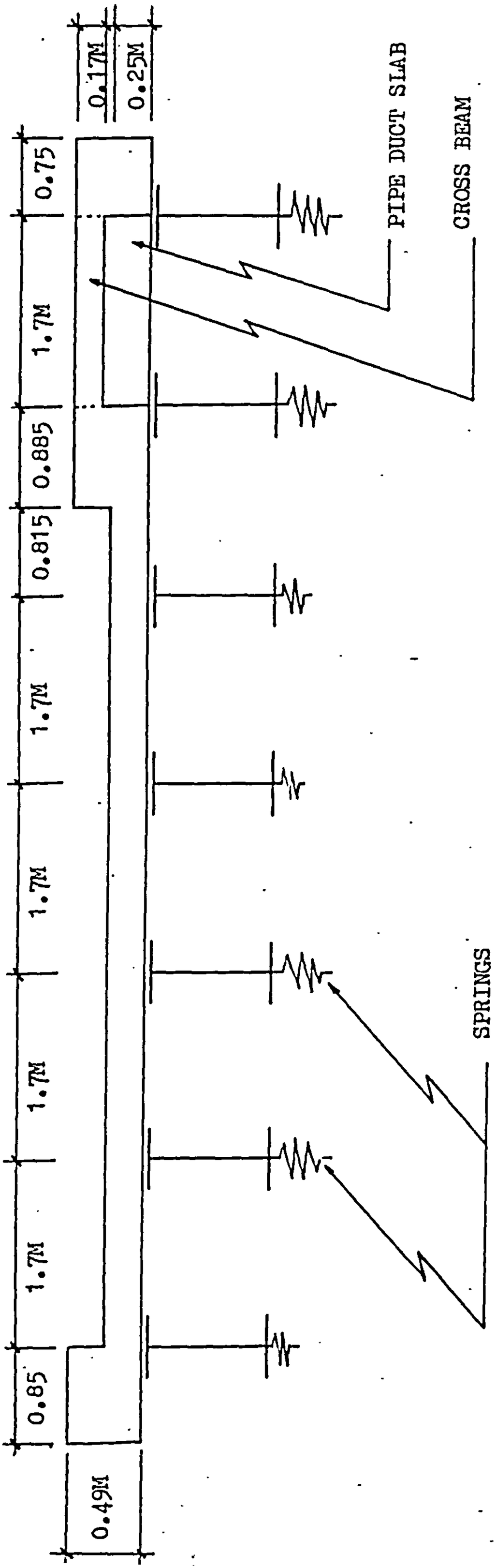

Figure 2.7 WESTERHOUSE BRIGDE
FINITE ELEMENT CROSS.- SECTION

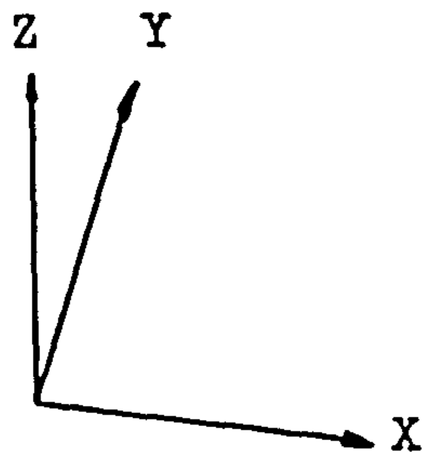

Number of Nodes = 342
Total Number of Degrees of Freedom = 2052

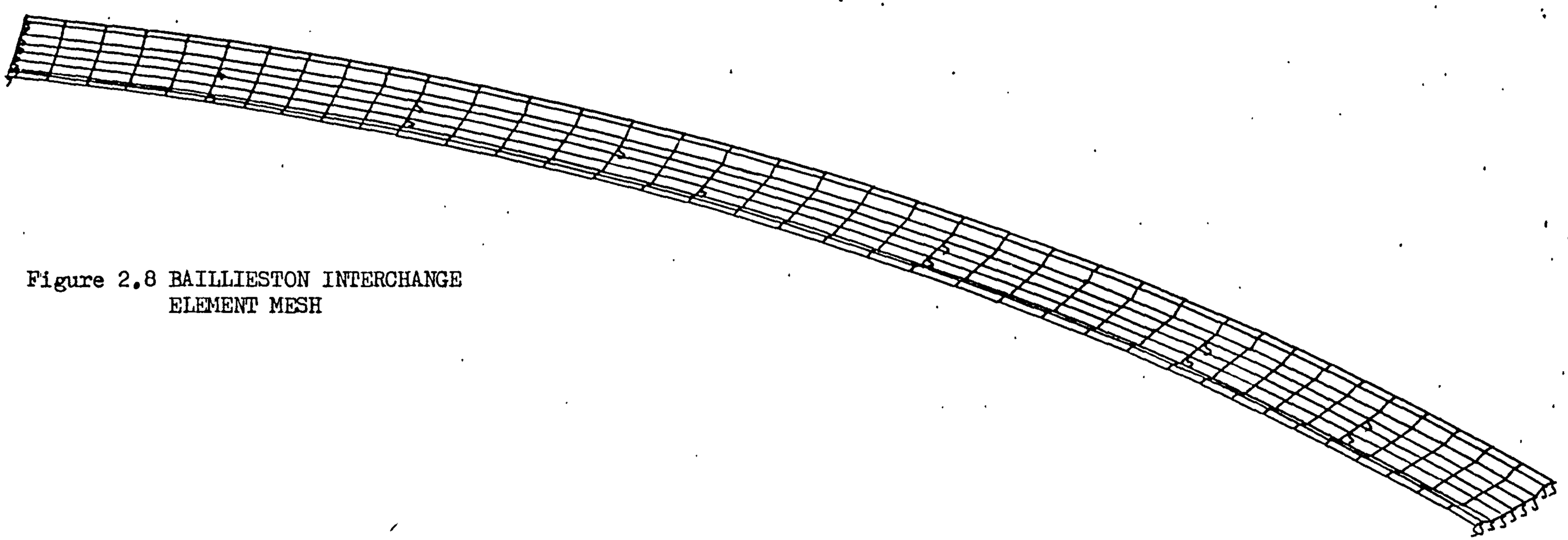

Figure 2.8 BAILLIESTON INTERCHANGE
ELEMENT MESH

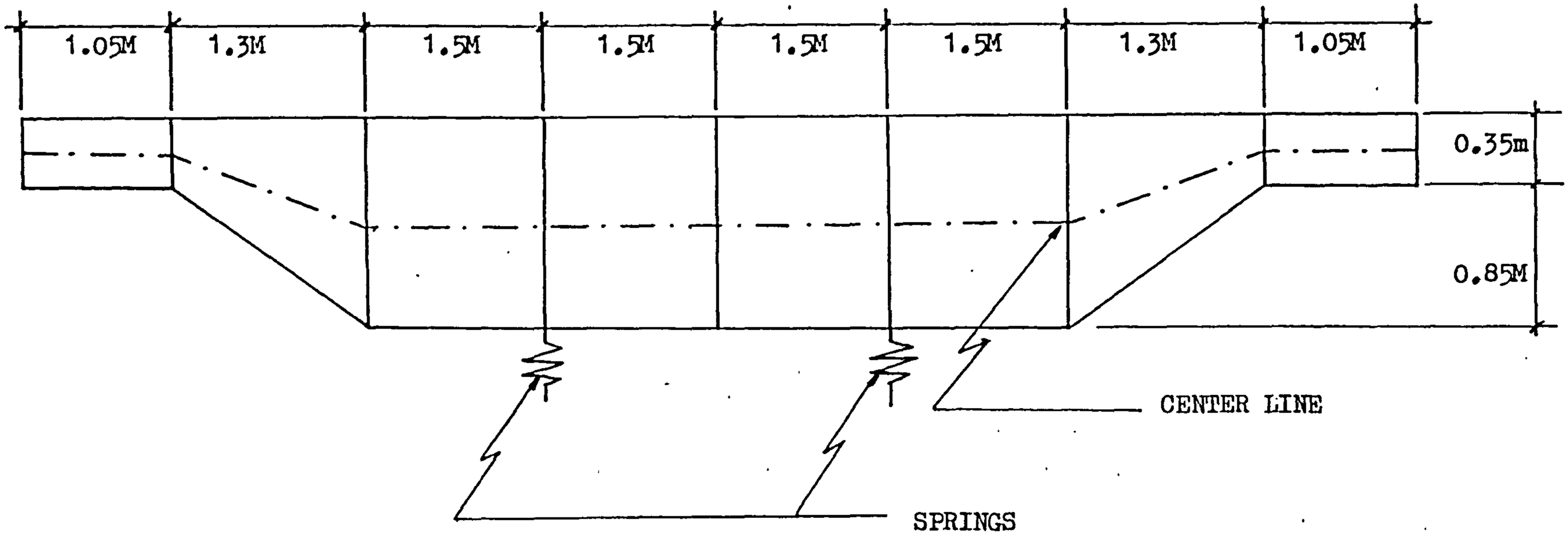

Figure 2.9 BAILLIESTON INTERCHANGE
FINITE ELEMENT CROSS - SECTION

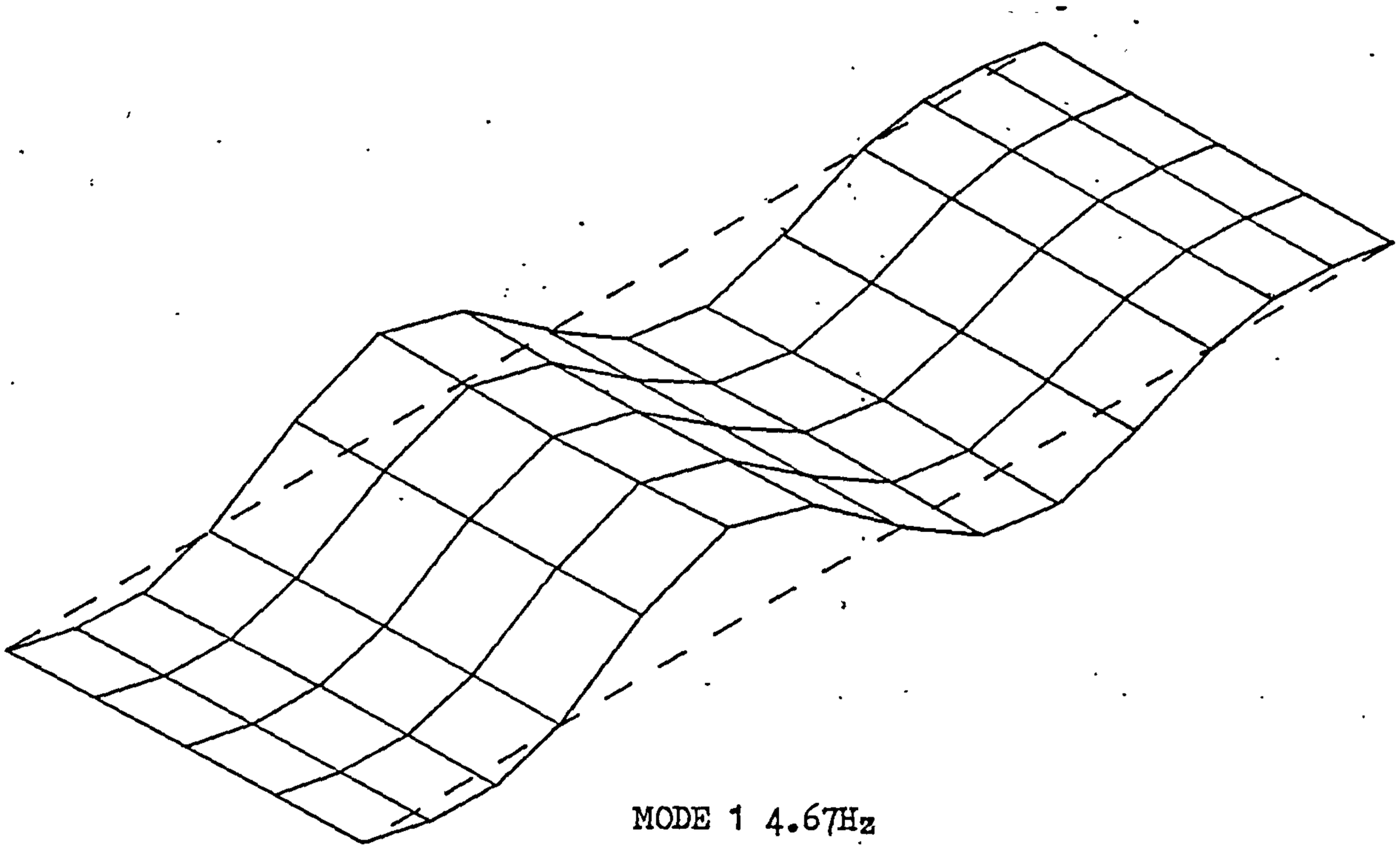

MODE 1 4.67Hz

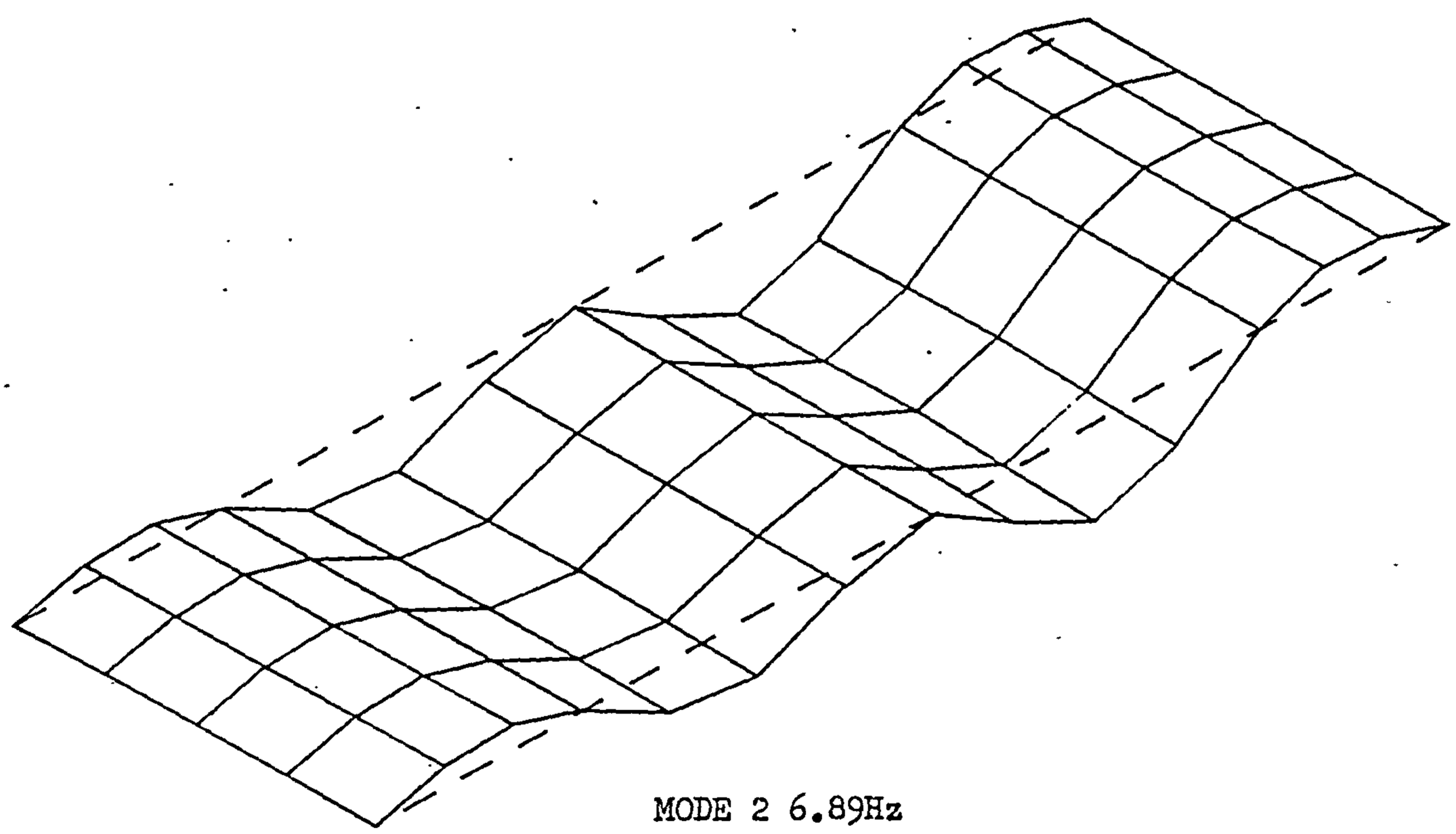

MODE 2 6.89Hz

Figure 2.10 SOUTHFIELD BRIDGE
FLASH MODE SHAPES

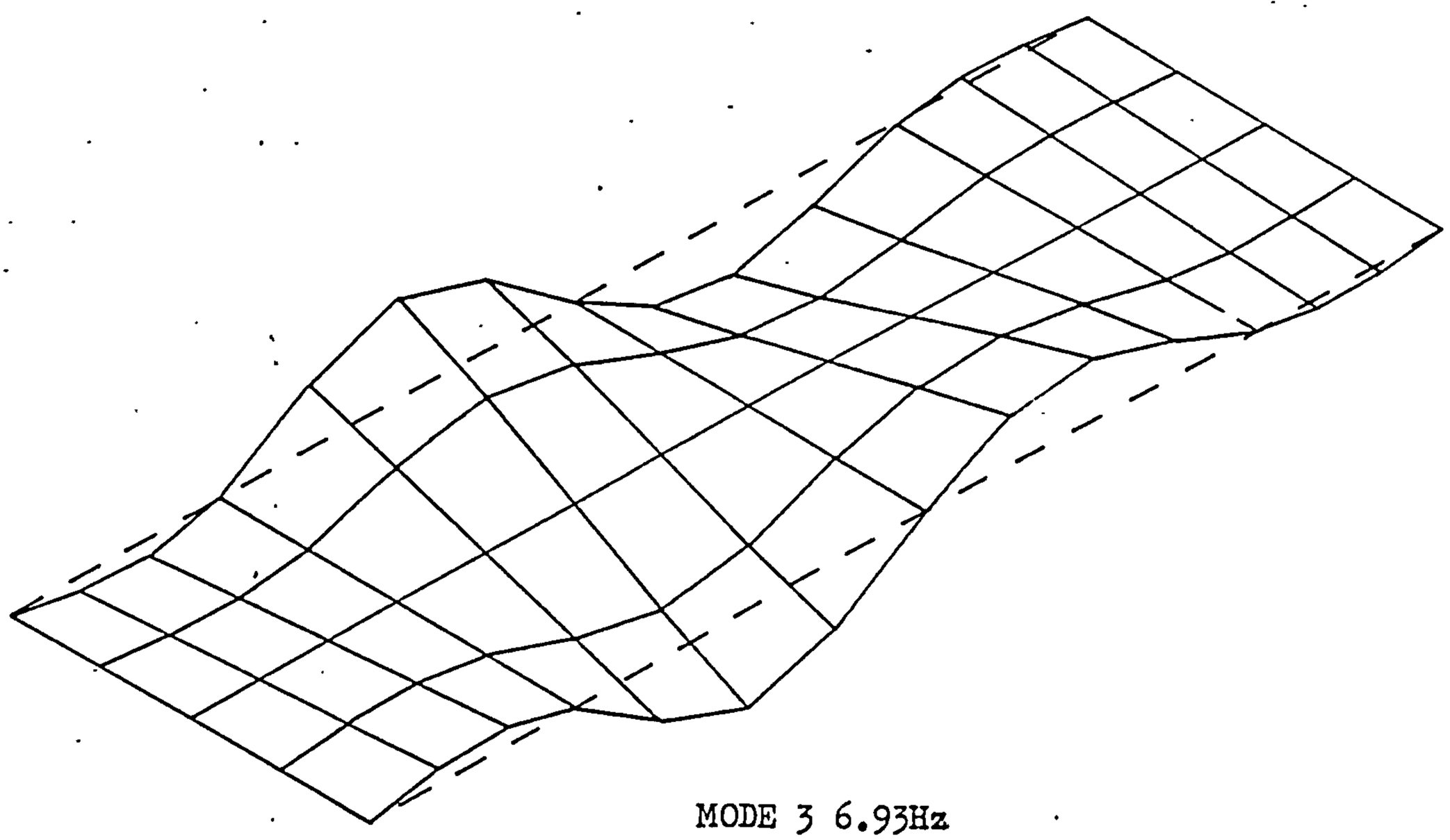

MODE 3 6.93Hz

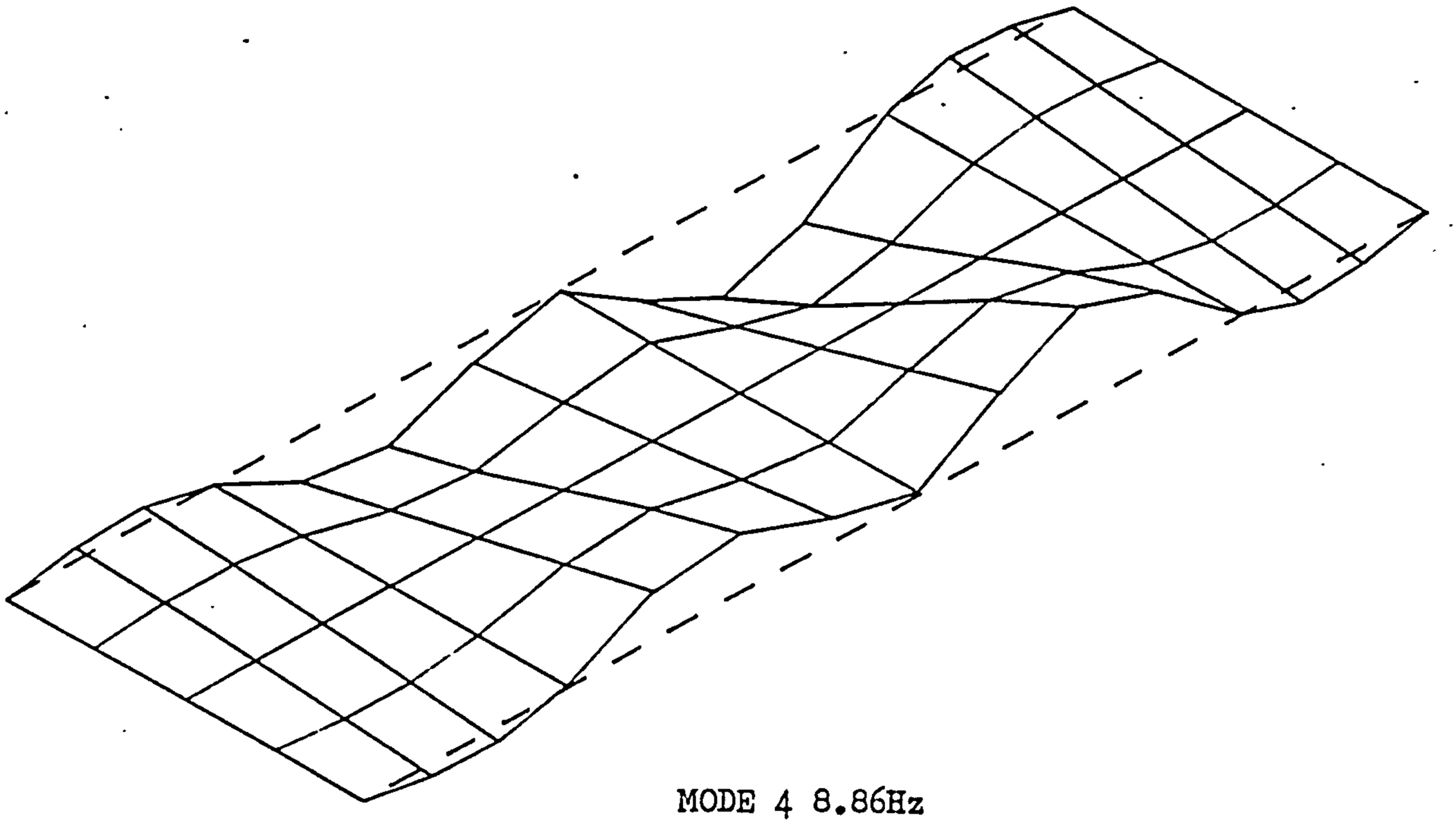

MODE 4 8.86Hz

Figure 2.10 (cont) SOUTHFIELD BRIDGE
FLASH MODE SHAPES

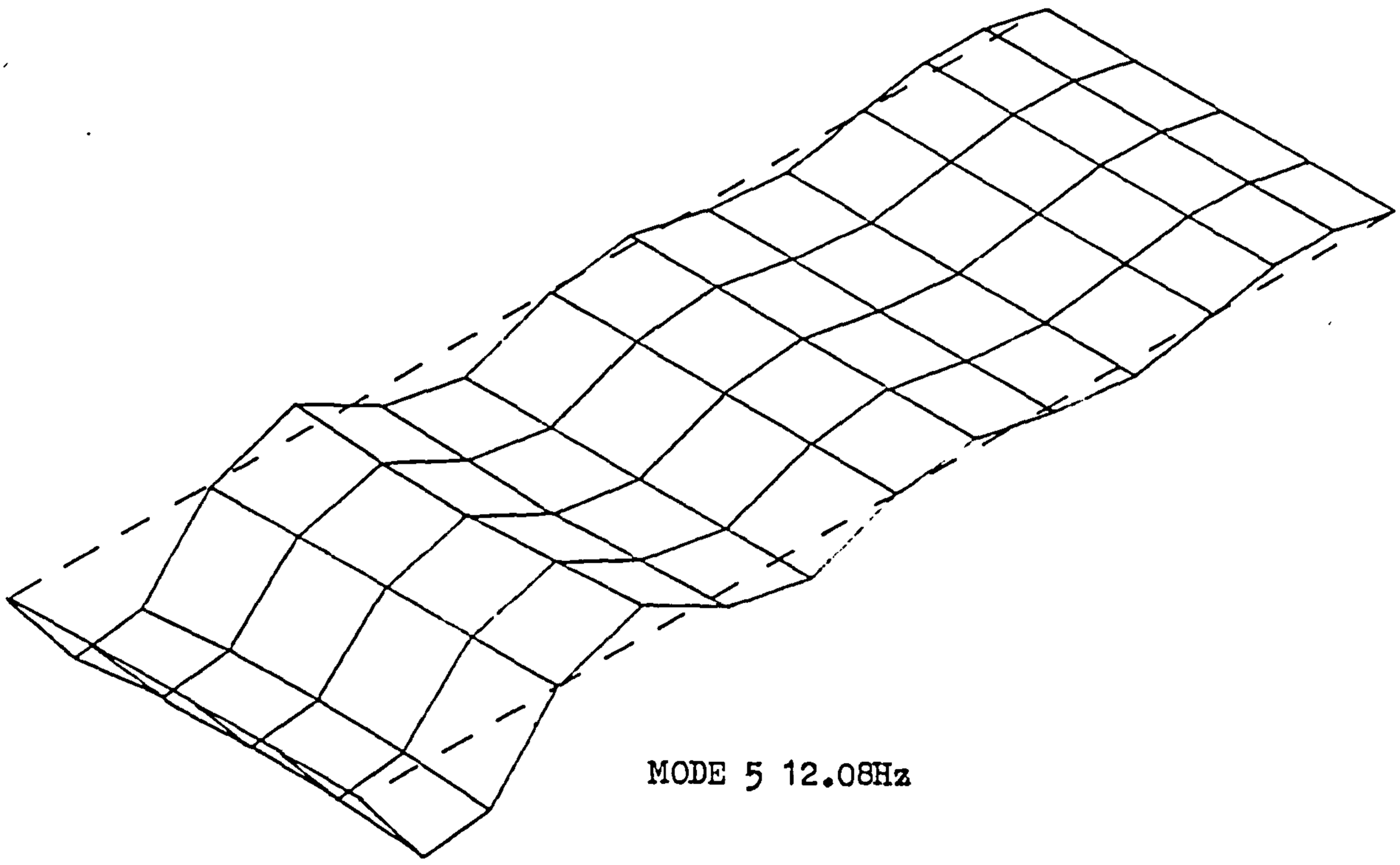

MODE 5 12.08Hz

Figure 2.10 (cont) SOUTHFIELD BRIDGE
FLASH MODE SHAPES

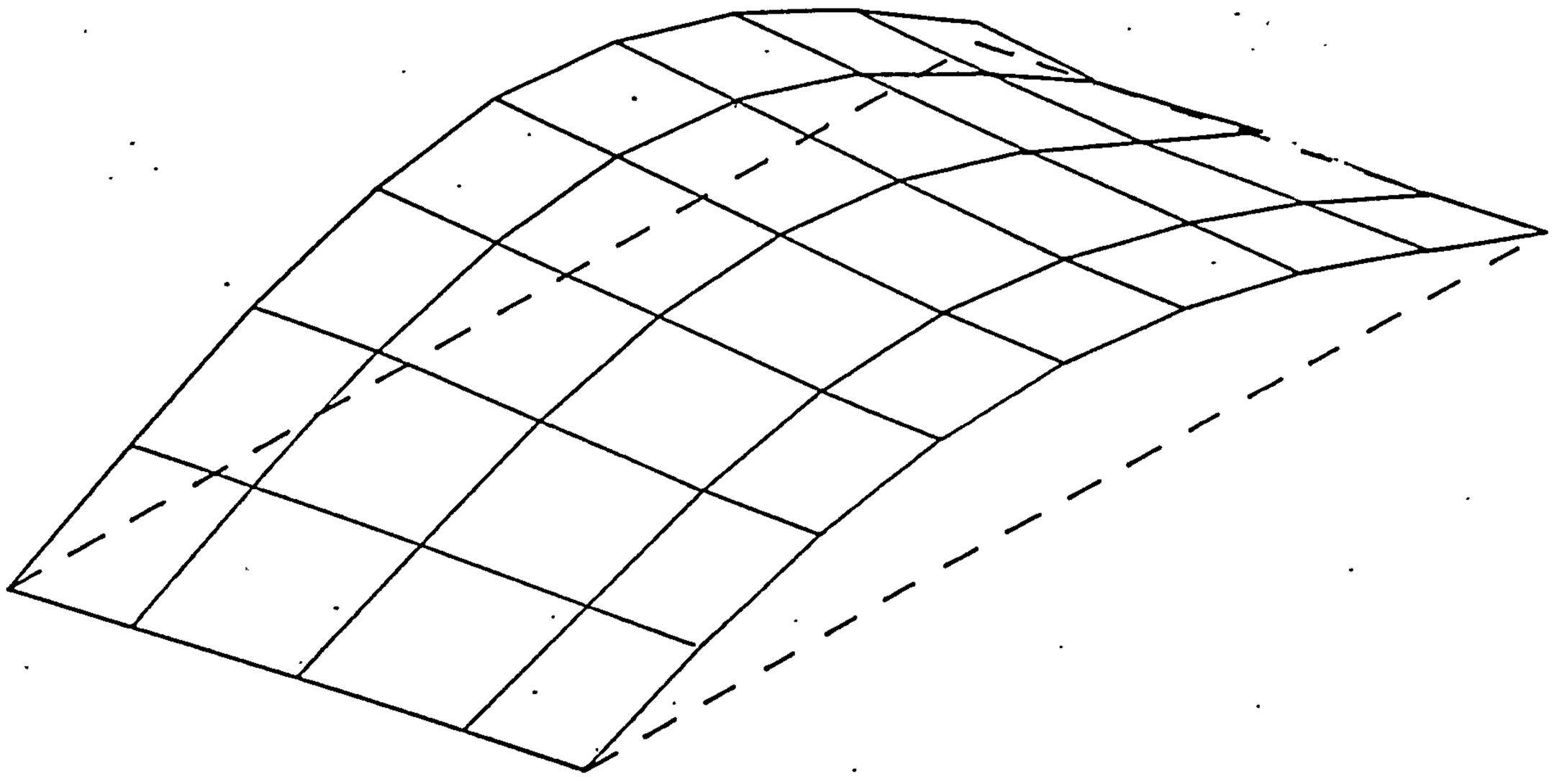

MODE 1 3.55Hz

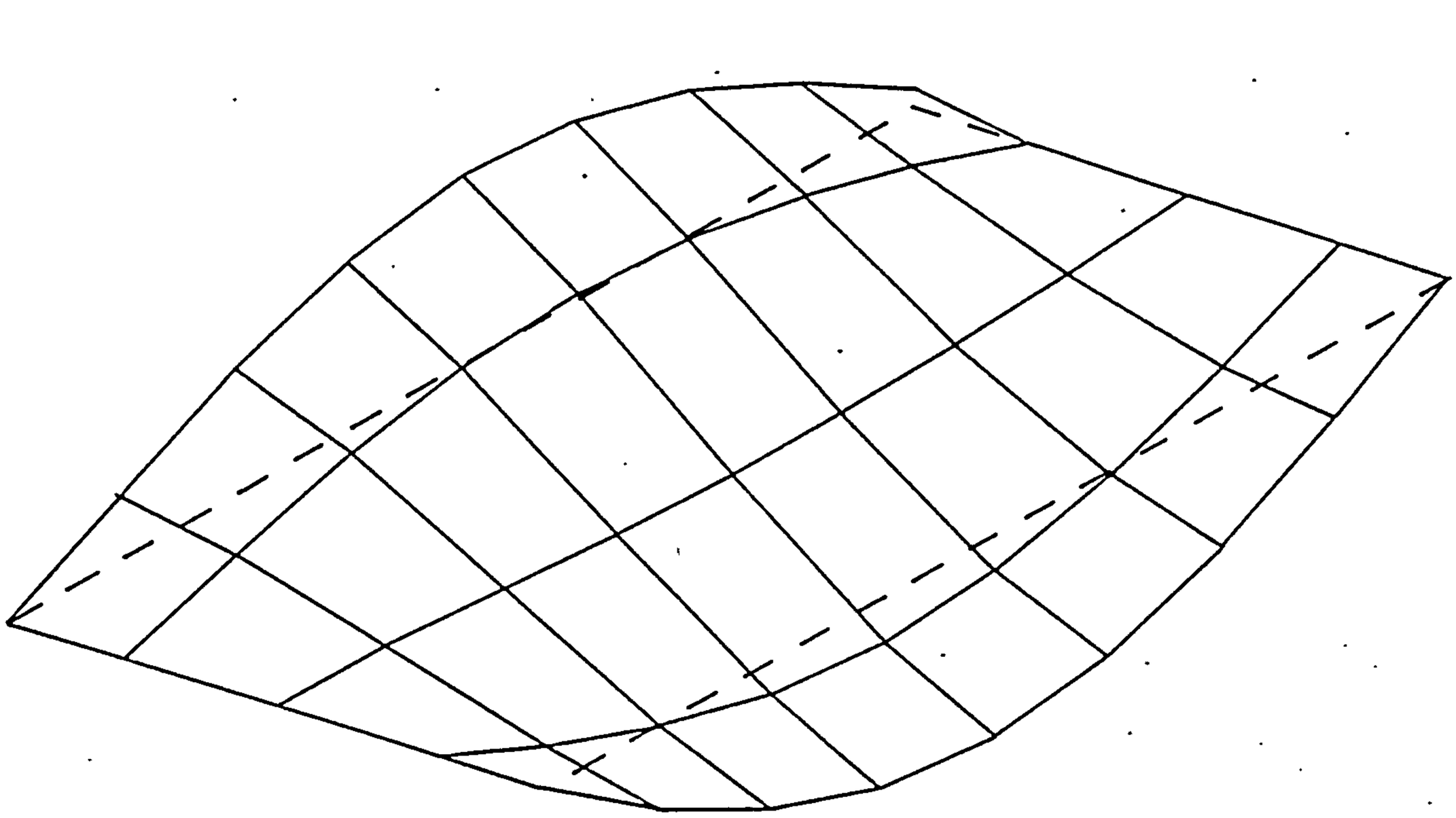

MODE 2 4.04Hz

Figure 2.11 WESTERHOUSE BRIDGE
FLASH MODE SHAPES

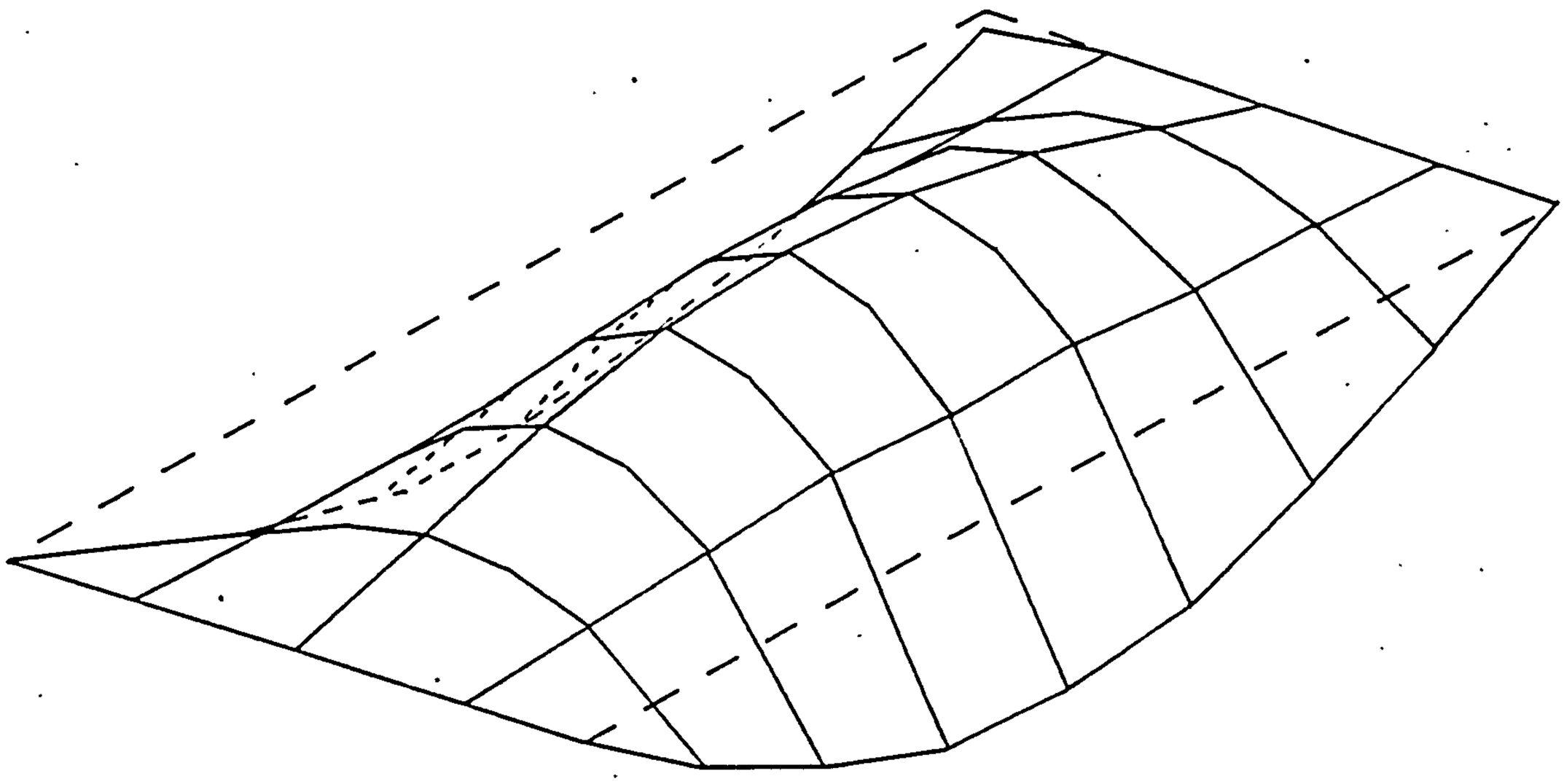

MODE 3 6.84Hz

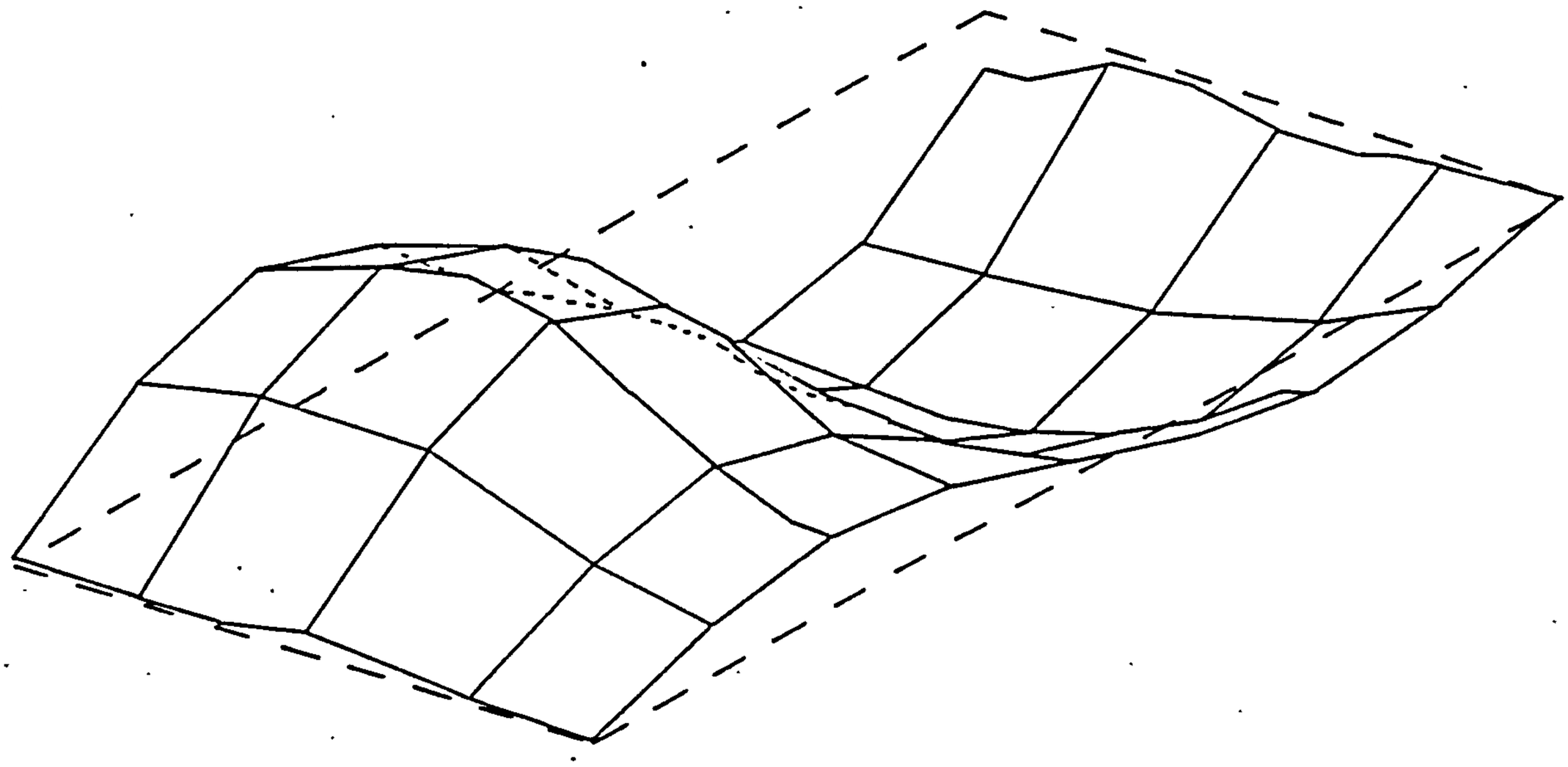

MODE 4 9.68Hz

Figure 2.11 (cont) WESTERHOUSE BRIDGE
FLASH MODE SHAPES

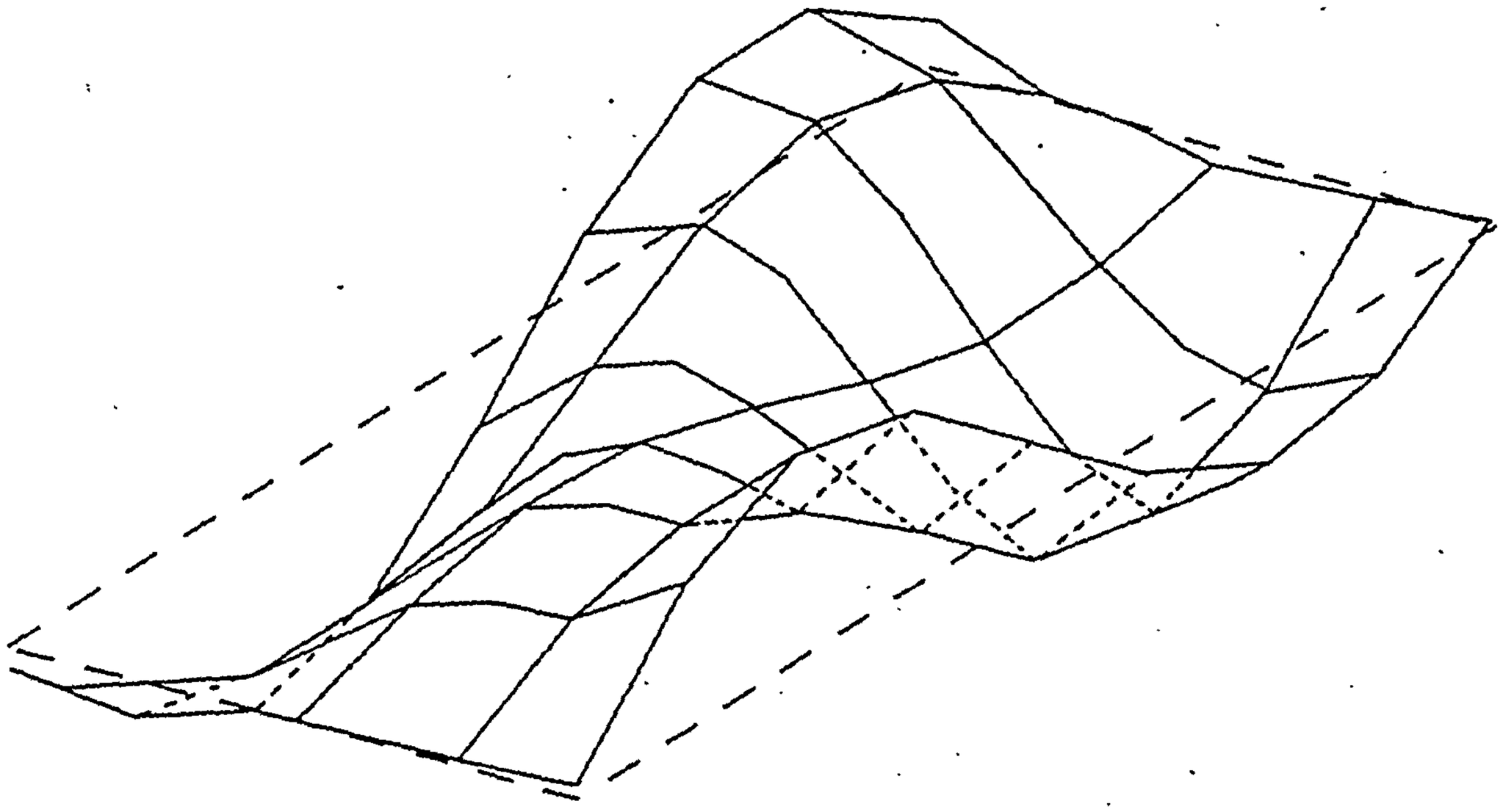

MODE 5 10.89Hz

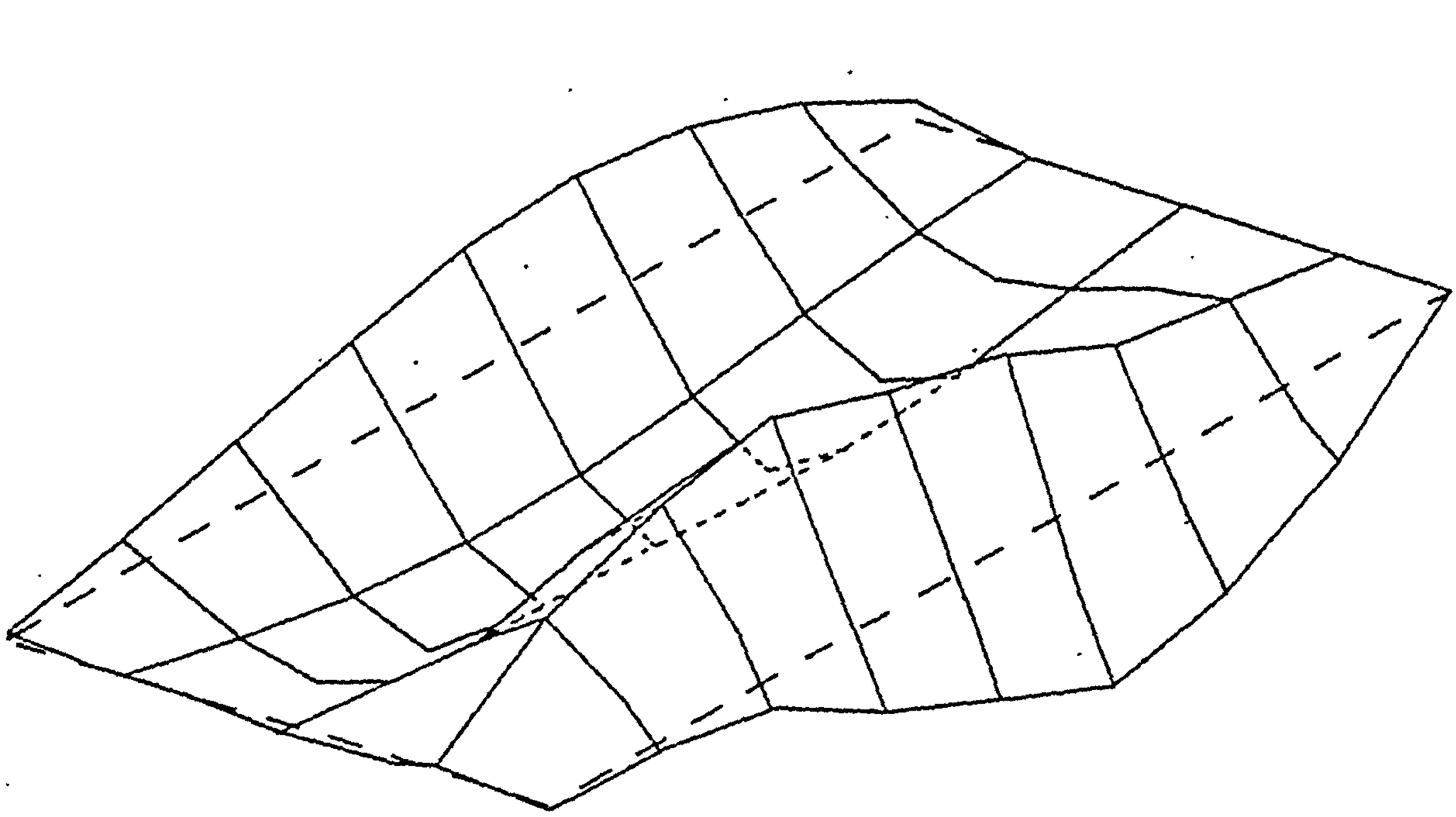

MODE 6 11.57Hz

Figure 2.11 (cont) WESTERHOUSE BRIDGE
FLASH MODE SHAPES

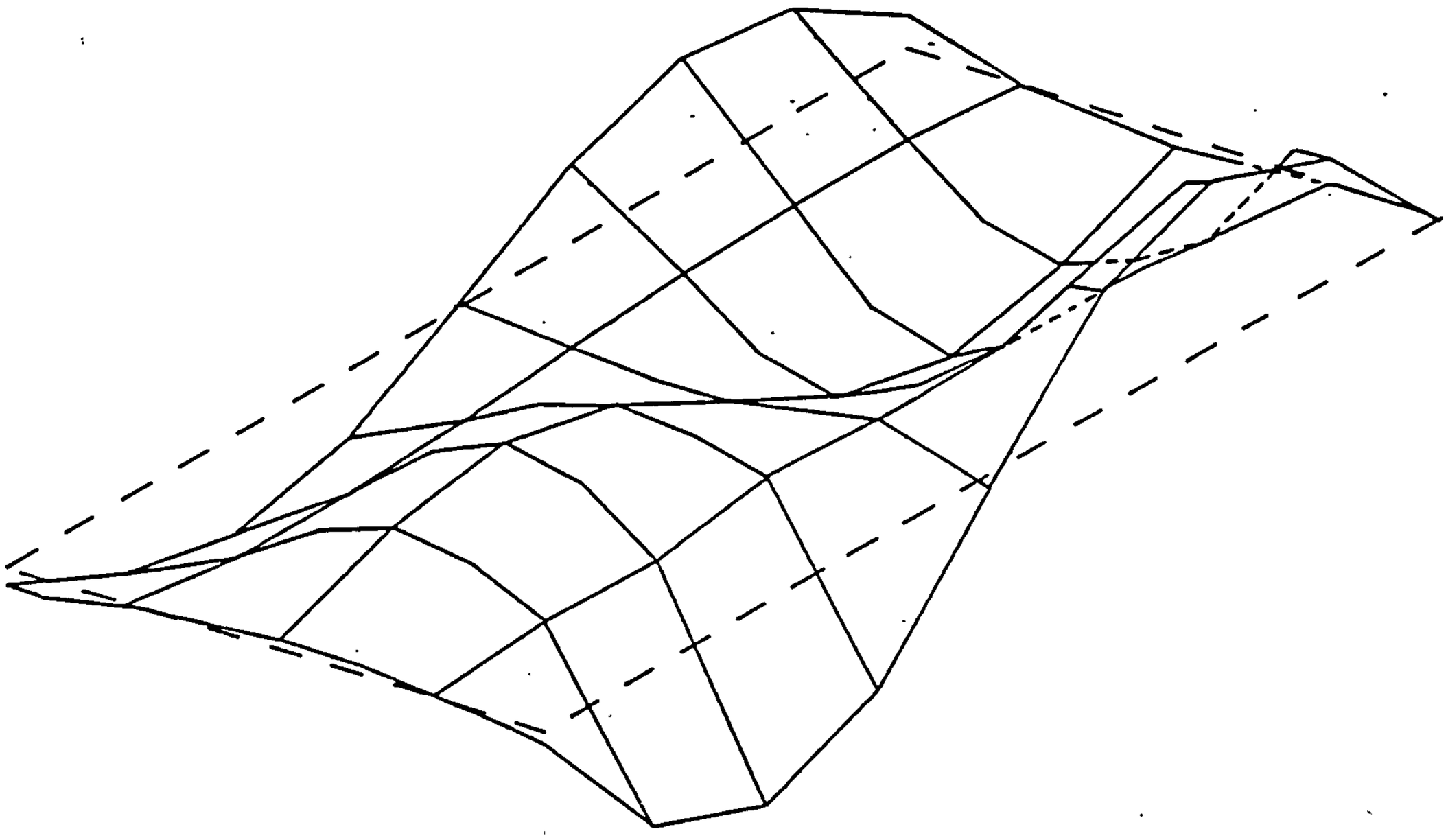

MODE 7 13.03Hz

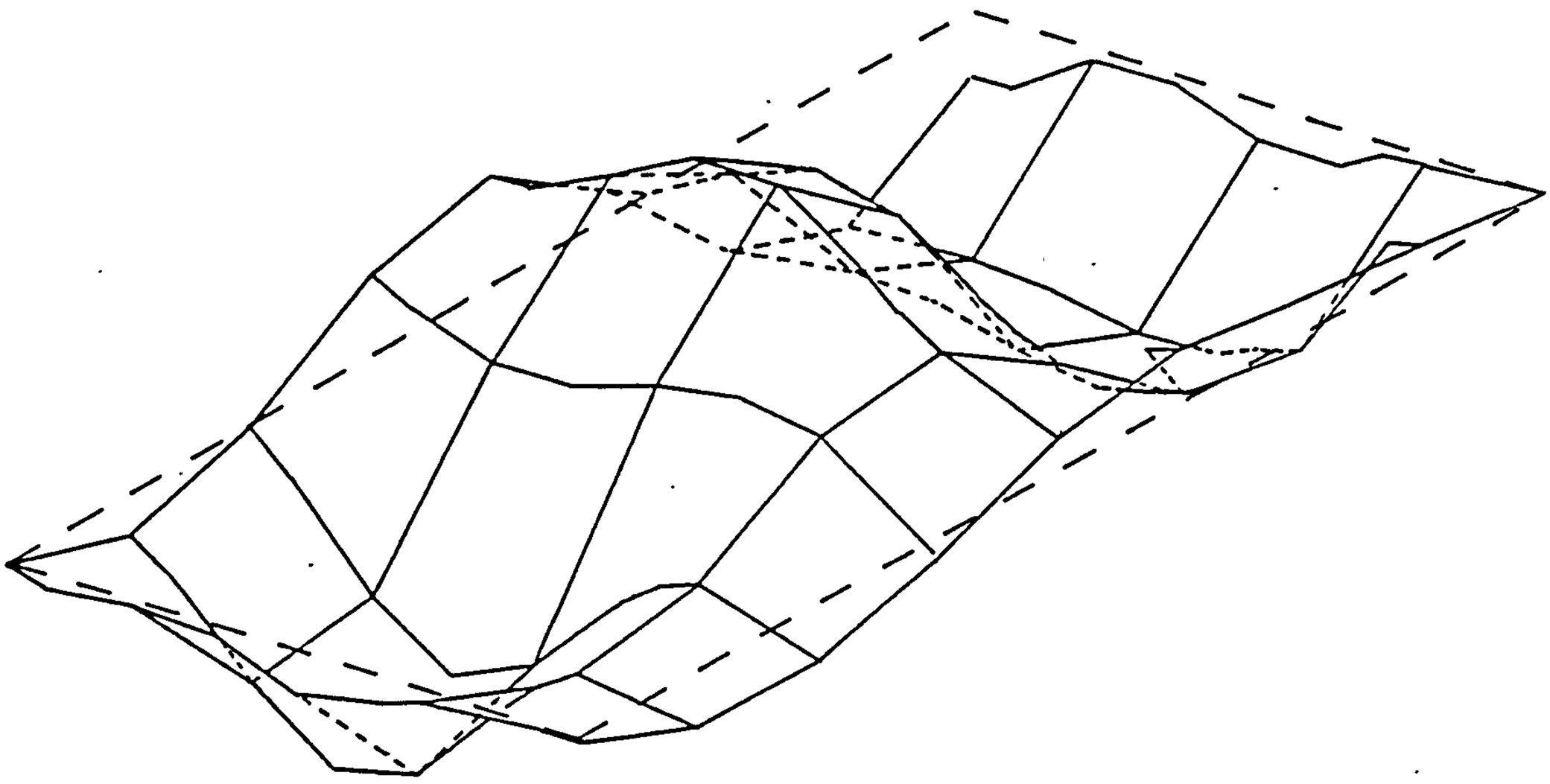

MODE 8 15.86Hz

Figure 2.11 (cont) WESTERHOUSE BRIDGE
FLASH MODE SHAPES

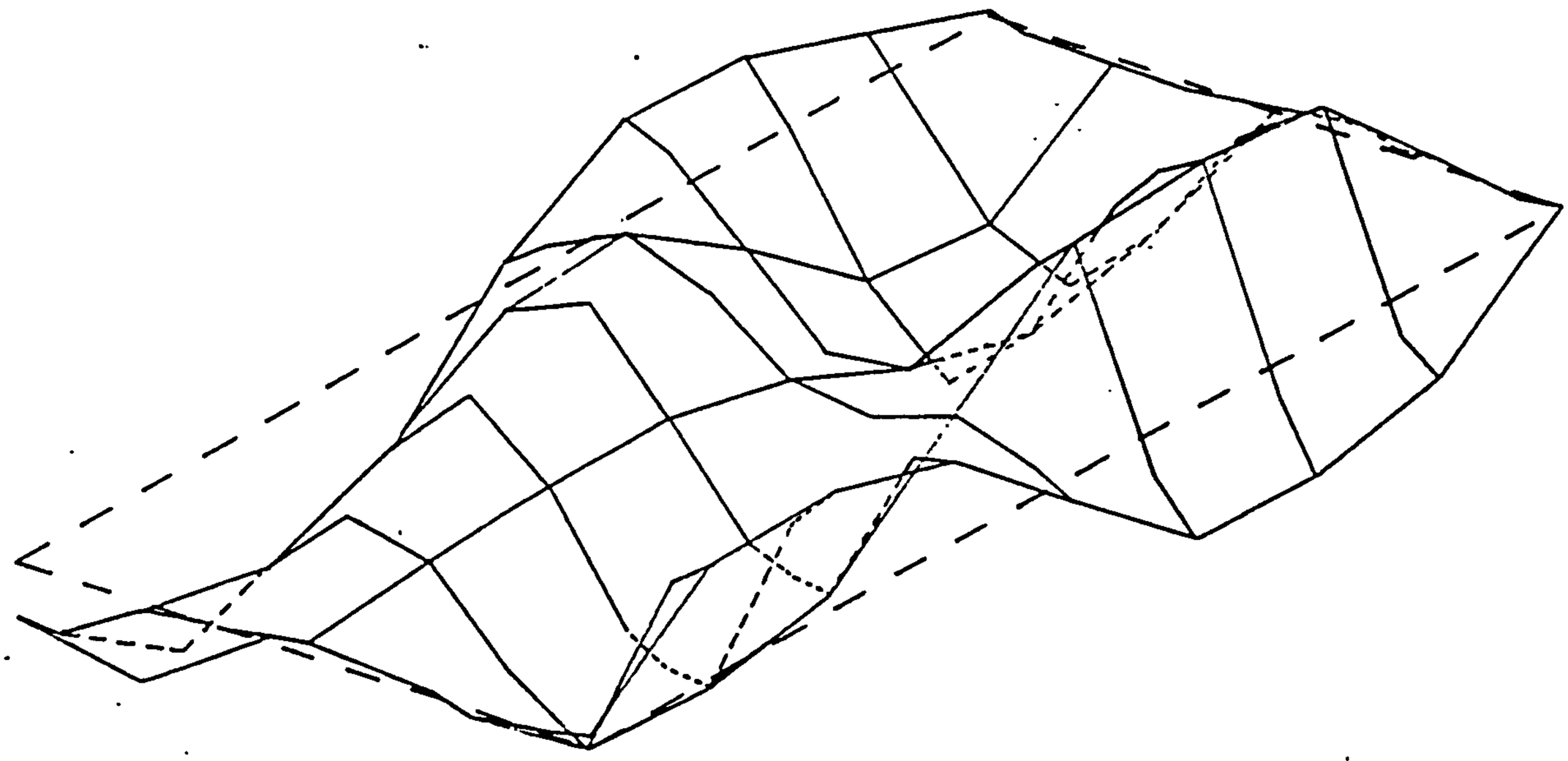

MODE 9 16.87Hz

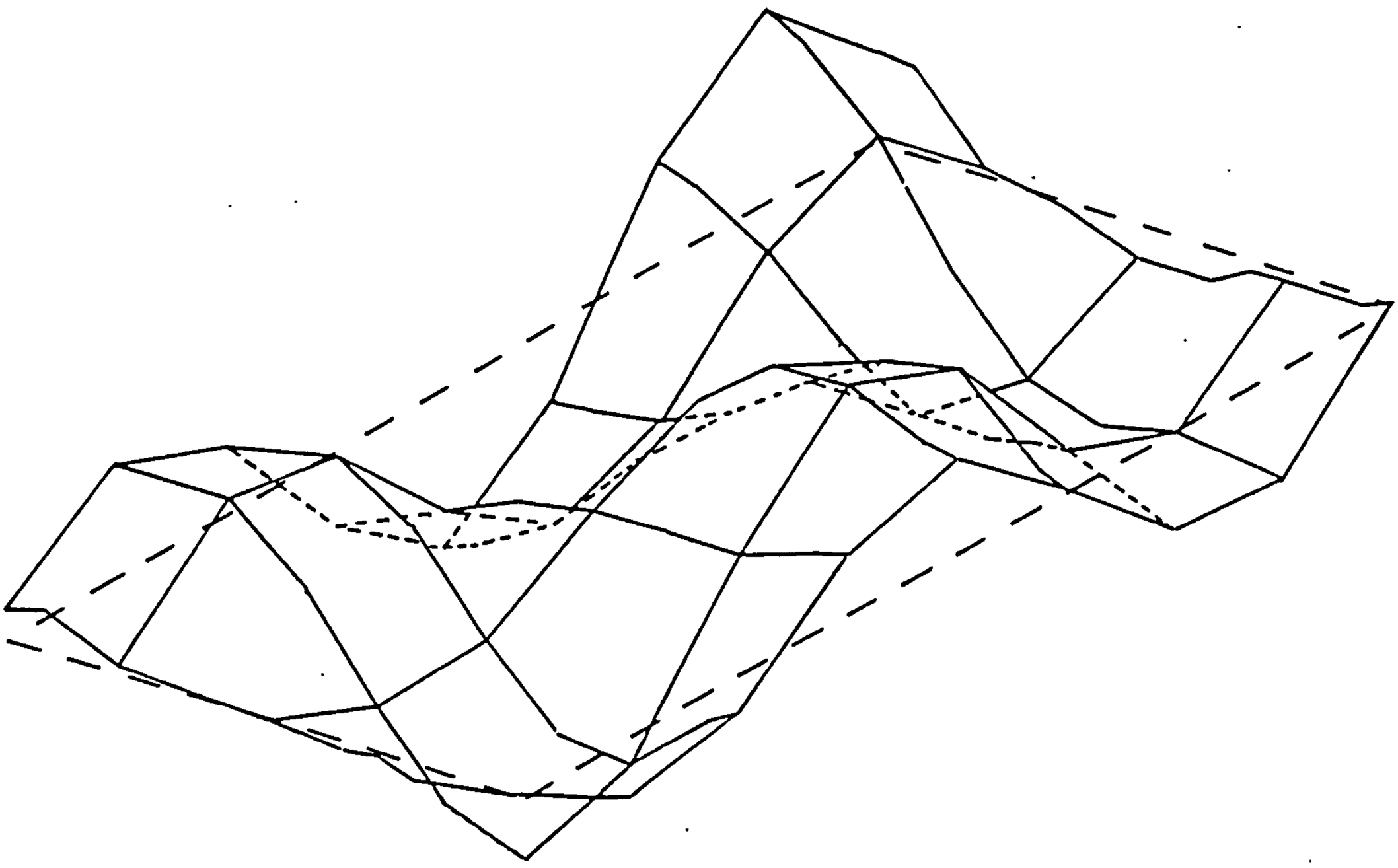

MODE 10 18.42Hz

Figure 2.11 (cont) WESTERHOUSE BRIDGE
FLASH MODE SHAPES

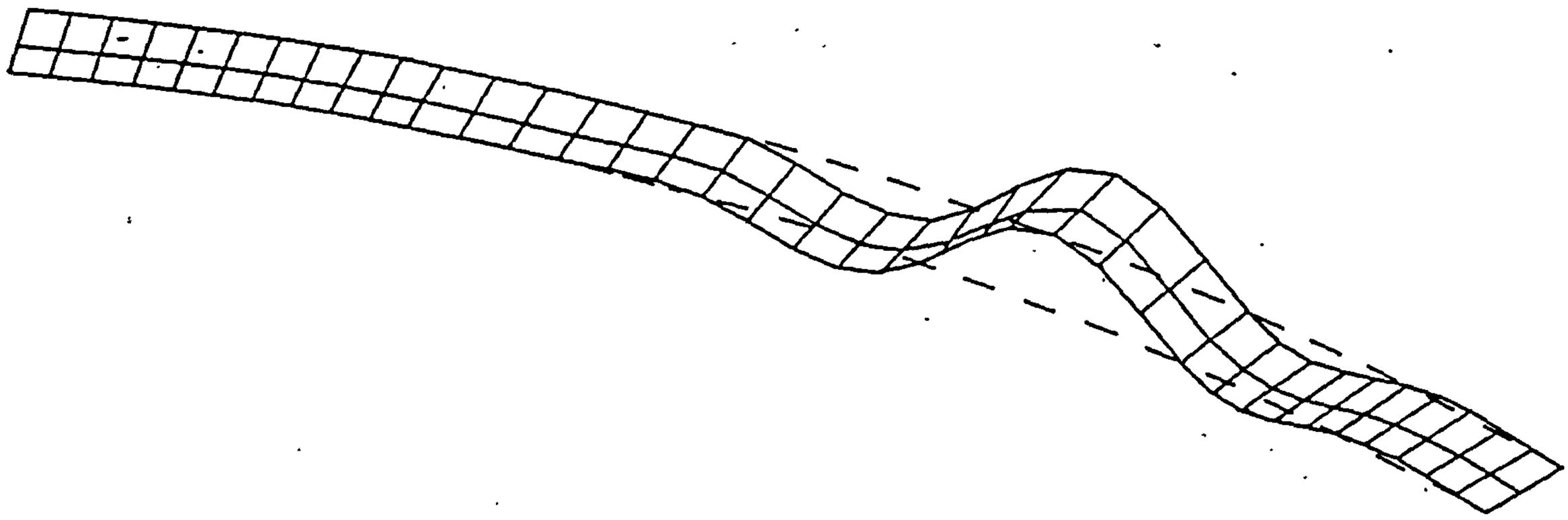

MODE 1 3.08Hz

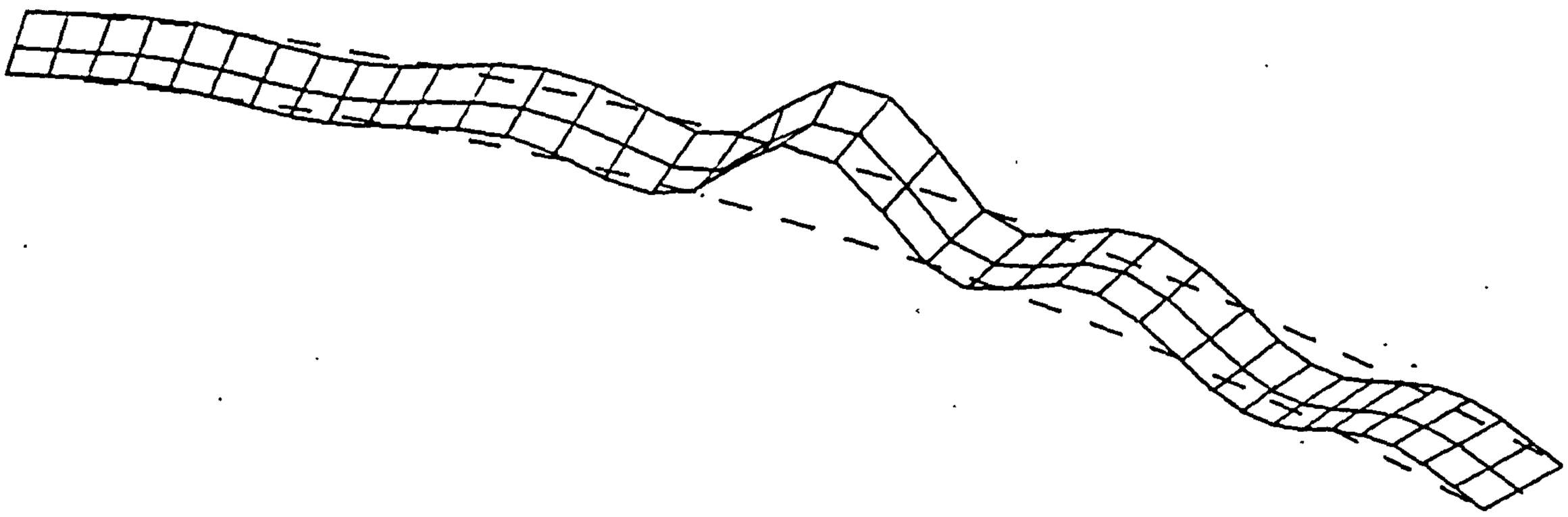

MODE 2 4.99Hz

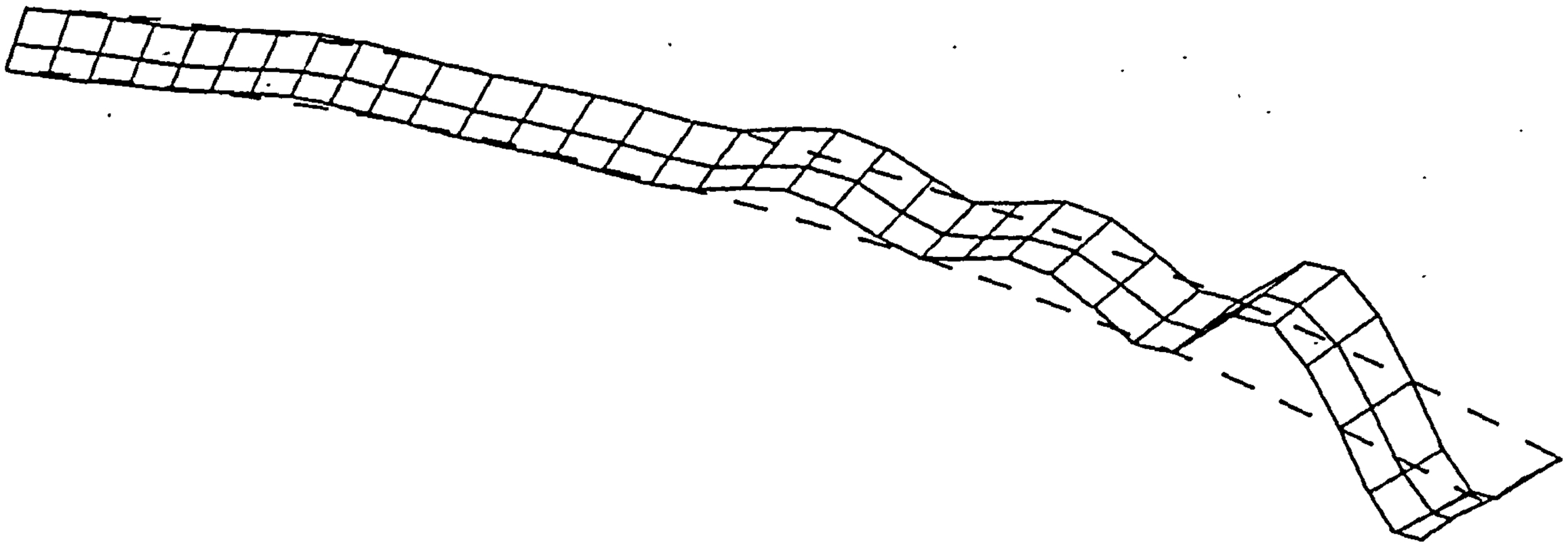

MODE 3 6.09

Figure 2.12 BAILLIESTON INTERCHANGE - FLASH MODE SHAPES

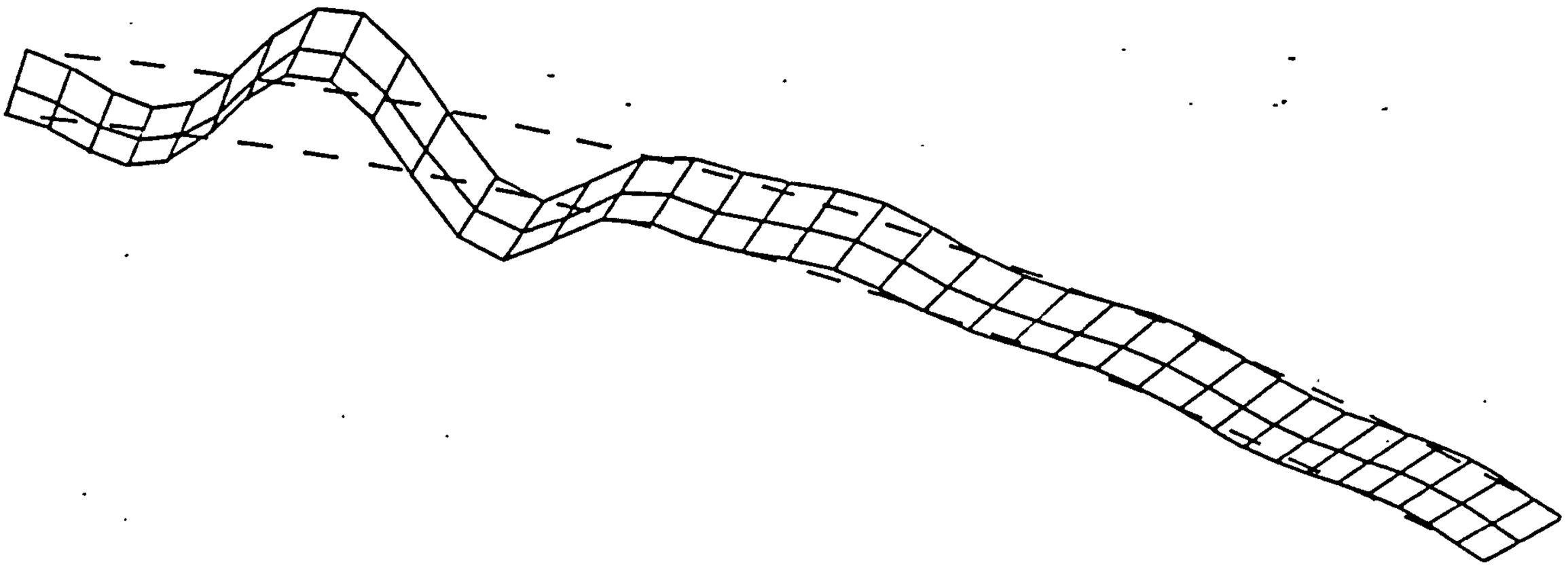

MODE 4 6.21Hz

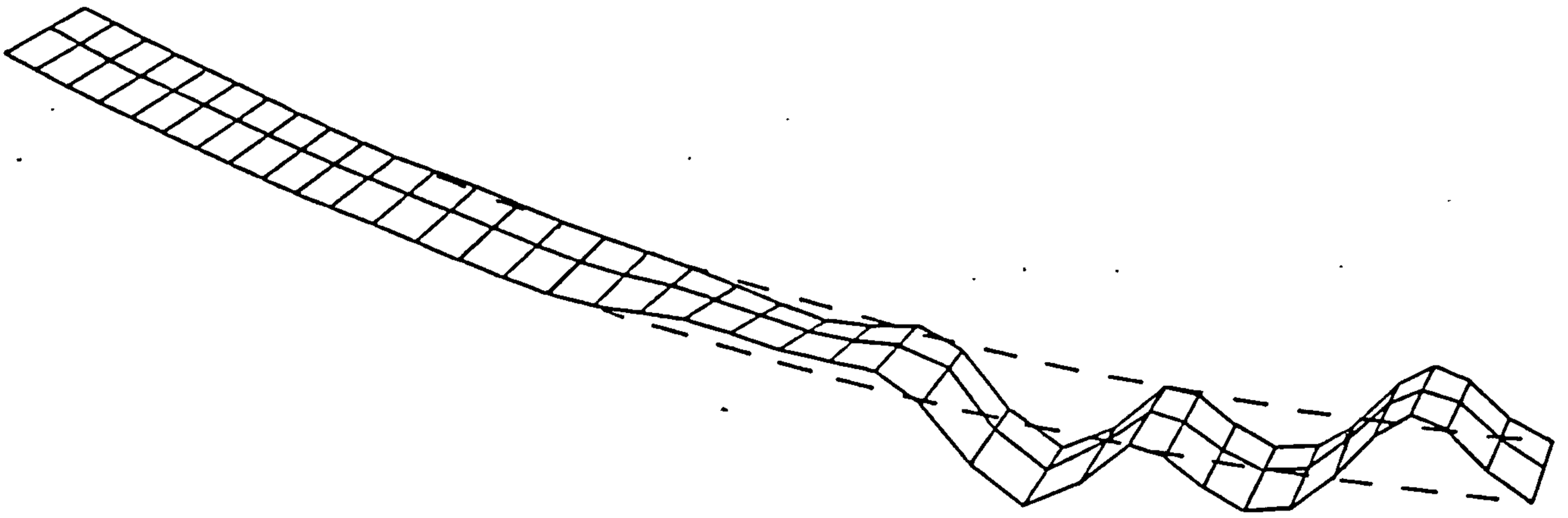

MODE 5 7.74Hz

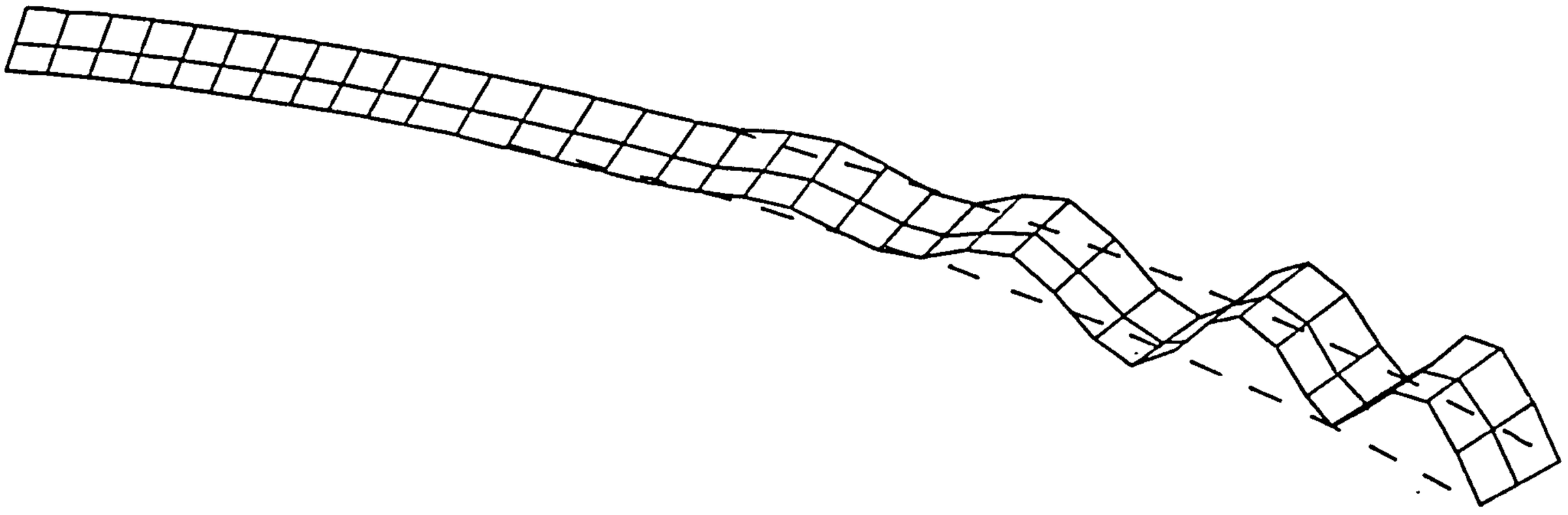

MODE 6 8.27

Figure 2.12 (cont) BAILLIESTON INTERCHANGE - FLASH MODE SHAPES

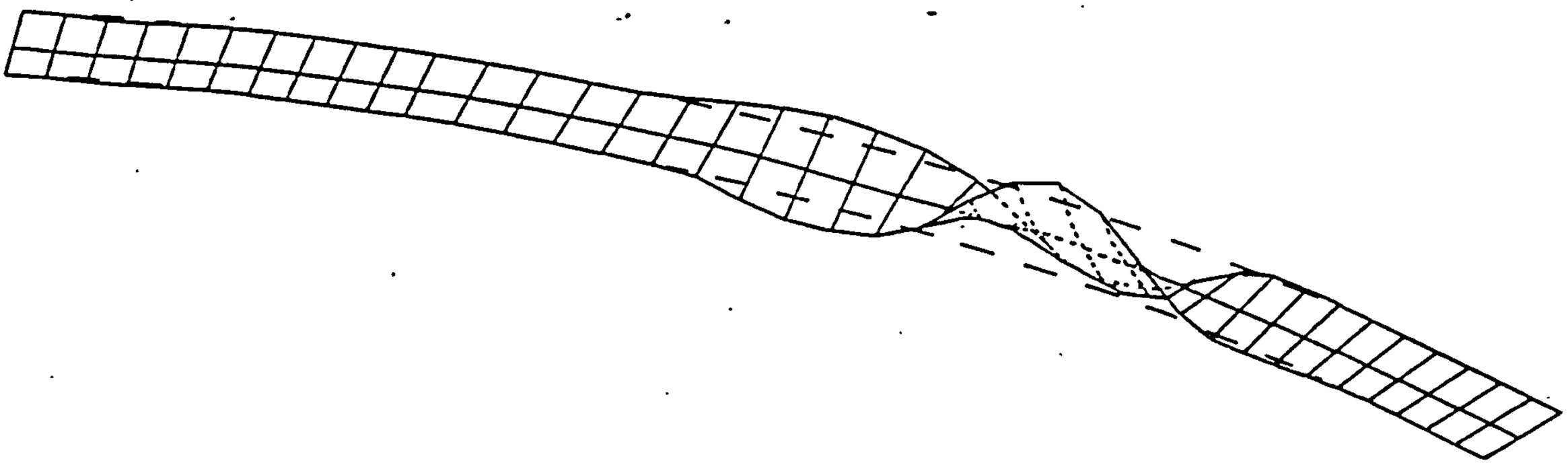

MODE 7 8.79Hz

Figure 2.12 (cont) BAILLIESTON INTERCHANGE - FLASH MODE SHAPES

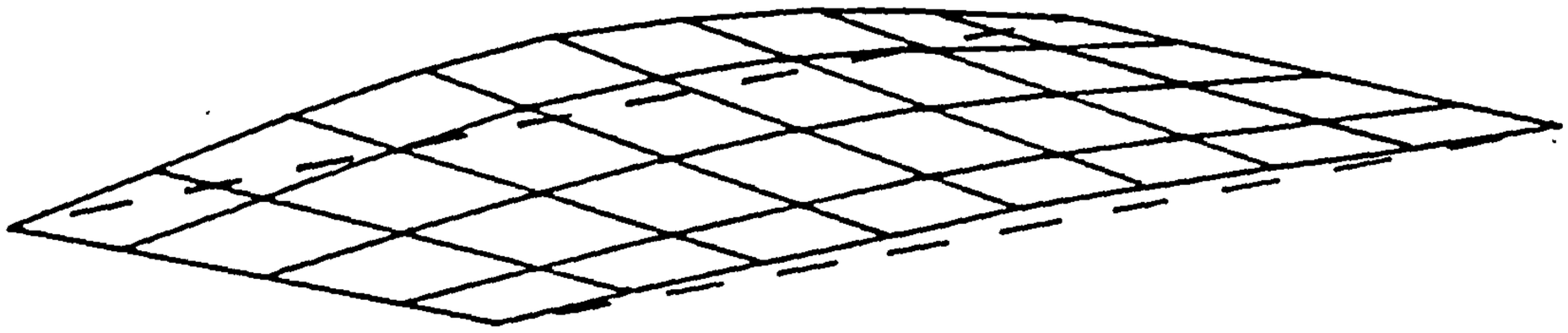

MODE 1 3.5Hz

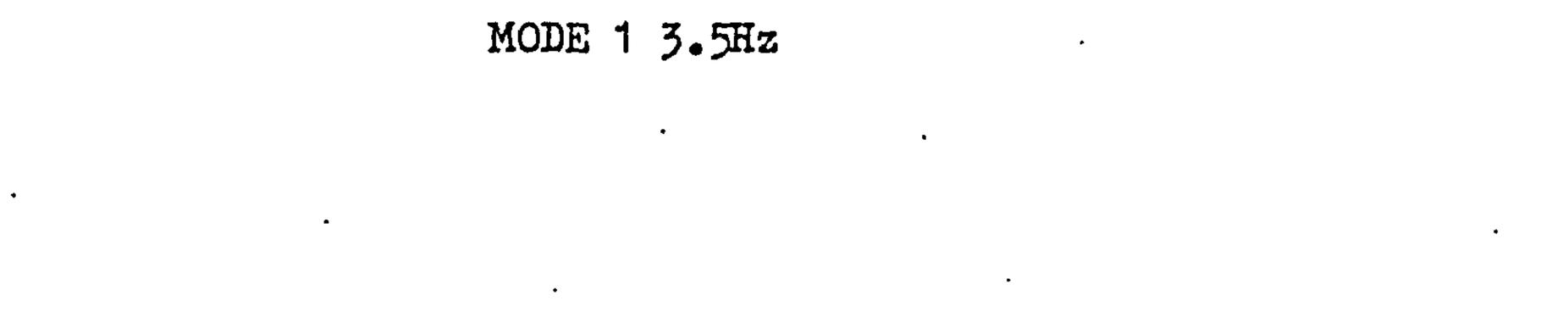

MODE 2 3.94Hz

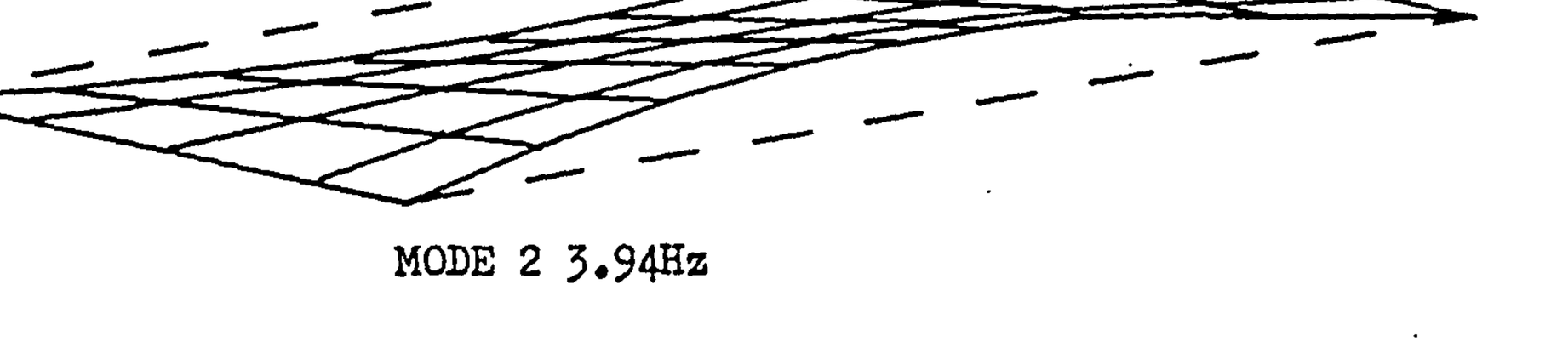

MODE 3 6.73Hz

Figure 2.13 WESTERHOUSE BRIDGE MSC/NASTRAN MODE SHAPES

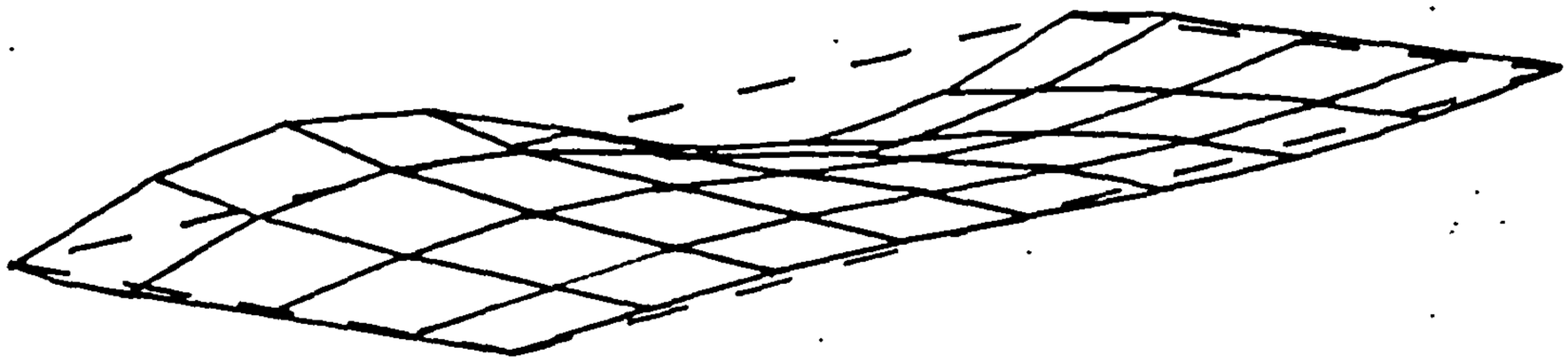

MODE 4 11.63Hz

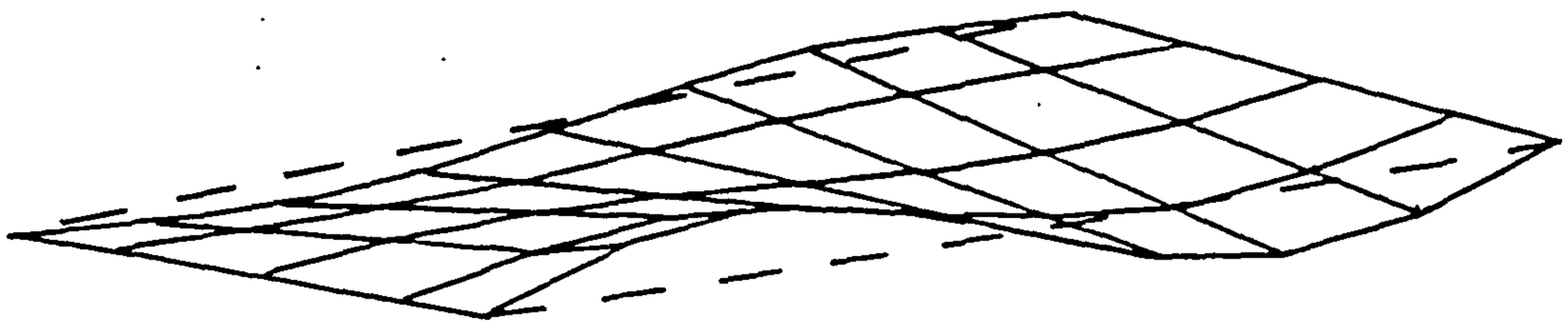

MODE 5 12.54Hz

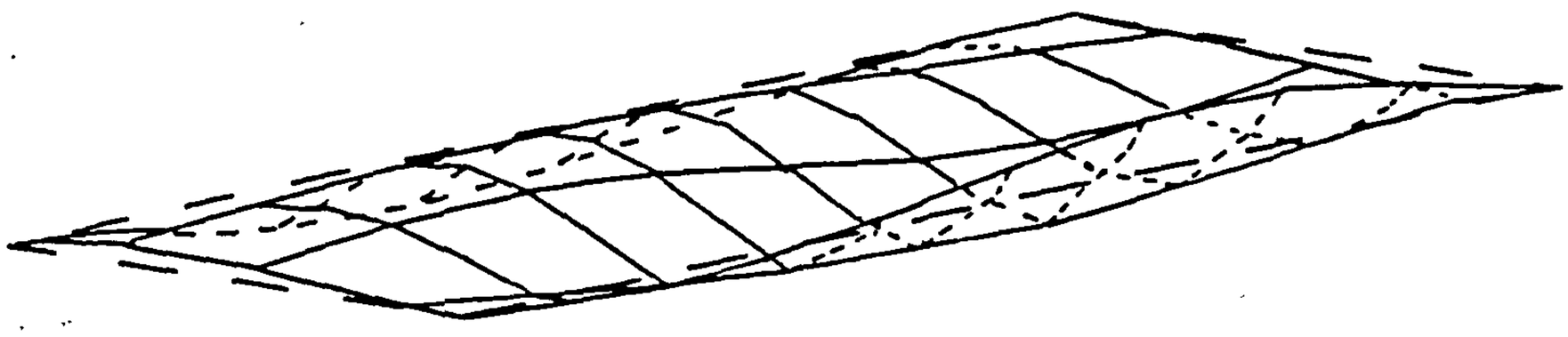

MODE 6 13.43Hz

Figure 2.13 (cont) WESTERHOUSE BRIDGE MSC/NASTRAN MODE SHAPES

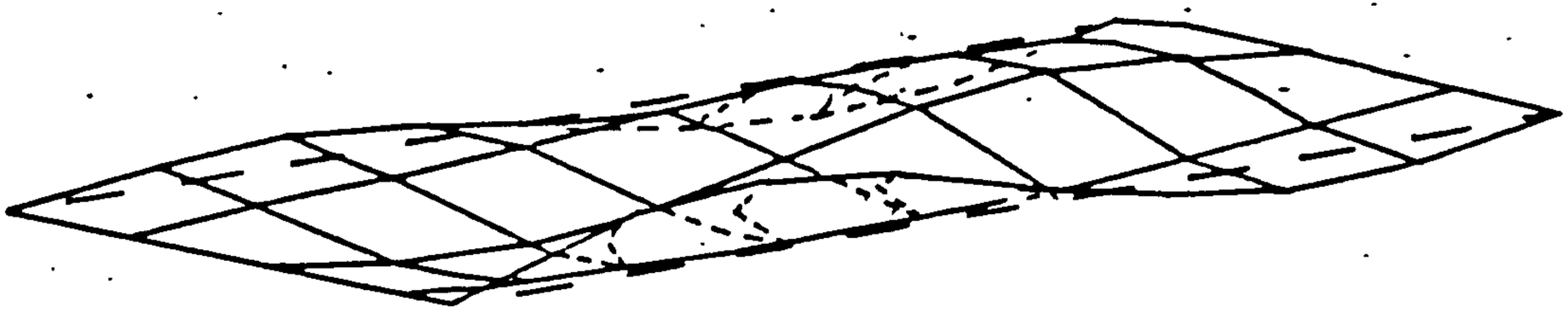

MODE 7 14.31Hz

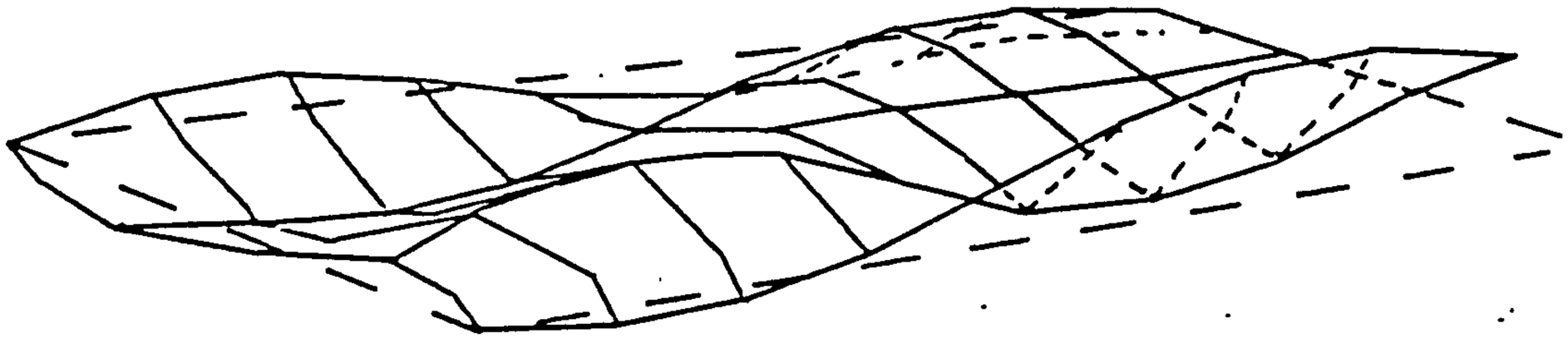

MODE 8 20.03Hz

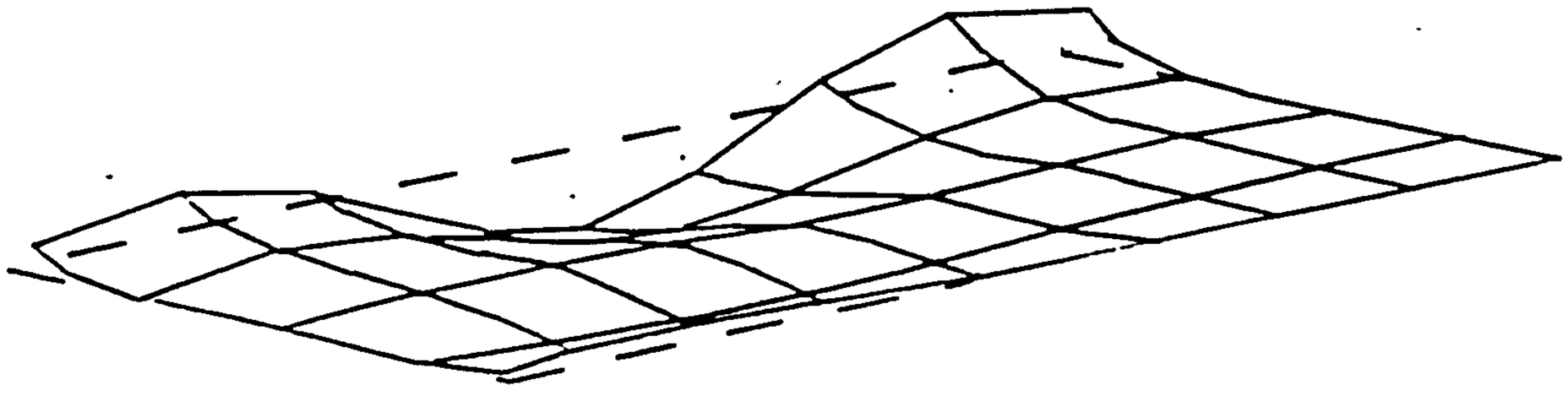

MODE 9 22.36Hz

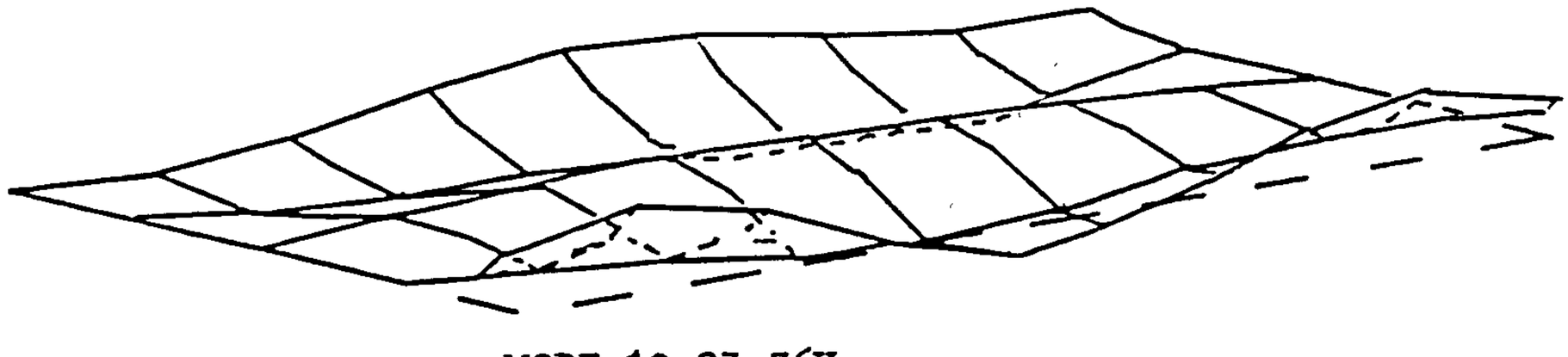

MODE 10 23.56Hz

Figure 2.13 (cont) WESTERHOUSE BRIDGE MSC/NASTRAN MODE SHAPES

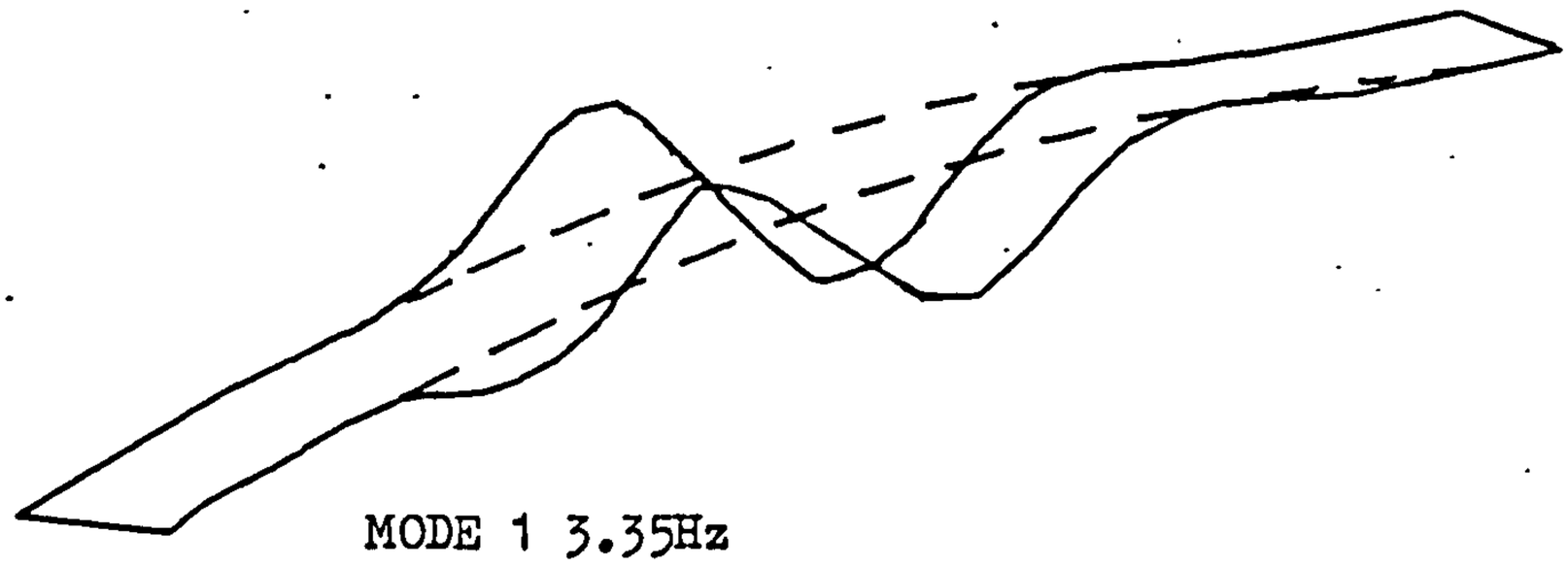

MODE 1 3.35Hz

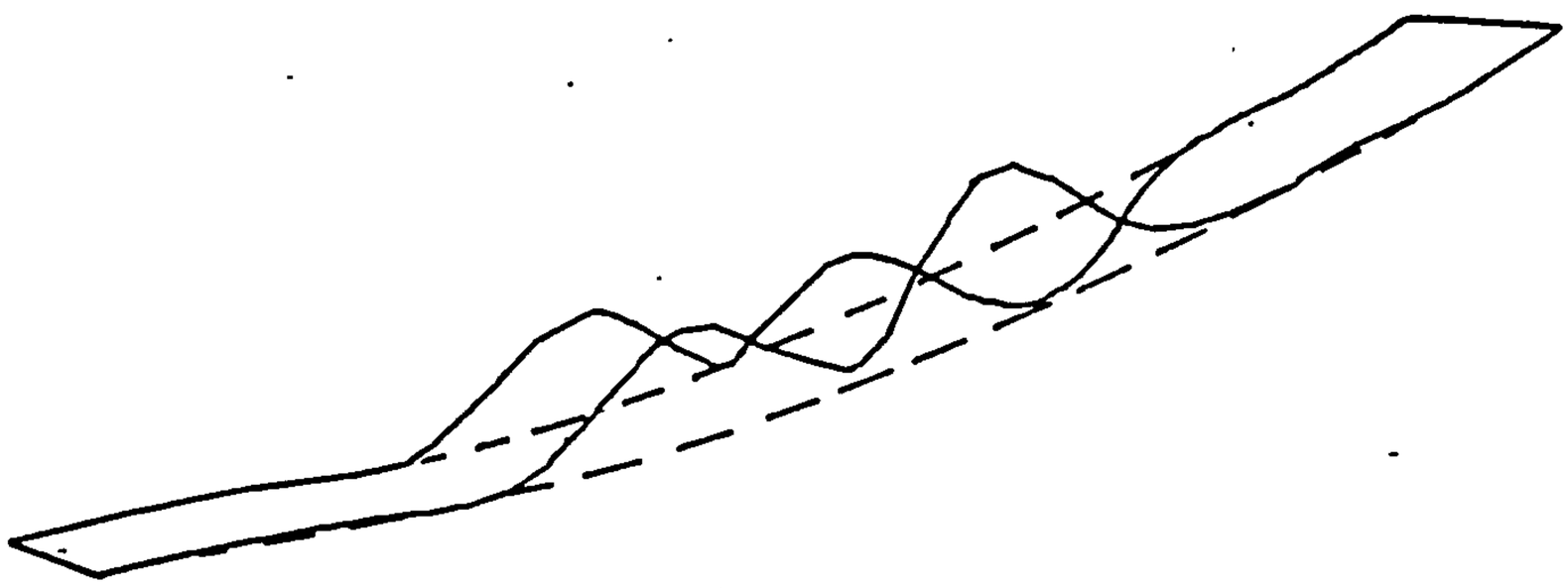

MODE 2 3.97Hz

MODE 3 3.97Hz

Figure 2.14 BAILLIESTON INTERCHANGE MSC/NASTRAN MODE SHAPES

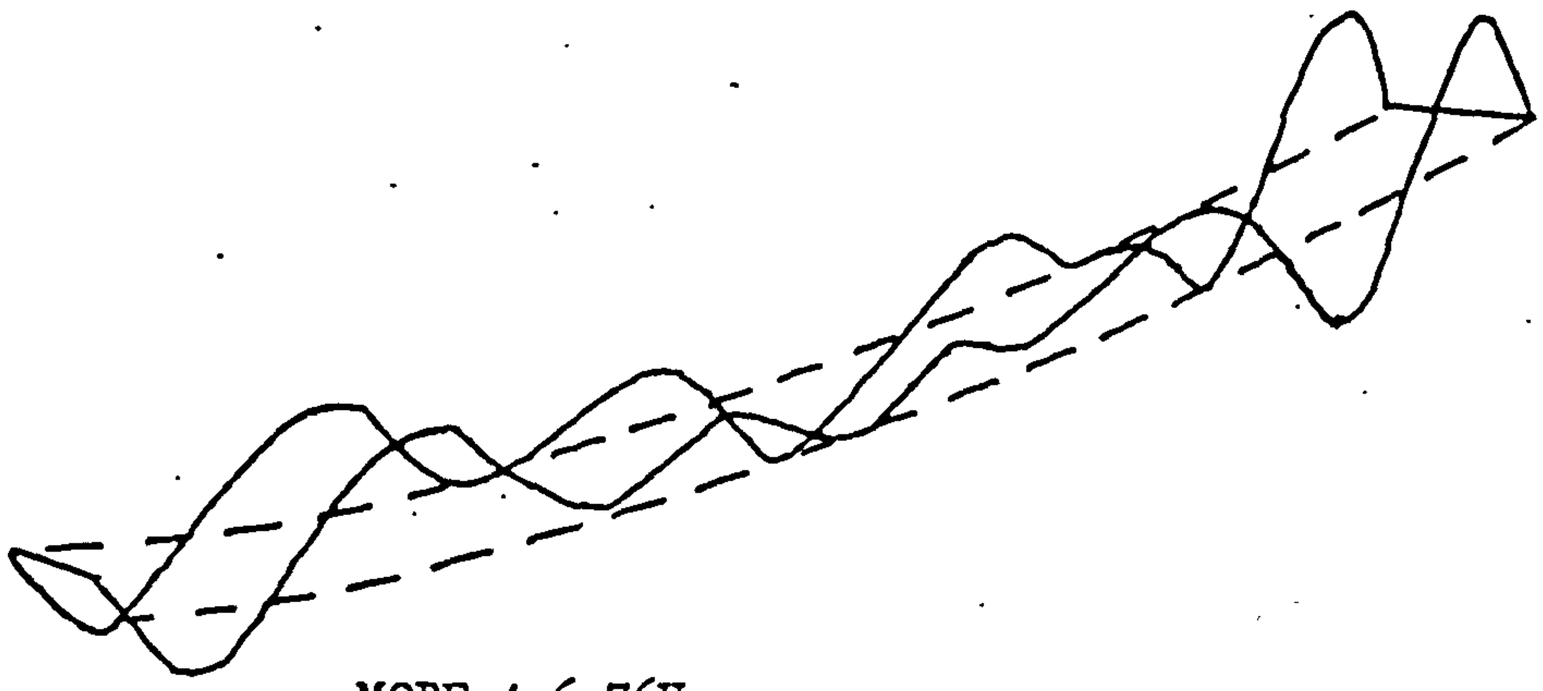

MODE 4 6.76Hz

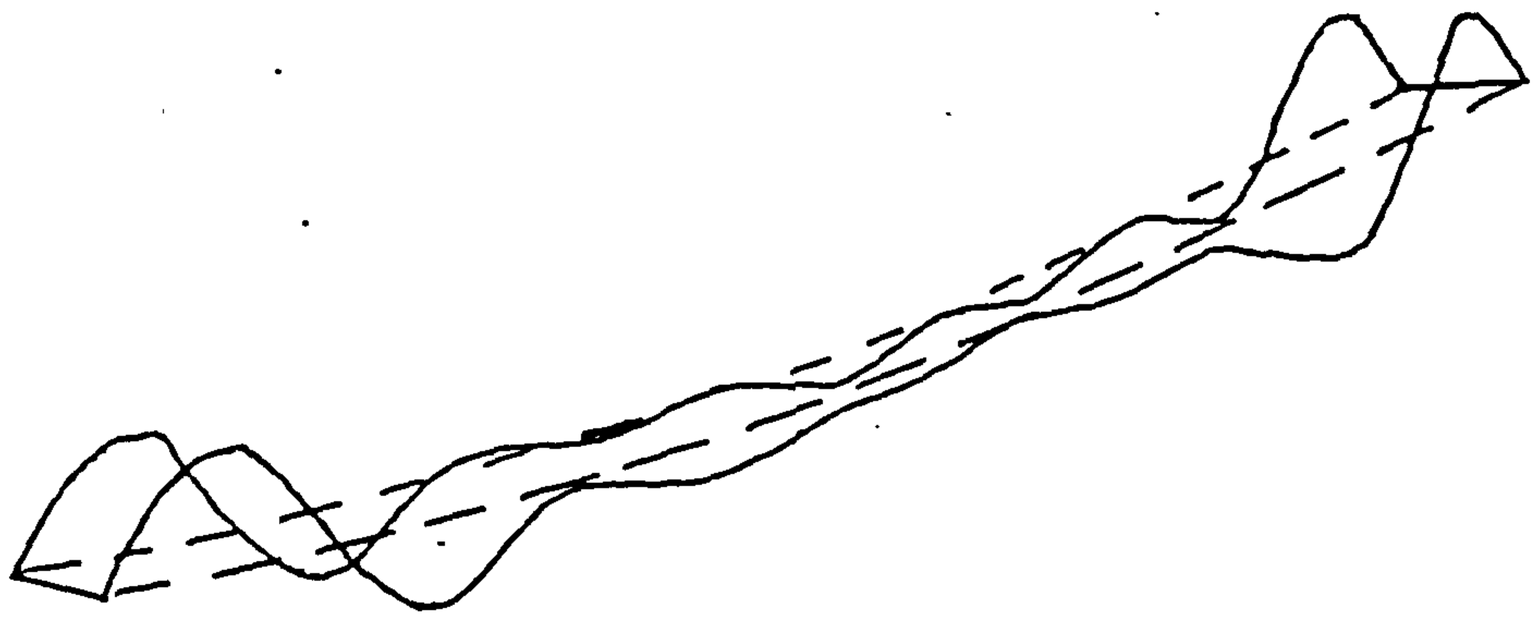

MODE 5 6.86Hz

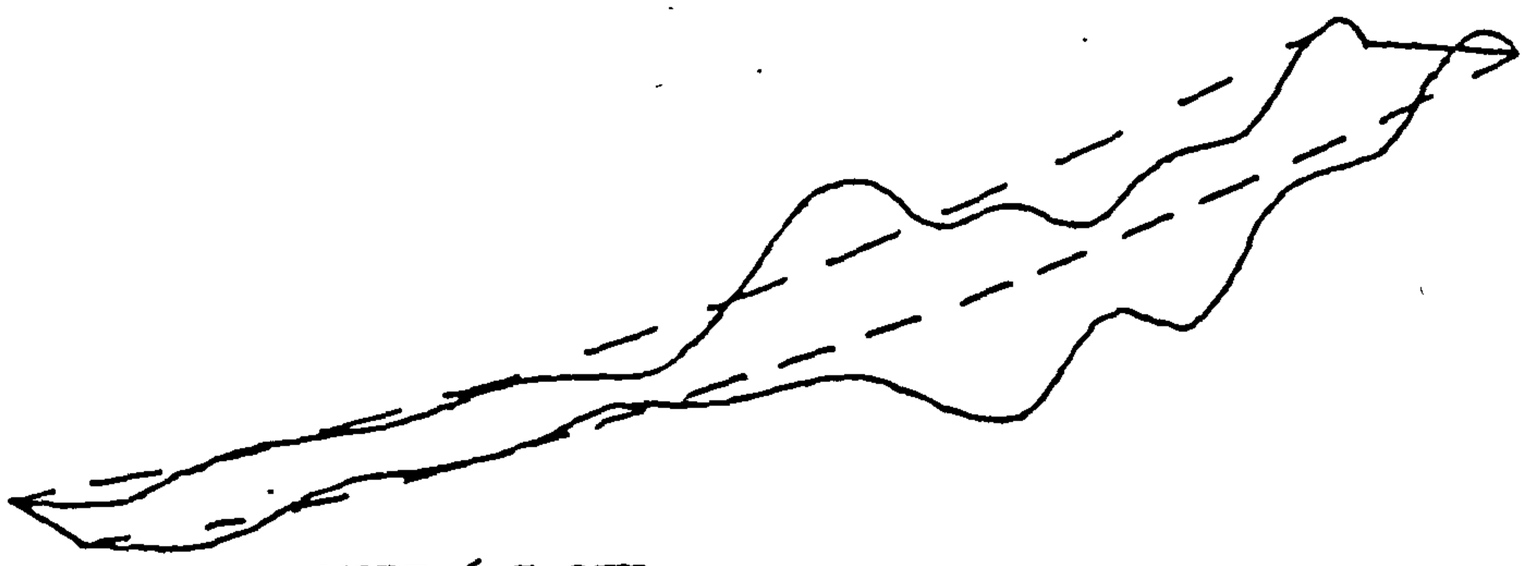

MODE 6 7.27Hz

Figure 2.14(cont) BAILLIESTON INTERCHANGE MSC/NASTRAN MODE SHAPES

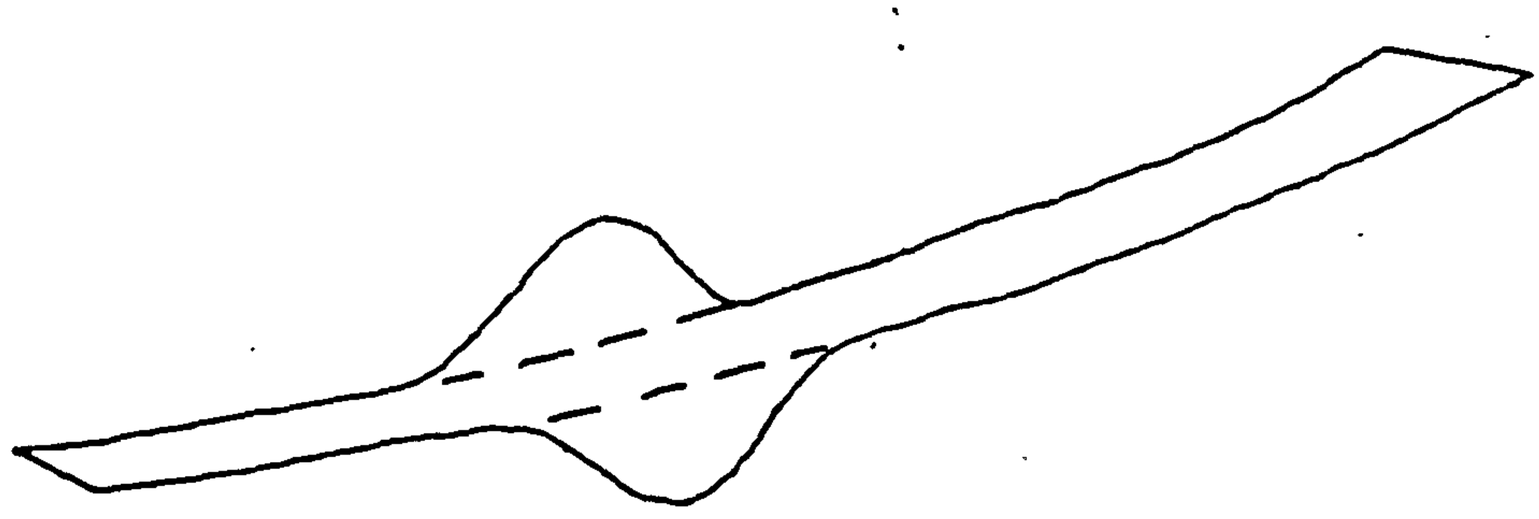

MODE 7 7.99Hz

MODE 8 8.43Hz

Figure 2.14 (cont) BAILLIESTON INTERCHANGE MSC/NASTRAN MODE SHAPES

CONTENTS OF CHAPTER 3

CHAPTER 3 DYNAMIC FINITE ELEMENT THEORY

3.1 Introduction

Since the technique proposed in Chapter 1 involves a large number of dynamic analyses which cover a range of variations in stiffness and mass of some basic structural form, to carry out each analysis from scratch would be prohibitively expensive. In order to make the technique cost effective for bridge monitoring a method of re-analysis must be developed which involves operating on the basic structural matrices. This chapter gives an outline of such a method of dynamic re-analysis.

Since a large proportion of this research work involves the solution of dynamic finite element equations, this chapter shows how these equation of motion of a body can be solved. Before any of the methods are discussed, some important definitions are given.

3.2 Definitions

a) A collection of vectors $\phi_1, \phi_2, \ldots\ldots, \phi_q$ is said to be LINEARLY DEPENDENT if there exist numbers $\alpha_1, \alpha_2, \ldots\ldots \alpha_q$ not all zero such that,

$$\alpha_1 \phi_1 + \alpha_2 \phi_2 + \alpha_3 \phi_3 + \ldots\ldots\ldots\ldots + \alpha_q \phi_q = 0 \qquad (3.1)$$

If the vectors are not linearly dependent they are said to be LINEARLY INDEPENDENT.

As a consequence of the above definition it can be shown that, if the set of q vectors $\phi_1, \phi_2 \ldots\ldots\ldots \phi_q$ are linearly independent, then any subset P of q ($P < q$), are also linearly independent (Ref 22).

b) A set of vectors is said to form a VECTOR SPACE if any linear combination (addition, multiplication) of any two members of the set also results in a member of the set.

c) A BASIS for a vector space is a set of linearly independent vectors that spans the space.

d) A SUBSPACE of a vector space is a vector space such that any vector in the subspace is also in the original space. If ϕ_1, ϕ_2,.....,ϕ_p are the basis vectors of the original space, any subset of these vectors forms the basis of a subspace. The dimension of the subspace is equal to the number of base vectors selected.

e) If a set of q vectors, of which P vectors (P<q) are linearly independent, these vectors are said to SPAN a P-dimensional vector space.

f) A matrix P is an orthogonal matrix if

$$p^T p = pp^T = 1 \qquad (3.2)$$

Hence for an orthogonal matrix we have

$$p^{-1} = p^T$$

g) If there is a matrix A, the EIGENVALUES of A are the scalars λ for which $AX = \lambda X$ possess non zero solutions. The corresponding non zero solution X are the EIGENVECTORS.

h) If all the eigenvalues of a matrix are positive, it is said that the matrix and the operator that the matrix represents are POSITIVE DEFINITE. And if all the eigenvalues are greater than or equal to zero the matrix is POSITIVE SEMIDEFINITE.

3.3 Equation of Motion of a Body

The equation of motion of a multi degree of freedom system can be derived from Newton's Second Law which states: "the rate of change of momentum of any mass is equal to the forces acting on it"

In mathematical form

$$\underline{P}(t) = \frac{d}{dt}\left(M \frac{d\underline{X}}{dt}\right) \tag{3.4}$$

where $\underline{P}(t)$ - applied force vector

$\underline{X}(t)$ - position (displacement) vector of the systems mass (M)

In structural dynamics it may be assumed that the mass does not vary with time. Hence equation (3.4) can be written as:

$$\underline{P}(t) = M \frac{d^2\underline{X}}{dt^2} = M\ddot{\underline{X}}(t) \tag{3.5}$$

The force $\underline{P}(t)$ may be considered to include many types of forces acting on the mass: elastic constraints which oppose displacements, viscous forces which resist velocity etc. By applying d'Alembert's principle to equation (3.5) it can be shown that (Ref 3).

$$M\ddot{X}(t) + C\dot{X}(t) + KX(t) = F(t) \tag{3.6}$$

where K represents the elastic constraints and is known as the system stiffness

C represents the viscous forces and is known as the system damping

If free vibrations are only considered, then the damping and forcing function can be neglected, and hence equation (3.6) can be written as:

$$M\ddot{X} + KX = 0 \tag{3.7}$$

3.4 Solution of the Equation of Free Vibration

If equation (3.7) is premultiplied by M^{-1} then the equation becomes

$$M^{-1} * M\ddot{X} + M^{-1} * KX = 0 \tag{3.8}$$

$$I\ddot{X} + AX = 0 \tag{3.9}$$

where $M^{-1} * M = I$ (a unit matrix)

and $M^{-1} K = A$

Equation (3.9) is the equation of harmonic motion in which

$$\ddot{X} = -\omega^2 X \qquad (3.10)$$

Hence the solution to equation (3.9) is:

$$(A-\omega^2 I) X = 0 \qquad (3.11)$$

which is the characteristic equation of the system and is known as a STANDARD EIGENPROBLEM. The roots of the characteristic equations are called the EIGENVALUES, and the vectors of displacements X are known as the EIGENVECTORS. The solution to equation (3.7) can also be obtained by substituting

$$X = \phi \text{ SIN } (t-t_o) \qquad (3.12)$$

to produce the GENERALIZED EIGENVALUE PROBLEM

$$K\phi = \omega^2 M\phi \qquad (3.13)$$

in which the eigenvalues ω^2_i gives the natural frequencies f_i

$$f_i = \frac{\omega i}{2\pi} \qquad i = 1, 2, \ldots\ldots, n \qquad (3.14a)$$

and the corresponding eigenvectors ϕ_i gives the mode of vibration.

3.5 Methods of Solution of the Generalised Eigenvalue Problem

The equation which is under consideration is equation (3.13) where K and M are the stiffness and mass matrices respectively of an n degree of freedom assemblage. If K and M result from a finite element idealisation both matrices have special properties. These special properties are that, K is symmetric, has a constant lower profile (bandwidth), and is positive semidefinite or positive definite. M has the same properties as K plus it can have the same bandwidth

(consistent mass analysis) as K, or it is a diagonal matrix (lumped mass analysis). The generation of finite element stiffness matrices and mass matrices are given in many finite element texts e.g. reference (3).

If the order of the matrices in equation (3.13) is n then there are n eigenvalues and corresponding eigenvectors satisfying equation (3.13). The i th equation is denoted as (ω^2_i, ϕ_i), where the eigenvalues are ordered according to their magnitudes.

$$0 < \omega^2_1 < \omega^2_2 \ldots\ldots\ldots\ldots < \omega^2_i < \ldots\ldots\ldots \omega^2_n \qquad (3.14b)$$

The aim is to solve equation (3.13) for the q lowest solutions and hence equation (3.13) can be written as:

$$K\underline{\Phi} = M\underline{\Phi}\,\Omega^2 \qquad (3.15)$$

where $\underline{\Phi}$ is an n*q matrix with each column corresponding to the q eigenvectors.

Ω^2 is an q*q diagonal matrix with each diagonal member corresponding to the q eigenvectors.

$$\text{Hence } \underline{\Phi} = [\,\phi_1, \phi_2, \phi_3, \ldots\ldots\ldots\ldots \phi_q] \qquad (3.16)$$

$$\text{and } \Omega^2 = \text{diag}\,(\omega_i^2) \qquad i = 1, 2, \ldots\ldots\ldots q \qquad (3.17)$$

Before trying to solve for the eigensystem it is necessary to give some fundamental properties of the eigensystems, because all the solution methods are, in essence, based on these fundamental properties.

3.6 Fundamental Properties

a) As it was stated in section 3.4 the solution of the generalized eigenproblem $K\phi = \omega^2 M\phi$ yields n eigenpairs (ω^2_i, ϕ_i) and each pair satisfies equation (3.18).

$$K\phi_i = \omega^2_i M\phi_i \qquad i = 1, 2, 3, \ldots\ldots\ldots n \qquad (3.18)$$

b) If in equation (3.18) a vector $\omega_i^2 M\phi_i$ is established and it is used as a load vector F in equation (3.18) then it becomes

$$K\phi_i = F \tag{3.19}$$

This immediately suggests the use of static solution algorithms i.e. decomposition, for the calculation of an eigenvector. Later it will be shown that the "LDL^T" decomposition algorithms are a very important part of eigensolution procedures.

c) It can be shown that an eigenvector is only defined within a multiple of itself, hence equation (3.18) becomes

$$K(\alpha\phi_i) = \omega^2_i M(\alpha\phi_i) \tag{3.20}$$

where α is a nonzero constant. Hence, with ϕ_i being an eigenvector, $\alpha\phi_i$ is also an eigenvector, and it can be said that an eigenvector is only defined by its direction in the n-dimensional space considered.

d) A very important property is the Orthonormality of the eigenvectors, that is:

$$\phi_i^T M\phi_j = \delta_{ij} \tag{3.21}$$

$$\text{and } \phi_i^T K\phi_j = \omega^2\delta_{ij} \tag{3.22}$$

where δ_{ij} is the Kronecker Delta

$$\text{that is } \delta_{ij} = \begin{cases} 0 \text{ if } i \neq j \\ 1 \text{ if } i = j \end{cases}$$

The meaning of the above two equation (3.21) and (3.22) is that the eigenvectors are M- and K- orthogonal. It follows from equation (3.21) and (3.22)

$$\text{that } \underline{\Phi}^T K\underline{\Phi} = \Omega^2 \tag{3.23}$$

and $\Phi^T M \Phi = I$ (3.24)

where the P columns of ϕ are the eigenvectors and Ω^2 is a diagonal matrix containing the eigenvalues. .If the M-orthonormality and K-orthogonality are satisfied, the P vectors need not necessarily be eigenvectors unless P=n. Assume that X stores P vectors P<n then equation 3.23 and 3.24 become

$$X^T KX = D \quad (3.25)$$

and $X^T MX = I$ (3.26)

then the vectors in X and the diagonal elements in D may or may not be eigenvectors and eigenvalues of equation (3.15). If P=n then $X = \phi$ and $D = \omega^2$ because only the eigenvectors span the complete n- dimensional space.

e) An important property of the eigensystem is that the eigenvalues are the roots of the characteristic polynomial:

$$P(\Omega^2) = \det (K-\Omega^2 M) \quad (3.27)$$

and $P(\omega^2_i) = 0$ because $\phi_i \neq 0$

f) Finally another important property of an eigensystem is shifting. If a shift of ρ is performed on K to produce $\hat{K} = K - \rho M$ ($K = \hat{K} + \rho M$) then equation (3.13) becomes

$$(\hat{K} + \rho M)\, \phi = \omega^2 M\phi$$

$$\hat{K}\phi = \omega^2 M\phi - M\phi$$

$$K\phi = (\omega^2 - \rho)\, M\phi \quad (3.28)$$

The solution to equation (3.28) produces the eigenvectors to equation (3.13) but the eigenvalues produced have to be increased by ρ to produce the solution to equation (3.13).

g) If it is assumed that the matrix [K-μM] can be factorized into "LDL^T" form, and all the associated eigenvalues are nonzero and there are no multiple eigenvalues, the number of negative elements in det (K-μM) is equal to the number of eigenvalues smaller than μ. This property is known as the STURM SEQUENCE PROPERTY.

h) Before the solution methods are considered, a very important principle will be discussed. The Rayleigh's quatient $\rho(v)$ of the eigenproblem $Av = \lambda v$ is defined as:

$$\rho(v) = \frac{v^T A v}{v^T v} \qquad (3.29)$$

and $\lambda_1 \leq \rho(v) \leq \lambda_n$

or $\rho(v) \geq \lambda_1$ (3.30)

If v is made any vector, then considering the problem of varying v, $\rho(v)$ will always be greater than or equal to λ_1, and the minimum is reached when $v = v_1$, in which $\rho(v_1) = \lambda_1$. If a restriction is imposed on v, such that it is to be orthogonal to any vector u (ie $v^T u=0$) and u can be varied to produce a number of minimum values of $\rho(v)$, It can be shown that the maximum value of the minimum values equals λ_2 (Ref 9) or more general, equation 3.31.

$$\lambda_r = \max \left[\min \frac{v^T A v}{v^T v} \right] \quad r=1, 2, \ldots\ldots\ldots\ldots n \qquad (3.31)$$

and the principle is called the MINIMAX CHARACTERIZATION OF EIGENVALUES.

3.7 Approximate Solution Methods of the Eigenvalue Problem

The primary interest in Structural Mechanics is the first q lowest eigenpairs of a larger system of order n.

A number of methods will be given which, in practice, because the solution procedure becomes inefficient as the order n increases, are basically only used in "small" eigenvalue problems. Two methods which are used in the solution of "large" eigenvalue problem will also be developed section 3.8. These techniques for the solution of large eigenvalve probems are based on the principles outlined in Section 3.6.

The solution methods for small eigensystems can be divided into four groups.

a) Group One - Vector Iteration Methods. This group uses the basic property of:

$$K\phi_i = \omega^2_i M\phi_i \quad i = 1, 2, \ldots\ldots\ldots\ldots n \qquad (3.18)$$

b) Group Two - Transformation Methods. This group uses the basic property of:

$$\underline{\Phi}^T K \underline{\Phi} = \Omega^2 \qquad (3.23)$$

$$\underline{\Phi}^T M \underline{\Phi} = I \qquad (3.24)$$

c) Group Three - Polynomial Iteration Methods. This Group uses the basic property of:

$$\rho(\Omega^2) = \det (K - \Omega^2 M) \qquad (3.27)$$

and $\rho(\omega^2_i) = 0$

d) Group four - This group employs the Sturm sequence property of the characteristic polynominals

In addition to using the basic properties summarized above, the techniques also use the Rayleigh quatient.

3.7.1 Rayleigh - Ritz Analysis

The eigenproblem that is under consideration is:

$$K\underline{\Phi} = M\underline{\Phi}\Omega^2 \qquad (3.15)$$

It is assumed that K and M are both positive definite which assumes that all the eigenvalues are positive,

i.e. $\omega^2_i > 0 \quad i = 1, 2,.....N$ where N is the rank of the eigenproblem

(K can be assumed positive definite because a shift can always be applied to satisfy this condition. In the case of the mass matrix it has to be assumed that M is a consistent mass matrix or a lumped mass matrix with no zero diagonal terms).

The Rayleigh minimum principle state that:

$$\lambda_1 = \min \rho(\phi) \tag{3.31}$$

where the minimum is taken over all possible vectors ϕ and $\rho(\phi)$. The Rayleigh quotient of the standard eigenvalue problem $Kv = \lambda v$ can be defined for the generalized eigenvalue problem (Ref 3) as:

$$\rho(\phi) = \frac{\phi^T K \phi}{\phi^T M \phi} \tag{3.32}$$

The bounds of Rayleigh quotient are defined as

$$0 < \omega^2_i \leq \rho(\phi) \leq \omega^2_n < \infty \tag{3.33}$$

considering a set of vectors $\bar{\phi}$ which are a linear combination of basis vectors $\psi i \quad i = 1, 2,.....q$ these vectors are known as the Ritz basis vectors. A typical vector is defined as:

$$\bar{\phi} = \sum_{i=1}^{q} X_i \psi_i \tag{3.34}$$

where X_i = Ritz coordinates

ψ_i = Ritz basis vectors

Since $\bar{\phi}$ is a linear combination of the Ritz basis vectors, these vectors lie in the subspace spanned by the Ritz basis vectors which are called V_q. Since the vectors are linearly independent, the

subspace they span has dimension q and also noting the n-dimensional vector space in which the matrices K and M span V_n, hence:

$$V_q \in V_n \tag{3.35}$$

Before the Rayleigh minimum principle on $\bar{\phi}$ can be applied, the Rayleigh quotient must be first evaluated. The Rayleigh quotient on $\bar{\phi}$ is:

$$\rho(\bar{\phi}) = \frac{\bar{\phi}^T \; K\bar{\phi}}{\phi^T \; M\phi} \tag{3.32}$$

The numerator is evaluated as:

$$\bar{\phi}^T \; K\bar{\phi} \;=\; \sum_{i=1}^{q} \; (X_i \; \psi_i)^T \quad K \sum_{j=1}^{q} \; (X_j \; \psi_j) \tag{3.36}$$

$$= \sum_{j=1}^{q} \; \sum_{i=1}^{q} \; (X_i \; \psi_i)^T \; K \; (X_j \; \psi_j) \tag{3.37}$$

$$= \sum_{j=1}^{q} \; \sum_{i=1}^{q} \; X_i \; X_j \; \psi_i^T \quad K \; \psi_j \tag{3.38}$$

since X_i, and X_j are not vectors.

The denominator gives a similar result and hence the quotient becomes:

$$\rho(\bar{\phi}) \quad \frac{\displaystyle\sum_{j=1}^{q} \; \sum_{i=1}^{q} \; X_i \; X_j \; \psi_i^T \quad K \; \psi_j}{\displaystyle\sum_{j=1}^{q} \; \sum_{i=1}^{q} \; X_i \; X_j \; \psi_i^T \quad M \; \psi_j} \tag{3.39}$$

The condition for a minimum value of a function is determined by equating its derivative to zero i.e.:

$$\text{Min } \rho(\bar{\Phi}) \qquad \frac{\delta}{\delta X_i}\rho(\bar{\Phi}) = 0 \quad i = 1, 2, \ldots\ldots\ldots \tag{3.40}$$

Hence we require

$$\frac{\delta}{\delta X_i}\left[\frac{\sum_{j=1}^{q}\sum_{i=1}^{q} X_i\, X_j\, \psi_i^T\, K\, \psi_j}{\sum_{j=1}^{q}\sum_{i=1}^{q} X_i\, X_j\, \psi_i^T\, M\, \psi_j}\right] = 0 \tag{3.41}$$

or

$$\frac{\delta}{\delta X_i}\frac{\left[\sum_{j=1}^{q}\sum_{i=1}^{q} X_i\, X_j\right]\left[\bar{K}_{ij}\right]}{\left[\sum_{j=1}^{q}\sum_{i=1}^{q} X_i\, X_j\right]\left[\bar{M}_{ij}\right]} = 0$$

where $K_{ij} = \psi^T_i\, K\, \psi_j$ $\qquad \bar{K} = X_i X_j \bar{K}_{ij}$ (3.42)

and

$$\bar{M}_{ij} = \psi^T_i\, M\, \psi_j \qquad \bar{M} = X_i X_j \bar{M}_{ij}$$

that is $\dfrac{\delta}{\delta X_i}\left[\dfrac{\bar{K}}{\bar{M}}\right] = 0$ is required

that is $$\frac{\delta}{\delta X_i}\left[\frac{\bar{K}}{\bar{M}}\right] = \frac{\delta \bar{K}\quad \bar{M} \;-\; \delta \bar{M}\quad \bar{K}}{\bar{M}^2} \tag{3.43}$$

therefore $\dfrac{\delta \rho(\bar{\Phi})}{\delta X_i} = 0$ gives

$$2\bar{M} \sum_{j=1}^{q} X_j \bar{K}_{ij} - 2\bar{K} \sum_{j=1}^{q} X_j \bar{M}_{ij} = 0 \qquad (3.44)$$

$$\sum_{j=1}^{q} \left[X_j \bar{K}_{ij} - \frac{\bar{K}}{\bar{M}} X_j \bar{M}_{ij} \right] = 0 \qquad (3.45)$$

$$\sum_{j=1}^{q} \left[\bar{K}_{ij} - \frac{\bar{K}}{\bar{M}} \bar{M}_{ij} X_j \right] = 0 \qquad (3.46)$$

If $\rho = \frac{\bar{K}}{\bar{M}}$

Hence

$$\sum_{j=1}^{q} \left[\bar{K}_{ij} - \rho \bar{M}_{ij} X_j \right] = 0 \qquad (3.47)$$

In actual analysis the q equations in (3.47) are in matrix form, this obtaining the eigenproblem

$$\bar{K} X = \rho \bar{M} X \qquad (3.48)$$

Where $\bar{K}$ and $\bar{M}$ are q * q matrices with typical elements defined in (3.42) and X is a vector of the Ritz coordinates. The solution (3.48) yeilds, q eigenvalues $\rho_1, \rho_2 \ldots\ldots\ldots \rho_q$ which are an approximation to $\omega^2_1, \omega^2_2, \ldots\ldots\ldots\ldots \omega^2_q$, and the vector X_i which is are an approximation to the eigenvector ϕ_i.

It should be noted that this eigenvalue approximation analysis produces an upper bound approximation to the problem considered because of equation (3.30) i.e.:

$$\omega^2_1 \leq \rho_1 : \omega_2^2 \leq \rho_2 : \ldots\ldots\ldots\ldots \omega_q^2 \leq \rho_q \leq \omega^2_n \qquad (3.49)$$

The errors of the method depend .on the selection of Ritz basis vectors. Good results can be obtained if the basis vectors span the subspace V_q, in other words are "close to the least dominant subspace of K and M spanned by $\underline{\bar{\Phi}}$ (Ref 4). However, this does not mean that the basis vectors should be close to the eigenvalues sought, but that linear combination of the basis vectors will give good approximations to the required eigenvectors.

To summarize the Rayleigh Ritz Method the procedure to calculate the eigenproblem $K\underline{\bar{\Phi}} = M\underline{\bar{\Phi}}\Omega^2$ is now presented as:-

a) First it is assumed that a load vector F which if possible, excites the eigenvalues required and from this load vector by considering a static solution the Ritz basic functions ψ can be calculated i.e.

$$K\psi = F \tag{3.50}$$

where ψ is a matrix storing the Ritz basis functions.

b) The reduced stiffness and mass matrices, are calculated that is:

$$\bar{K} = \psi^T K \psi \tag{3.51}$$

$$\bar{M} = \psi^T M \psi \tag{3.54}$$

c) The new eigenproblem for the eigenvalues is solved thus:

$$\bar{K}\, x = \rho \bar{M}\, x \tag{3.53}$$

d) The approximation to the eigenvectors of the problem $K\underline{\bar{\Phi}} = M\underline{\bar{\Phi}}\Omega^2$ are calculated as:

$$\bar{\Phi} = \psi X \tag{3.54}$$

From the Rayleigh - Ritz Method above it is implied that an iterative process could be used. For example if the following step is added, the procedure then would become an iterative process.

This step would be:

e) From the approximation to the eigenpairs (ρ_i $\bar{\phi}_i$), calculate a new load vector F_k for increment k;k = 1, 2,.....as:

$$F_k = \rho M\phi \tag{3.55}$$

and proceded to step (b) until convergence is reached.

Hence $\rho \longrightarrow \omega^2_i$, $\bar{\phi}_i \longrightarrow \phi_i$ as $k \longrightarrow \infty$ (3.56)

3.7.2 Vector Iteration Method

The technique of vector iteration is used to calculate an eigenvector, and at the same time the corresponding eigenvalues can be calculated.

The aim is to solve equation (3.15) by operating on it

$$K\phi = M\phi^{\,2} \tag{3.15}$$

If vector X_1 is assumed as an approximation to vector ϕ_1 and a value for ω^2_1 is assumed as $\omega_1{}^2 = 1$. Hence evaluating the right hand side of equation (3.13).

$$F_1 = 1 * MX_1 \tag{3.57}$$

and in general

$$KX_1 \neq F_1 \tag{3.58}$$

Hence introducing a new vector X_2 such that

$$KX_2 = F_1 \tag{3.59}$$

Where X_2 is the displacement solution corresponding to the applied force F_1. In this iterative solution of (3.13) it may be considered that X_2 is a better approximation to the eigenvector ϕ_1. The above technique may be refined into a more effective process by using "weighting". This technique is known as Inverse Iteration Method.

3.7.3 Inverse-Iteration Method

In this method an intermediate step is introduced between assuming X_2 is a better approximation to an eigenvector than X_1. That is X_2 is mass weighted as follows:

$$X_2 \text{ (weighted)} = \frac{X_2}{(X_2^T \; MX_2)} \tag{3.60}$$

Because of the mass orthonormality $X_2^T \, MX_2 \longrightarrow 1$ as $X_2 \rightarrow \phi$.

Also a Rayleigh quotient is introduced to calculate the corresponding eigenvalues.

To summarize the inverse iteration procedure to calculate the eigenproblem $K\phi = M\phi\Omega^2$ is presented as:

a) First a starting iteration vector X_1 is assumed, and hence Y_1 is calculated that is

$$Y_1 = MX_1 \tag{3.61}$$

or

$$Y_k = MX_k$$

b) Calculate $K\bar{X}_{k+1} = Y_k$ (3.63)

c) Calculate Rayleigh quotient $\rho(\bar{X}_{K+1})$

$$\rho(X_{k+1}) = \frac{\bar{X}_{k+1} \quad K\,\bar{X}_{k+1}}{\bar{X}_{k+1} \quad M\,\bar{X}_{k+1}} \tag{3.64}$$

d) Applying the mass weighting

$$Y_{k+1} = \frac{\bar{X}_{k+1}}{(X^T_{k+1} \; M\,\bar{X}_{k+1})^{1/2}} \tag{3.65}$$

e) Return to (b) until convergence is reached that is:

$$Y_{k+1} \rightarrow M\phi_1 \quad \text{and} \quad \rho(X_{k+1}) \rightarrow \omega_1^2 \quad \text{as } k \rightarrow \infty \tag{3.66}$$

By assuming different starting vectors X or by applying a shift it is possible to calculate other eigenpairs.

3.7.4 Transformation Method

This method employs the basic properties of the orthonormality of the eigensystem that is:

$$\phi^T M \phi = I$$

$$\phi^T K \phi = \Omega^2$$

The basic scheme is to reduce K and M into diagonal form using successive pre- and postmultiplication by matrixes P^T_k and P_k respectively where k = 1, 2, ..., that is

$$M_{k+1} = P^T_k M_k P_k \tag{3.69}$$

$$\text{and} \quad K_{k+1} = P^T_k K_k P_k$$

and where the matrices P_k, k = 1, 2,..... are selected to bring K and M closer to diagonal form hence producing.

$$K_{k+1} \rightarrow \Omega^2 \quad \text{and} \quad M_{k+1} \rightarrow I \text{ as } k \rightarrow \infty$$

In practice it is not necessary that K_{k+1} and M_{k+1} converge to Ω^2 and I respectively but only that they should converge to diagonal form and

$$\Omega^2 = \text{diag} \quad \frac{K_{k+1}}{M_{k+1}} \tag{3.70}$$

and

$$\underline{\bar{\Phi}} = P_1 P_2 \ldots\ldots\ldots P_k \text{ diag } \left(\frac{1}{\sqrt{M_{k+1}}} \right) \qquad (3.71)$$

practical applications of this method are the Jacobi Method and Householder - QR Method. Only the Jacobi methods will be discussed.

3.7.4.1 Jacobi Method

This method was developed for the solution of the case where M is the identity matrix. It is initially developed in this form but later the generalized eigenvalue problem will be discussed. The major advantage of this method is that it is simple and very stable, since the eigenvalues properties in equations 3.23 and 3.24 are applicable to all symmetric matrices K and M with no restriction on the eigenvalues. The Jacobi method can be used to calculate negative, zero or positive eigenvalues.

Consider the Problem

$$K\phi = \omega^2 \phi \qquad (3.72)$$

In which equation (3.69) reduces to for the k^{th} iteration step.

$$K_{k+1} = P^T_k \; K_k \; P \qquad (3.73)$$

and

$$I = P^T_k \; P_k$$

In this method the matrix P_k is a rotation matrix which is selected in such a way that an off-diagonal element K_k is zero. For example, if, element (i,j) is required to be reduced to zero then the P_k matrix is:

$$P_k = \begin{array}{c} \\ \\ \\ \\ \\ \\ \\ \\ \\ \\ \\ \end{array} \begin{array}{c} \begin{matrix} \overset{t^{th}\ \text{Column}}{} & & & & & & \overset{j^{th}\ \text{Column}}{} \end{matrix} \\ \begin{bmatrix} 1 & & & & & & \\ & \ddots & & & & & \\ & & 1 & & & & \\ & & & \cos\theta & & -\sin\theta & \\ & & & & 1 & & \\ & & & & & \ddots & \\ & & & \sin\theta & & \cos\theta & \\ & & & & & & 1 \\ & & & & & & & \ddots \\ & & & & & & & & 1 \end{bmatrix} \end{array} \begin{array}{l} \\ \\ \\ \\ \\ \\ \\ \\ \\ \\ \\ \end{array} \begin{array}{l} \\ \\ \\ \\ i^{th}\ \text{Row} \\ \\ \\ \\ \\ j^{th}\ \text{Row} \\ \\ \\ \end{array} \qquad (3.75)$$

where θ is found by multiplying ${}_kP_k^T\,K\,{}_kP_k^T$ out and equating the term required of the result to zero, hence θ is taken as

$$\theta \text{ is } \begin{cases} \tan 2\theta = \dfrac{2K_{ij}}{K_{ii} - K_{jj}} & K_{ii} = K_{jj} \\ \theta = \dfrac{\pi}{4} & K_{ii} = K_{jj} \end{cases} \qquad (3.77)$$

An important point to remember is that the above transformation will reduce element (i,j) to zero but this element will again become nonzero during the transformation which follows. So the choice of which elements to reduce is important. The most efficient way is to select the largest off-diagonal term for reduction until the diagonal form is reached.

3.7.5 The Generalized Jacobi Diagonalization Method

In order to solve the generalized eigenvalue problem it could be reduced to standard form. However an alternative approach is to use the generalized Jacobi Method where the matrices K and M can be operated on simultaneously. In this method the P_k matrix has the following form:

$$P_k = \begin{bmatrix} 1 & & & & & & & \\ & \ddots & & & & & & \\ & & 1 & & \alpha & & & \\ & & & \ddots & & & & \\ & & \gamma & & 1 & & & \\ & & & & & \ddots & & \\ & & & & & & 1 & \end{bmatrix} \begin{matrix} \\ \\ \text{ith Row} \\ \\ \text{jth Row} \\ \\ \\ \end{matrix} \qquad (3.78)$$

ith Column jth Column

where the constants α and γ are selected to reduce to zero the (i,j) term in K_k and M_k simultaneously, α and γ are found in a similar way to θ in the Jacobi Method.

Hence:

$$\alpha = \frac{\bar{K}_{jj}}{X} \qquad (3.79)$$

$$\gamma = \frac{\bar{K}_{ii}}{X} \qquad (3.80)$$

$$\text{where} \quad X = \frac{\bar{K}}{2} + \text{sign}(\bar{K}) \sqrt{\left(\frac{\bar{K}}{2}\right)^2 + \bar{K}_{ii} * \bar{K}_{jj}} \qquad (3.81)$$

$$\text{and} \quad \bar{K}_{ii} = K_{ii}\,M_{ij} - M_{ii}\,K_{ij}$$
$$\bar{K}_{jj} = K_{jj}\,M_{ij} - M_{jj}\,K_{ij} \qquad (3.82)$$
$$\bar{K} = K_{ii}\,M_{jj} - M_{jj}\,M_{ii}$$

Equation (3.78) to (3.82) represent one increment k, of matrices K_k and M_k.

To summarize the gneralized Jacobi method the procedure to calculate the eigenproblem $K\phi = \omega^2 M\phi$ is presented as follows:

a) The elements in the stiffness and mass matrices to be zeroed are chosen.

b) The constants α and γ of equation (3.78) are calculated.

c) The pre-and postmultiplication to K_k and M_k are preformed.

d) (a) is returned to until all the off-diagonal elements are zeroed or have reached the correct tolerance.

e) The eigenvalues and eigenvectors are calculated

$$\text{Eigenvalues} \quad \omega^2 = \text{diag} \left(\frac{K_{k+1}}{M_{k+1}} \right) \qquad (3.83)$$

$$\text{Eigenvectors} \quad \phi = P_1\,P_2 \ldots\ldots P_k \,\text{diag} \left(\frac{1}{\sqrt{M_{k11}}} \right) \qquad (3.84)$$

It should be noted that the Jacobi Diagonalization method solves simultaneously for eigenvalues and corresponding eigenvectors.

3.7.6 Polynormial Iteration Techniques

These methods use the eigensystem property of the characteristic polynomial $\rho(\omega^2)$, where

$$\rho(\omega^2) = \det\ (K - \omega^2 M) \qquad (3.85)$$

and the zeros of $\rho(\omega^2)$ are the eigenvalues of the eigenproblem $K\phi = \omega^2 M\phi$. Hence to find the eigenvalues the roots of the polynomial $\rho(\omega^2)$ need to be extracted. There are two main ways of calculating the root of equation (3.85). These methods are explicit and implicit polynormal iteration.

3.7.6.1 Explicit Polynomial Iteration

In explicit polynomial iteration the solution to equation (3.86) is required.

$$\rho(\omega^2) = a_0 + a_1\ \omega^2{}_1 + a_2\omega^2{}_2 + \ .....a_n\ \omega^2{}_n \qquad (3.86)$$

This is carried out by first evaluating the polynomial coefficients $a_0, a_1, ...a_i, ...a_n$, and then calculating the roots of the polynomial.

This method is almost completely abondoned for the solution of equation (3.15). This is because the solution is very heavily dependent on calculating the polynomial coefficients a_i, and small errors in a_i will cause a large error in the roots of the polynomial. But small errors are almost unavoidable, owing to computer rounding errors.

3.7.6.2 Implicit Polynomial Iteration

In implicit polynomial iteration the values of $\rho(\omega^2)$ are evaluated directly without calculating the coefficients a_i. The values of $\rho(\omega^2)$ can be obtained effectively by the decomposition of $(K-\omega^2M)$ into lower (L) and upper (S) triangular matrices, hence:

$$K-\omega^2M = LS \qquad (3.87)$$

$$\text{and} \quad \det\ (K-\omega^2M) = S_{11} * S_{22} * .....S_{nn} = \prod_{i=1}^{n} S_{ii} \qquad (3.88)$$

In the Gauss elimination procedure, if no column interchanges are carried out, $(K-\omega^2M)$ will be symmetric and hence equation (3.88) can be re-written as:

$$\det(K-\omega 2M) = \det\ ("LDL^T") = \prod_{i=1}^{n} d_{ii} \qquad (3.89)$$

Since an accurate solution to $\rho(\omega^2)$ is available, a number of iteration schemes can be used to calculate the roots of the polynomial (Ref 3).

Finally, polynomial iteration methods, only calculate the eigenvalues and the corresponding vectors have to be found by another method, say by inverse iteration, with the application of shifting.

3.7.7 Methods Based on the Sturm Sequence Properties

The Sturn sequence property is that if a shift of μ is applied to equation (3.15) and after decomparing $(K-\mu M)$ into LDL^T, the number of negative elements in D is equal to the number of eigenvalues smaller than μ.

3.7.7.1 Bisection Method

In the Bisection method, a Sturm sequence is applied to find out how many eigenvalues are below a certain value. Simple schemes of bisection are applied to identify the intervals within which the individual eigenvalues lie. In this process, those intervals in which more than one eigenvalue is found to lie as processive bisection are applied, then a Strum sequence is carried out to check to see if all the eigenvalues are isolated.

The above technique is straightforward, but the method is very inefficient, because each bisection requires LDL^T factorization and this may be very time consuming because convergence can be very slow when a cluster of eigenvalues has to be solved.

However the Sturm sequence property can be employed in conjunction with other solution methods to make sure that no eigenvalues have been omitted.

3.8 Solution of Large Eigenvalue Problems

The previous methods given so far as said, are for the solution of "small" eigenvalue problems, i.e. stiffness and mass matrices with small rank. If used on matrices with large rank the methods become very inefficient and time consuming and great care has to be taken. The methods are not recommended for general use since in engineering problems the P smallest eigenvalues are only required. Both methods in the following discussion have been developed for the solution of the P smallest eigenvalues and corresponding eigenvectors.

The methods presented so far are based mainly on one fundamental property. The two methods to be discussed are based on a number of fundamental properties. These methods are;

The DETERMINANT SEARCH Method which uses the properties of:

i) Characteristic Polynomial

ii) Shifting

iii) Eigenpairs satisfying the generalized eigenproblem

The SUBSPACE ITERATION Method which uses the properties of:

i) Rayleigh minimum principle

ii) Orthonormality of the eigenvectors

iii) Shifting

3.8.1 The Determinant Search Method

This method as the name suggests is very heavily dependent on the polynomial iteration method. The first operation to be carried out is to find an approximation to ω^2_i i=1,2,....n by applying a shift to the eigenproblem. This is carried out by using an accelerated bisection method, known as Secant iteration (Ref 3). In the Secant method two lower bounds to ω^2_i are required. The initial two values

required for ω^2_1 (μ_1, μ_2) are taken as $\mu_1 = 0.0$ and the other is obtained from an approximation to ϕ_1 calculated by inverse vectors iteration with ω^2_1 equal to zero, hence

$$\mu_2 = (1-0.01)\ \frac{X^T_k\ K\ X_k}{X^T_k\ M\ X_k}\ . \tag{3.90}$$

where X_k is the iteration vector after (k-1) iteration. If μ_2 is larger than ω^2_1, this is detected by the Sturn sequence count in the factorization of $(K-\mu_2 M)$. By leting γ be the number of negative pivots in the triangular factorization, μ_2 is divided by $(\gamma+1)$ until γ equal zero.

A shift is continuously applied until it has been established that the bisection method has jumped over one or more eigenvalues. It does not matter if one root, or a cluster of roots have been jumped over because a Sturm sequence is applied to detect the number of changes, if any, in the signs of the diagonal elements of the triangular factorization of the shifted eigenvalue problems.

Vector inverse iteration is applied with vector deflation (Vector orthogonalization). The basis of vector deflation is that in order for an interation vector to converage to the required eigenvector using vector interaction, the iteration vector must not be orthogomal to it. Or conversely if the iteration vector is orthogonalized to the eigenvectors already calculated, the possibility that the iteration converges to any one of them is eliminated, and guarantees that, it converges instead to another eigenvector. At the same time as the inverse vector iteration is applied to calculate the eigenvector, the application of Rayleigh quotient is applied to calculate the corresponding eigenvalue.

To summarize the Determinant Search Method the procedure to calculate the eigenproblem $K\underline{\Phi} = M\underline{\Phi}\Lambda^2$ is presented now for the P lowest eigenpairs:

a) The first two lower bounds on ω^2_1 (μ_1, μ_2) to start the secant iteration are calculated.

b) With the two lowest bounds to ω^2_i a secant iteration is carried out to find a better approximation to ω^2_i

c) A shift of μ on the eigenproblem under consideration is carried out.

d) A sturm sequence to the eigenproblem $(K-\mu_k M)$ is applied to see if there has been any change in the number of negative diagonal terms in the LDL^T formulation. If no change has occurred, step (b) is returned to until changes have occurred.

e) Since the above value of shift is an approximation to ω^2_i, using this value, as an eigenvalue, the corresponding eigenvector, is calculated. This in turn, can be used as the starting vector X_1 in the inverse vector iteration procedure, with 1 = 1,2,..... until convergence is reached.

i) calculate: $Y_1 = MX_1$ (3.91)

ii) then $\bar{K}\bar{X}_{1+1} = (K-\mu_k M)\ \bar{X}_{1+1} = Y_1$ (3.92)

iii) calculate Rayleight quatient $\rho(\bar{X}_{1+1})$

$$\rho(\bar{X}_{1+1}) = \frac{\bar{X}^T_{1+1}\ \bar{K}\ \bar{X}_{1+1}}{\bar{X}_{1+1}\ M\ \bar{X}_{1+1}} \qquad (3.93)$$

iv) During the mass weighting vector deflation is applied to vector $\bar{X}_{1+1}$

This is carried out as follows:

a vector x_{1+1} which is M- orthogonal to the eigenvectors ϕ_m m=1, 2,.....(i-1) is calculated and is carried out as follows:

$$\tilde{X}_{1+1} = \bar{X}_{1+1} - \sum_{m=1}^{i-1} \alpha_m\ \phi_m \qquad (3.94)$$

where the coefficients α_m are obtained by using the condition of M- orthogonal. i.e.

$$\phi^T_m \; M \; \tilde{X}_{l+1} = 0$$

and (3.95)

$$\phi_i{}^T \; M \; \phi_j = \delta_{ij}$$

Hence giving

$$\alpha_m = \phi^T_m \; M \; \bar{X}_{l+1} \quad m = 1,2,.....(i-1) \tag{3.96}$$

v) (i) is returned to until convergence is reached, that is

$$X_l \rightarrow \phi_i \text{ and } (X_{l+1}) \longrightarrow \omega^2_i \text{ as } l \longrightarrow \infty \tag{3.97}$$

f) If the Sturm sequence in (d) shows there was more than one eigenvalue the shift "jumped", then step (e) is returned to until all the jumped eigenvalues have been calculated, but increasing i each time by one.

g) Finally (b) is returned to until all the eigenvalues which are required are calculated.

The major advantage of this solution procedure is that each eigenpair is obtained independently from the previously calculated pairs. Hence the eigenvalues and eigenvectors, need not be calculated to very high precision. This solution procedure is most effective as an in-core solver, but it may place considerable limitations on the problem size.

3.8.2 The Subspace Iteration Method

The aim is to solve the eigenproblem $K\bar{\phi} = M\bar{\phi}\,\Omega^2$ for the P- lowest eigenvalues. In this method of subspace iteration the main operation is a repeated application of the Rayleigh - Ritz method. Hence the subspace iteration method uses the fact that the eigenvectors form an

M-orthonormal basis of P- dimensional, i.e. least dominant subspace of the matrices K, and M, and is denoted by E_∞.

The essential idea of subspace iteration is to iterate simultaneously with P linearly independent vectors which initially span the starting subspace E until they span E_∞ to the required accuracy (Hence the name of the method). It follows that convergence is not dependent on individual iteration vectors to the eigenvectors but on the subspace E_k.

It was observed that during the subspace iteration, i.e. as $E_k \rightarrow E_{k+1}$ k = 1, 2, ..., the reduced matrices, K_{k+1} and M_{k+1} (Section 3.7.1) tend towards diagonal form. Hence the generalized Jacobi method is used to solve, very effectively, the new eigenproblem of the reduced matrices, given in equation (3.53).

$$\bar{K}X = \rho \bar{M}X \tag{3.53}$$

Since the eigenvalues of the reduced problem are equal to the eigenvalues for the original problem $K\bar{\Phi} = M\bar{\Phi}\Omega^2$ and X are the Ritz coordinates, and these can be used to calculate the eigenvectors of the problem given in equation (3.53). These approximate to the eigenpairs are used to update the iteration vectors.

Bathe found, that if P eigenpairs are required q eigenpairs (q>P) must be calculated. This causes the convergence rate to increase, but using more iteration vectors will increase the computer effort for an individual iteration (Ref 4, 5, 6). In practice he found that

$$q = \min (2P, P+8) \tag{3.98}$$

gives the best compromise between convergence and computer effort.

Since convergence is not dependant on the iteration vectors but on the subspace E_1, so the method's effectiveness lies in finding P linearly independent vectors which initially span the starting subspace E_1, and which are as close to E as possible. Also the starting iteration vectors should excite the q lowest eigenvalues. In other words this should include all the degrees of freedom, up to q, with which are associated a large mass and a small stiffness. The starting iteration vectors take the form given in equation (3.99)

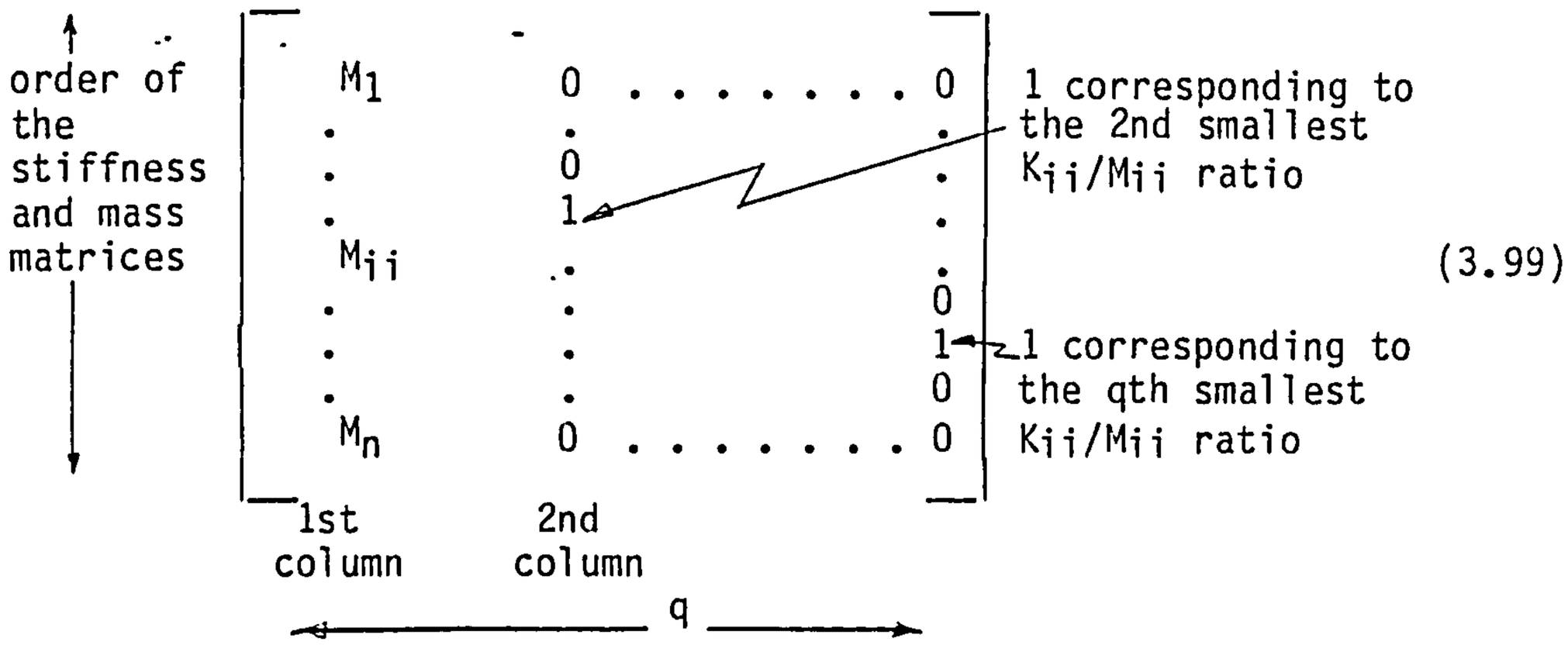

(3.99)

To summarize the Subspace Iteration procedure to calculate the eigenproblem $K\Phi = M\Phi\omega^2$ will be presented now for the P lowest eigenpairs is as follows

a) From p the rank q of the subspace of the operators K and M are calculated using equation (3.98) i.e.:

$$q = \min.(2P,\ P+8) \tag{3.98}$$

b) The first q degrees of freedom which have a large mass with corresponding small stiffness are identified.

c) The starting iteration vectors (X) which will excite the q lowest eigenvalues, by using equation (3.99) are calculated.

d) The load vector F, is calculated, as:

$$F = MX \tag{3.100}$$

so the Ritz basis functions ,($\bar{X}$), can be calculated as

$$K\bar{X} = F \quad \text{i.e. } \bar{X} = K^{-1}\ F \tag{3.101}$$

e) Now the reduced, or projected, stiffness and mass matrices on the subspace E_{k+1} are calculated,

$$Y = K\bar{X} \quad \text{ie } \bar{X} = K^{-}Y \tag{3.102}$$

$$\bar{K} = \bar{X}\ \ Y \tag{3.103}$$

$$\bar{Y} = M\,\bar{X} \tag{3.104}$$

$$\bar{M} = \bar{X}\;\; Y \tag{3.105}$$

f) The new eigenproblem is solved

$$\bar{K}Q = \bar{M}Q\;\;\bar{\Omega}^2 \tag{3.106}$$

using the generalized Jacobi Diagonalization method.
Where Q are the Ritz coordinates, and $\bar{\Omega}^2$ are the eigenvalues of $K\phi = M\phi\Omega^2$ (Section 3.7.5).

g) From the Ritz coordinates, the improved eigenvector are calculated as

$$X = \bar{X}Q \tag{3.107}$$

h) Step (d) is returned to with X as the iteration vectors, and the process is repeated from $E_k \rightarrow E_{k+1}$, k = 1, 2,..... until E_{k+1} spans E_∞ to the required accuracy. Before iteration, is carried out a check is applied to see if the eigenvalues are in ascending order, since the convergence is increased by reordering them in ascending order.

i) After the q lowest eigenpairs have been calculated to the required accuracy, a Sturm sequence is applied to the eigenproblem $K\phi = M\phi\Omega^2$ with a shift of μ, where μ is just greater than ω^2_q to check that the number of negative elements in D, of the LDL^T factorization of $(K - \mu M)$, is equal to the number of eigenpairs calculated. This verifies that none of the eigenpairs have been omitted.

3.9 Dynamic Re-analysis

If the method of dynamic monitoring of bridge structures is going to be cost effective, a method of dynamic re-analysis must be developed. The reason for such a method is that during the monitoring process a data bank of natural frequencies associated with a number of structural changes is required. At present to produce such a data bank is very

expensive since for each structural change a complete new dynamic model must be constructed.

Three proposed methods of re-analysis are given. These methods are based on the use of Subspace Iteration, and the rate of change of equation (3.15) with respect to any disturbance i.e. with respect to any change in stiffness or mass.

3.9.1 Differentiation of $K\phi = \omega^2 M\phi$ with Respect to any Disturbance

Rewriting equation (3.15) for the ith solution

$$K\phi_i - \omega^2_i M\phi_i = 0 \tag{3.108}$$

$$(K - \omega^2_i M)\,\phi_i = 0 \tag{3.109}$$

If let $F_i = (K - \omega_i^2 M)$ (3.110)

It follows that

$$F\phi_i = 0 \tag{3.111}$$

Premultiplication of equation (3.111) by ϕ^T_i gives

$$\phi^T_i F_i \phi_i = 0 \tag{3.112}$$

Differentiation of equation (3.112) with respect to any disturbances δ_j, yields:

$$\phi^T_{i,j} F_i \phi_i + \phi^T_i F_{i,j} \phi_i + \phi^T_i F_i \phi_{i,j} = 0 \tag{3.113}$$

The first and third terms of equation (3.113) are zero, owing to the symmetry of F_i and because of equation (3.111) hence:

$$\phi^T_i F_{i,j} \phi_i = 0 \tag{3.114}$$

If equation (3.110) is differentiated with respect to any disturbance δ_j,

$$F_{i,j} = K_{,j} - \omega^2_i M_{,j} - \omega^2_{i,j} M \tag{3.115}$$

(Note ω^2_i denotes the ith eigenvalue, hence if it is differentiated with respect to $_j$ it gives $\omega^2_{i,j}$ NOT $2\omega_{i,j}$)

By combining equation (3.114) and (3.115) and using the M-orthonormality of eigenvectors give

$$\omega^2_{i,j} = \phi^T_i \quad [\, K,_j - \omega^2_i \, M,_j \,] \, \phi_i \qquad (3.116)$$

3.9.2 Methods of Re-analysis

The three methods which are presented here can be placed in two categories

i Full matrices: the complete stiffness and mass matrices are worked on

ii Changed Matrices: the stiffness and mass matrices have entries associated only with the structural change.

Both categories are two stage processes. The first stage of the methods is to carry out a complete dynamic analysis of the structure under consideration using Subspace Iteration. The working matrices from this first analysis are saved, to be operated on later by the second stage analysis associated with changes in the original structure. The second stage of the analysis, can if required be repeated as many times as required.

3.9.2.1 Category One : Full Matrices

In this category the stiffness and mass matrices are formulated in the same way as a complete original analysis, that is, the data input to any program is the same as the original analysis, but the data are adjusted to taken into consideration the structural changes. Hence the stiffness and mass matrices are formulated in such a way that

$$K_{new} = K \text{ original} + K_{change} \qquad (3.117)$$

$$M_{new} = M \text{ original} + M_{change} \qquad (3.118)$$

After the formulation of the new matrices, the procedure in as follows: -

a) the stiffness matrix is reduced

$$K_{new}\ \bar{X}_{new} = Y \qquad \text{i.e. } \bar{X}_{new} = K^{-1}_{new}\ Y \tag{3.119}$$

where Y are iteration vectors from the original analysis
Hence

$$\bar{K}_{new} = \bar{X}_{new}\ Y \tag{3.120}$$

b) The mass matrix is reduced by first calculating $\bar{Y}_{new}$

$$\bar{Y}_{new} = M_{new}\ \bar{X}_{new} \tag{3.121}$$

and hence:

$$\bar{M}_{new} = \bar{X}^{T}_{new}\ \bar{Y}_{new} \tag{3.122}$$

c) The changed reduced matrices are calculated, that is

$$\delta\bar{K} = \bar{K}_{new} - \bar{K}_{original} \tag{3.123}$$

$$\delta\bar{M} = \bar{M}_{new} - \bar{M}_{original} \tag{3.124}$$

d) Application of equation (3.116) to equation (3.123) and (3.124) gives the change in eigenvalue associated with a structural change:

$$\delta\omega^2_i = \phi^T_i\ (\delta\bar{K} - \omega^2_i\ \delta\bar{M}\ )\phi_i \tag{3.125}$$

e) The new eigenvalues corresponding to the new structural idealization are calculated as

$$\omega^2_{i\ new} = \omega^2_{i\ old} + \delta\omega^2_i \tag{3.126}$$

3.9.2.2 Category Two : Changed Matrices

In this category there are two methods discussed. Both methods but the stiffness and mass matrices formulation are only the formulations of the changed structural idealization, that is, K_{change} (δK) and M_{change} (δM) are only formulated.

As in the case of operations on the full matrix (equation 3.119) the first step is to find the inverse of the matrix $(K+\delta K)$. The two methods in this category give two possible methods of calculation of $(K+\delta K)$ knowing the inverse of K.

3.9.2.2.1 Method One

a) The inverse of the new stiffness matrix needs to be calculated, with only knowing the original inverse and the changed stiffness matrix (δK)

i.e. $(K+\delta K)^{-1}$ is required

$$(K+\delta K)^{-1} = \frac{1}{K+\delta K} \tag{3.127}$$

$$= \frac{1}{K(I+K^{-1}\delta K)} \tag{3.128}$$

$$= (I+K^{-1}\delta K)^{-1}K^{-1} \tag{3.128}$$

(because $(AB)^{-1} = B^{-1}\ A^{-1}$)

now consider at $(a+b)^n$

$$(a+b)^n = a^n\ (1 + {}^{b}/_{a})^n$$

$$= a^n\ (1 + X)^n \quad \text{where } X = {}^{b}/_{a} \tag{3.129}$$

$$(1+X)^n = 1 + \binom{n}{1} X + \binom{n}{2} X^2 + \binom{n}{3} X^3 + \ldots\ldots\ldots \tag{3.130}$$

where $\binom{n}{k} = \frac{n(n-1).....(n-k+1)}{k}$

Hence $(I+K^{-1} \cdot K)^{-1} = 1 + \binom{1}{1} X + \binom{1}{2} X^2 + ...$ (3.131)

where $X = k^{-1}\delta K$

$= 1 - X + X^2 - X^3 + X^4 + ...$ (3.132)

$= I - K^{-1}\delta K + (k^{-1}\delta K)^2 - .....$ (3.133)

Hence $(K+\delta K)^{-1} = K^{-1} - K^{-1}\delta KK^{-1}$ + higher order terms (3.134)

b) Using the original iteration vectors (y), gives

$$X = (K^{-1} - K^{-1}\delta KK^{-1})Y \quad (3.135)$$

c) New reduced stiffness matrix is calculated

$$\bar{K} = \bar{X}^T Y \quad (3.136)$$

d) The new reduced mass matrix is calculated

i $\bar{Y} = M \bar{X}$ (3.137)

ii $\bar{M} = \bar{X}^T \bar{Y}$ (3.138)

e) Now applying equation (3.114) to the reduced matrices equations (3.136) and (3.138) give the i^{th} changed eigenvector;

$$\delta\omega^2_i = \phi^T_i (\delta\bar{K} - \omega^2_i \delta \bar{M})\phi_i \quad (3.139)$$

f) The new eigenvalues corresponding to the new structural idealization are calculated as:

$$\omega^2_{i\ new} = \omega^2_{i\ old} + \omega^2_i \quad (3.140)$$

3.9.2.2.2 Method_Two-

a) Rewriting equation (3.114)

$$K\bar{X} = Y \tag{3.102}$$

If changes are induced to the stiffness matrix (δK), this cause changes in $\bar{X}$ also, hence equation (3.114) becomes

$$(K+\delta K)\ (\bar{X}+\delta\bar{X}) = Y \tag{3.141}$$

$$K\bar{X} + \delta K\bar{X} + K\delta\bar{X} + \delta K\delta\bar{X} = Y \tag{3.142}$$

Since $K\bar{X} = Y$ and neglecting second order terms equation (3.142) becomes.

$$K\delta\bar{X} + \delta K\bar{X} = 0 \tag{3.143}$$

$$\delta\bar{X} = - K^{-1}\delta K\bar{X} \tag{3.144}$$

b) The changed stiffness matrix is calculated

$$\delta\bar{K} = \delta\bar{X}^{T}Y \tag{3.145}$$

Where Y is the iteration vectors from the original analysis.

c) Rewriting equation (3.104)

$$\bar{Y} = M\bar{X} \tag{3.104}$$

If changes are induced to the mass matrix (δM), this causes changes in $\bar{Y}$ also, hence equation (3.104) becomes

$$Y + \delta Y = (M + \delta M)\bar{X} \tag{3.146}$$

$$\bar{Y} + \delta\bar{Y} = (M\bar{X} + \delta M\bar{X}) \tag{3.147}$$

since $\bar{Y} = M\bar{X}$ equation (3.147) becomes

$$\delta\bar{Y} = \delta M\bar{X} \tag{3.148}$$

d) The changed mass matrix is calculated

$$\delta\bar{M} = \bar{X}^T \delta Y \tag{3.149}$$

e) Now applying equation (3.116) to the reduced changed matrix, equation (3.145) and (3.149) hence

$$\delta\omega^2_i = \phi^T_i \, (\delta\bar{K} - \omega^2_i \delta\bar{M}) \, \phi_i \tag{3.150}$$

f) The new eigenvalues corresponding to the new structural idealization are calculated as

$$\omega^2_{i\ new} = \omega^2_i + \delta\omega^2_i \tag{3.151}$$

3.10 Conclusion

In this chapter a number of methods for dynamic finite elements and re-analysis of bodies are presented.

In the dynamic finite element analysis the subspace iteration method was used in this research work because:

a) Subspace iteration method, at present, is the most effective and accurate method of extracting P eigenvalues and eigenvectors from an eigensystem of rank n were P<M.

b) It was already computer coded into the computer program FLASH.

c) The method can be easily extended to be used in dynamic re-analysis.

In this chapter three methods of re-analysis are given, but only one method can be developed further to be used in dynamic monitoring of structures or dynamic design of structures.

The full matrix method is very simple, but has the disadvantage that the complete structure needs to be remodelled to include the structural changes. It has the advantage that when the new structural eigenvalues are calculated, these and the corresponding eigenvectors could be used as the starting values and vectors in the subspace iteration algorithm, so the subspace iteration method can continue, but the number of iterations for convergence is unknown. Hence the method was eliminated.

The remaining two methods are based on the changed matrices, hence they have the advantage of just generating the changed structural matrices. This is very important since the design engineer can "forget about" the full structure, but just consider, what changes he/she would like to analysis. Method one in this category has also the advantage in that $(K+SK)^{-1}$ is calculated. Hence the method could also be used in static re-analysis of the same structural change. This method, was also eleminated, since a lower bound to the bandwidth (K^{-1}) can not be calculated.

Thus eliminating the full matrix method and the first of the changed matrix methods, it was decided to use the second of the two changed matrix methods. Implementation of the chosen method is given in Chapter 4 and Chapter 5 where tests of the method on five examples are explained in assessing the savings made in cost at the expence of accuracy.

CONTENTS OF CHAPTER 4

CHAPTER 4 THE FLASH PROGRAM

4.1 Introduction

As discussed in previous chapters, in this research it was decided to use the general purpose Civil Engineering Computer program FLASH. The reason for this choice was that the technique outlined in chapter 3 has to be as general as possible so that the technique of dynamic reanalysis can be applied to any structure in conjunction with dynamic response measurements outlined in chapter 1. In this chapter is given a brief history and description of the finite element program FLASH and how it works. The description of the program is in the form of a simple and brief outline of each of the subroutines which form the program FLASH.

This chapter also includes what changes had to be made to the program so that the new solution technique of dynamic reanalysis given in chapter 3, section 9 could be implemented.

4.2 History of Flash

The computer program FLASH (Finite eLement Analysis of SHells) analyses by the finite element method elastic homogeneous shells (SHELL ANALYSIS), plate in bending (PLATE ANALYSIS), plates in stretching (INPLANE ANALYSIS), axisymmetric structure (AXISYMMETRIC ANALYSIS) and also it can analyse ribbed slabs, plane and space frames and trusses under static loads. The program is supported and developed by Dr. Walder and Partner A.G. Tannackerstrasse 2, CH-3073 Bern-Guemligen Switzerland (Ref.14).

The program was basically introduced as a "black box" computer program for practising engineers and as a teaching tool at University for students whose knowledge of finite elements is minimal.The above project was started in 1972 under the leadership of Prof E Anderbeggen by U. Walder at the Swiss Federal Intitute of Technology (E.T.H.) Zurick Switzerland helped by D. R. Green of Glasgow University.

The program uses a hybrid finite element technique which includes elements which allow the investigation of plate and shells on elastic foundations (Ref.28). With the same elements columns under flat slabs can be approximated to avoid the moment singularities occurring when working with nodal point supports. Taking into account the shear deformation in plates and shells, also relatively thick structures as well as sandwich plate problems can be analysised. The elastic material properties may be isotropic (thin) or orthotropic (thick). Stiffness of plates and shells can be modelled with eccentrically connected beams which gives the possibility of treating ribbed plates as a plane problem. As usual in finite element analysis arbitrary support and edge conditions can be considered.

The program can accept a large number of loadcases or combinations of concentrated, uniformly distributed loads and prescribed joint displacement. The results can be obtained in the form of displacement, moments or stress in the nodes or in the centre of the elements for loadcase or combinations or section forces envelopes either numerically or graphically in the form of contour plot. Furthermore the reinforcement moments can be calculated from the superposition of the bending and twisting moments.

Over the years new versions of the program have been developed which include, 2nd order displacement theory, dynamic eigenvalue calculation and additional co-ordinate systems. The program at present has over 30,000 lines of executable FORTRAN code.

4.3 The Fortran Program

The program is split into 7 sections which are summarized as

OV00 - Main program and auxiliary routines which are called throughout the whole program

OV10 - Data input

OV20 - Local element generation.
OV30 - Loadcase generation.
OV40 - Generation and solution of the global equations.
OV50 - Output of the results.
OV60 - Plotting of results and the reinforecement calculation.

4.3.1 Main Program

The main program calls in turn all the main programs section as described above, but if any error is found the program automatically stops all the "heavy" calculations i.e. calculation of the local matrices, global matrices, solution of the global matrices etc, but continues checking the data for any more errors. Between sections of the program there are facilities for the program to restart with, more time, more loadcase or combinations etc. If any error is found during a section all the programs direct access file are closed, ready for a restart if it is a normal termination.

NOTE: All subroutines which start with OV__ have no arguments apart from OV13.

4.3.2 Section OV00

As mentioned above this section contains the program's auxiliary routines which are called throughout the whole program. Some of these are are

BLOCK DATA The program's main data base.
Number packing routine, i.e. PACK, UNPACK, PUTBIT etc
Direct access files routines:
READOF reads file of direct access files through system routines.
WRITTO writes files to direct access file through system routines.
OPENRA opens a direct access file through system routines.
CLOSRA closes a direct access file through system routines etc.
System routines e.g. TIME, DATA, FILES etc.

4.3.3 Section OV10

In this section the program calls from the main program three subsections OV11, OV12, OV13( ), which carry out the data input, mesh plotting and the bandwidth optimization (if required) respectively. This section also contains an auxiliary function LESE which reads the data in, in free format.

4.3.3.1 Section OV11

This section inputs the problem analysis i.e. if under data CHECK mode, or BEGIN mode, or a RESTART mode. It also inputs the problem type, IN-PLANE, AXISYMMETRIC, PLATE, SHELL analysis with the problem size, the number of nodes, elements, and types, prints out the Programs Banner and input problem definition and finally calculates the arrays dimensions for entry into subroutines EINGAB.

EINGAB Reads in the problem geometry using mesh generator. In the process it calls the following subroutines.

TANSK displacement generators.

ROTENO Rotation generators.

GENKNO generates between two points.

ORDKL converts the arbitrary input numbering system to a sequence numbering system.

Then eingab echos the problem geometry in coordinate form.

Subroutine MATPRO is called which reads in the problems material properties,element incidences and elements type, using mesh generators. In its process it calls FPROF which is used to check an input beam element profile which is stored in the programs data base.

-Then eingab echos the problem material properties for each type and echos each element's nodes and types.

Then eingab reads in the problems boundary condition using mesh generators. Subroutine

CONINP is called which reads in the nodal constraints and in coninp process it calls the following routines.

MCHECK checks the master nodes.

SCHECK checks the slave nodes.

Then eingab echos the properties boundary conditions and constraints.

Finally eingab opens the main programs direct access file (JX) which stores information about each node, element and type.

4.3.3.2 Section OV12

Subroutine OV12 calculates the arrays dimensions for entry into zeichen.

ZEICHEN This subroutine calculates and plots the problems elements meshes with node numbers, element numbers and type numbers if required. In its process it call the following routines.

ORDS Optimize the element mesh for plotting.

PLOTIN Initialize a plot frame.

PLOTP Plots a line.

SYMP Writes text.

NEWP Changes pens.

4.3.3.3 Section OV13

Subroutine OV13 calculates the arrays dimensions for bandwidth calculation before entry into colh if no optimization is required or setup if optimization is required.

COLH for each degree of freedom the subroutine calculates its bandwidth and hence the skyline profile of the global system.

SETUP as with colh, setup calculates for each element a bandwidth, but it renumbers the elements nodes to produce a mimimum skyline profile. In setup process it calls the following subroutines.

BAND calculate the problems original elements bandwidth and hence skyline profile.

OPTNUM carries out the renumbering of the problem elements nodes to produce a mimimum profile and optnum in its process calls the following routines FNDIAM, TREE, SORTDG, SET, PIKLUL, NUMOPT, DELECT, FORMLY, CHECK.For information about these routines see reference (1).

4.3.4 Section OV20

This subroutine calculates the arrays dimensions for entry into stiffn.

STIFFN This subroutine calls routines for each element type which calculate the element stiffness and mass matrices and stores them on a newly open direct access file KX; if an axisymmetic element it calls WIETYP; if an inplane element it calls SCHEIB and the inplane process calls the following routine which calculate:-

PSICH triangular shape functions.

PSISAZ quadrilateral shape function.

MSCH3 triangular consistent mass formulation.

MASH4 quadrilateral consistent mass formulation.

If a plate element it calls PLATTE and the plate process calls the following routine which calculate:-

PSIPLA elements shape functions.

MPLA3 triangular consistent mass formulation.

MPLA4 If a shell element, it set up the mass matrix of the combinations (see later).

If a shell element is required, stiffn call schecib then followed by Platte because in FLASH the shell elements are formed by adding the the inplane degrees of freedom to the plate degrees of freedom to produce the 6 degrees of freedom per nodes required for the shell element matrices.

If a beam element is required in any of the above analysis stiffn calls STAB which is a general purpose three dimensional stiffness, geometric and mass matrix formulation. In its process stab calls the following routines.

BSTRES calculates the element stress matrices.

LDVEC Reduce the 3-dimensional problems to an inplane or plate problem by removing non-contributory degrees of freedom.

SMAT Removes the stiffness, geometric stiffness and consistent mass matrices from incore and converts them into standard storage form.

SUM lumped mass formulation.

4.3.5 Section OV30

This subroutine calculates the arrays dimensions for entry into lasten.

LASTEN This subroutine reads in the problem loadcase using generations. From the input data it calculates for each loadcase the corresponding load vector. Also it echos out for each loadcase the applied loads. In its process it calls LASTIT which generates the loadvectors for the 2nd order calculations.

4.3.6 Section OV40

This section contains all the programs solution routines and if a subroutine is required it is called from the main program. There are three type of solution available in FLASH, these are:-

a static solution, uses a skyline block solution.

b free vibration solution, uses a suspace interation solution.

c 2nd order solution.

The solution routines are as follows.

4.3.6.1 Section OV41

This subroutine calculates the arrays dimensions for entry into blokl.

BLOKL evaluates the necessary blocklength for the most efficient solution (i.e. in or out of core).

4.3.6.2 Section OV42

This subroutine calculates the arrays dimensions for entry into bldab.

BLDAB assembles the global equation systems node by node into the global stiffness and mass matrices to produce the skyline profile and it opens the direct access file (LX) which stores the global matrices block by block. In its process it calls the following routines.

CONSTR adds the nodel constraints.

PUTROW introduces the constraint parameters into the master row of block.

PUTCOL introduces the constraint parameters into the master columns of a block.

PICK picks local nodal stiffness and mass matrices and places them into working space incore.

ROTATE Rotates a local nodel matrix.

PUT Inserts local stiffness and mass matrices into the global system.

GETTK Brings local element matrix into core.

4.3.6.3 Section OV43

This subroutine calculates the arrays dimensions for entry into crout.

CROUT This subroutine carries out the stiffness matrix traingularization and opens the following two direct access files.

(MX) - stores the triangularized matrix.

(NX) - stores the traingularization pivots.

4.3.6.4 Section OV44

This subroutine calculates the arrays dimensions for entry into reduc.

REDCU This subroutine carries out the elimination and back substitution for each loadcase.

4.3.6.5 Section OV45

This subroutine calculates the arrays dimensions for entry into eigen.

EIGEN This routine carries out the solution of the generalized eiginvalue problem using the subspace iteration method. In the process it calls the following routines.

REDCU2 carries out the elemination and back substitution of the iteration vectors.

MULT multiplies two matrices together taking into account the matrices skylines and blocks.

JACOBI carries out a Jacobian diagonalization.

4.3.6.6 Section OV46

This subroutine calculates the arrays dimensions for entry into reorg.

REORG This routine carries out the solution of the 2nd order theory.

4.3.7 Section OV50

This subroutine calculates the arrays dimensions for entry into ausgab.

AUSGAB This subroutine inputs all the required results for each loadcase or combination using mesh generators. For the required results it calculates all the stress, moments reactions etc, for the calculated displacement from section 4.3.6 and it prints out the required results.

Finally it closes all the solution direct access files and opens two new ones (KRA) - results for the flat element and (KRB) - results for the beam elements.

In the above process it calls the following routines.

AUSBER For each loadcase/combination, it read the required problems output with the use of generators.

AUSPLS Prints the section forces at the element centroids and averages joint section forces for plate and inplane analysis.

AUSSCH as above but for shell analysis.

GSW calculates and prints out the section forces resultants.

AWU Generators

HAUPITS Formulae.

WINKEL Formulae.

ARMIER Formulae.

INPTH2 Calculates and prints all the second order loadcases/combination results.

RANDSP Calculates and prints the surface and centroid stresses in the element centres.

4.3.8 Section OV60

This subroutine calculates the arrays dimensions for entry into ausgre.

AUSGRE This subroutine inputs the required information so that plotting of loadcases/combinations of results can be achieved It also inputs the required loadcases/ combinations to be combined so that stress, moments, reactions envelopes can be calculated and it reads in the information required so that reinforcement for the calculated envelops can be evaluated. In the above process the following routines are called.

GRENZW calculates and prints the required envelopes.

BEM1 calculates the problems reinforcement.

BEM2 sets up the required information so reinforcesment contours can be plotted.

RICHT Formulae.

RISSR Formulae.

BETEPS Formulae.

BOLTZ Prints the reinforcement results.

ZARW Loadcase/combination results plotting.

ELPLOT As above but only for requested elements.

SEREBZ Calculates envelopes for beam section forces.

ZSGRW Plots the beam section forces.

Plus also the plotting routine given in section 4.4.3.2.

4.4 Changes to FLASH

Since the changed stiffness or mass matrices were only required in the new solution method as described in chapter 3, so it was decided to change the whole program input system so that it would deal with the following structural changes.

a) change in element properties

b) make elements INACTIVE or ACTIVE

c) changes in boundary conditions.

which produced changed local stiffness or mass matrices but the structural changes were limited so that the number of degrees of freedom DID NOT alter.

The above changes were made in such a way as to minimise the changes to the program input flow chart, Figure 4.1. This was carried out by introducing a new program switch, which overruled the program error checks, but introduced new checks. Also a number of new routines were introduced and are described below, as well as extending the existing routines. Since there was a time limit in this research a number of the program parts were not permitted to be accessed under this restart mode and are shown in Figure 4.2

4.4.1 New Subroutines

ACTIVE (called from EINGAB) which checks to see if an element was already INACTIVE or ACTIVE and prints the correct error message if required.

COLHR (called from OV13) which calculates the skyline for the stiffness matrices and the skyline for the mass matrix because the skyline for both matrices now could be different or some could be zero. From the skylines it decides if there is

a) change to the stiffness matrix only

b) change to the mass matrix only

c) change to both matrices

so the correct solution can be carried out.

CALBAN (called from COLHR) which calculates the bandwidth of an element.

CALCOL (called from COLHR) which calculates the global matrices column heights.

ICHECK (called from STIFFN) which compares the old element material properties with the new to see if any of the new properties are zero, if so then there has been no change in the property but the old value may be required so that the change in local stiffness can be calculated. (e.g. element thickness).

BCOND (called from STIFFN) which checks to see if there have been any changes to the problems boundary conditions.

IDCODE (called from STIFFN) which decodes the old beam element boundary conditions to see if there has been any change.

DYNWRT (called from EIGEN) if dynamic restart mode is required in late runs of FLASH the subroutine stores the data files which are required in this restart mode.

In the solution section, if dynamic restart is required a new solution method is picked in sburoutine OV45 and these subroutines are as follows.

OV47 calculates the arrays dimensions before entry into fox.

FOX solves the changed stiffness and mass matrices using equation (3.141) to (3.151) given in chapter 3.

In the above process it calls the following routines .

PROJEC projects the changed matrices on to subspaces.

ARRAY1 solves equation (3.150) for changes in the stiffness matrix only.

ARRAY2 solves equations (3.150) for changes in the mass matrix only.

ARRAY3 solves equation (3.150) for changes in the mass and stiffness matrices.

MULTRN multiplies a two dimensional array with a single dimensional array.

4.5 Computes Implementation of Equation (3.150)

As mentioned in section (4.4) above there are three subroutines (ARRAY1, ARRAY2, ARRAY3) which are used to solve equation (3.150) which is:-

$$\delta\omega^2_i = \bar{\phi}^T_i \quad (\delta\bar{K} - \omega^2_i \delta \bar{M}) \bar{\phi}_i \qquad (3.150)$$

The three subroutines are used for numerical slability since

$$(\delta K - \omega^2_i \delta M) \qquad (4.1)$$

can produce very small number because of computer rounding. Hence there are three methods of solving equation (3.150). These methods were found by trial and error and are:

4.5.1 Change to Stiffness Matrix Only

Equation (3.150) reduces to

$$\omega^2_i = \bar{\phi}^T_i \quad (\delta\bar{K}) \bar{\phi}_i \qquad (4.2)$$

and subroutine ARRAY 1 is used to solve this equation.

4.5.2 Change to Mass Matrix Only

Equation (3.150) reduces to

$$\delta\omega^2_i = \bar{\phi}^T_i \, (-\omega^2_i \, \bar{M} \,) \, \bar{\phi}_i \qquad (4.3)$$

but the order of multiplication has to be changed since ω^2_i can often be very small, which can cause large rounding errors. Hence re-writing equation (4.3) gives

$$\delta\omega^2_i = (\bar{\phi}^T_i \, (\delta M \,) \, \bar{\phi}_i) * (-\omega^2_i) \qquad (4.4)$$

and subroutine ARRAY2 is used to solve this equation.

4.5.3 Changes to Both Matrices

In this method equation (4.2) is calculated and solved, then equation (4.4) is calculated and solved with the results added to produced the correct results.

Subroutine ARRAY3 carries this out by calling subroutine ARRAY1, followed by subroutine ARRAY2.

4.6 Conclusion

The chapter gives a brief outline of the computer program FLASH, and shows how the new method of solution given in chapter 3 has been carried out.

The method produced has a good advantage in that only the changed stiffness and mass details have to be inputted and hence solved. To bring about this advantage a great deal of time consuming effort had to be made in introducing into the program a switch which overrules error checks and introduce new ones.

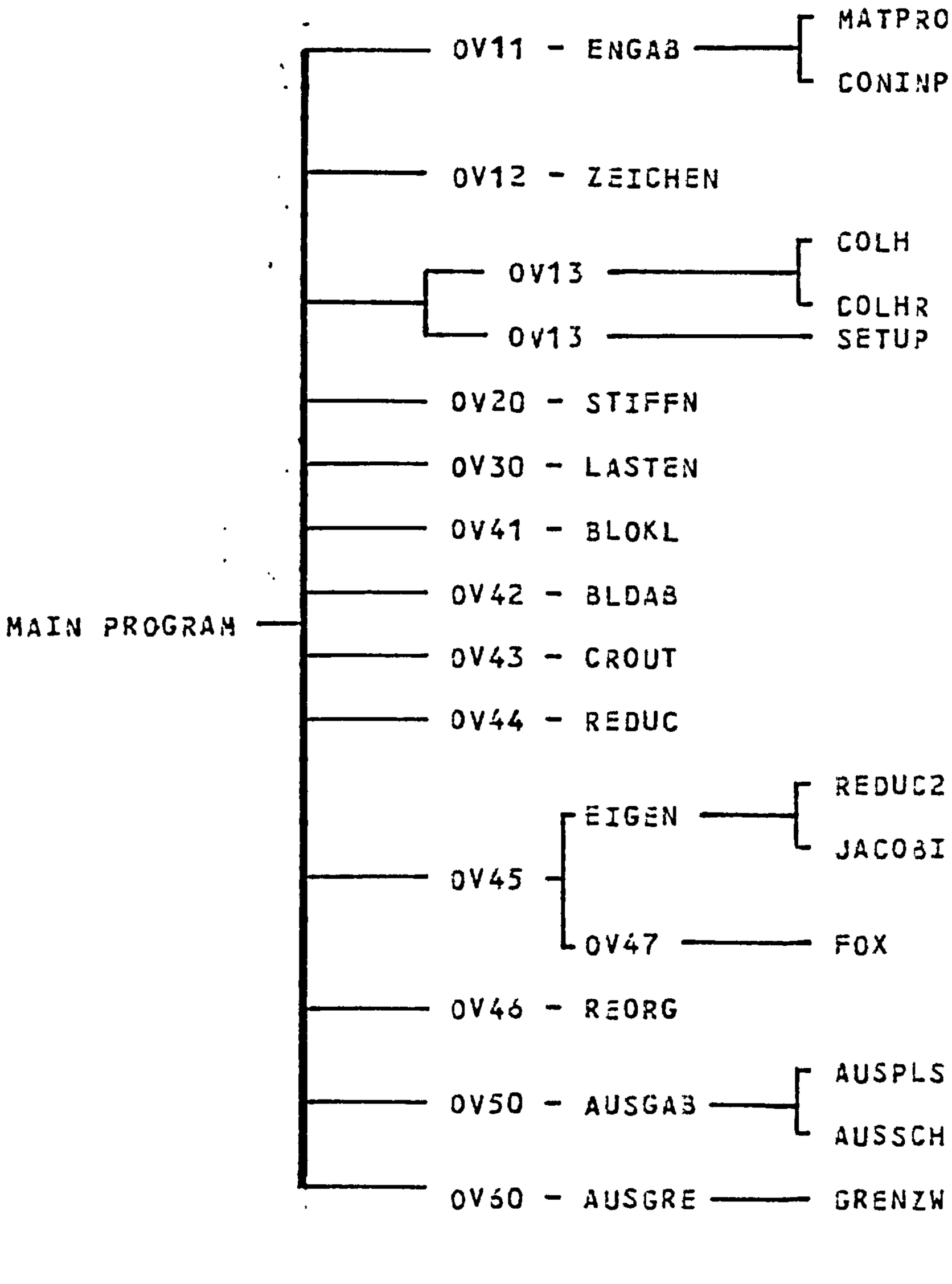

FIGURE 4.1 FLOWCHART OF THE MAIN PROGRAM SUBROUTINES

INPUT SCHEME FOR THE PROGRAM FLASH

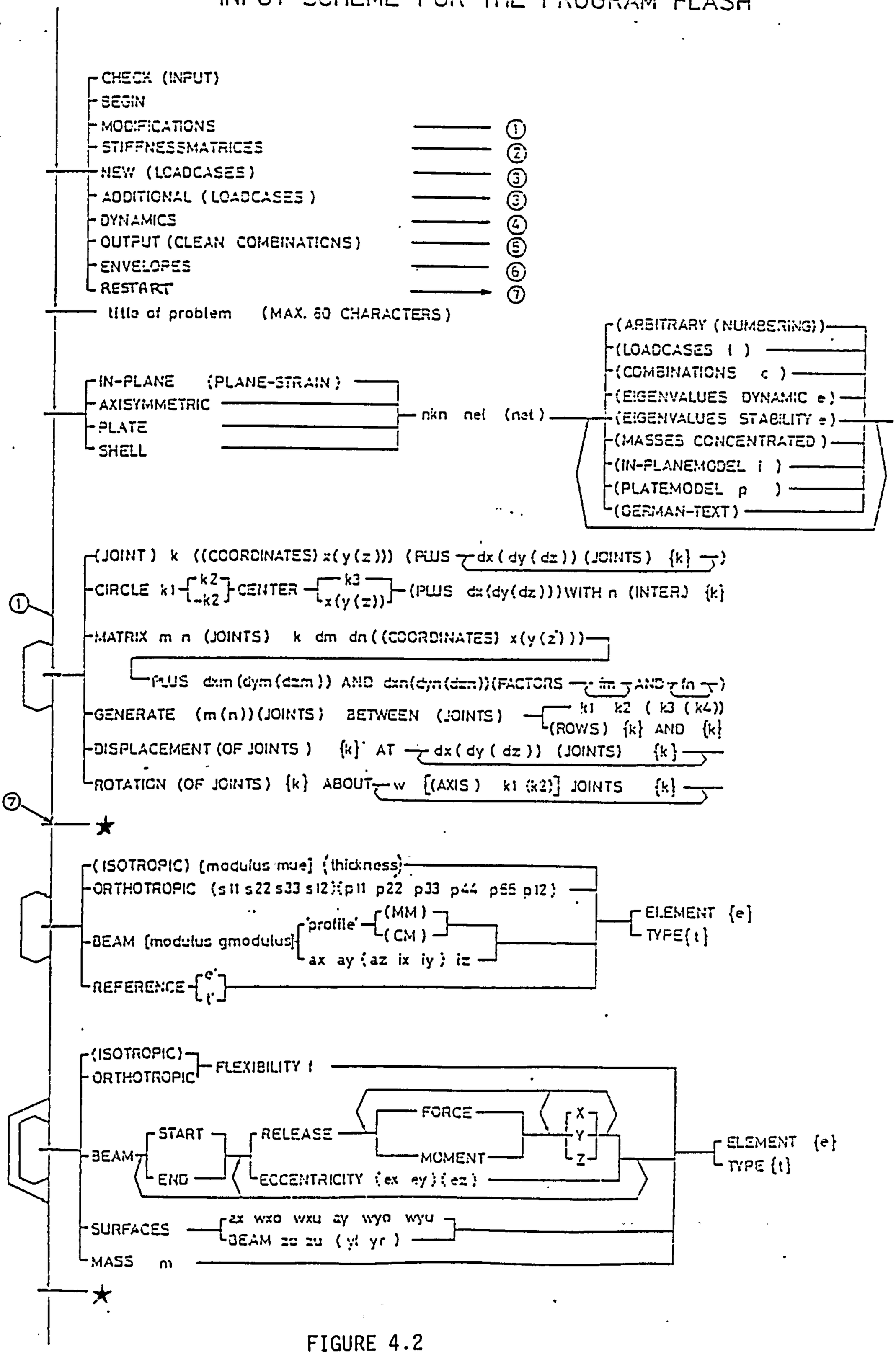

FIGURE 4.2

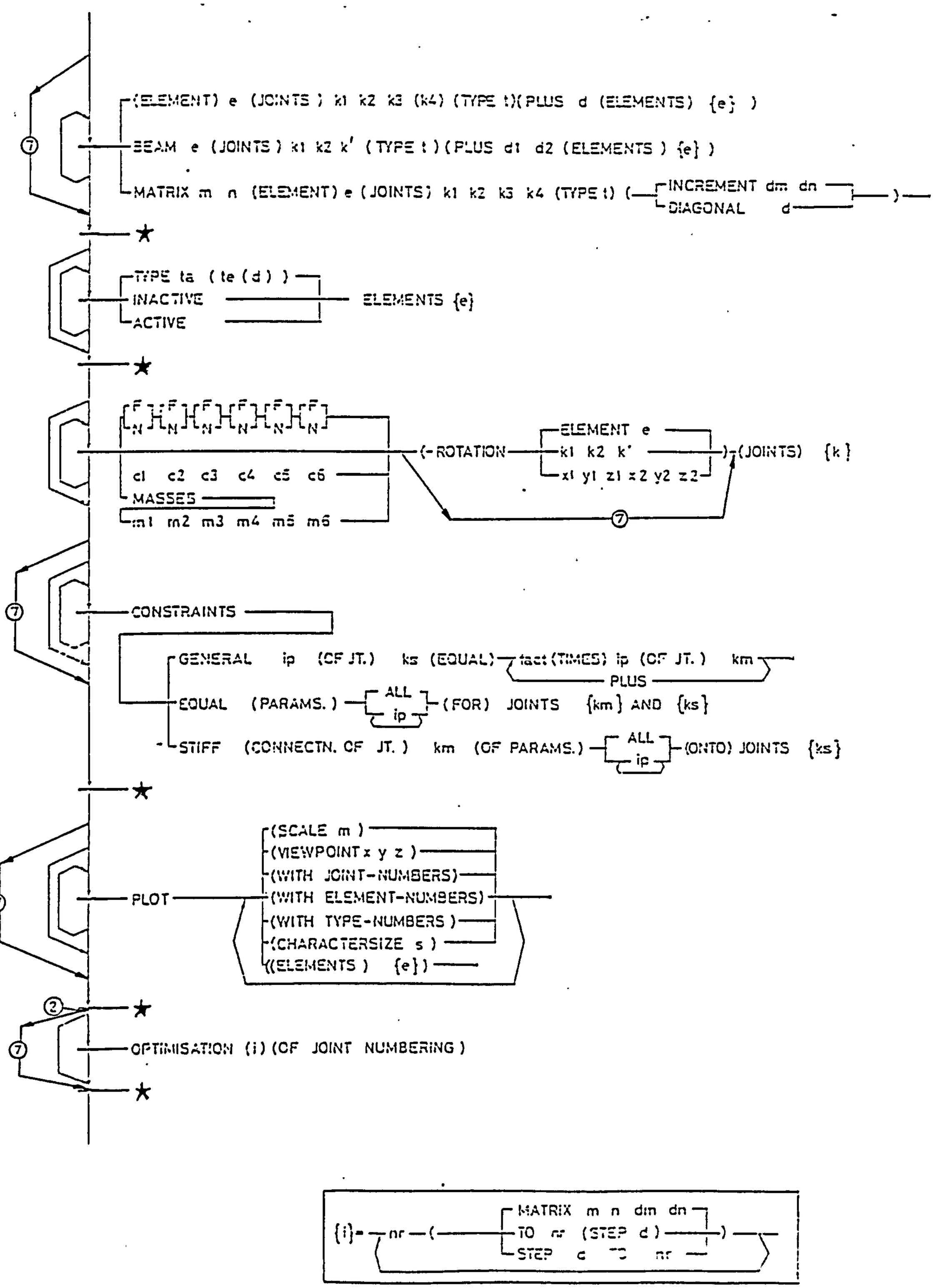

FIGURE 4.2 (cont)

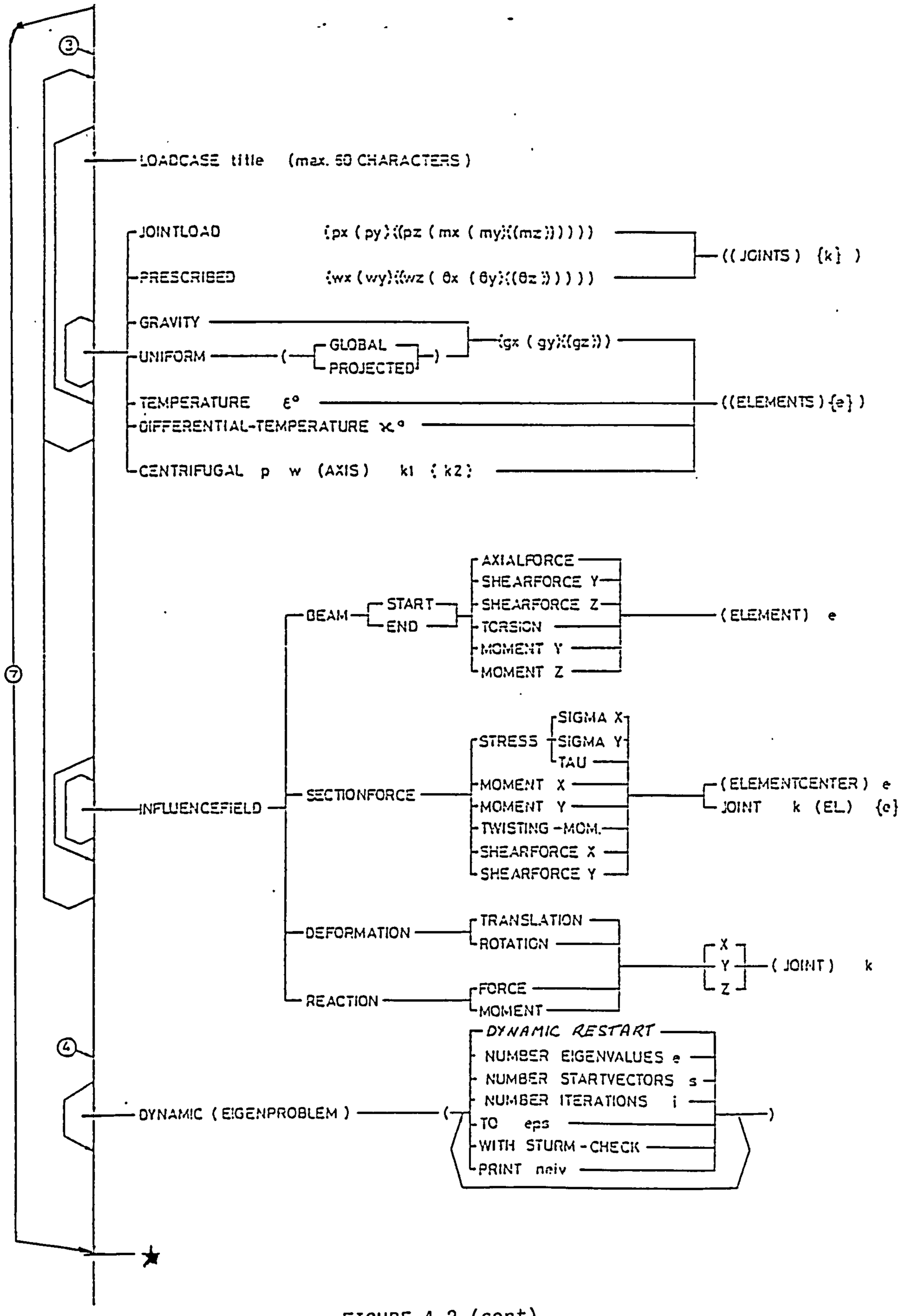

FIGURE 4.2 (cont)

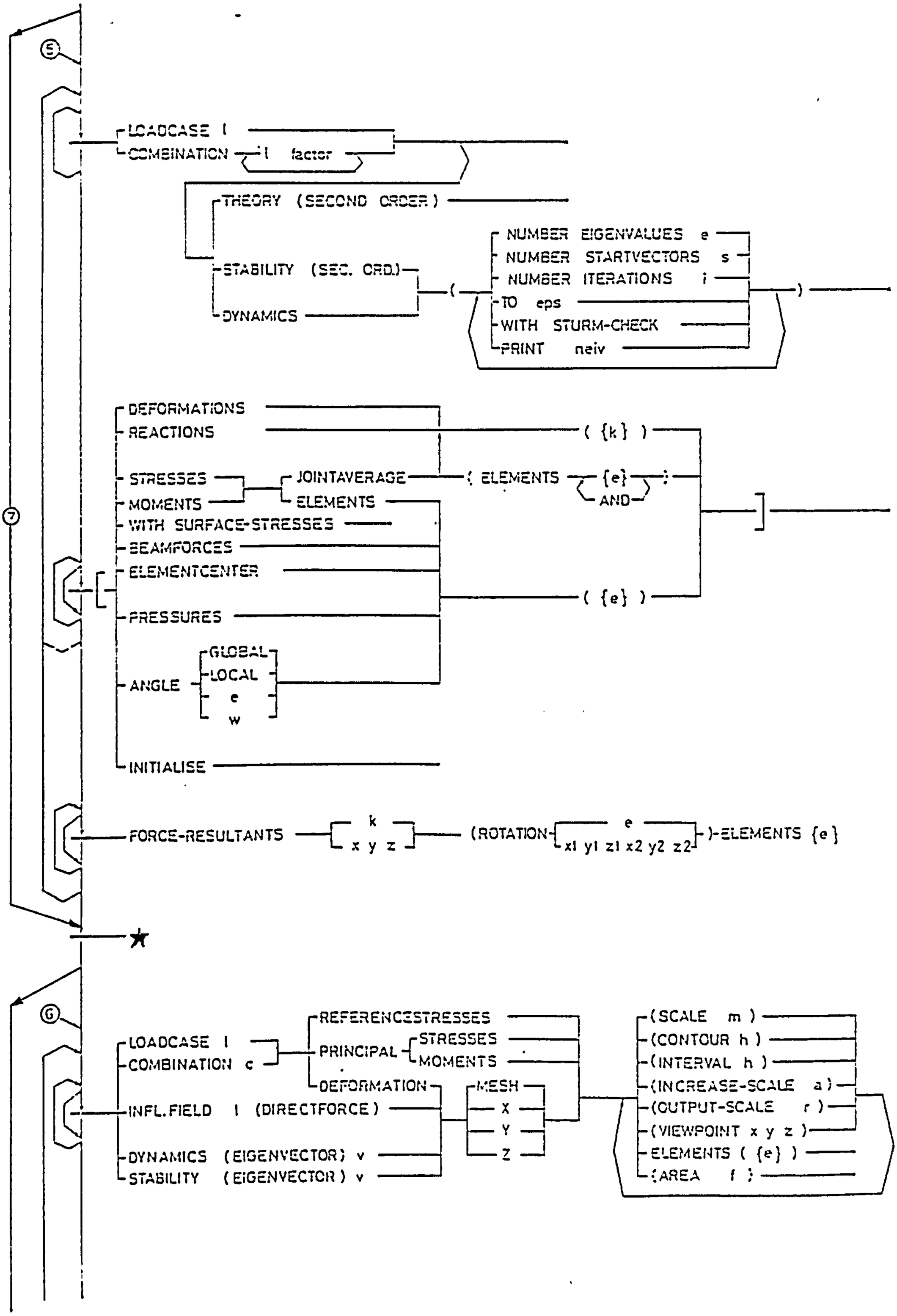

FIGURE 4.2 (cont)

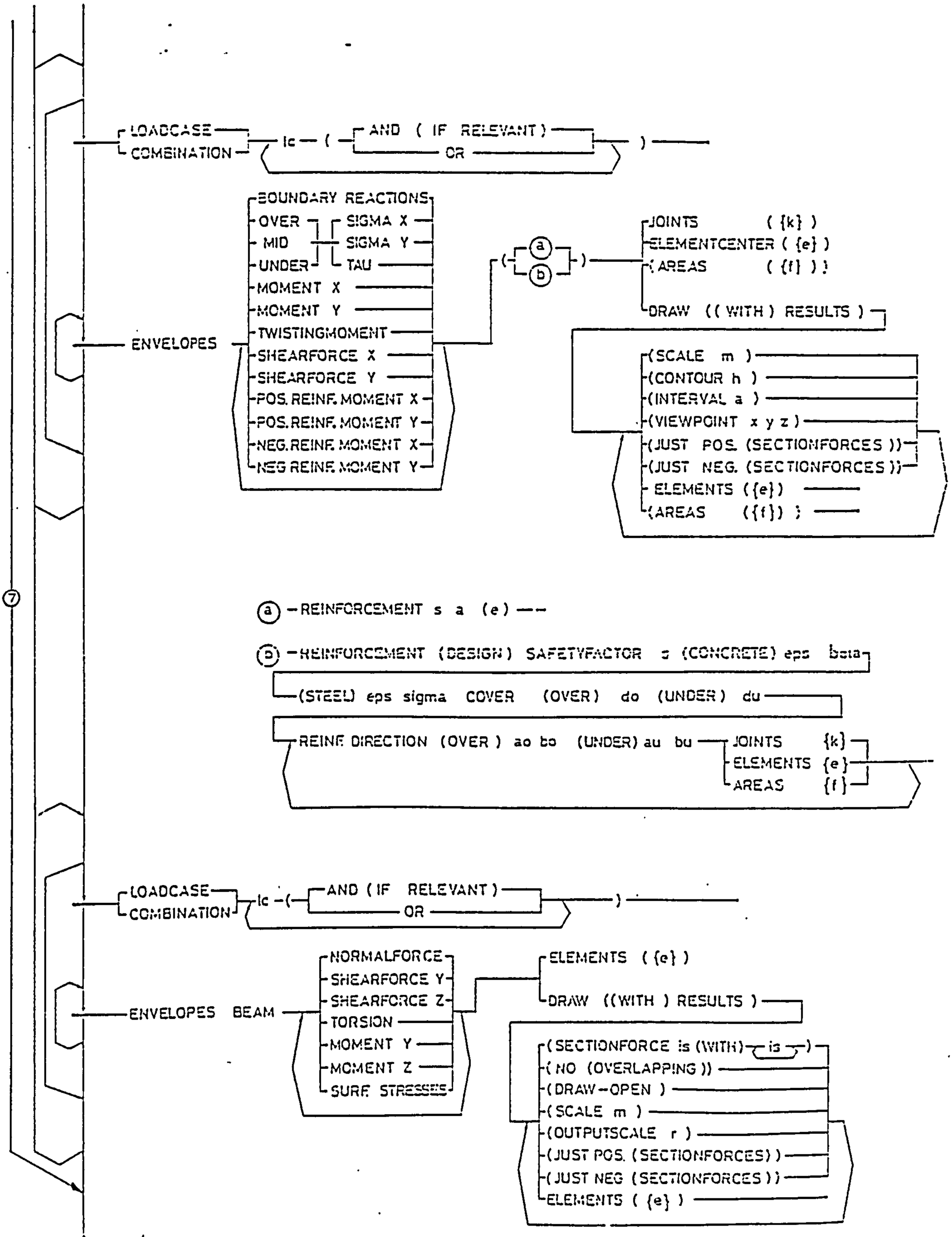

FIGURE 4.2 (cont)

CONTENTS OF CHAPTER 5

CHAPTER 5 RESULTS OF COMPUTER RESEARCH

5.1 Introduction

In this Chapter, five examples of dynamic re-analysis are given using equation (3.150) as its sub-equations (4.2) and (4.4). The following examples will attempt to illustrate different aspects of the equation, i.e.

Change in stiffness only	examples 1, 2 and 4
Change in mass only	example 5
Change in both stiffness and mass	example 3

In addition an example is given which examples the effects of the method when "very" local changes occur in the structural stiffness. The five examples are:-

1) Skew Isotropic Slab

2) Beam Element Problem

3) Southfield Bridge

4) Westerhouse Bridge

5) Baillieston Interchange

For each of the five examples a number of different changes were introduced into the structural models to see what effect there changes have on the structural natural frequencies. These structural changes were introduced into two computer models of the example under consideration.

The models were

a) A dynamic re-analysis using the new method given in Chapter 3 (i.e. a form of equation 3.150) in which the structural changes were the only data input to the program.

b) . A complete new analysis was carried out with the data modified to take the structural changes into account.

The errors between the complete new analysis (FULL) and the dynamic re-analysis (NEW) were calculated as follows:

$$\% \text{ ERROR} = \frac{fi(FULL) - fi(NEW)}{fi(FULL)} \qquad (5.1)$$

5.2 Example 1 - Skew Isotropic Slab

This example is based on the Department of the Environment, Highway Engineering Computer Branch, Program calibration problem 6.4 and is shown in Figure 5.1. The slab has the following material properties:

Young's Modulus	75.0 E6 N/m^2
Poisson's Ratio	0.215
Thickness	0.12m
Density	2.4 E3 Kg/m^3

It is simply supported along the shorter edges and free along the other two edges.

The slab computer model was analysed with 72 plate bending elements as shown in Figure 5.2, with the above material properties. The slabs supports are modelled using vertical stiff strings at the element boundaries. Since this example was idealised as a plate, the slab was modelled using 216 degrees of freedom, with only the first ten natural frequencies extracted, and these frequencies are given in Table 5.1. (Note: the rank (order) of finite element matrices equals the total number of degrees of freedom used).

This example is only concerned with changes to the structural stiffness matrices. The reduced changes were changes in the slabs Youngs Modules, but were made out as a "growth" process from joint 1 (see Figure 5.1), i.e. the changes were introduced into 2, 8, 18, 32, 50, 72, elements consecutively (see Figure 5.2) to produce an envelope of errors for the first ten natural frequencies. Three growth studies were carried out for 10%, 20%, 30% decrease in Youngs Modulus, and the

above study could simulate different levels of progressive cracking in a concrete slab.

A graph of the error envelopes plotted against the percentage growth in the number of elements affected is given in Figure 5.3. Tables 5.6, 5.7, 5.8 give the numerical comparison between the two types of analysis. These show that for a maximum overall decrease in the value of the first natural frequency of 16.3% associated with a 30% reduction in Youngs Modules, there was only a 2.6% difference between the two methods of analysis. This occurs when the region of changed elements covers 30% of the idealisation; thereafter the error decreases. This could be due to the effects of the unaffected boundary springs being very close to the boundary between changed and unchanged elements.

5.3 Example 2 - Beam Element Problem

Figure 5.4 shows a three span continuous beam, with one support completely fixed in all directions and positions. The beam's cross-section is taken as a standard hot-rolled universal beam of serial size 610 x 305 and a mass per metre of 238Kg/metre. The computer model of the beam was constructed with 12 3-D beam element with the following material properties.

Young's Modulus = $210E9N/m^2$

Shear Modulus = $81E9N/m^2$

Density = $77E3Kg/m^3$

The beam boundary conditions were modelled by springs, but joint 1 (see Figure 5.4) instead of having very stiff springs, it was modelled using a spring of stiffness equal to $1E10N/m^2$. As a 3-D analysis the beam model has 72 degrees of freedom. Only the first ten natural frequencies are given in Table 5.2.

The local changes to the structural stiffness matrices in this example are associated with support conditions. The spring support stiffness of the six degrees of freedom of joint 1 were halved in each successive

analysis. This simulates different levels of relaxation of the support.

Since this was only a local effect, only four of the ten natural frequencies were affected. Figure 5.5 gives a graph of errors of the affected frequencies plotted against the percentage change in the spring stiffness. Table 5.9 gives the numerical comparison between the full and re-analysis results.

The results of this example demonstrate that the method can be used for very local changes. (In this case 6 degrees of freedom out of 72 degrees of freedom only were affected).

However care has to be taken since the reanalysis technique introduced changes in some natural frequencies which should not have been affected by the particular change in stiffness. In this example these changes were insignificant errors of "round off" magnitude but this effect may be significant in longer studies and care should be taken. But again example 2 has shown that equation (3.150) seems to work since the maximum recorded error was only 0.067% in the fifth natural frequency, and that was after progressively reducing the support stiffness to 96.875% of its original value.

5.4 Example 3 - Southfield Bridge

This bridge and the computer model of it are fully described in chapter two. The bridge deck was modelled as a plate analysis using 225 degrees of freedom and from the analysis the first five natural frequencies were calculated. These frequencies are given in Table 5.3.

This test problem was used to study simultanuously changes to the structural stiffness and the structural mass. The parameters varied in this study were again Youngs Modules (stiffness matrix) and the mass of the deck (mass matrix). These two properties were varied in different proportions so that the mass changes were twice as large as the stiffness changes. The variation in the material properties was carried out twice, once as a decrease and the other as an increase. These studies could simulate removing, increasing structural tarmac or concrete running courses.

These changes were made over the whole bridge and hence the effect is seen in every degree of freedom of the structure. The errors fall into two zones; one for the increase in properties, the other for the decrease. Figure 5.6 gives a graph of these zones plotted against dual axis scales of percentage changes in density and percentage change in young's modulus. Tables 5.10 and 5.11 gives the numerical comparison between the two types of analysis.

In this example, both parts of equation (3.150) have been affected by different propositions so one effect would not cancel out the other. Since the study was a global change affecting every degree of freedom, this produced the zone effect, seen in Figure 5.6.

Again the success of the method is demonstrated because after introducing a 50% reduction in density coupled with a 25% reduction in Youngs modulus, an error of the order of 6% occurs.

Note that the difference in the two error zones could be attributed to the fact that both the stiffness and mass matrices had diagonal contribution due to boundary springs and mass point loads, thus producing the non-linear error difference between the increase and decrease study.

5.5 Example 4 - Waterhouse Bridge

The description of the bridge and computer model used are given in chapter two. This example was modelled as a plate analysis with eccentrically connected beam stiffners. The computer model had 270 degrees of freedom, and the first ten natural frequencies were calculated. These frequencies are given in Table 5.4.

A new aspect introduced by the example was of large bandwidth. This was because of the concrete cross beams causing an uneven element mesh, see Chapter Two. For example the bandwidth in this example was almost three times greater than in example 3.

Since this structure was of composite construction form it led to the study of the effect of the connections between the two types of

materials i.e. the shear connectors. This type of problem is analysed in such a way that local displacements (or strains) at the interface between the two materials are constant (see Figure 5.7). In the ribbed plate analysis this was modelled using stiff eccentricity beam elements so a study was carried out in such a way as to reduce the degree of shear connectors between the two elements of the structure. To model this effect correctly the eccentricity of the stiff connectors was reduced in such a way as to keep the local axis of both elements parallel. If the axis of the stiffener element is not parallel to that of the plate elements the axial stiffness of the stiffener contributes to the transverse stiffness of the plate.

This effect is described in detail in Figure 5.8a. The vertical stiffness (degree of freedom (1)) is not affected by eccentricity of the beam. If the eccentricity at each end is the same, the flexural shear stiffness of the beam is added to the plate. But the flexural stiffness (degree of freedom (3)) is increased by the flexural stiffness times the eccentricity. The torsional stiffness (degree of freedom (2)) of the beam is neglected in this type of analysis. Figure 5.8b gives the relationship described above in mathematical form. Hence decreasing the eccentricity between the plate and beam elements models less than 100% shear connection between the two materials.

If uneven eccentricity is applied the stiffness is increased because the beams axial stiffness would increase the plate vertical (shear) stiffness. Figure 5.8c gives the relationship for uneven eccentricity in mathematical form.

Figure 5.9 gives a graph of the errors plotted against percentage reduction in the rigid connector, and table 5.12 gives the numerical comprison between the two types of analysis.

During this study, a local effect was studied by removing the rigid connectors over a central 9.5 meter section of one of the central beams. Table 5.13 gives the results of this study.

In this example the study was carried out for a full range of reduction of the rigid connectors. This study has shown very good results from zero reduction up to about 40% reduction, that is errors less than 5%. If the reduction is continued right up to 100%, the error increases to a maximum of just under 25%. As seen from Figure 5.9 the errors fall into 3 zones, that is bending, torsion and cross bending eigenvalues/vectors, with much greater errors occurring on the bending and torsional modes, because the rigid connectors affect the longitudinal bending of the structure. In this example when 100% reduction has been carried out, the reduction in the bending stiffness is of the order of 90%. This is because the total bending stiffness has three components, that is the bending stiffness of the plate elements (concrete check), the bending stiffness of the beam elements and, the axial stiffness times the eccentricity of the beam elements, and this total stiffness reduces to only the two bending stiffnesses. That is

$$M_{PLATE} + M_{BEAM} + ECC * A_{BEAM} \longrightarrow M_{PLATE} + M_{BEAM} \qquad (5.1)$$

For this example an elastic "composite construction" analysis is carried out. The stiffness for one steel beam plus the effective concrete slab the EI values (hence the bending stiffness) reduces from 95.16 NM^3 to 10.14NM^3 i.e. a 89% reduction.

The errors falling into 3 zones can be seen very clearly in Table 5.13. The error for the local reduction in the rigid connectors are very high for the bending modes, that is the first, fourth, and eighth natural frequencies. Hence great care has to be taken so that a local change, or a global change which seems to be small but which actually affects a global degree of freedom very significantly, hence affecting the natural frequencies significantly.

5.6 Example Five - Baillieston Interchange

For description of the bridge and computer model used see Chapter Two. Since this example was modelled as a shell analysis the bridge deck was modelled with 2052 degrees of freedom, with the first seven natural

frequencies extracted. These are given in Table 5.5. [Please note the difference in the results from Table 2.3 and Table 5.5 for the third and fourth frequencies; this is due to the fact that after the results in Table 2.3 were produced, the Glasgow University main frame computer was upgraded from an ICL 2976 to an ICL 2988].

As given in the introduction this example is concerned with changes to the structural mass. The parameter used in this study was again the density of the deck which was progressively reduced to simulate removing and replacing the tarmac by a much less dense material. This study was carried out over the whole bridge and hence the changes affect every degree of freedom of the structure, and the errors fall into a zone the same as for example two. Figure 5.10 gives a graph of this error zone plotted against the percentage change in density, and Table 5.14 gives the numerical comparisons between the two types of analysis.

As seen from Figure 5.10 the maximum error for a global change in density of 40% was only 7% so again equation (3.150) seems to work.

5.7 Computer savings

As mentioned before, equation (3.150) only deals with the changed stiffness and mass matrices, hence the only data input is these changes. Given in Figures 5.11 and 5.12 are two examples of the data input for

a full analysis
b restart analysis

The two examples are for the skew slab and the beam element problem. It can be seen from these figures that if the structure was very large the restart analysis for a number of different changes would be much easier and simpler than a complete full new analysis.

The most important point of the new solution method is not the data input, but the savings in computer time, and hence COST. To assess the

time factor a detailed study was carried out for each part of the analysis, that is the time saved in data input, matrix generation, solution time and hence the total time, for example one; the skew slab. Figure 5.13 gives a graph of these savings, plotted against the growth in the structural defect.

For all the other examples, a study of only the total time was carried out, owing to a computer system problem, and the results are given in Table 5.15. (Also given in this table are the computer savings in carring out a restart analysis for the model bridge used in this research (see later)).

5.8 Conclusion

The method given in Chapter 3 of this thesis, has been tested over five different problems, with each one looking at a different aspect of the method. It seems to produce very good results, for large structural changes to both the stiffness and mass, but as seen in example four, care has to be taken when introducing a structural change, which is too large. From the results, a reasonable upper limit would be 40% change in structural properties which would place an upper limit to the errors of about 7% in natural frequencies.

The other good point about the method apart from its accuracy is the saving in computer time. In the Baillieston Interchange example, the full analysis took over 3800 computer processor seconds, which at Glasgow University put the analysis into the overnight batch queue, but the restart analysis only took less than 280 seconds and could be executed almost immediately (depending on how many people are using the computer).

The method described in Chapter 3 applies equation (3.150) to reduced stiffness and mass matrices, i.e. the projected matrices. Equation (3.150) may also be applied to the full changed matrices, i.e. no reduction to the matrices were carried out. This approach may be faster than the technique which includes reduction, so a short study was carried out using example one, (Ref 15, 30, 32).

The results are given in Table 5.16 and show that this method is not very accurate since it did not predict any changes above the third natural frequency. Also the error for the first three natural frequencies were large. These errors could be due to the computer rounding and to the fact that the stiffness and mass matrices represent the full structure whereas the reduced matrices represent the structural properties of the eigenvalues/vectors under consideration and hence lead to more accurate and useful results.

MODE -	FREQUENCY
1	0.336638
2	0.986545
3	2.371438
4	3.468227
5	4.547134
6	5.609734
7	5.550049
8	3.089236
9	10.09023
10	10.47138

TABLE 5.1 EXAMPLE ONE - SKEW SLAB
--------- NATURAL FREQUENCIES (HZ)

MODE	FREQUENCY
1	3.749775
2	4.730255
3	6.431323
4	7.866933
5	9.302883
6	10.16875
7	12.65235
8	14.38037
9	16.52464
10	17.72368

TABLE 5.2 EXAMPLE TWO - BEAM ELEMENT PROBLEM
--------- NATURAL FREQUENCIES (HZ)

MODE	FREQUENCY
1	4.671113
2	6.895181
3	6.932759
4	8.864517
5	12.07479

TABLE 5.3 EXAMPLE THREE - SOUTHFIELD BRIDGE
--------- NATURAL FREQUENCIES (HZ)

MODE	FREQUENCY
1	3.553119
2	4.035084
3	6.835774
4	9.680708
5	10.88918
6	11.57487
7	13.03246
8	15.86477
9	16.37473
10	13.41756

TABLE 5.4 EXAMPLE FOUR - WESTERHOUSE BRIDGE
--------- NATURAL FREQUENCIES (HZ)

MODE	FREQUENCY
1	3.080773
2	4.996823
3	5.842380
4	6.095642
5	7.399362
6	8.269837
7	8.795681

TABLE 5.5 EXAMPLE FIVE - BAILLIESTON INTERCHANGE BRIDGE
--------- NATURAL FREQUENCIES (HZ)

NUMBER OF ELEMENT / MODE	RESTART 2	FULL 2	RESTART 8	FULL 8	RESTART 18	FULL 18	RESTART 32	FULL 32	RESTART 50	FULL 50	RESTART 72	FULL 72
1	0.834422	0.834302	0.828509	0.828084	0.820020	0.819393	0.811033	0.810440	0.802541	0.802231	0.793704	0.793705
2	0.981850	0.981792	0.976132	0.976061	0.970178	0.970121	0.961580	0.961595	0.950558	0.950581	0.935918	0.935919
3	2.367968	2.367830	2.356406	2.355812	2.338782	2.337892	2.316431	2.315329	2.286116	2.285434	2.249743	2.249744
4	3.462186	3.461967	3.451250	3.450558	3.430367	3.429449	3.395159	3.393721	3.343662	3.342783	3.290249	3.290249
5	4.531034	4.530245	4.498035	4.496229	4.469231	4.466344	4.429461	4.425878	4.376203	4.374245	4.313838	4.313840
6	5.605481	5.605374	5.590733	5.590412	5.562955	5.561639	5.506890	5.504644	5.424649	5.422621	5.321906	5.321911
7	7.541984	7.541549	7.508458	7.505041	7.431799	7.424299	7.331036	7.321846	7.222413	7.218941	7.162603	7.162608
8	8.083591	8.083347	8.064660	8.064332	8.026421	8.026590	7.950624	7.948478	7.831528	7.827950	7.674124	7.674129
9	10.06489	10.06489	10.02981	10.02476	9.949705	9.927666	9.833743	9.813363	9.723829	9.714748	9.572481	9.572489
10	10.46116	10.46123	10.42289	10.42266	10.32942	10.33324	10.21418	10.21444	10.05638	10.05432	9.934492	9.934498

TABLE 5.6 COMPARISON BETWEEN CALCULATED FREQUENCIES DUE TO A 10% REDUCTION IN YOUNG'S MODULUS FOR A SKEW SLAB
--------- (HZ)

NUMBER OF ELEMENT / MODE	RESTART 2	FULL 2	RESTART 8	FULL 8	RESTART 18	FULL 18	RESTART 32	FULL 32	RESTART 50	FULL 50	RESTART 72	FULL 72
1	0.832201	0.831682	0.820300	0.818449	0.803059	0.800339	0.784594	0.782036	0.766929	0.765582	0.748312	0.748312
2	0.977132	0.976891	0.965608	0.965333	0.953531	0.953327	0.935950	0.936027	0.913153	0.913250	0.882393	0.882393
3	2.364492	2.363900	2.341272	2.338716	2.305664	2.301798	2.260087	2.255259	2.197483	2.194458	2.121078	2.121078
4	3.456134	3.455189	3.434192	3.431214	3.392084	3.388143	3.320482	3.314173	3.214275	3.210359	3.102077	3.102078
5	4.514827	4.511432	4.448343	4.440636	4.389894	4.377307	4.308527	4.290590	4.198262	4.189790	4.067125	4.067125
6	5.601175	5.600721	5.571618	5.570257	5.515730	5.509982	5.402040	5.392079	5.232971	5.223952	5.017543	5.017546
7	7.533909	7.531993	7.466637	7.451660	7.311639	7.279891	7.105279	7.066779	6.879191	6.864667	6.752967	6.752970
8	8.077939	8.076887	8.040006	8.038718	7.963112	7.962815	7.809549	7.798373	7.565044	7.548951	7.235233	7.235235
9	10.03944	10.03306	9.968963	9.947397	9.807115	9.714401	9.570330	9.489815	9.343014	9.302013	9.025024	9.025027
10	10.45044	10.45072	10.37367	10.37189	10.18499	10.19660	9.949823	9.942164	9.622966	9.615661	9.365330	9.366332

TABLE 5.7 COMPARISON BETWEEN CALCULATED FREQUENCIES DUE TO A 20% REDUCTION IN YOUNG'S MODULUS FOR A SKEW SLAB
--------- (HZ)

NUMBER OF ELEMENT / MODE	RESTART 2	FULL 2	RESTART 8	FULL 8	RESTART 18	FULL 18	RESTART 32	FULL 32	RESTART 50	FULL 50	RESTART 72	FULL 72
1	0.830271	0.823706	0.813118	0.867444	0.788064	0.779061	0.760937	0.751002	0.734671	0.726260	0.706616	0.699982
2	0.973025	0.971825	0.956393	0.954378	0.938865	0.936197	0.913156	0.909806	0.879450	0.874364	0.833227	0.825403
3	2.361476	2.359554	2.328078	2.319773	2.276572	2.262543	2.210094	2.190309	2.117670	2.097493	2.002893	1.984088
4	3.450878	3.447777	3.419339	3.409824	3.358554	3.343755	3.254375	3.228317	3.097771	3.069527	2.929232	2.901729
5	4.500731	4.490267	4.404822	4.379469	4.319955	4.278006	4.200897	4.164373	4.037711	3.991554	3.840508	3.804448
6	5.597443	5.595781	5.554999	5.549176	5.474470	5.453786	5.309494	5.270016	5.060979	5.011151	4.737970	4.693482
7	7.526905	7.521028	7.430202	7.387406	7.205880	7.113929	6.903651	6.780536	6.567240	6.483490	6.376698	6.316826
8	8.073038	8.069709	8.018577	8.012405	7.907831	7.895881	7.685190	7.633948	7.326256	7.247798	6.832093	6.767943
9	10.01733	9.998590	9.915929	9.855332	9.681835	9.446517	9.336027	9.121560	8.999480	8.842357	8.522160	8.442141
10	10.44113	10.44032	10.33082	10.31763	10.05813	10.04969	9.714894	9.638700	9.230892	9.154141	8.844448	8.761402

TABLE 5.8 COMPARISON BETWEEN CALCULATED FREQUENCIES DUE TO A 30% REDUCTION IN YOUNG'S MODULUS FOR A SKEW SLAB
--------- (HZ)

SPRING STIFF--NESS MODE	RESTART 50%	FULL 50%	RESTART 75%	FULL 75%	RESTART 87.5%	FULL 87.5%	RESTART 93.73%	FULL 93.73%	RESTART 96.8%	FULL 96.8%
1					NO CHANG					
2	4.73024	4.730226	4.730233	4.730167	4.730228	4.730051	4.730228	4.729817	4.730226	4.729354
3					NO CHANG					
4					NO CHANG					
5	9.302776	9.302671	9.302723	9.302249	9.302696	9.301409	9.302684	9.299740	9.302670	9.296447
6	10.16871	10.16868	10.16870	10.16854	10.16869	10.16828	10.16868	10.16774	10.16868	10.16667
7					NO CHANG					
8					NO CHANG					
9	16.52464	16.52461	16.52457	16.52458	16.52441	16.52411	16.52457	16.52350	16.52457	16.52228
10					NO CHANG					

TABLE 5.9 COMPARISON BETWEEN CALCULATED FREQUENCIES FOR PERCENTAGE REDUCTION IN SUPPORT STIFFNESS --------- FOR A BEAM ELEMENT PROBLEM (HZ)

	RESTART	FULL	RESTART	FULL	RESTART	FULL	RESTART	FULL	RESTART	FULL
DECREASE MODE	10XDENSITY 5X YOUNG'S		20X DENSITY 10X YOUNG'S		30X DENSITY 15X YOUNG'S		40X DENSITY 20X YOUNG'S		50X DENSITY 25X YOUNG'S	
1	4.762702	4.771482	4.852565	4.890642	4.940792	5.034635	5.027473	5.212450	5.112685	5.438169
2	7.034386	7.047512	7.170883	7.227792	7.304837	7.445008	7.436373	7.712528	7.565627	8.038969
3	7.065840	7.078426	7.196462	7.251009	7.324753	7.459038	7.450836	7.715141	7.574821	8.051289
4	9.041053	9.057425	9.242080	9.285113	9.384170	9.558585	9.551108	9.894148	9.715178	10.31714
5	12.31857	12.34165	12.55763	12.65767	12.79222	13.03867	13.02258	13.50828	13.24894	14.10344

TABLE 5.10 COMPARISON BETWEEN CALCULATED FREQUENCIES FOR PERCENTAGE REDUCTION IN DENSITY AND YOUNG'S MODULUS FOR SOUTHFIELD BRIDGE (HZ)

	RESTART	FULL	RESTART	FULL	RESTART	FULL!	RESTART	FULL	RESTART	FULL
INCREASE MODE	10%DENSITY 5% YOUNG'S		20% DENSITY 10% YOUNG'S		30% DENSITY 15% YOUNG'S		40% DENSITY 20% YOUNG'S		50% DENSITY 25% YOUNG'S	
1	4.580020	4.585331	4.484603	4.511111	4.387109	4.446211	4.287401	4.388945	4.185318	4.338006
2	6.760288	6.764551	6.611338	6.651115	6.462877	6.551544	6.310925	6.463328	6.155224	6.384523
3	6.800523	6.808041	6.662001	6.699965	6.520538	6.605330	6.375936	6.521727	6.227977	6.447276
4	8.688797	8.698681	8.504762	8.554362	8.316655	8.427423	8.124195	8.314748	7.927064	8.213921
5	11.83197	11.84606	11.57768	11.64754	11.31768	11.47336	11.05156	11.31910	10.77888	11.18134

TABLE 5.11 COMPARISON BETWEEN CALCULATED FREQUENCIES FOR PERCENTAGE INCREASE IN DENSITY AND YOUNG'S MODULUD
---------- FOR SOUTHFIELD BRIDGE (HZ)

DECREASE IN ECCEN (mm) MODE	RESTART 100	FULL 100	RESTART 200	FULL 200	RESTART 300	FULL 300	RESTART 400	FULL 400	RESTART 500	FULL 500	RESTART 600	FULL 600
1	3.348903	3.331828	3.163382	3.095626	3.000028	2.851330	2.862642	2.610895	2.755110	2.392926	2.681026	2.222702
2	3.827171	3.813293	3.639491	3.585794	3.475358	3.360435	3.338244	3.148548	3.231593	2.965161	3.158495	2.827933
3	6.744280	6.736101	6.664713	6.634192	6.597676	6.533942	6.543554	6.440408	6.502666	6.359633	6.475262	6.298539
4	9.440603	9.399076	9.229816	9.057824	9.050410	8.655388	8.904284	8.204244	8.793097	7.742678	8.718183	7.344087
5	10.61186	10.55535	10.36800	10.14705	10.16031	9.675444	9.991057	9.164892	9.862207	8.663883	9.775364	8.248820
6	11.52847	11.52669	11.48845	11.47169	11.45500	11.39204	11.42817	11.25972	11.40800	11.35677	11.39454	10.83926
7	12.79906	12.76733	12.59476	12.47507	12.42195	12.17565	12.28195	11.91394	12.17590	11.74135	12.10468	11.65337
8	15.69228	15.65594	15.54285	15.38823	15.41722	15.04889	15.31598	14.63398	15.23960	14.16776	15.18847	13.72878
9	16.72952	16.69916	16.60371	16.48099	16.49815	16.21814	16.41321	15.90822	16.34921	15.54531	16.30640	15.15677
10	18.16498	18.11613	17.94550	17.74196	17.76053	17.29041	17.61116	16.78024	17.49829	16.28160	17.42265	15.90517

TABLE 5.12 COMPARISON BETWEEN CALCULATED FREQUENCIES FOR DECREASE IN THE RIGID CONNECTION
---------- FOR WESTERHOUSE BRIDGE (HZ)

DECREASE IN ECCEN (mm) MODE	RESTART 700	FULL 700
1	2.603207	2.127887
2	3.121303	2.753876
3	6.461516	6.264807
4	8.680485	7.106551
5	9.731651	8.009440
6	11.38780	10.70062
7	12.06891	11.61721
8	15.16284	13.45043
9	16.28496	14.88471
10	17.38490	15.71057

TABLE 5.12 (CONT) COMPARISON BETWEEN CALCULATED FREQUENCIES FOR DECREASE IN THE RIGID CONNECTION FOR WESTERHOUSE BRIDGE (HZ)

MODE	RESTART	FULL	%ERROR
1	3.355038	3.082384	8.83
2	3.840385	3.877276	0.951
3	6.777163	6.755874	0.315
4	9.503167	3.940500	6.349
5	10.69533	10.52061	1.66
6	11.59439	11.58327	0.096
7	12.94698	12.85253	0.735
3	15.77663	15.57751	1.28
9	16.73137	16.61623	0.994
10	18.20879	18.00739	1.12

TABLE 5.13 EXAMPLE FOUR
---------- LOCAL COMPARISON RESULTS
(HZ)

DECREASE IN DENSITY MODE	RESTART 10%	FULL 10%	RESTART 20%	FULL 20%	RESTART 30%	FULL 30%	RESTART 40%	FULL 40%
1	3.219723	3.233507	3.352920	3.411469	3.481024	3.622467	3.604574	3.878175
2	5.221880	5.244172	5.437632	5.532308	5.645144	5.873832	5.845294	6.287560
3	6.104948	6.130892	6.356680	6.466847	6.598815	6.864354	6.832375	7.346714
4	6.370236	6.397438	6.633472	6.749006	6.886654	7.165725	7.130854	7.670568
5	7.731189	7.763896	8.049351	8.188198	8.355404	8.690614	8.650638	9.298466
6	8.641028	8.677614	8.996917	9.152201	9.339254	9.714027	9.669478	10.39340
7	9.176129	9.212212	9.541418	9.694252	9.893229	10.26107	10.23295	10.94102

TABLE 5.14 COMPARISON BETWEEN CALCULATED FREQUENCIES FOR DECREASE IN DENSITY
---------- FOR BAILLIESTON INTERCHANGE

EXAMPLE	FULL TIME (S)	RESTART TIME(S)	% OF FULL ANALYSIS
SKEW SLAB(MAX)	354.9	73.1	20.6
BEAM ELEMENT	44.1	10.0	22.7
SOUTHFIELD	135.6	27.8	20.5
WESTERHOUSE	360.3	36.7	10.2
BAILLIESTON	3362.0	278.8	7.2
MODEL BRIDGE	38.5	891.5	4.3

TABLE 5.15 AVERAGE PERCENTAGE SAVING IN COMPUTER TIME

NUMBER OF ELEMENT / MODE	RESTART 2	FULL 2	RESTART 8	FULL 8	RESTART 18	FULL 18	RESTART 32	FULL 32	RESTART 50	FULL 50	RESTART 72	FULL 72
1	0.836635	0.834302	0.836627	0.828084	0.836616	0.819393	0.836605	0.810440	0.836594	0.802231	0.836583	0.793705
2	0.986542	0.981792	0.986538	0.976061	0.986534	0.970121	0.986528	0.961595	0.986521	0.950581	0.986511	0.935919
3	2.371437	2.367830	2.371437	2.355812	2.371437	2.337892	2.371436	2.315329	2.371436	2.285434	2.371435	2.249744
4	3.468227	3.461967	3.468227	3.450558	3.468227	3.429449	3.468227	3.393721	3.468227	3.342783	3.468227	3.290249
5	4.547184	4.530245	4.547184	4.496229	4.547184	4.466344	4.547184	4.425878	4.547184	4.374245	4.547184	4.313840
6	5.609784	5.605374	5.609784	5.590412	5.609784	5.561639	5.609784	5.504644	5.609784	5.422521	5.609784	5.321911
7	7.550049	7.541549	7.550049	7.505041	7.541549	7.424299	7.541549	7.321846	7.541549	7.218941	7.541549	7.162608
8	8.089236	8.083347	8.089236	8.064332	8.089236	8.026590	8.089236	7.948478	8.089236	7.827950	8.089236	7.674129
9	10.09028	10.06489	10.09028	10.02476	10.09028	9.927666	10.09028	9.813363	10.09028	9.714748	10.09028	9.572489
10	10.47188	10.46123	10.47188	10.42266	10.47188	10.33324	10.47188	10.21444	10.47188	10.05432	10.47188	9.934498

TABLE 5.15 COMPARISON BETWEEN FULL ANALYSIS AND JUST EQUATION 3.150 APPLIED TO THE FULL STRUCTURAL MATRICES
---------- (HZ)

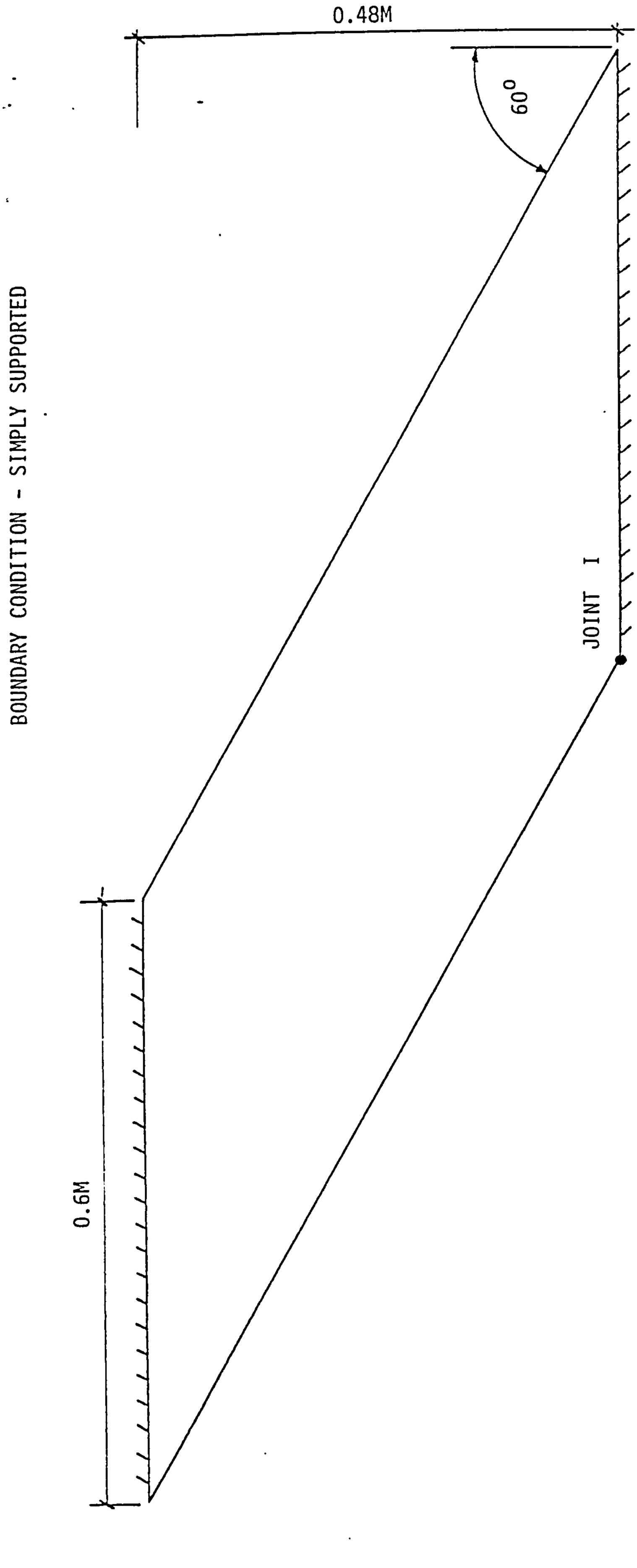

FIGURE 5.1 DIAGRAM OF EXAMPLE ONE - SKEW ISOTROPIC SLAB

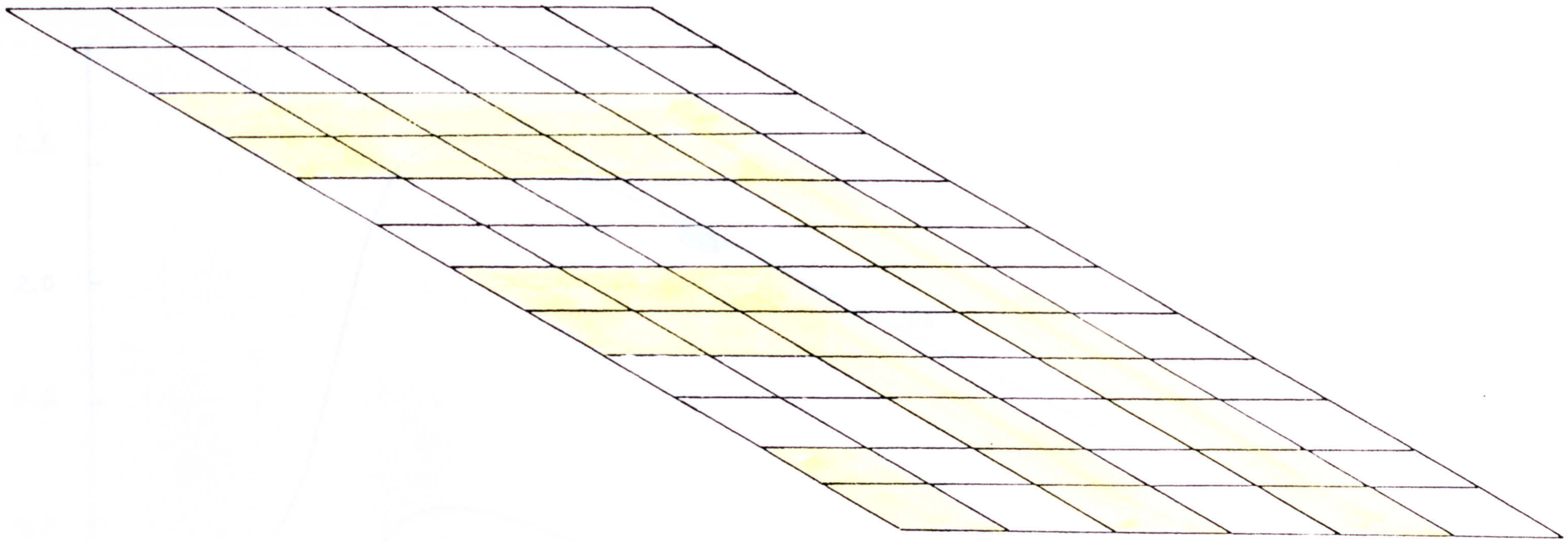

FIGURE 5.2 ELEMENT MESH FOR A SKEW ISOTROPIC SLAB SHOWING ELEMENT GROWTH CHANGE

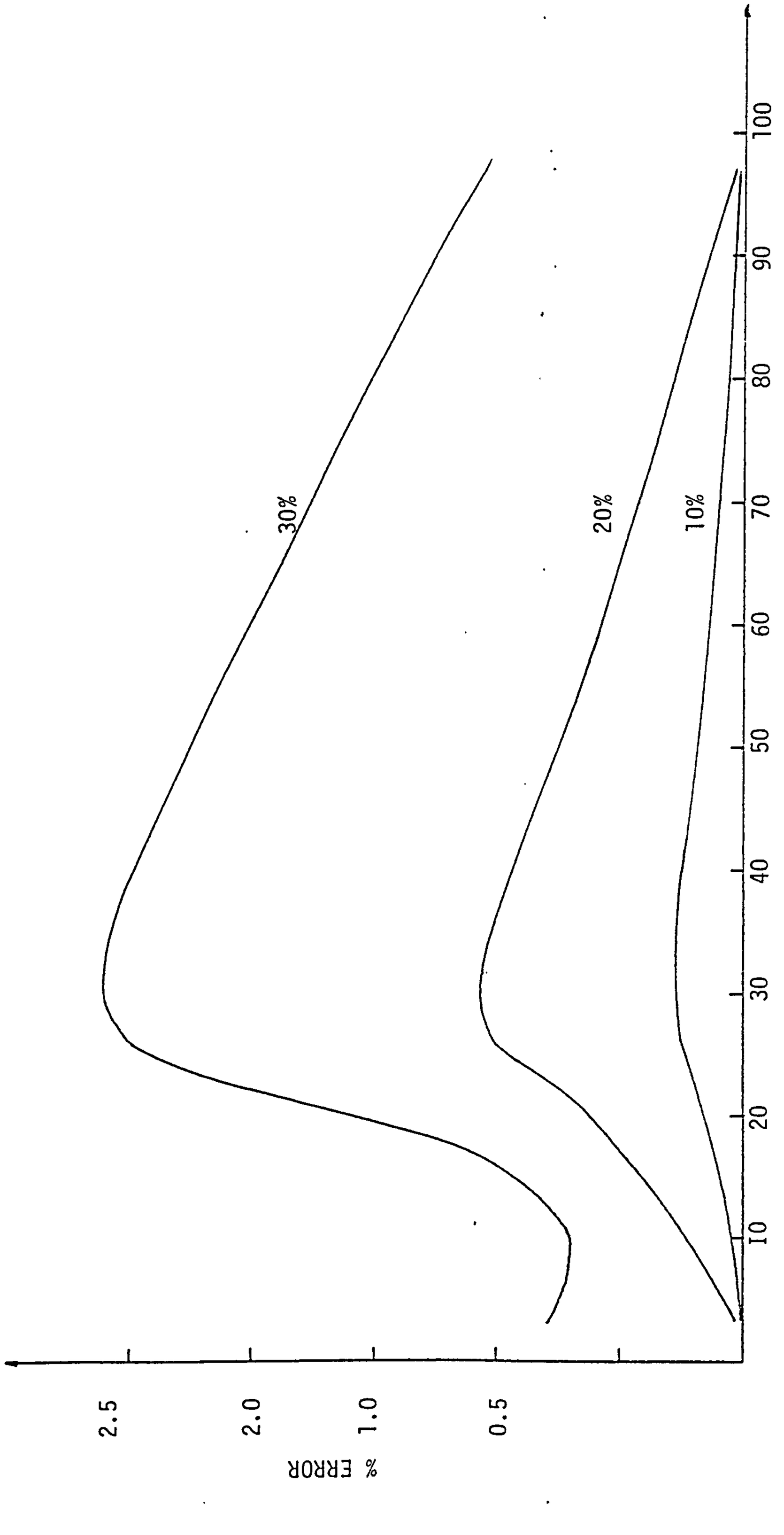

FIGURE 5.3 ENVELOPE OF ERRORS FOR 10,20,30% CHANGE IN YOUNG'S MODULUS OF A SKEW SLAB

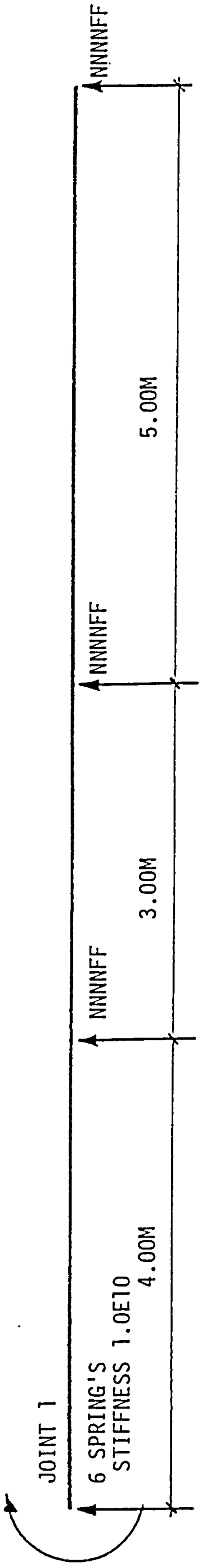

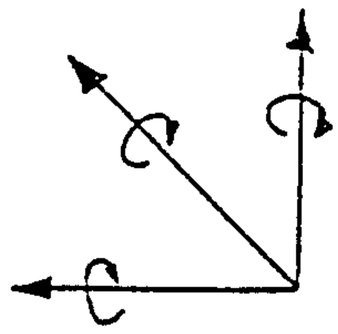

Ux,Uy,Uz,Rx,Ry,Rz
N DENOTES NOT FREE
F DENOTES FREE

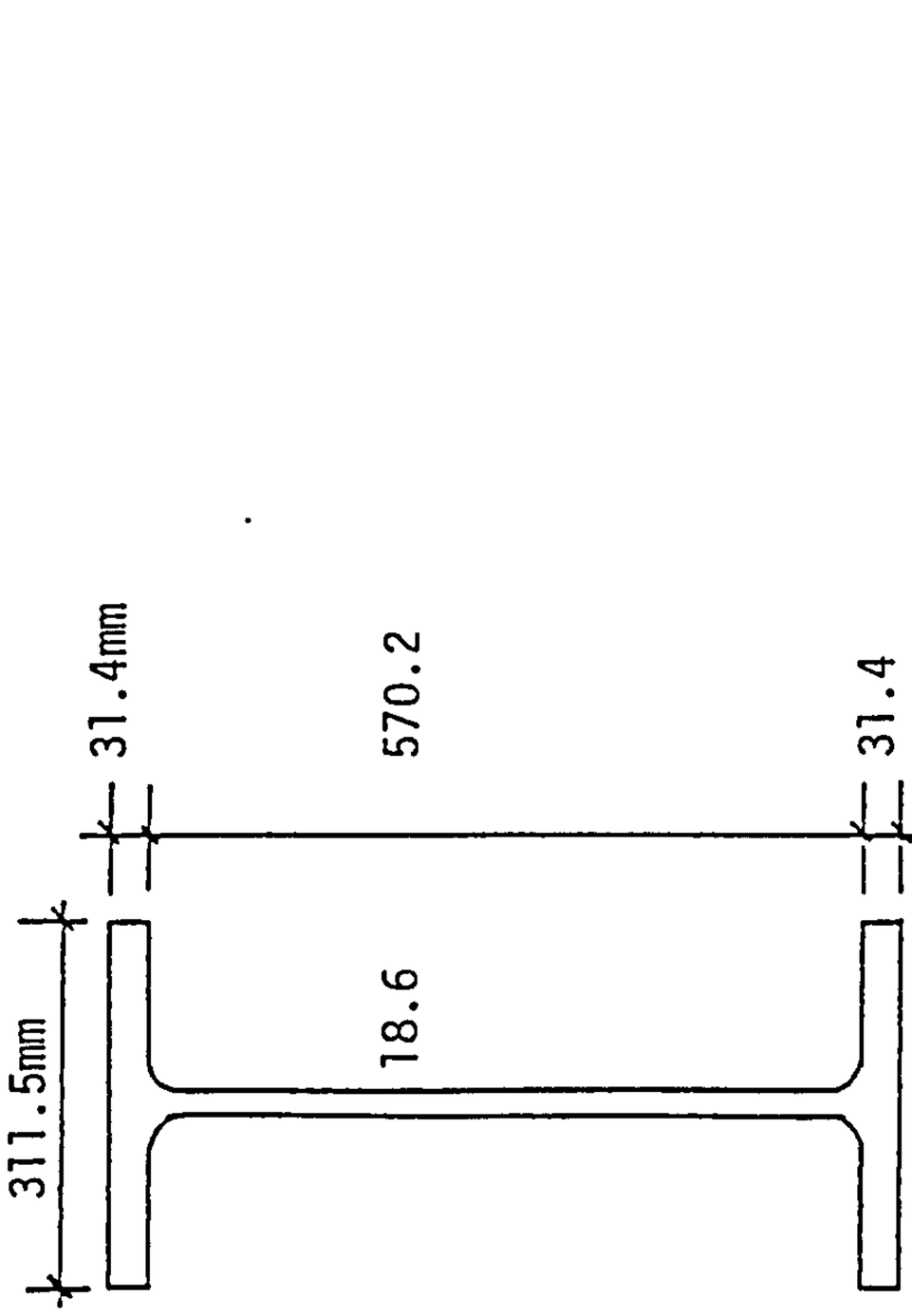

SECTION
OF
610*305*238Kg UB

FIGURE 5.4 DIAGAM OF EXAMPLE TWO - BEAM ELEMENT PROBLEM

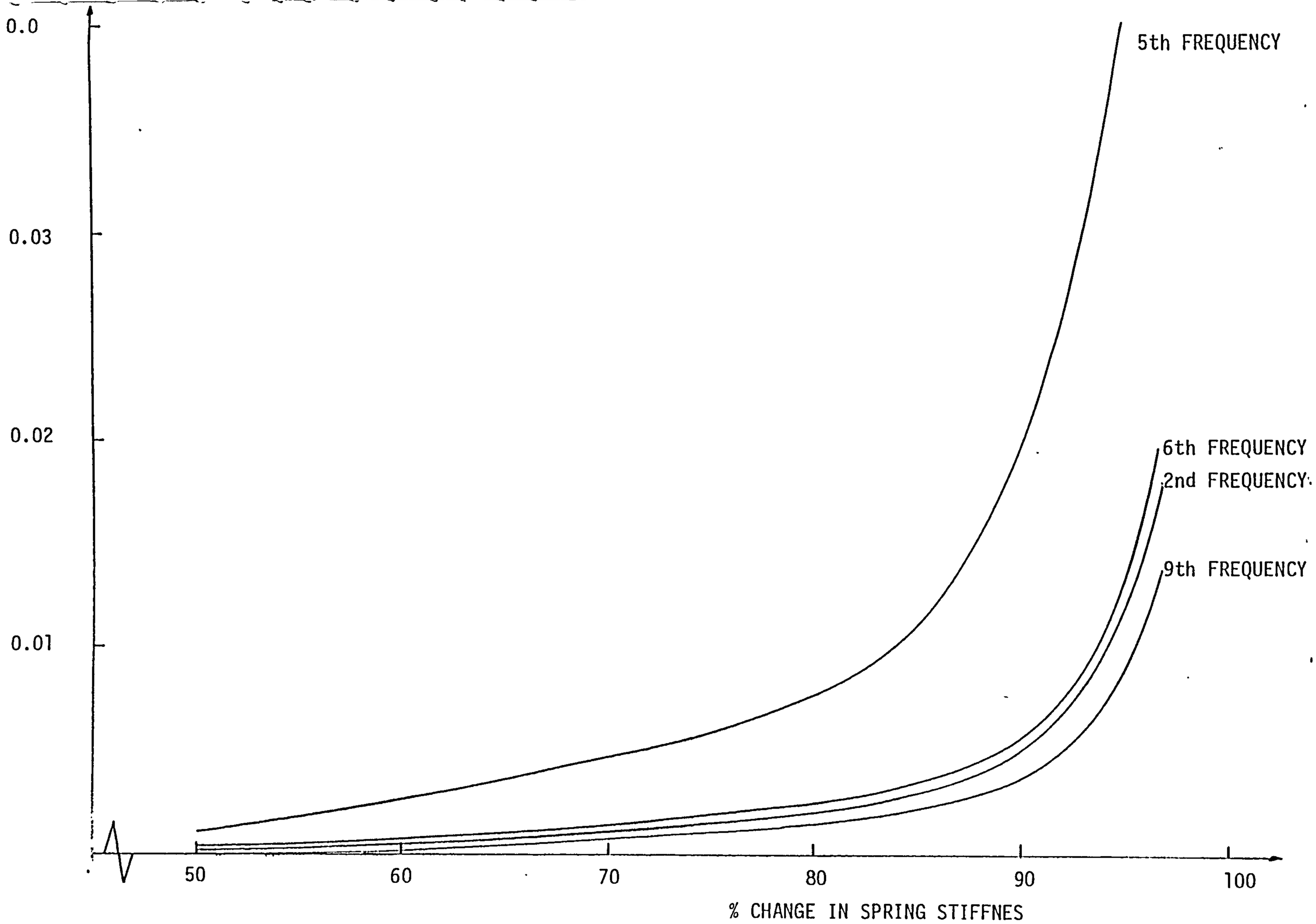

FIGURE 5.5 ERRORS IN FREQUENCIES FOR CHANGE IN SPRING STIFFNESS IN JOINT 1 OF THE BEAM ELEMENT PROBLEM

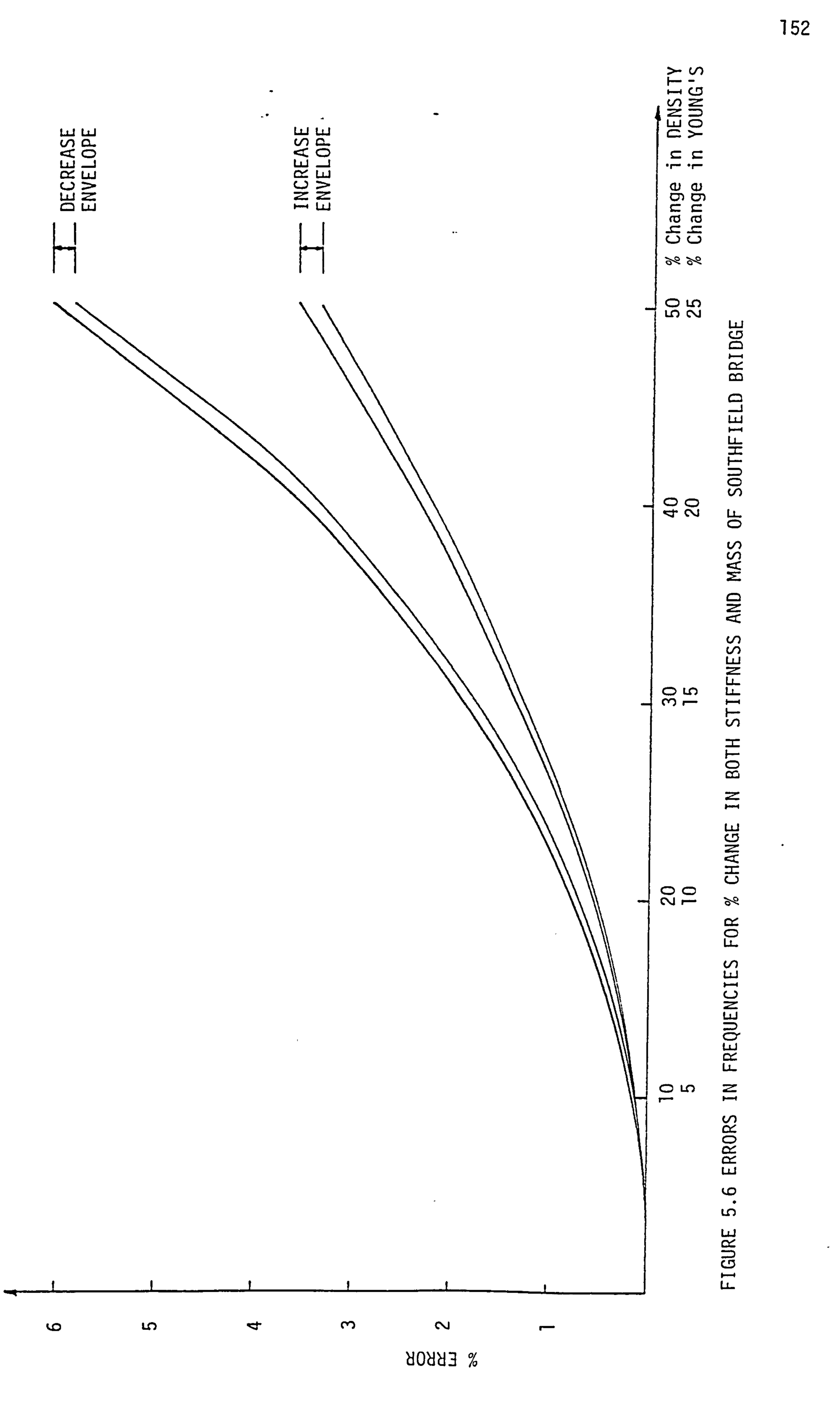

FIGURE 5.6 ERRORS IN

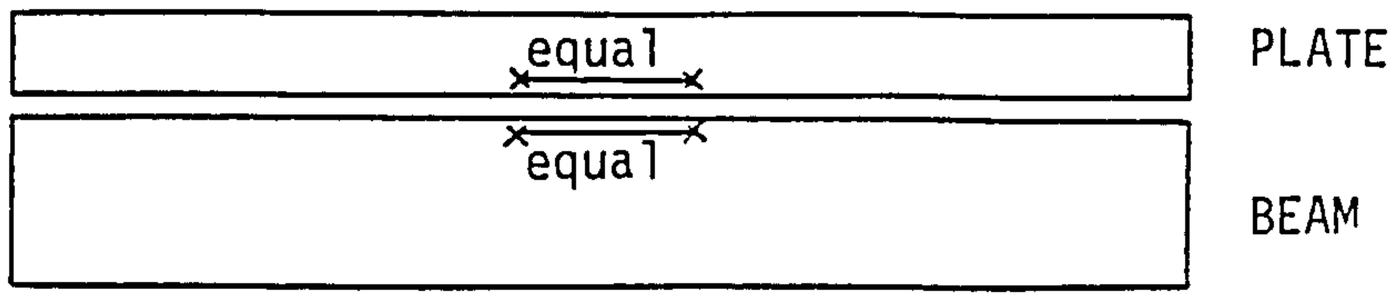

(a) COMPOSITE SECTION
BEFORE DEFLECTION

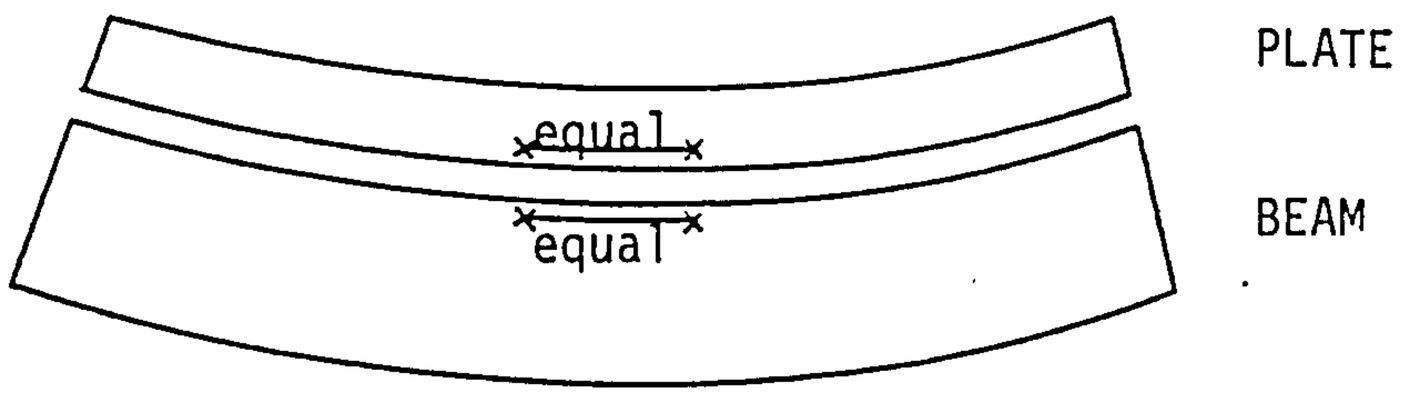

(b) COMPOSITE SECTION
AFTER DEFLECTION

Diagrams show that a composite section, after deflection, the strains at the interface are constant in both materials

FIGURE 5.7 STRAINS AT INTERFACE OF A COMPOSITE SECTION

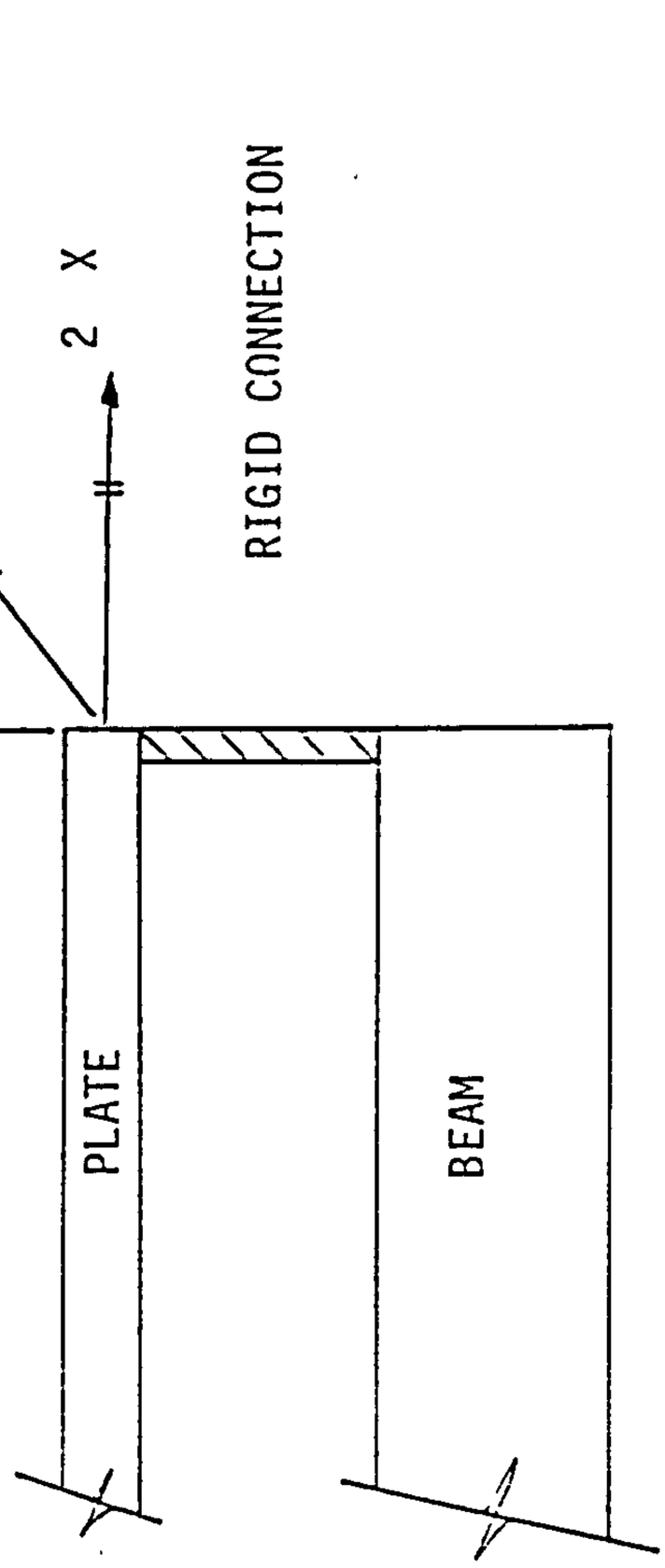

(a)

FIGURE 5.8 EQUATIONS OF STIFFNES TRANSFER FOR A RIBBED SLAB ANALYSIS

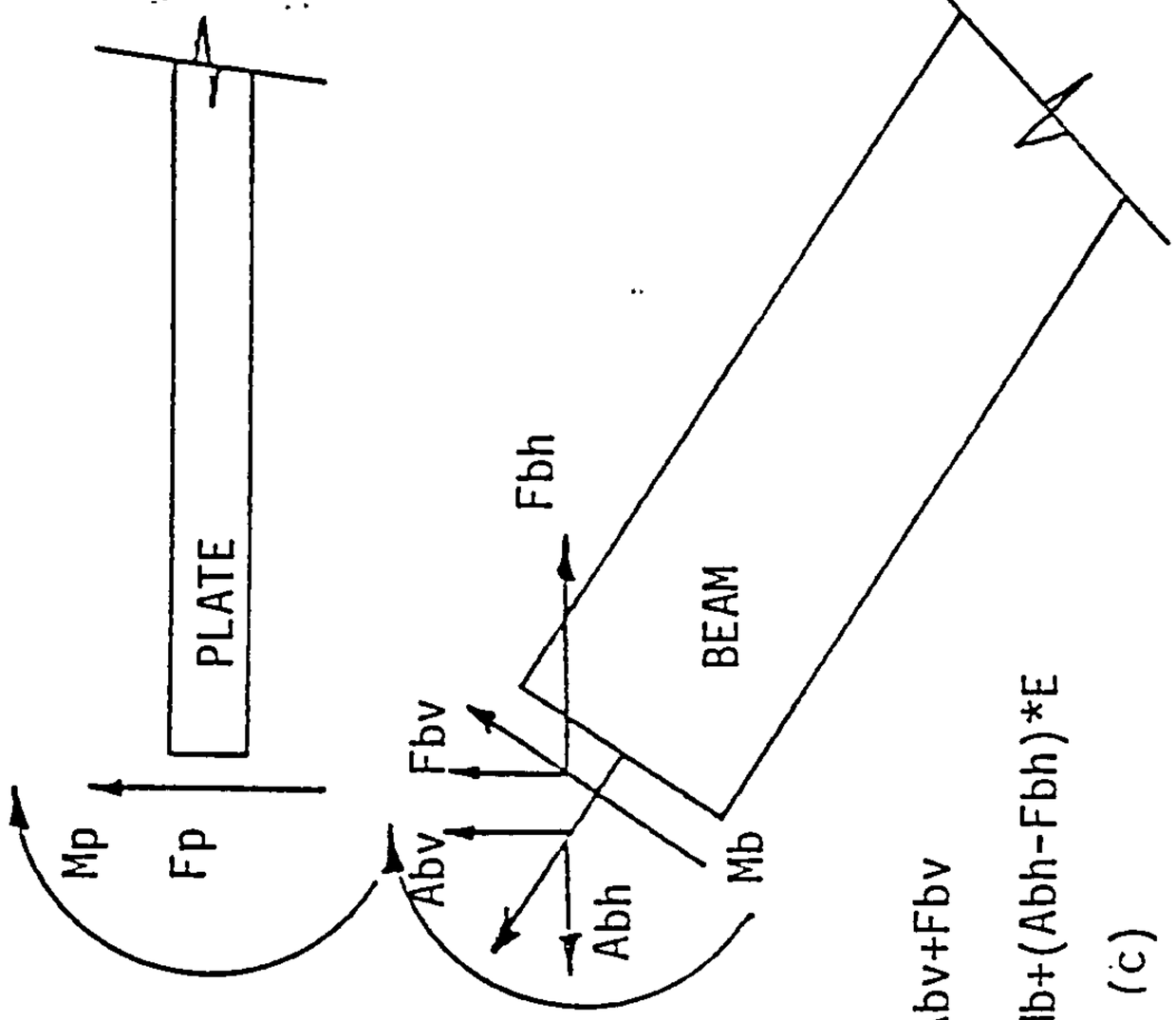

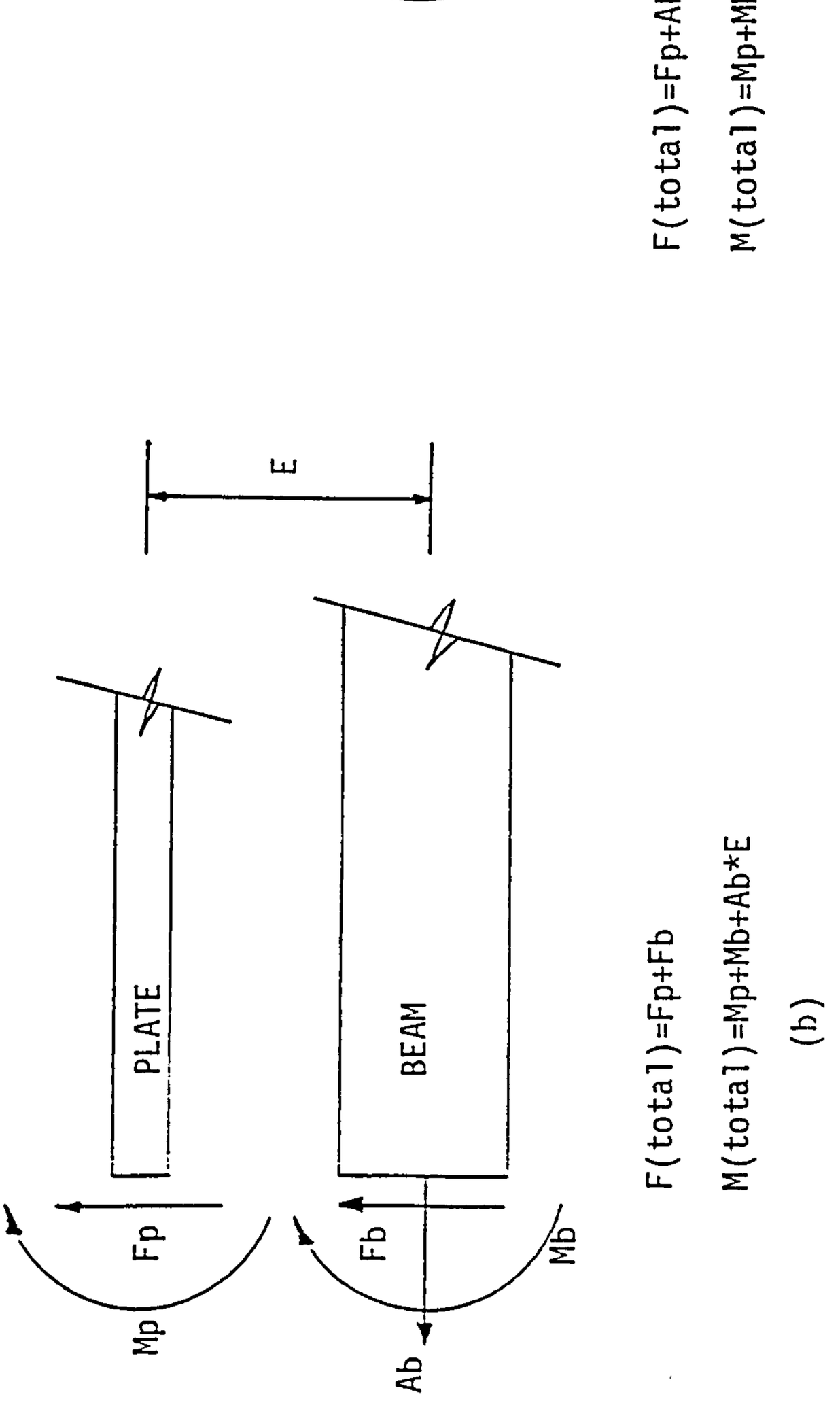

FIGURE 5.8 EQUATIONS OF STIFFNESS TRANSFER FOR A RIBBED SLAB ANALYSIS

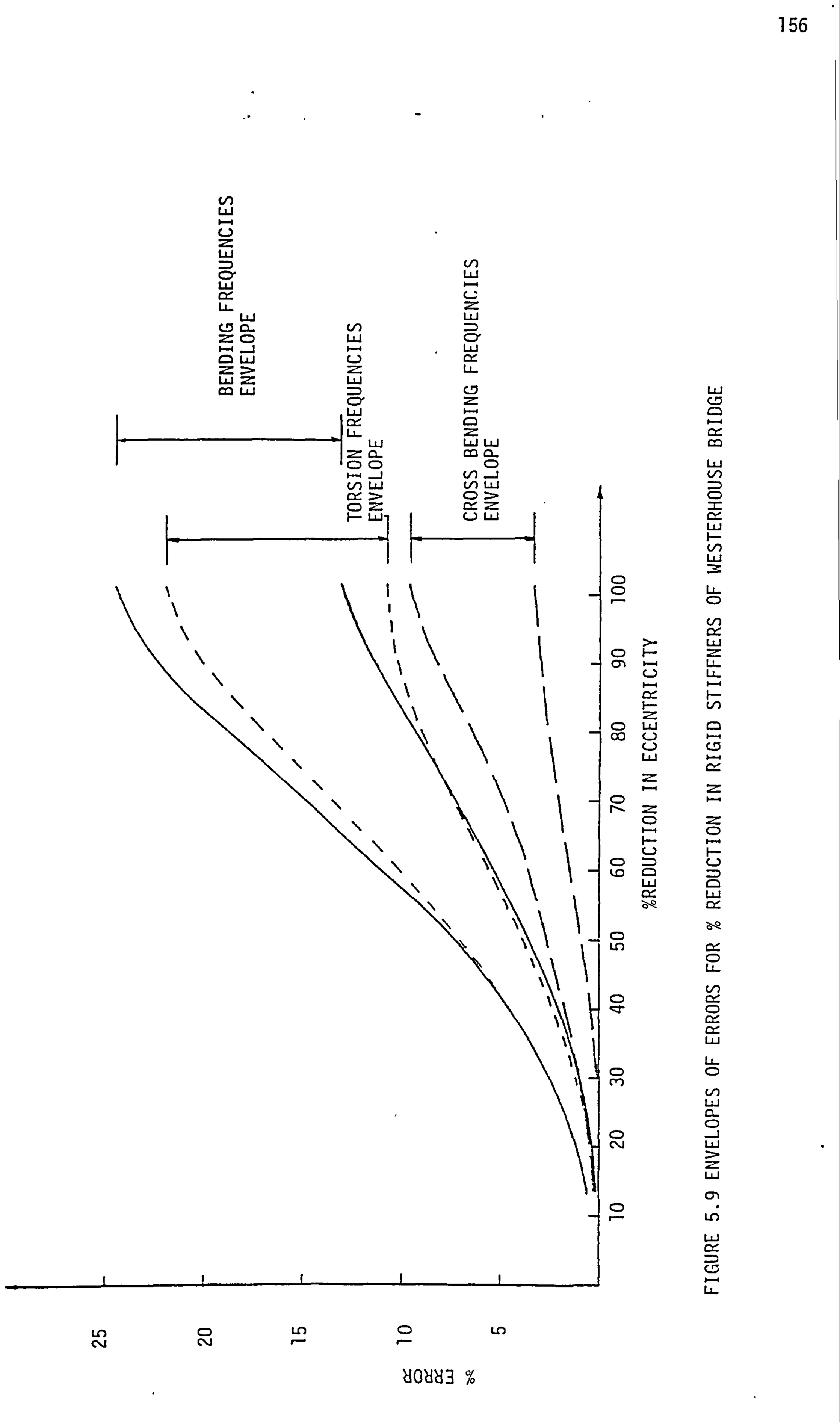

FIGURE 5.9 ENVELOPES OF ERRORS FOR % REDUCTION IN RIGID STIFFNERS OF WESTERHOUSE BRIDGE

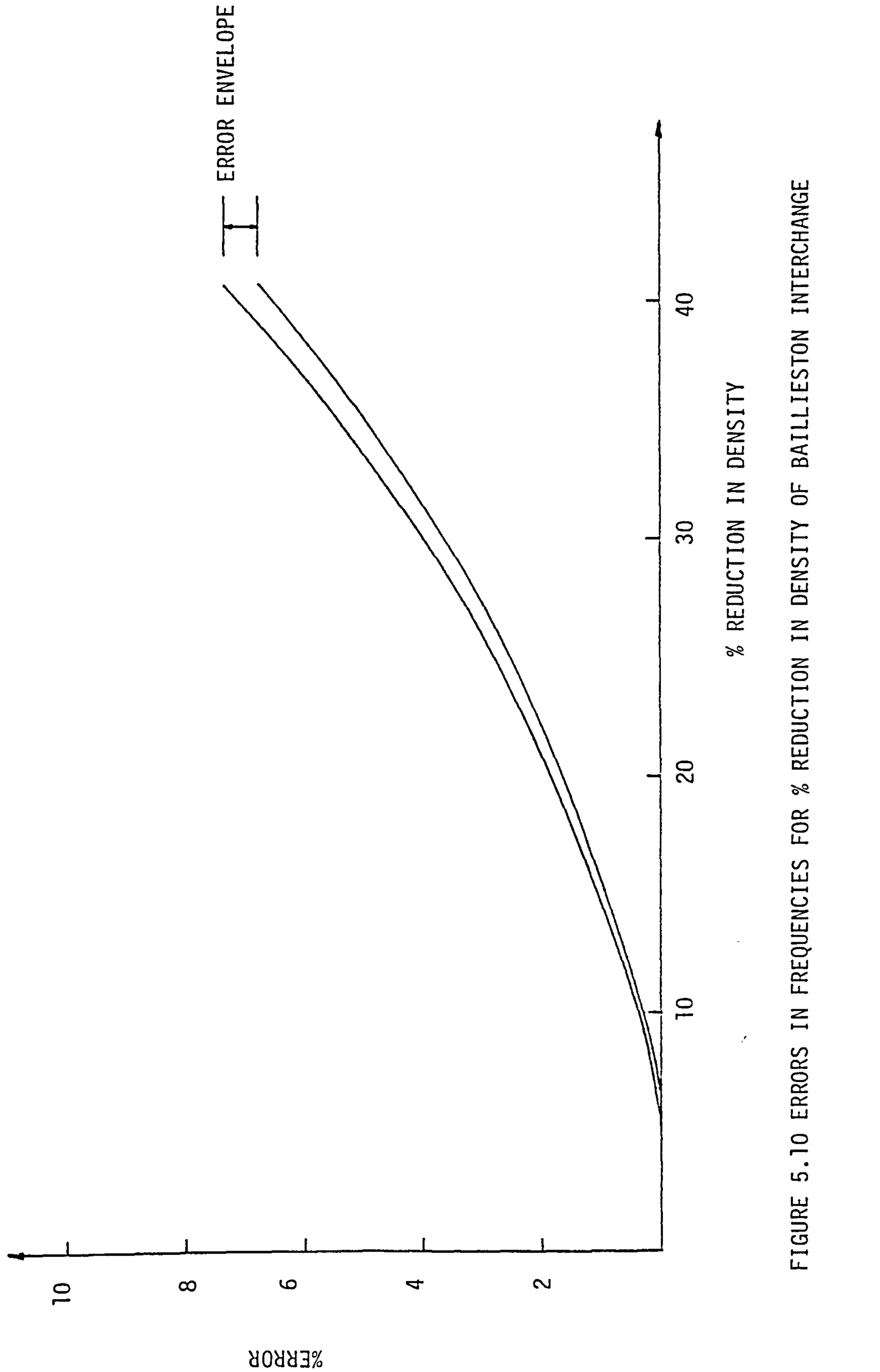

FIGURE 5.10 ERRORS IN

```
BEGIN
SKEW ISOTROPIC SCAB
PLATE 91 72 72 EIGENVALUES DYNAMIC 10
MATRIX 7 13 JOINT 1 1 7 COOD 0·0 PLUS 10·0 AND -6·928 4·0
*
ISOTROPIC 75·0E9  0·215  1·2 TYPE 3 TO 72
ISOTROPIC 67·5E9  0·215  1·2 TYPE 1 TO 2
MASS 2·4E3 TYPE 1 TO 72
*
MATRIX 12 6 ELEMENT 1  JOINT 2 9 8 1
*
TYPE   1 72 ELEMENT 1 TO 72
*
N F F  JOINT 1 TO 7
N F F  JOINT 85 TO 91
*
*
*
DYNAMIC PRINT 10 RESTART
*
*
*
```

DATA INPUT FOR FULL ANALYSIS OF SKEW SLAB

```
RESTART
*
ISOTROPIC  75·0E8  0·215  1·2 TYPE 1 TO 2
*
*
*
*
*
*
*
*
*
*
*
```

DATA INPUT FOR RESTART ANALYSIS OF SKEW SLAB

EXAMPLE DATA INPUT FOR DYNAMIC REANALYSIS

FIGURE 5.11

```
BEGIN
BEAM  ELEMENT  PROBLEM
SHELL  14  12  12 EIGENVALUES  DYNAMIC  10
JOINT 1   COOD  0.  PLUS  1·0   JOINTS  2  TO 13
JOINT 14  COOD  0.  1·0
*
BEAM 210·E9  81·E9  303·8E-4  82·1E-4  168·8E-4  2·895E-6
     20·8E-4  1·58E-4    TYPE  1  TO 12
MASS 77·0E3    TYPE  1  TO 12
*
BEAM 1  JOINT  1  2  14  PLUS  1 1  ELEMENTS  2  TO 12
*
TYPE 1 12  ELEMENTS 1 TO 12
*
0·5E10  0·5E10  0·5E10  0·5E10  0·5E10  0·5E10 JOINT 1
NNNNFF   JOINT  5  8  13
*
*
*
*
DYNAMIC  PRINT  10  RESTART
*
*
*
*
```

DATA INPUT FOR FULL ANALYSIS OF BEAM PROBLEM

```
RESTART
*
*
*
*
*
0·5E10  0·5E10  0·5E10  0·5E10  0·5E10  0·5E10  JOINT 1
*
*
*
*
*
*
*
*
```

DATA INPUT FOR RESTART ANALYSIS OF BEAM PROBLEM

EXAMPLE DATA INPUT FOR DYNAMIC REANALYSIS

FIGURE 5.12

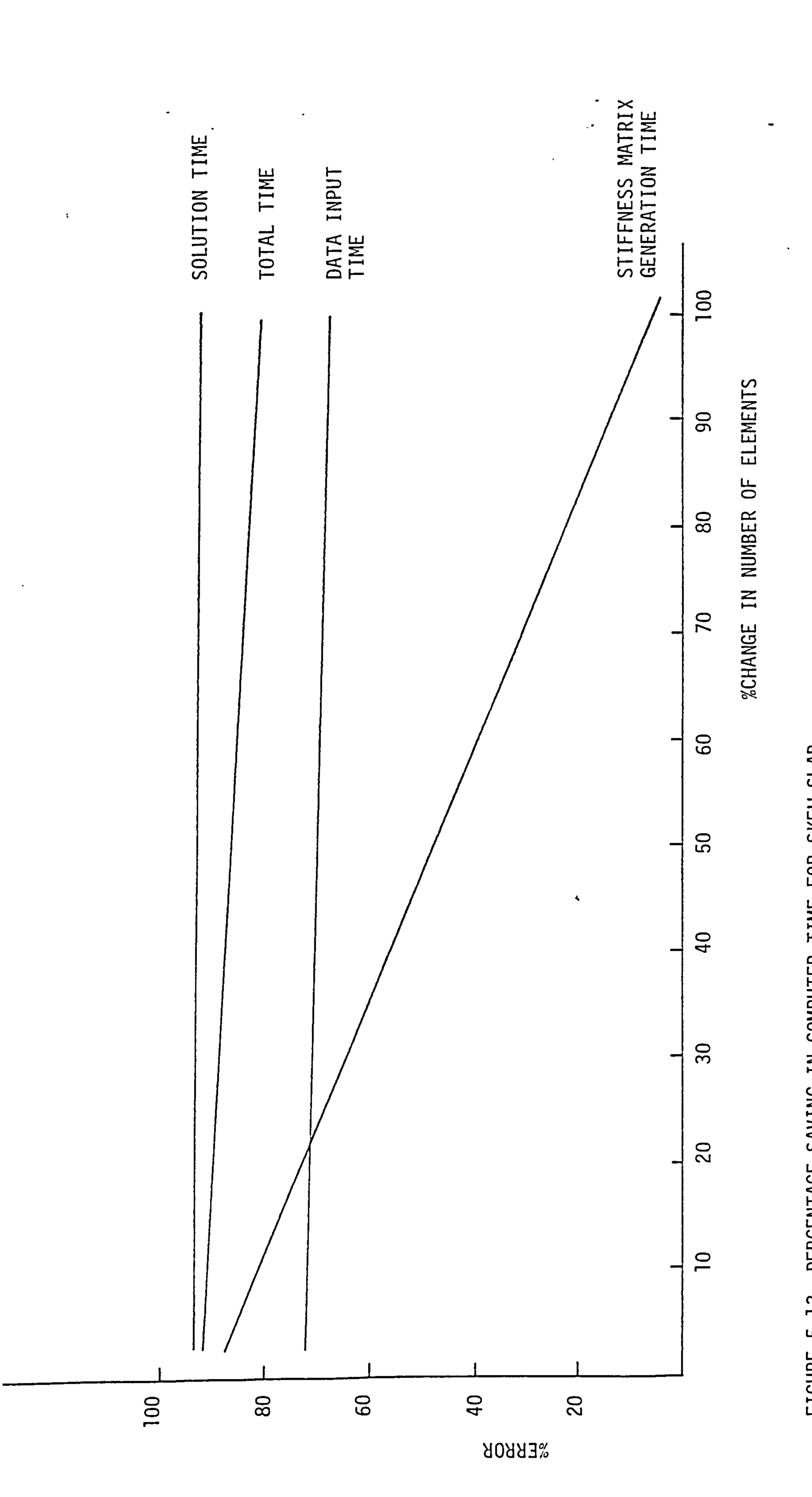

FIGURE 5.13 PERCENTAGE SA

SECTION TWO

CONTENTS OF CHAPTER 6

CHAPTER 6 RESPONSE MEASUREMENT

6.1 Introduction

The literature review of chapter 1 identifies several studies (Ref 17) where response analysis has been used to monitor the long-term integrity of structures. The proposals made in this study are to extend the technique to bridge structures. Dynamic monitoring is generally more expensive than visual inspection. For oil rigs, however, since large parts of the structure are inaccessible, i.e. below the water line, dynamic monitoring is less expensive than visual inspection. When the technique is extended to bridges the overall structure is more accessible for inspection, but parts which may deteriorate and affect the structural integrity are less accessible, e.g. internal stiffness in box structures, the deck under the bitumen pavement. If dynamic monitoring is to be extended to bridge structures it is desirable to develop methods which reduce costs and are more attractive or simpler to apply.

The cost differences between dynamic monitoring and visual inspection are associated with two factors. Firstly, dynamic monitoring analysis requires the construction of a large number of finite element models. Each model is associated with a change to the original structural configuration and the range of changes must be comprehensive enough to cover the most likely sources of deterioration in the sturcture. For each model the response of the structure must be evaluated. The techniques developed in chapters 2 to 5 considerably reduce the cost of computer modelling. Secondly high costs arise from the method of frequency extraction from the random signal produced by the accelerometers used in the response measurements. The Maximum Entrophy Method used in earlier dynamic response monitoring (Ref 7), requires the use of large amounts of computer equipment. It may be possible to reduce costs by using simpler methods of measurement of natural frequencies. Such techniques are developed and described in this chapter.

In order to assess the applicability of the technique to bridge structures experimental evidence is required to show that these simpler methods can be used to measure the dynamic responses of bridge structures. Also evidence is required to show that changes in dynamic response can be used to identify changes that have occurred in the structure.

The following possibilities were considered to provide the experimental evidence to validate the simplified measurement techniqes and to correlate changes in structural integrity with changes in dynamic response.

a) Monitoring of a real structure

This proposal has the attraction that, if a real structural change occurs during the monitoring period and the change can be correlated with calculated response, the technique is proved to work. The disadvantages of this approach are : firstly the period of the study is indeterminate. Structural Monitoring Limited's study of the bridges described in chapter 2 (Ref 17) lasted 18 months during which time the dynamic response did not change. Secondly, structural changes may occur which are not apparent to visual inspection and hence are difficult to quantify.

b) Monitoring of a real structure with controlled structural changes introduced systematically.

This approach has all the advantages of the previous proposal and in addition measured structure changes can be introduced in a systematic way and the structure monitored to see if correlation is achieved. The disadvantage is one of availability of a suitable bridge structure and the possibility of making structural changes to it.

c) Fabrication and Monitoring of a Simple Laboratory Model

This approach has the advantage that simple measurable structural changes can be introduced into the model in a controlled environment. The disadvantage is that it may not be valid to extrapolate the model response to that of a real structure.

Since there was a limited period of time available for the experimental study, it was important to be able to introduce known structural changes in a controlled environment. It was decided to construct a simple laboratory model.

6.2 Design and Construction of the Test Model

6.2.1 Choice of the Structural Form

The dimensions of the model were based on a footbridge over the river Kelvin in Glasgow. The footbridge, Figure 6.1, is part of the river's walkway system and is situated just north of Great Western Road in the West End of Glasgow. The footbridge is of composite construction, with two steel I-Beams running along the length of the deck and supporting a concrete slab with a light bitumen pavement. The steel I-Beams are supported on two concrete abutments.

6.2.2 Identification of Possible Structural Changes in the Footbridge

During the lifetime of a structure a number of different changes may occur which affect the structural stiffness and/or the mass. These may result from natural wear and tear or from modifications to the structure. These changes could be associated with the following effects:

i) cracking of the reinforced concrete deck which, depending on location, may cause a loss of structural stiffness and mass

ii) reduction in shear transfer between the steel I-Beams and the concrete deck so that the deck and stiffening beams act independently in the affected region at a reduced overall stiffness

iii) increased friction in the support region which may result in a change in structural stiffness associated with change in boundary conditions.

iv) delamination of the bitumen pavement which may result in a loss of structural stiffness of resurfacing which may result in a change in mass.

v) differential displacement between support regions may result in loss of structural stiffness during the lifetime of the structure.

6.2.3 Techniques of Modelling Structural Changes in the Footbridge -

It is desirable that the laboratory model should be capable of modelling the possible changes to the real structure listed above. The model therefore incorporates the following features :

i) The deck and stiffening beams are fabricated separately and can be caused to act together by discrete shear connection along the line of the stiffening beams. To simulate reduction in shear transfer, groups of these discrete shear connections would be removed.

ii) The support system of the model is constructed with independent bearings so that a differential displacement can be introduced by altering the relative levels of the individual supports. Individual bearings should also have the facility of introducing different degrees of restraint against translation and rotation.

iii) Cracking in the concrete deck can be simulated by fabricating the deck and stiffening beams separately, and by varying the model material of the different components. The reduced stiffness of the cracked deck is modelled by a lower modulus in the model deck. Also if a selection of stiffening beams are fabricated with different second moments of area these beams can be used to simulate different levels of corrosion.

In the limited time available to carry out this study not all the above changes could be studied. The following changes were chosen because they would be easy to introduce into the model and involved the construction of only one deck and one set of stiffening beams:

i) restraint of the bearings;
ii) differential displacement of the bearings;
iii) loss of shear connection between the I-beams and the deck.

6.2.4 Definition of the Test Model

To keep the model as simple as possible it was decided to construct the model from one material, perspex. Also for simplicity the number of different thicknesses of perspex was kept to a minimum, using 1/2" (12.7mm) for the bridge deck and 1/4" (6.3mm) for all the other members.

The model, shown in Figure (6.2) was of composite construction with two perspex I-Beams running along the length of the perspex deck. Three small perspex channel cross beams (see Figure 6.2) were used to give lateral stability to the longitudinal perspex I-Beams. The stiffening I-beams and the bridge deck were connected together with screws at 50mm centres. Loss of shear connection between the deck and the beams could be simulated by removing these screws.

The bridge supports were designed in such a way as to allow free rotation in support type A, Figures 6.3; 6.5; 6.24. In this case the changes in boundary conditions especially rotation were not intended to produce zero rotation, but rather the sort of restraint that might arise in practice. Rotation could be constrained by grub screws in the perspex bridge and the support brackets as shown in Figure 6.6. Rotational and translational movement were allowed by constructing bearing type B, Figures 6.4; 6.5; 6.25. This bearing could constrain translational and/or rotational movements by using the metal blocks, grub screws, and the black bolts shown in Figure 6.7. To help free rotation and translation in all bearing types, grease was applied to all surfaces.

The differential displacement could be introduced into the model by placing small thin plates, shims, under the bearings where differential displacement was required.

6.3 Design and Construction of the Test Rig

The test rig was connected to the laboratory floor with the bridge model located on it, clear of the floor to allow access underneath for an energy input device. The support frame had also to accommodate the following features :

a. it had to be possible to isolate the test rig from the random vibrations of the building

b. the fundamental frequency of the test rig had to be higher than the highest natural frequency of the bridge model to be recorded.

c. it had to be possible to move the energy input device so that the model can be vibrated at different locations.

6.3.1 Supporting Framework

The above requirements were met by using the double frame arrangement shown in Figure 6.8. The springs between the two frame systems (part A and B of Figure 6.8) isolated one system from the other. The frequencies of the springs separating the two rigs were selected so that the valve of transmissibility was as low as possible. Transmissibility is a measure of the amount of vibration transmitted through an isolation system. It is a function of damping and the ratio of the fundamental frequency of the element being isolated and of the fundamental frequency of the isolation system. For satisfactory isolation of two systems a minimum value of 2 is recommended (Ref 2).

The finite element analysis of the bridge (Chapter 7) gave the first ten natural frequencies within the range of 40-350Hz. Hence the support frame had to be designed to have a fundamental frequency greater than 350Hz. For the dimensions given in figure 6.8 the calculated fundamental frequency of the testing rig frame was 465Hz. The ratio of the fundamental frequency of the frame to that of the springs was =20 which produces a value of transmissibility of less than 0.1 in figure 6.9.

In order to be able to apply an excitation force at different locations, the vibrator could be placed at eight positions along the length of the bridge structure and three positions across the width. See Figure 6.10, 6.11.

Three types of excitation, viz, mass excitation, sine-wave excitation, and random-wave were attempted. the sine-wave excitation and random-wave excitation were applied to the structure through a connection which consisted of two small diameter rods which formed a "box" so that the small cross beams of the bridge would not effect the vibration system, and a longer diameter rod to connect the "box" with the appropriate vibration apparatus, see Figure (6.12) for details.

6.4 The Effects of Vibration on Young's Modulus of Perspex

Since the perspex bridge has to be vibrated a number of times under sine-wave excitation and random-wave excitation it was important to find out if sustained vibration would result in irreversible changes in material properties. Six 350x50x6mm thick perspex samples cut from the same perspex sheet as the longitudinal beams used in the bridge were tested.

There were two stages to this study. In the first stage, three of the six samples were vibrated, while the other three were used as the control samples. These samples were vibrated for $1x10^6$ cycles at frequencies of 480, 240, 120, 60, 30Hz with one hour relaxation time between frequencies. These frequencies and the vibration times are given in Table 6.1.

The second stage was to measure the Young's Modulus of the six samples, i.e. the three vibrated samples and the three control samples. After completing the study the variation of Young's Modulus between the vibrated and the unvibrated samples was less than 0.1%, so the effect of variations, of Young's Modulus due to vibration was neglected.

6.5 Evaluation of the Response of the Test Model

The dynamic response of the bridge model was measured under three types of excitation. In the first method, mass excitation, a large weight was suspended from the model and the structure was released from its displaced position by cutting the string connecting the weight to the model. This method proved to be unsuccessful for a number of reasons:

Because the model had a high flexural stiffness, large initial deformations were needed to excite more than the fundamental frequency. The loadings required to produce such deflections were excessive. In evaluating this method release loads of 12.7Kg were used, and release of this load did result in the first natural frequency being recorded. The recorded frequency was approximately 50Hz which coincides with the frequency of mains electricity. The effect of mains frequency interference could be reduced by increasing the magnitude of the release load, but it was clear that the method would prove unsuccessful since the bridge could not be isolated during this method of excitation.

6.5.1 Simple Sine Wave Excitation

From this simple excitation method a feeling of the response of the structure could be obtained. The simplicity of the excitation method limited the number of natural frequencies that could be excited at any particular input position. Therefore a study was necessary to determine how many different locations had to be used to generate all of the required frequencies.

A two dimensional structure like a bridge deck has three types of response modes, i.e. longitudinal bending, along the major axis cross bending along the minor axis, and torsion about the major axis. These mode types are shown in Figure 6.13. To excite the above modes by sine-wave excitation, two excitation positions were chosen. The first excitation location was chosen at the centroid of the model deck. This position is the most obvious in which to excite the fundamental frequency of the model. The second excitation location was at the 1/4 span of both the major and minor axis. This position was chosen to excite all longitudinal bending, cross bending and torsion response modes. Figure 6.14 identifies the vibrator position for both locations.

6.5.1.1 The Test Apparatus

In the sine-wave excitation study the experimental setup is shown in Figure 6.15. The basic components were the vibration system, the measurement system for the input signal, and measurement system for the output signal. Figures 6.15, 6.26 gives a line diagram and photograph of the equipment.

The vibrator system comprised :

a. a simusoidal generator, used to generate the simusoidal input which drives the vibrator;

b. an amplifier, rated power output of 300W, used to increase the input signal power to the vibrator;

c. a cooling fan, used to protect the moving coil assembly of the vibrator, from over heating;

d. the vibrator. This was a 400 series permanent magnet vibrator made by Ling Dynamic Systems Limted with a sine vector force (forced air cooled) of 196N.

Measurement system for the input signal :

Two accelerometers were used to measure the effect which the small rods forming the box of the vibration had on the input signal. The main accelerometer, the one used to measure the input signal was located above the connecting system on the bridge deck. See Figure 6.12. The signals of the above two accelerometers were processed as follows:

i) The signals from both the accelerometers were passed through a high impedance microdot cable. This high impedance cable was reduced to a low impedance cable by using a voltage amplifier. The reason for this impedance transfer is that if long lengths of cables are required on site where low impedance is necessary, so the loss of signal power would not be great.

ii) The signals from both accelerometers were fed through an oscilloscope, as the model resonance occurred which was associated with maximum amplitude on the oscilloscope screen.

iii) The signal from both accelerometers were passed through an attenuator and an amplifier which were used to decrease or increase the accelerometers' signals respectively before they were displayed on the oscilloscope.

iv. Permanent records of the input accelerometers' signals could be made on photographic paper by using an oscillograph.

Measurement systems for the Output Signals:

These signals were measured with similar duplicate instrumentation as the input signal, except that an oscilloscope was not used.

6.5.1.2 The Test Procedure

As was expected, the central vibration location (location b in Figure 6.14) only excited the fundamental frequency. The off-central vibration location (location a in Figure 6.14) was more successful in exciting higher modes, and only the results for this position are quoted.

Altogether nine tests were carried out with the vibrator position at location a and with the accelerometers placed at different locations. All the accelerometer positions were selected as anti-nodes of the first ten mode shapes found from the finite element analysis (Chapter 7). The number of accelerometers used for each test varied from 1 to 6 and depended on which natural frequencies were sought. In tests A, B, C, D a fixed number of natural frequencies were investigated, whereas in the remainder of the tests the maximum number of frequencies in the range of 40-500Hz were explored. Table (6.2) lists the tests and identifies the range of each study.

The test procedure was as follows:

Within a frequency range, the frequency fine control of the generator was adjusted until a point of maximum amplitude was recorded on the oscilloscope thus indicating a point of resonance. At this frequency, oscillograph traces of both the accelerometers measuring the input signals and the accelerometers measuring the response of the model were taken. With the input accelerometer being fixed in position, the use of the oscilloscope at higher frequencies proved to be unsuccessful since resonance could not easily be obtained.

To overcome this difficulty the output signals were examined through the oscillographs for a number of fine adjustments to each frequency until points of resonance were noted.

The results were measured from the input oscillograph traces as follows : the photographic paper of the oscillographs was fed through the oscillograph at a known speed, so that by measuring the distance along the trace for 20 cycles, the time for 1 cycle, and hence the frequency could be calculated.

6.5.1.3 Test Results

The frequencies measured for each test are given in the form of a Histogram in figure 6.16. Also given in this figure are the averages of these measured frequencies, and the natural frequencies calculated using the finite element model described in chapter 7.

Table (6.3) gives the average frequencies in numerical form, and the number of frequencies used to calculate these averages. By comparing the numerical frequency with the histogram it can be seen that these frequencies have been calculated within $\pm$10Hz.

By comparing the phase differences between the output signals, the mode shapes could be deduced. These modes are given in Table (6.3). Modes greater than the 5th mode were difficult to obtain, since at higher frequencies correlation was difficult owing to the considerable scatter of results, and hence interpretation for the mode shapes was impractical.

The effect of the small rods used in the device connecting the vibrator to the bridge was found to be insignificant, i.e. no difference was found between each trace.

6.5.1.4 Conclusion

In general the method of sinusoidal response measurement, as given in this section is a very simple method of measuring response, but it has two great disadvantages:

i) at higher frequencies resonances are difficult to detect

ii) the method is very time consuming

This method of excitation has the advantage that it is very simple to use and the user can get the feeling of the response of the structure from the accelerometer traces produced by the oscillograph very easily. The method although it may work successfully in the laboratory to evaluate the model response, it would be difficult to translate into a practical technique.

6.5.2 Random Wave Excitation

There are a number of methods of exciting bridge structures randomly. These include traffic flow, energy input devices etc., and are described in detail in Chapter 1. In this study an energy input method was used. This technique has the advantage that random vibration signals resulting from random vibration at a single location can be separated into a range of discrete natural frequencies. Success with the method depends on the number and location of accelerometers, and therefore a preliminary study was necessary to find the best locations and number of accelerometers required.

Although the technique has been applied successfully to a number of structures, in order that the method is cost effective when applied to bridge structures, simpler techniques must be developed. Hence the principal aim of this preliminary study was to produce a simple and inexpensive alternative to the rather expensive method of vibration monitoring which has proved to be successful for offshore platforms (Ref 17).

6.5.2.1 The Test Apparatus

There were four components in this test setup and the equipment used in each of the components is described in the following sections. Figures 6.16, 6.27 gives a line diagram and photograph of the test arrangement.

6.5.2.1.1 Vibration System

The vibration system comprises :

Random Noise Generator. The generator used was a Bruel and Kjaer Random noise generator which produces a Gaussian random noise signal with a uniform spectrum density, (also termed WHITE RANDOM NOISE), in the range 0-4000Hz. After a time T the signal output for each frequency is constant. This generator was used to drive the vibrator randomly and for all experiments the signal output was kept constant at 1 volt.

Band Pass Filter. The filter was a Barr and Stroud EF3. These filters allow only adjustable frequency ranges to pass and since from the finite element analysis it was shown that the first ten natural frequencies were below 500Hz, the filter was adjusted to pass frequencies in the range 0-500Hz.

Amplifier. The amplifier, a 1000w Ling Dynamics Ltd. Amplifier, was used to increase the signal input to an input signal to the vibrator of average valve of 1 amps R.M.S.

Vibrator. The Vibrator was a V455 series permanent magnet vibrator by Ling Dynamics Ltd. with a 1101b peak thrust force, air cooled to prevent overheating.

6.5.2.1.2 Response Measurement

Response measurement was made by using accelerometers. The signal from each accelerometer was fed into a microdot cable, and since the cable has a high impedance a voltage amplifier was used to convert the signal to low impedance. The signals from each of the accelerometers, up to a maximum of eight, were recorded on a frequency modulated (FM), eight channel tape recorder.

6.5.2.1.3 Signal Calculation

The background noise from the tape recorded signals from the accelerometers was filtered out through the use of band pass filters. Two filters were used since the analyser could deal with two accelerometer output signals simultaneously. A Hewlett Packard HP 3582A dual channel spectrum analyser was used to calculate the response spectra of the dual signals using the fast fourier transform technique (see Appendix).

6.5.2.1.4 Recording of the Results

Since the spectrum analyser results were produced on a small television screen, which was very difficult to read and digitise, the analyser was controlled through an IEEE interface thus allowing the screen results to be transferred to a micro computer. A program was developed for the micro computer (Commodore Pet) so that results could be recorded on a disc for permanent storage. These results were stored as digitised co-ordinates on disks, and the co-ordinates were also printed. (see figure 6.19 for a sample). Finally the co-ordinates were transmitted through another Pet micro computer to the University main frame computer so that the graphs on the analyser screen could be plotted. Figure 6.18 gives an example of the plots of the spectrum analyser screen.

6.5.2.2 The Test Procedure

From the sine wave excitation study it was found that the vibrator positioned at the $^1/_4$ longitudinal span gave better results than when positioned at mid-span. During this study the two vibration positions chosen were on the centre cross span, location a (Figure 6.20) and the $^1/_4$ cross span, location b (Figure 6.20).

For each of the two locations of the vibrator, tests were carried out to find the optimum number and positions of accelerometers to give results with the least scatter. Altogether 19 different accelerometer positions were investigated and up to a maximum of 7 accelerometers at any one time were used.

Procedure :

The model bridge was vibrated, and the accelerometer signals were recorded on the 8 channel tape recorder. One accelerometer in the frequency range 0-500Hz was used as reference .If(n) accelerometers were used (n-1) analyses were carried out. Channel A of the analyser was always taken as the reference accelerometer.

During each analysis, the results were extracted from the analyser to the pet computer for digitising and transfer to the university main frame for plotting. By studying the printed results, and graphs of each of the analyses, the natural frequencies were deduced. Also by studying the phases of the spectra the mode shapes were deduced.

6.5.2.3 Test Results

All of the results from each vibrator position were plotted on two histograms, given in Figure 6.21 for location a, and Figure 6.22 for location b. Comparison of the two histograms indicated that location b for the vibrator gave results with less scatter than location a. If the results from individual tests for each of the 19 positions were plotted on different histograms and these histograms were compared to Figures 6.22 it was found that the results for the accelerometer position given in Figure 6.23 matched most closely that of Figure 6.22. Hence the natural frequency of the model bridge using the accelerometer position given in Figure 6.23 are given in Table (6.4).

From the above results, the first nine natural frequencies were found, using a frequency range of 0-500Hz in the spectrum analyser. Each natural frequency could only be calculated to within $\pm$3.9Hz which was not accurate enough for this study. If instead of using one frequency range (0-500Hz), if five frequency ranges were used (0-100, 100-200, 200-300, 300-400, 400-500Hz) the natural frequencies were calculated within $\pm$0.78Hz.

The results from this more accurate analysis using the optimum accelerometer position found above are given in Table (6.5). Also given in Table (6.5) are the corresponding mode shapes. These modes were deduced from the phase differences of the accelerometers signals which were produced by the spectrum analyser.

6.5.2.4 Conclusion of the Random Excitation Method

A method of random response excitation using an energy input device in which the first ten natural frequencies of the model bridge were found has been described. Also during the study an optimum number and positions of accelerometers were identified and are given in Figure 6.23. Furthermore it has been shown that a simple method as described could be used to measure the response of bridge structures to within $\pm$ 0.78Hz.

The main difference between this method described above and the method used by S.M.L. is that Structural Monitoring Limited used Maximum Entropy Method which involves the use of much more computer arithmetic than the Fast Fourier Transform technique used in this study.

6.6 Conclusion

In this chapter methods are developed for the response measurement of bridge models. The sine wave excitation method is simple but gives a large scatter of results, i.e. within 10Hz, whereas the random method developed is also simple and semi-automatic, and gives the natural frequencies of the model to within $\pm$ 0.78Hz.

The most important aspect of this chapter is the development of a method of random response measurement, i.e. the test procedure is summarized as follows :

i) The bridge is vibrated, and the 7 accelerometer's signals are recorded on the 8 channel tape recorder.

ii) Taking the central accelerometer as reference, figure (6.22) six analyses in the frequency range 0-500Hz are carried out (channel A of the analyser was always taken as the reference accelerometer).

iii) As above but more detailed analysis in the frequencies ranges 0-100, 100-200, 200-300, 300-400, 400-500 are carried out, hence producing 30 more analyses.

iv) During each of the 36 analyses, the results were extracted from the analyser and fed into the University main frame computer for plotting.

v) By comparing the printed results, and graphs of each of the 36 analyses, the natural frequencies are deduced.

FREQUENCY (HZ)	TIME OF VIBRATION (MINS)
480	35
240	69
120	139
60	153
30	556

TABLE 6.1 VIBRATION FREQUENCIES AND VIBRATION TIMES OF THE PERSPEX SAMPLES

TEST	NUMBER OF ACCELEROMETERS	FREQUENCIES REQUIRED OR RANGE (HZ)	NUMBER OF TIMES THE TESTS WERE REPEATED
a	1	4	4
b	2	4	4
c	2	5	4
d	3	6	4
e	4	RANGE 40-500	2
f	4	RANGE 40-500	2
g	5	RANGE 40-500	2
h	6	RANGE 40-500	2
i	6	RANGE 40-500	2

TABLE 6.2 LISTS OF SINE WAVE EXCITATION TESTS

MODE NUMBER	AVERAGE FREQUENCY (HZ)	NUMBER OF RESULT USED TO CALCULATE THE AVERAGES	MODE SHAPES
1	40.9	26	1st BENDING
2	53.9	26	1st TORSION
3	131.1	18	2nd BENDING
4	172.5	17	2nd TORSION
5	229.1	10	1st CROSS - BENDING
6	249.7	6	
7	269.0	7	
8	302.54	10	

TABLE 6.3 AVERAGE NATURAL FREQUENCIES (HZ)

NODE NUMBER	FREQUENCY (HZ)
1	40.444
2	56.069
3	144.35
4	209.975
5	251.538
6	308.413
7	341.225
8	382.631
9	420.913

TABLE 6.4 RANDOM VIBRATION RESULTS

MODE NUMBER	FREQUENCY (HZ)	MODE SHAPE
1	41.225	1ST BENDING
2	60.756	1ST TORSION
3	148.256	2ND BENDING
4	221.694	1ST CROSS BENDING
5	279.506	3RD BENDING
6	291.225	
7	308.413	
8	331.85	3RD TORSION
9	416.225	
10	467.788	

TABLE 6.5 BRIDGE MEASURED NATURAL FREQUENCIES (HZ)
---------- USING THE MORE ACCURATE FREQUENCY RANGES

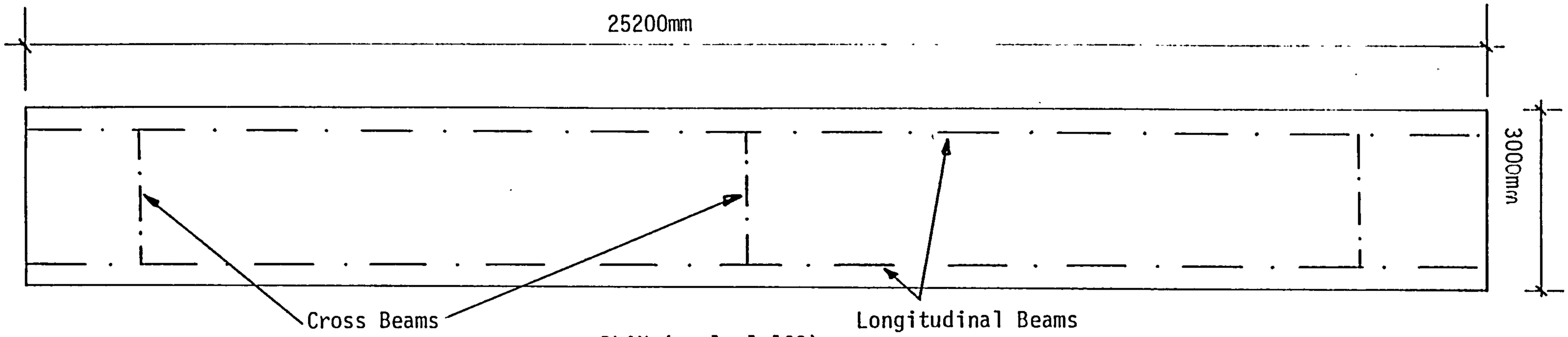

PLAN (scale 1:100)

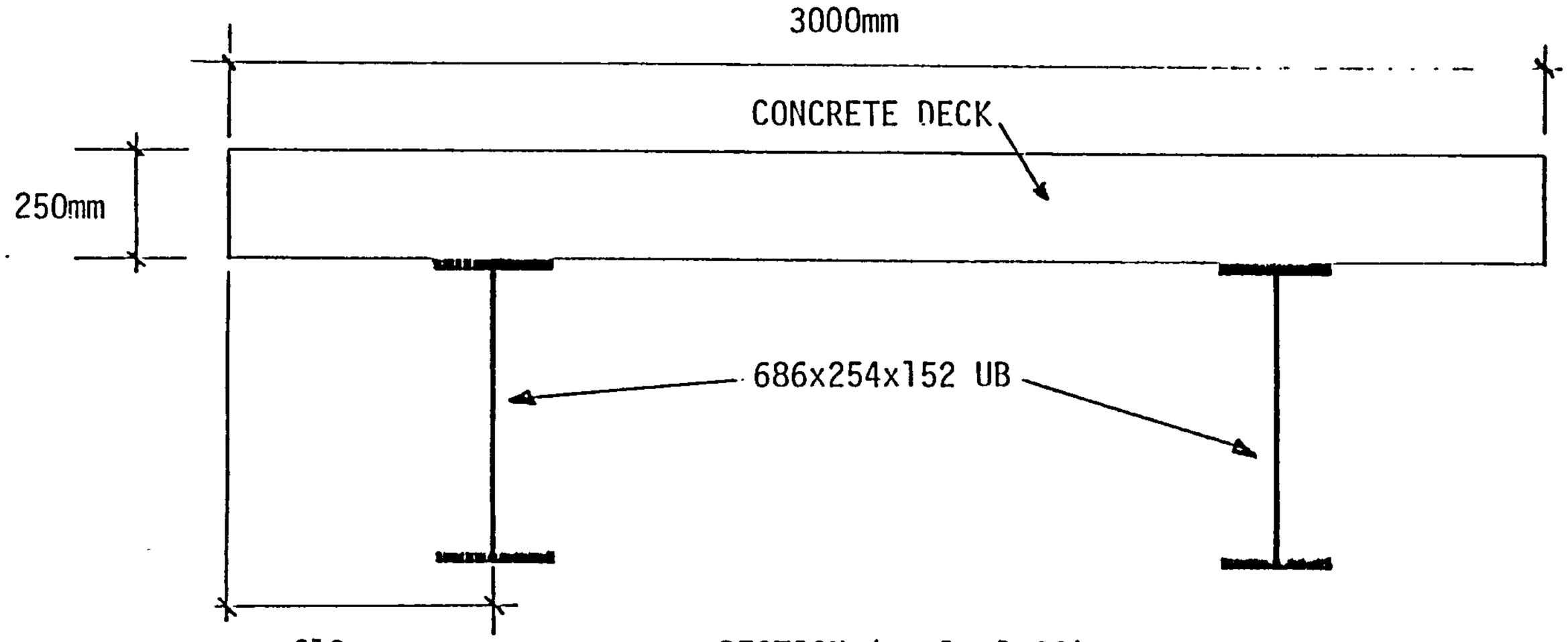

SECTION (scale 1:20)

FIGURE 6.1 FOOTBRIDGE OVER THE RIVER KELVIN

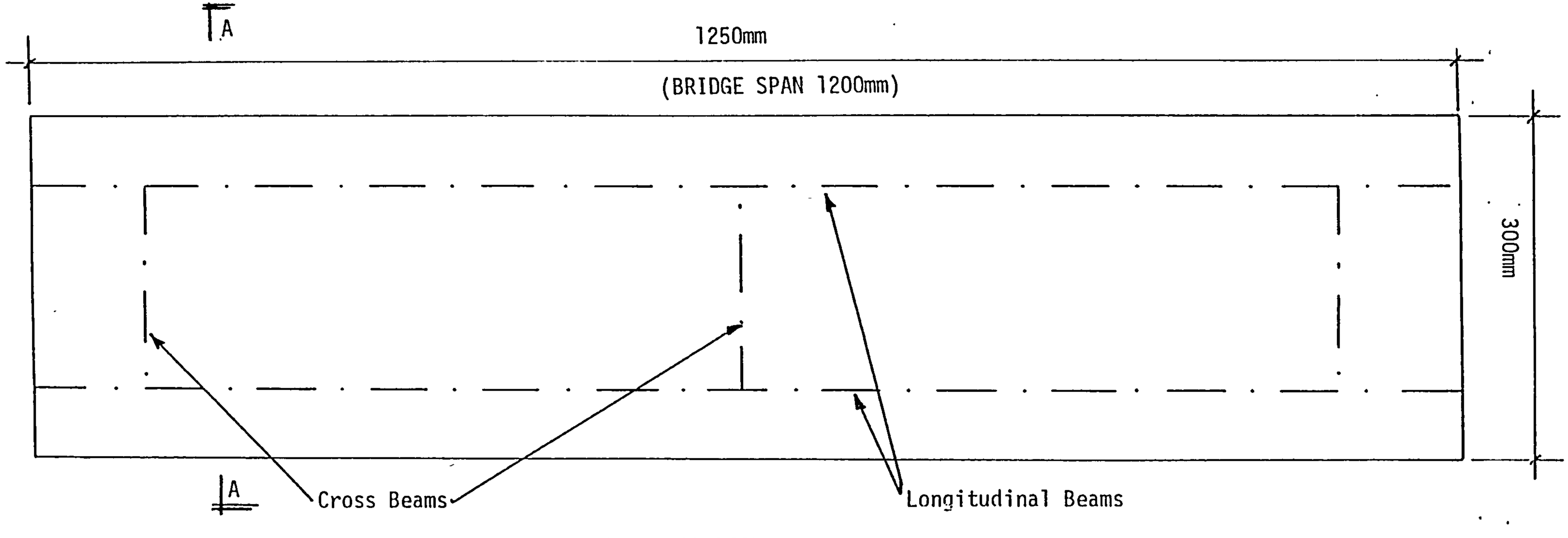

FIGURE 6.2a PLAN OF MODEL BRIDGE DECK

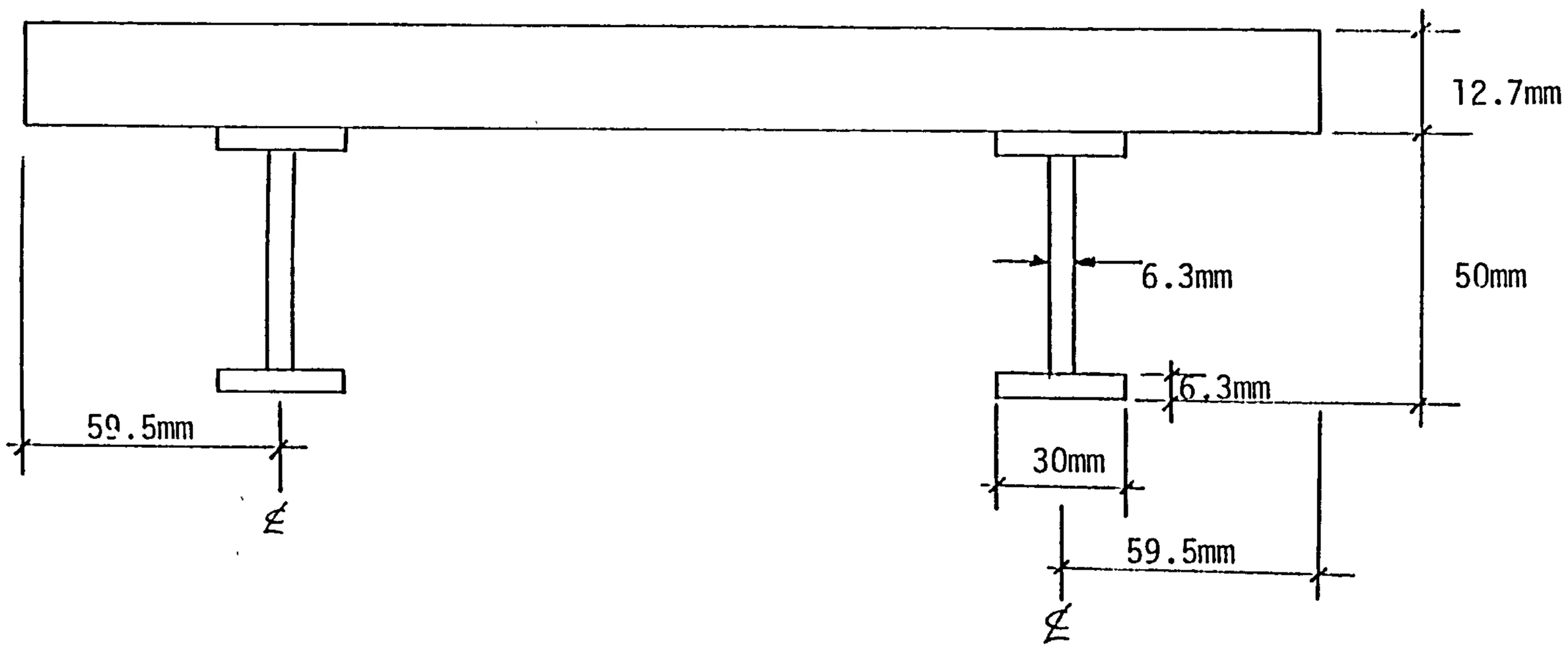

FIGURE 6.2b SECTION A-A OF THE MODEL BRIDGE

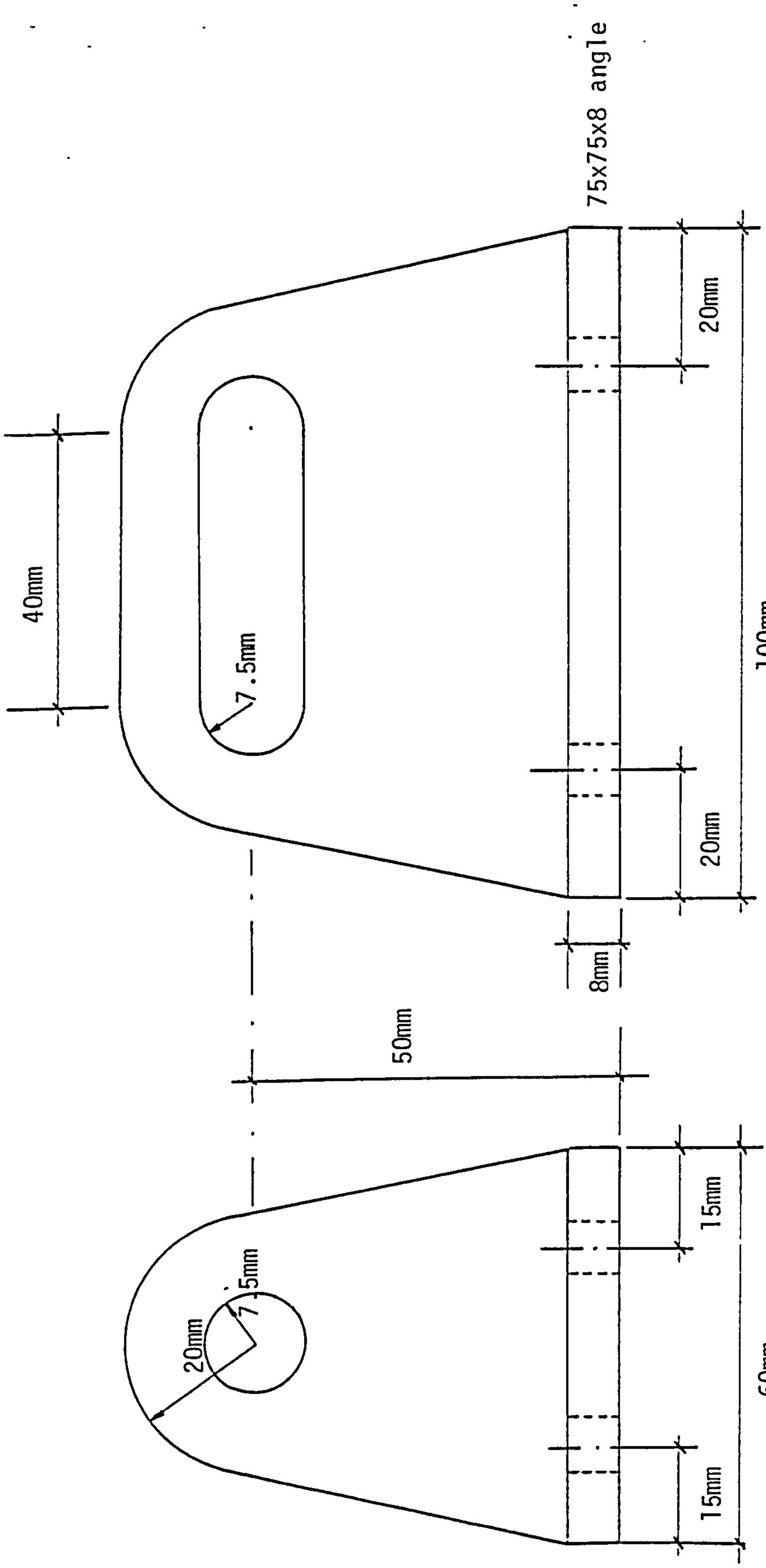

FIGURE 6.4 SUPPORT TYPE B

FIGURE 6.3 SUPPORT TYPE A

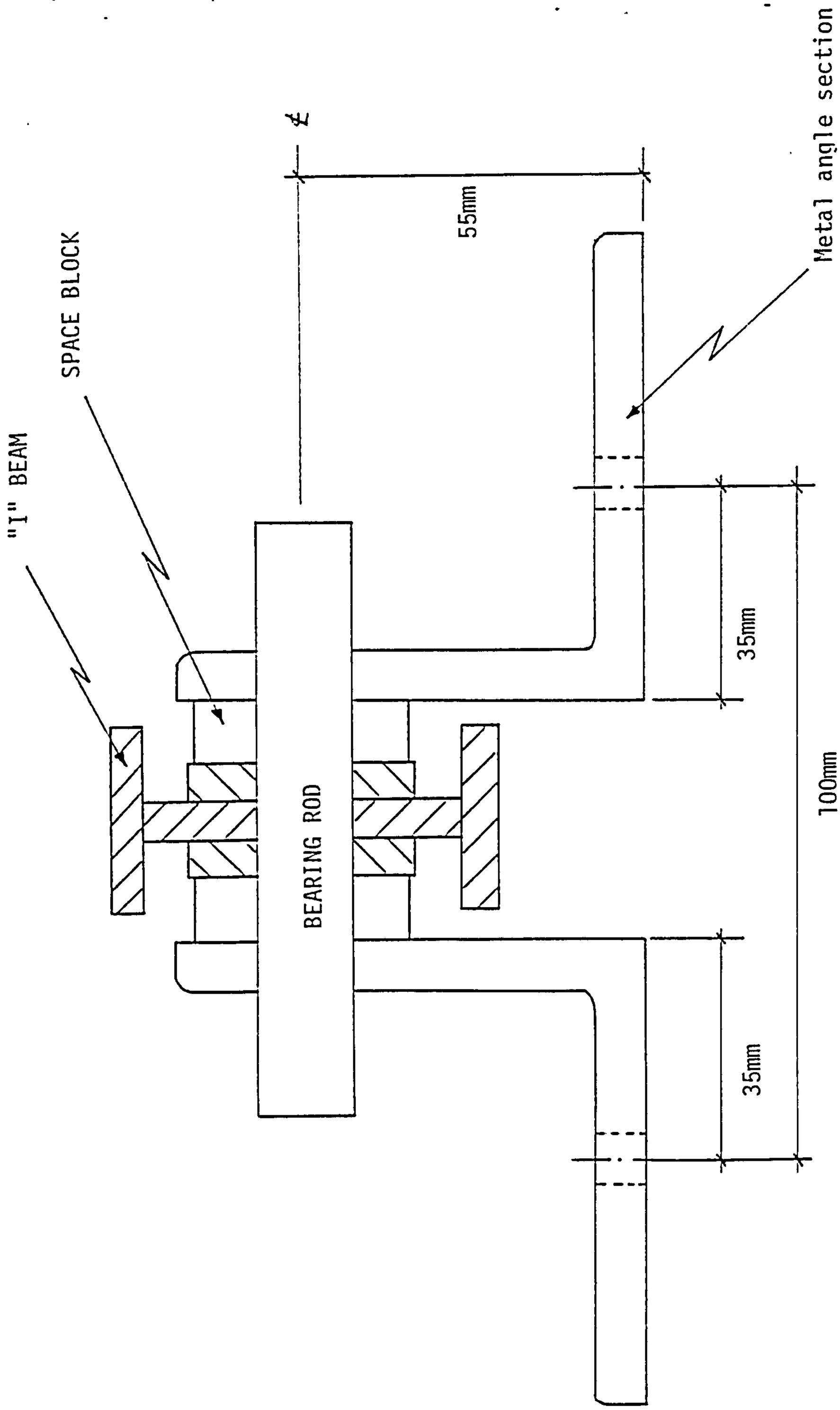

FIGURE 6.5 SECTION OF MODEL BRIDGE SUPPORTS

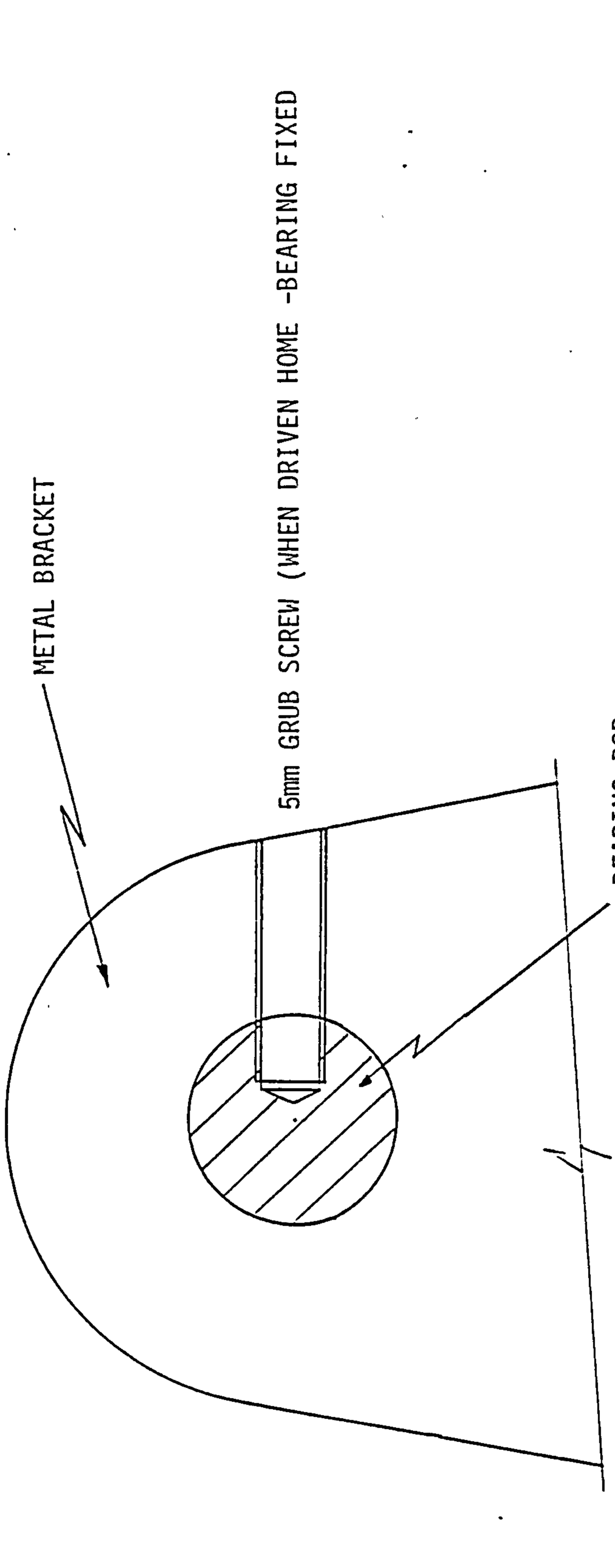

FIGURE 6.6 BEARING TYPE A SHOWING FIXING DEVICE

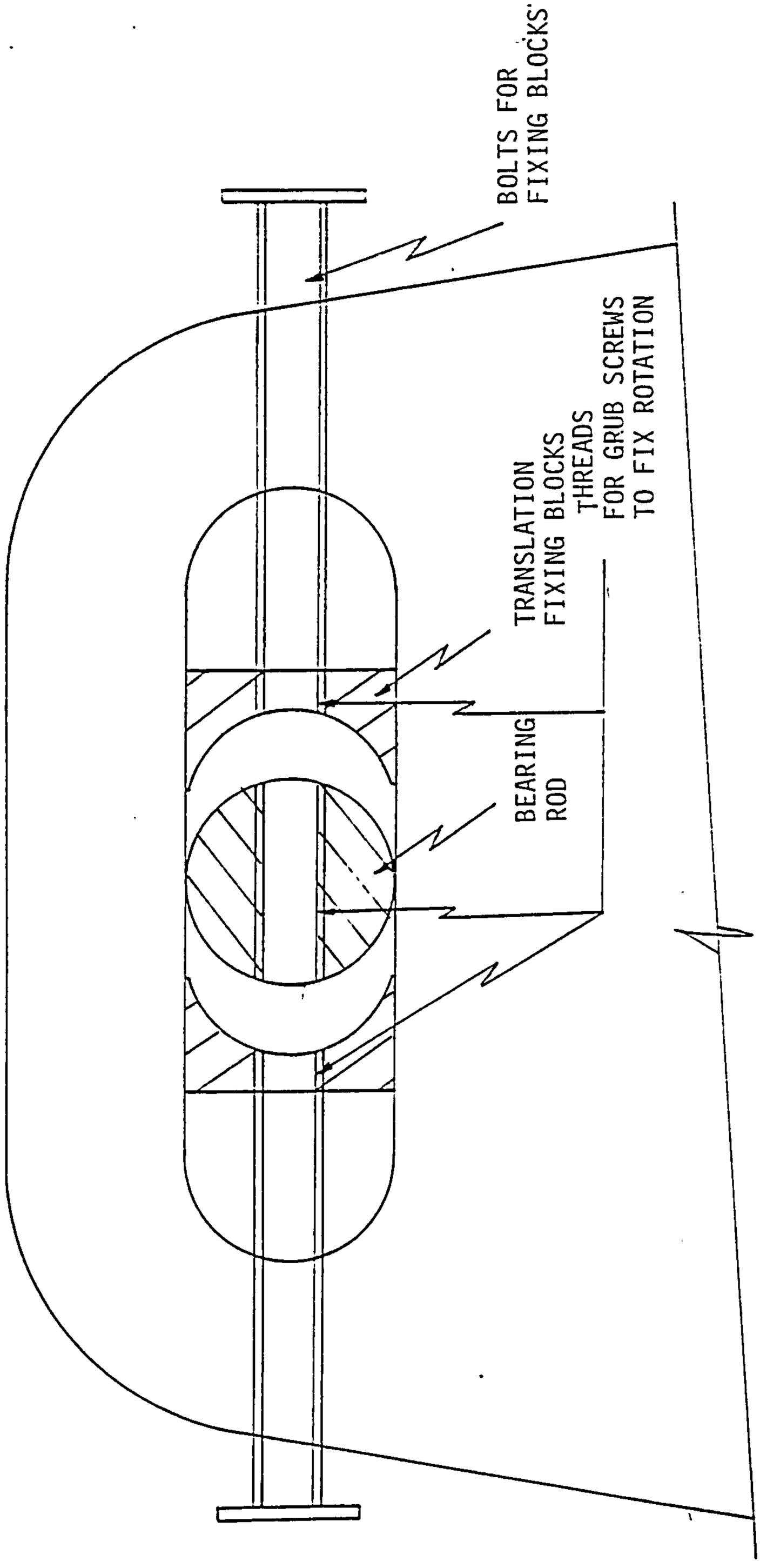

FIGURE 6.7 BEARING TYPE B SHOWING FIXING DEVICES

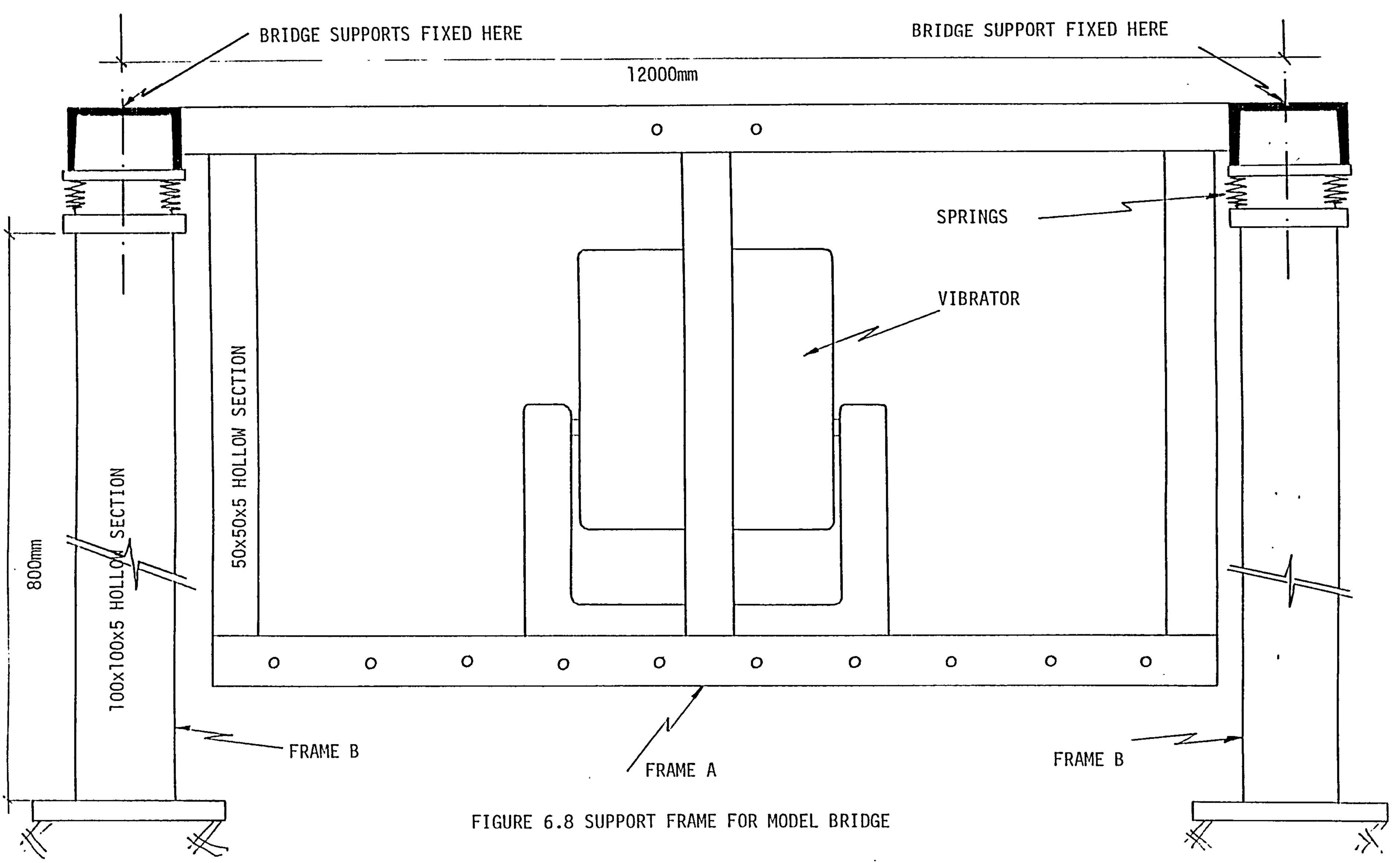

FIGURE 6.8 SUPPORT FRAME FOR MODEL BRIDGE

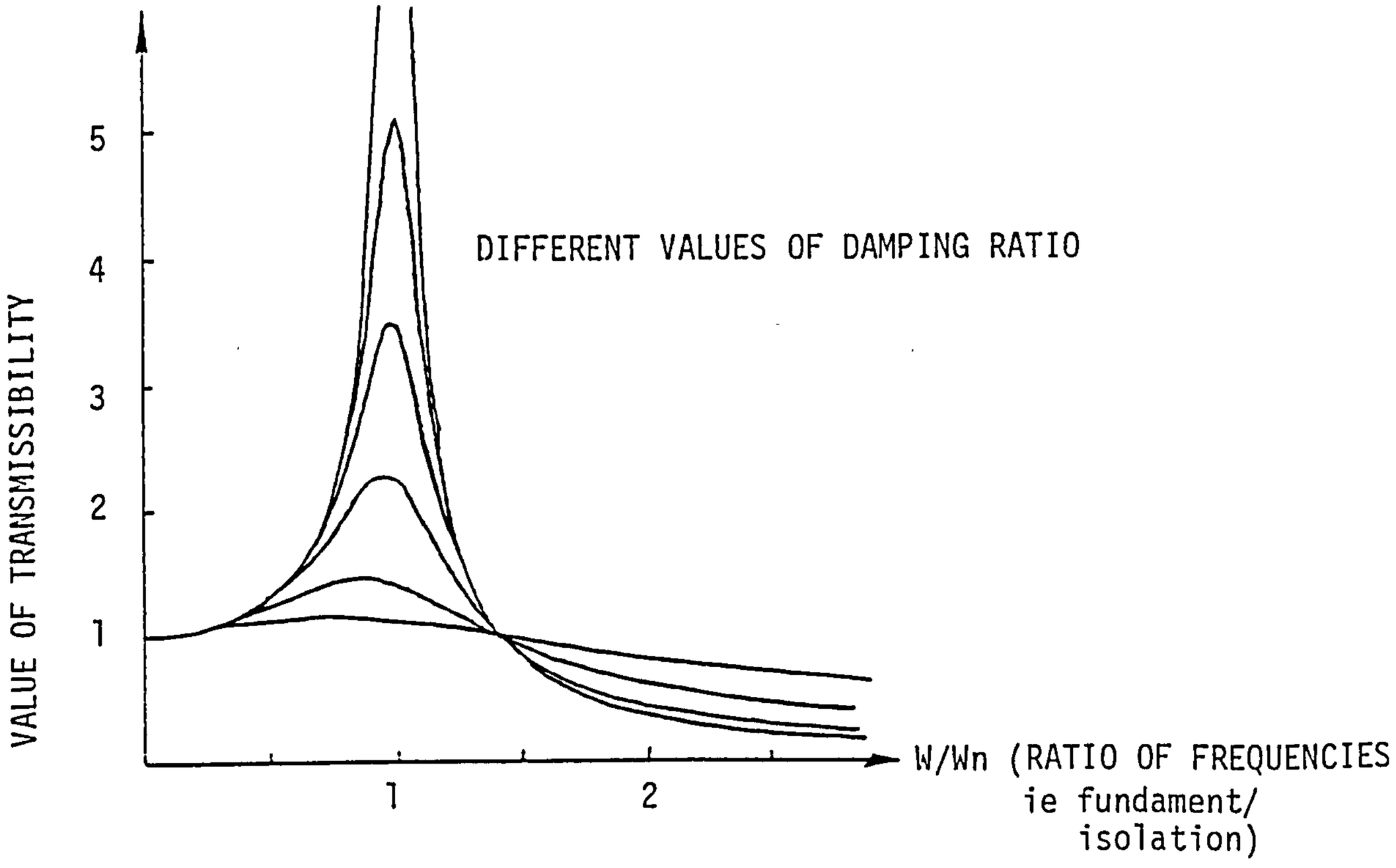

FIGURE 6.9 TRANSMISSIBILITY CURVES

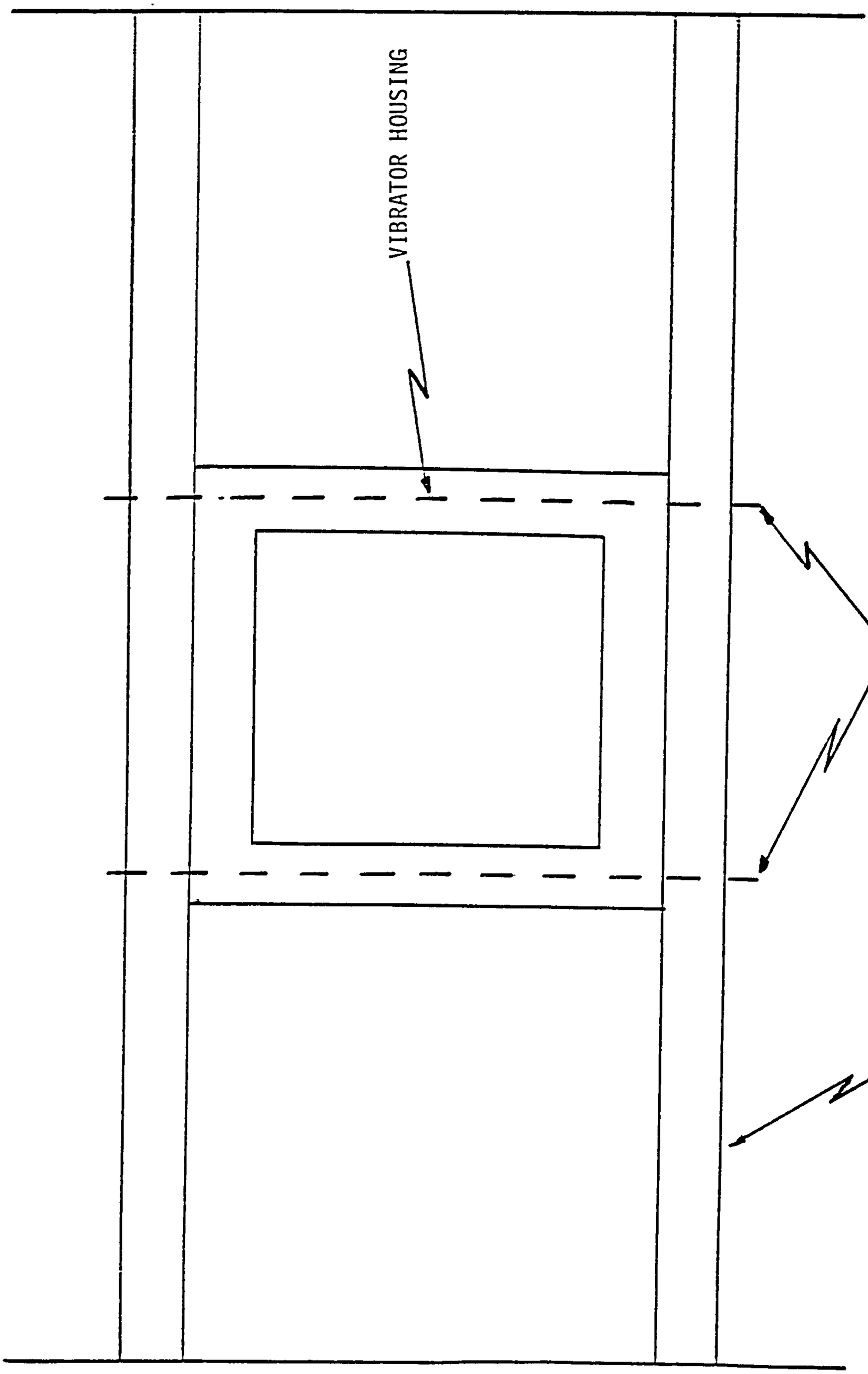

FIGURE 6.10 DIAGRAM SHOWING METHOD OF VIBRATOR SUPPORT
(VIBRATOR MAY BE MOVED TO REQUIRED POSITION USING THE THREAD ROD)

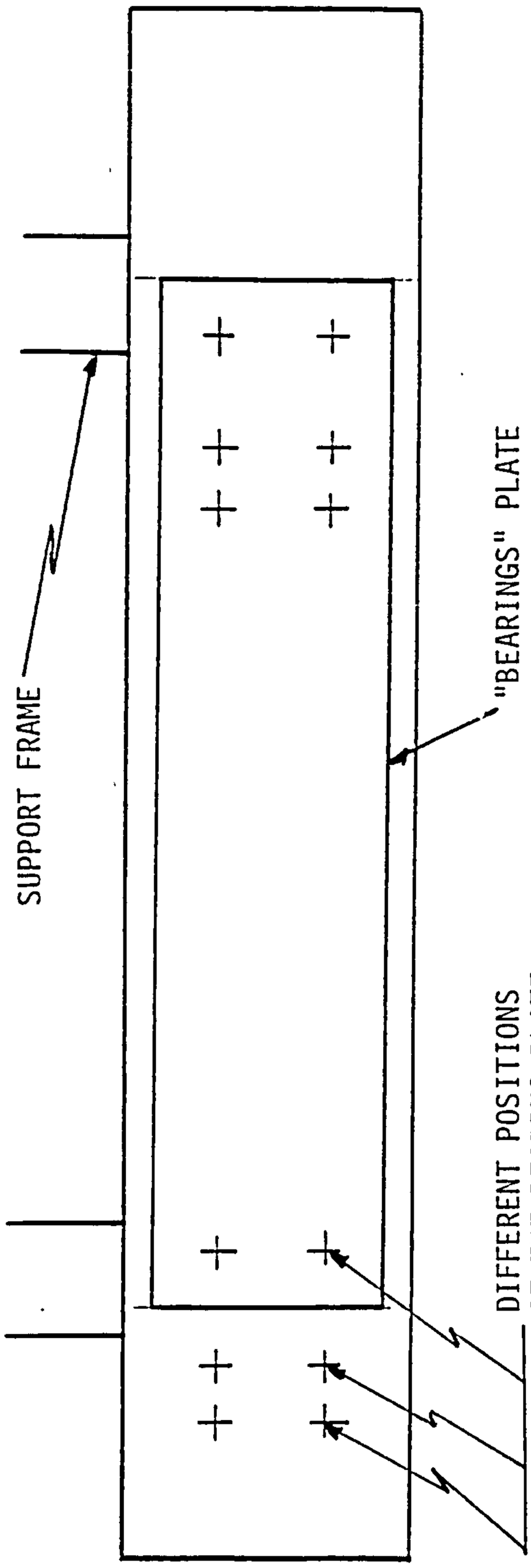

FIGURE 6.11 DIAGRAM SHOWING METHOD OF SIDE MOVEMENT

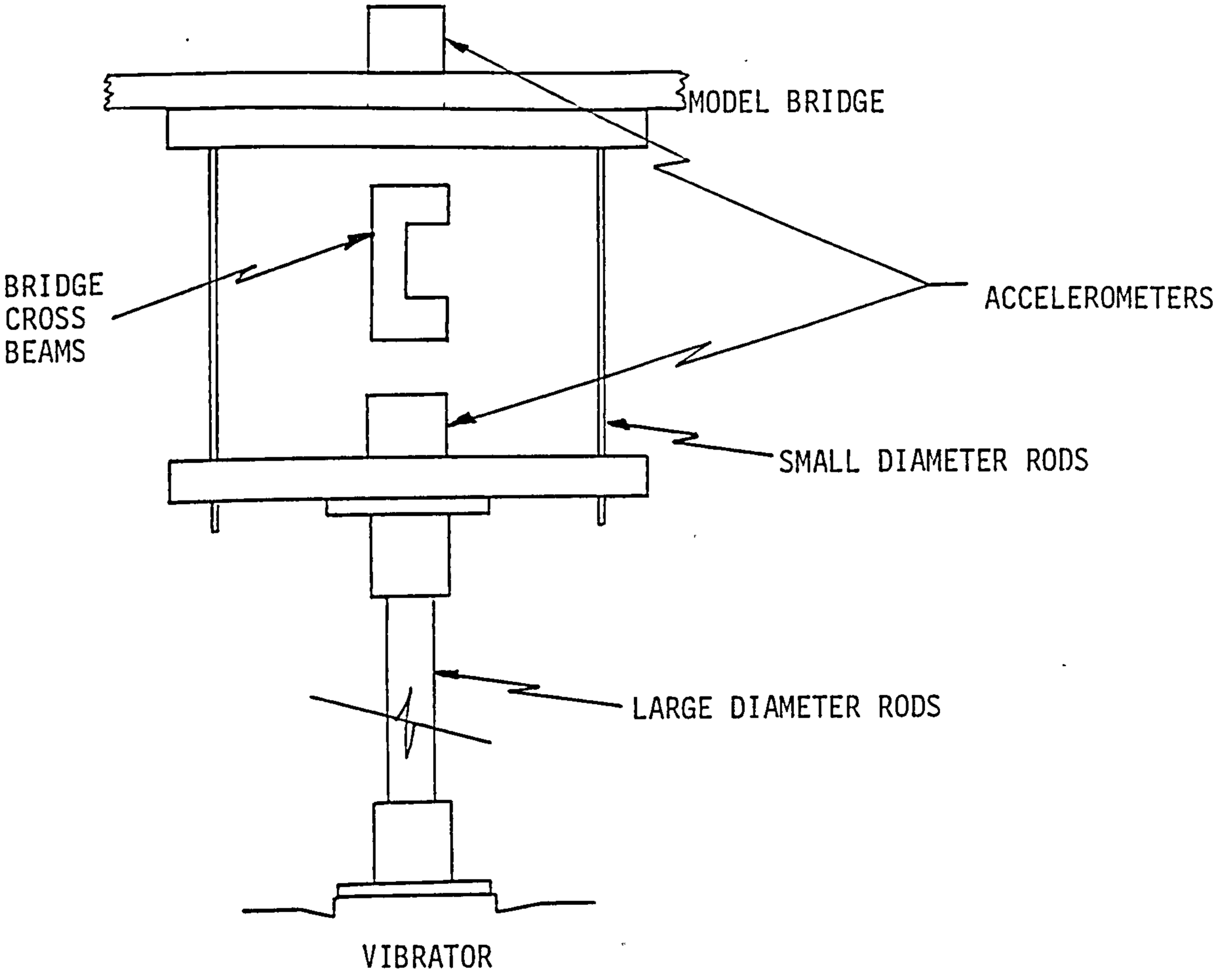

FIGURE 6.12 CONNECTOR BETWEEN MODEL BRIDGE AND VIBRATOR

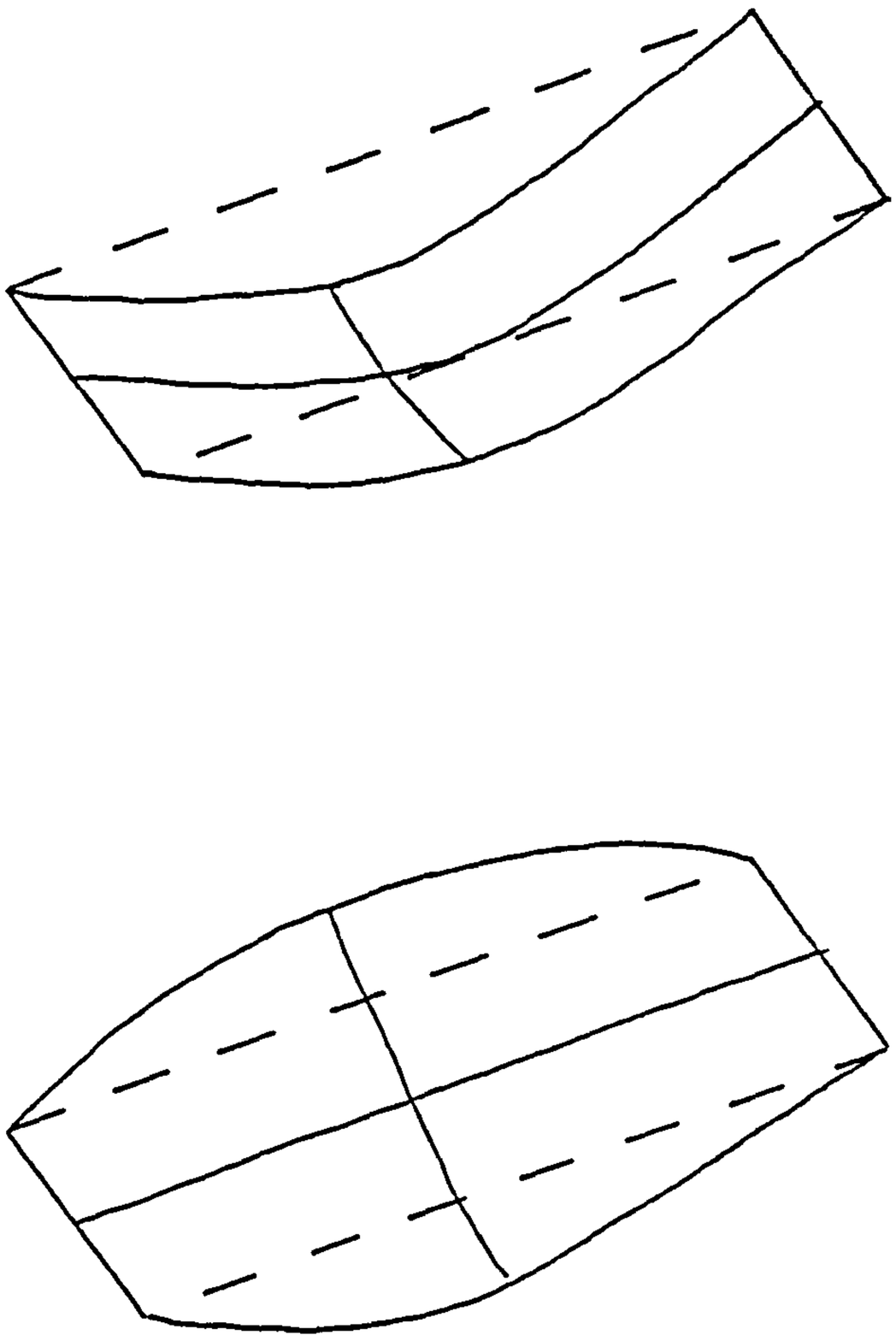

LONGITUDINAL BENDING

TORSION

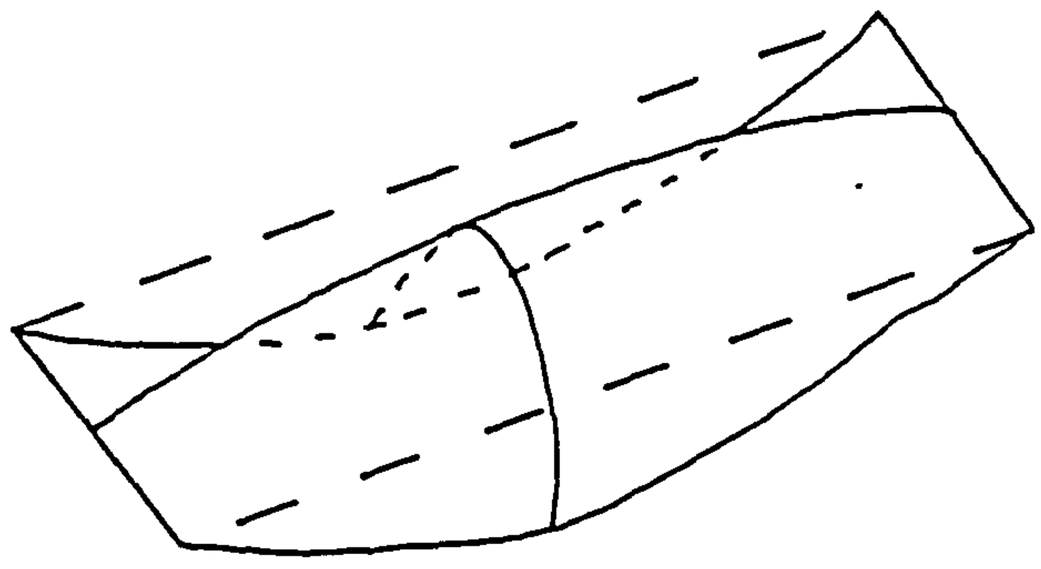

CROSS BENDING

FIGURE 6.13 2-D STRUCTURAL MODES SHAPES

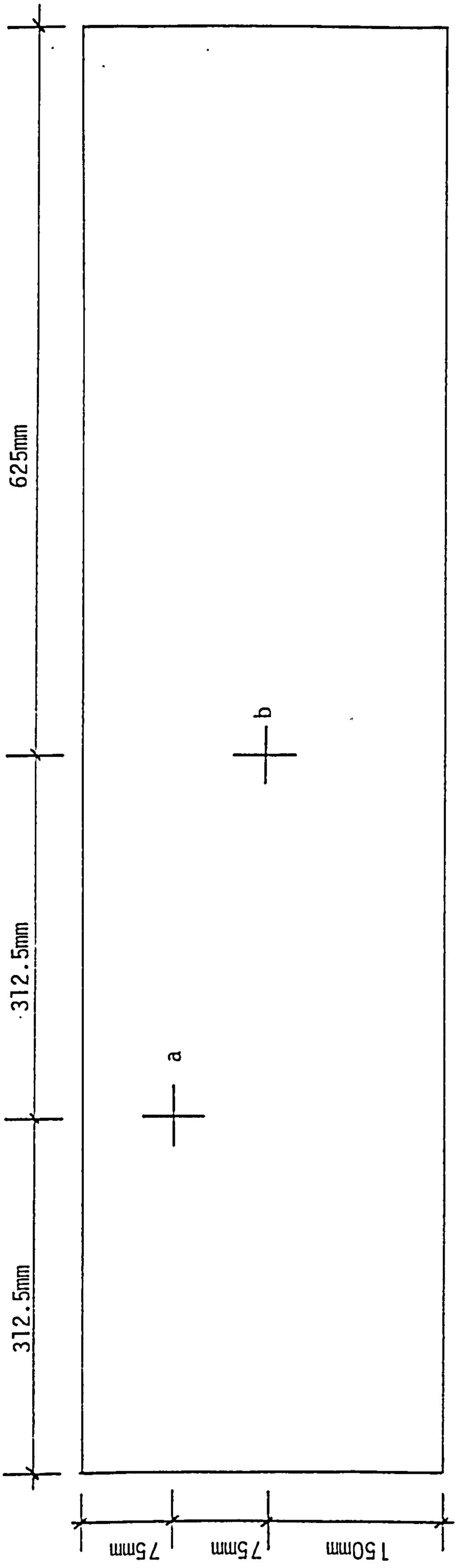

FIGURE 6.14 POSITIONS OF EXCITATION

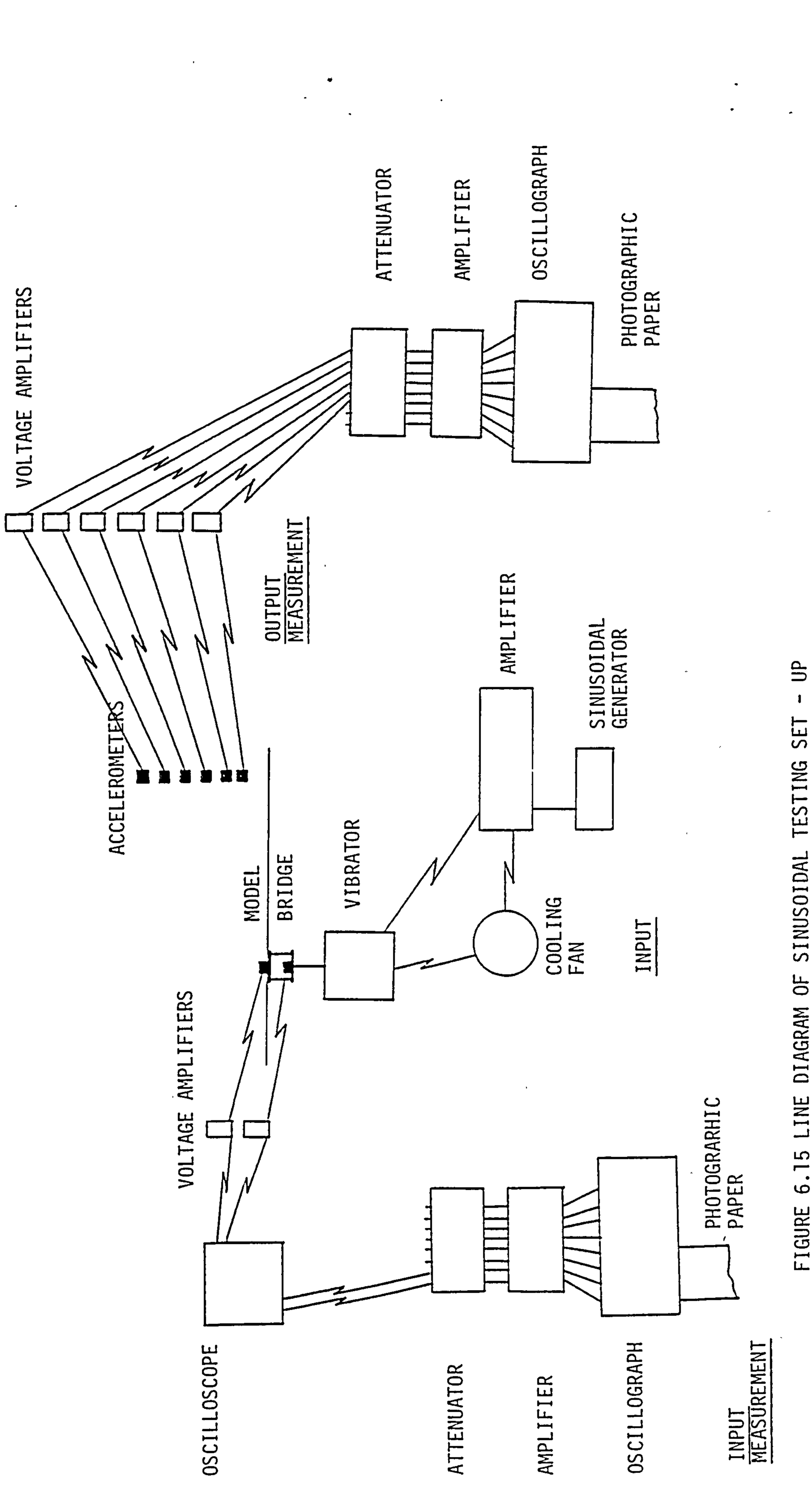

FIGURE 6.15 LINE DIAGRAM OF SINUSOIDAL TESTING SET - UP

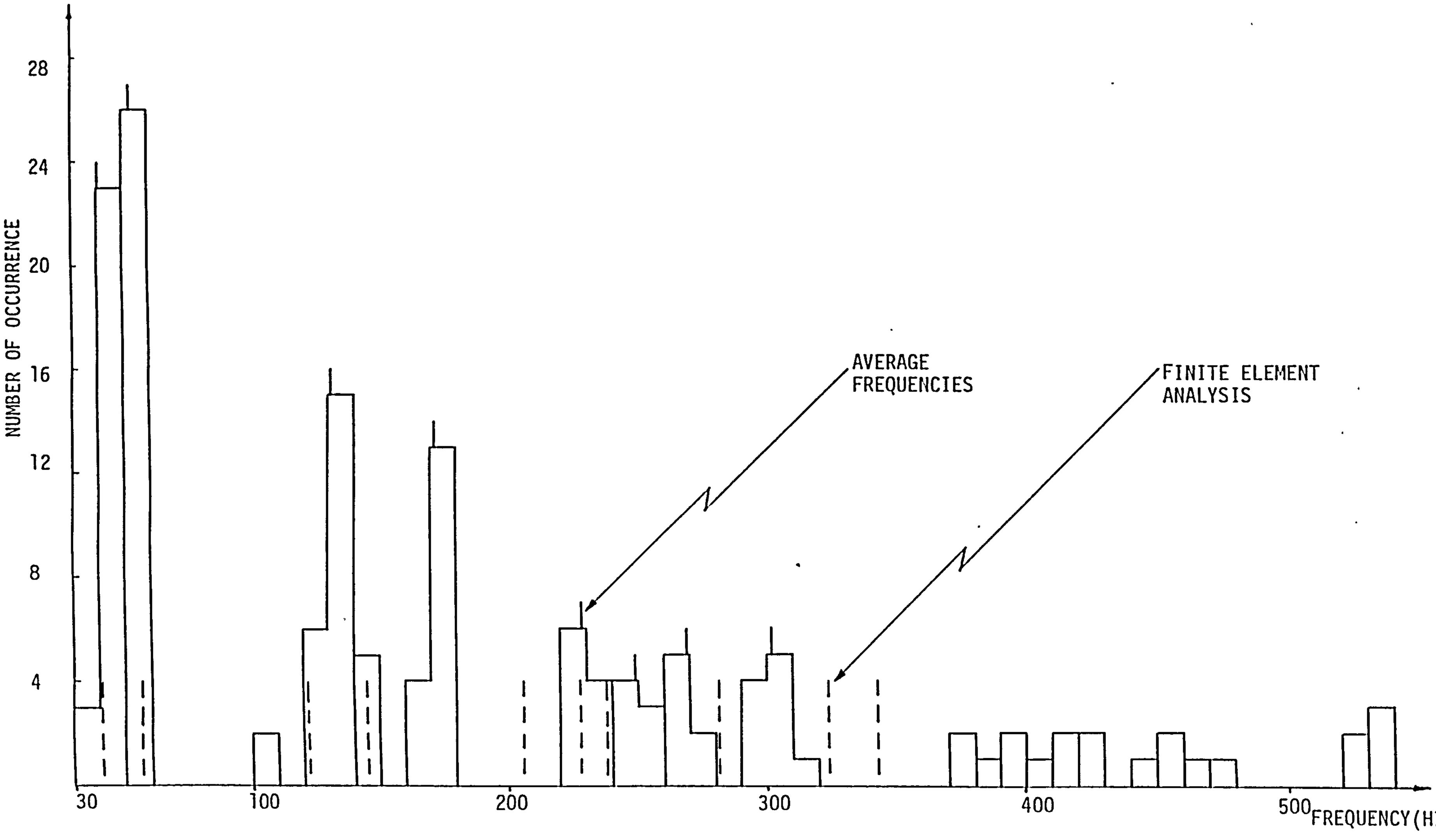

FIGURE 6.16 HISTOGRAM OF SINUSOIDAL TESTING RESULTS

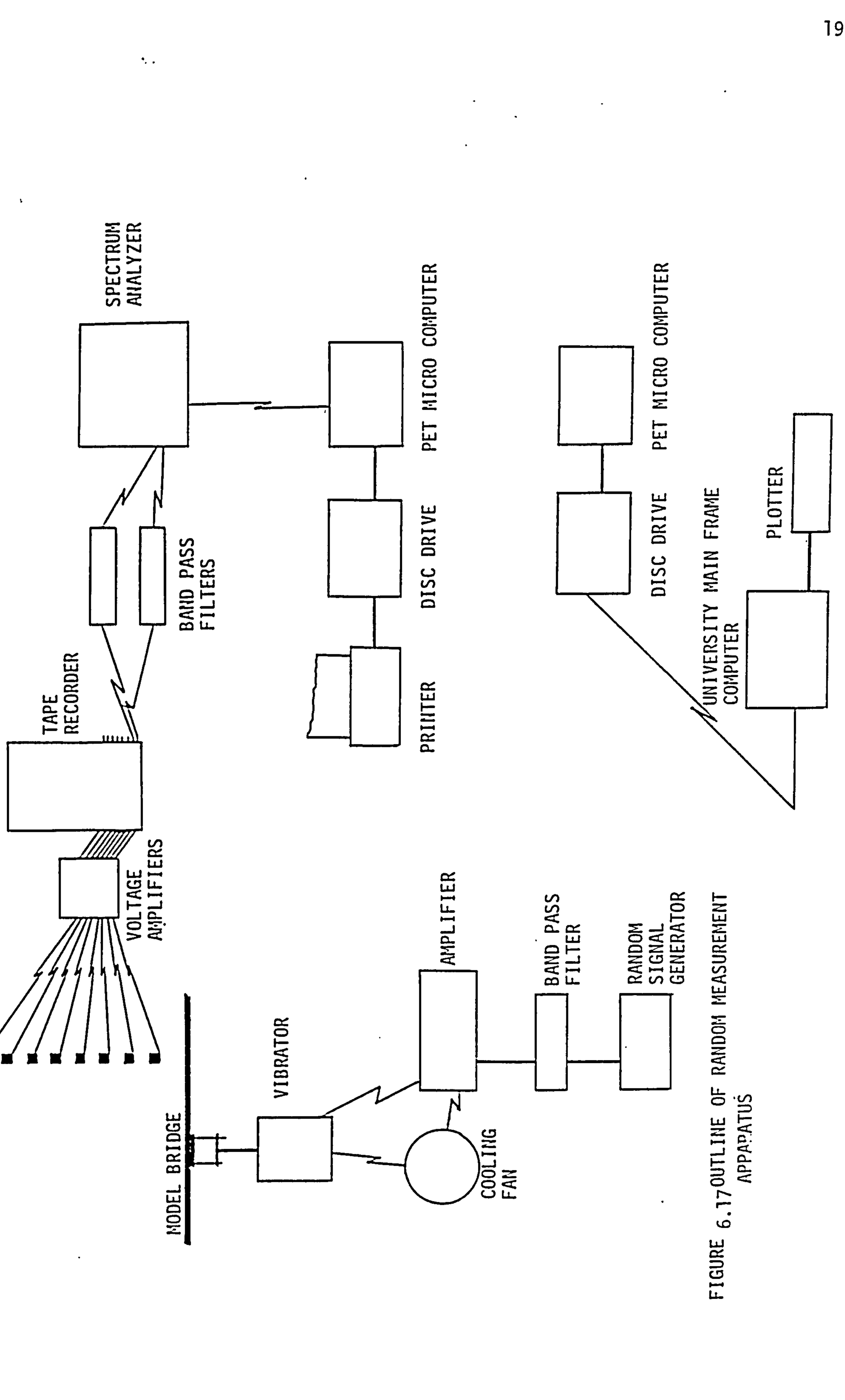

FIGURE 6.17 OUTLINE OF RANDOM MEASUREMENT APPARATUS

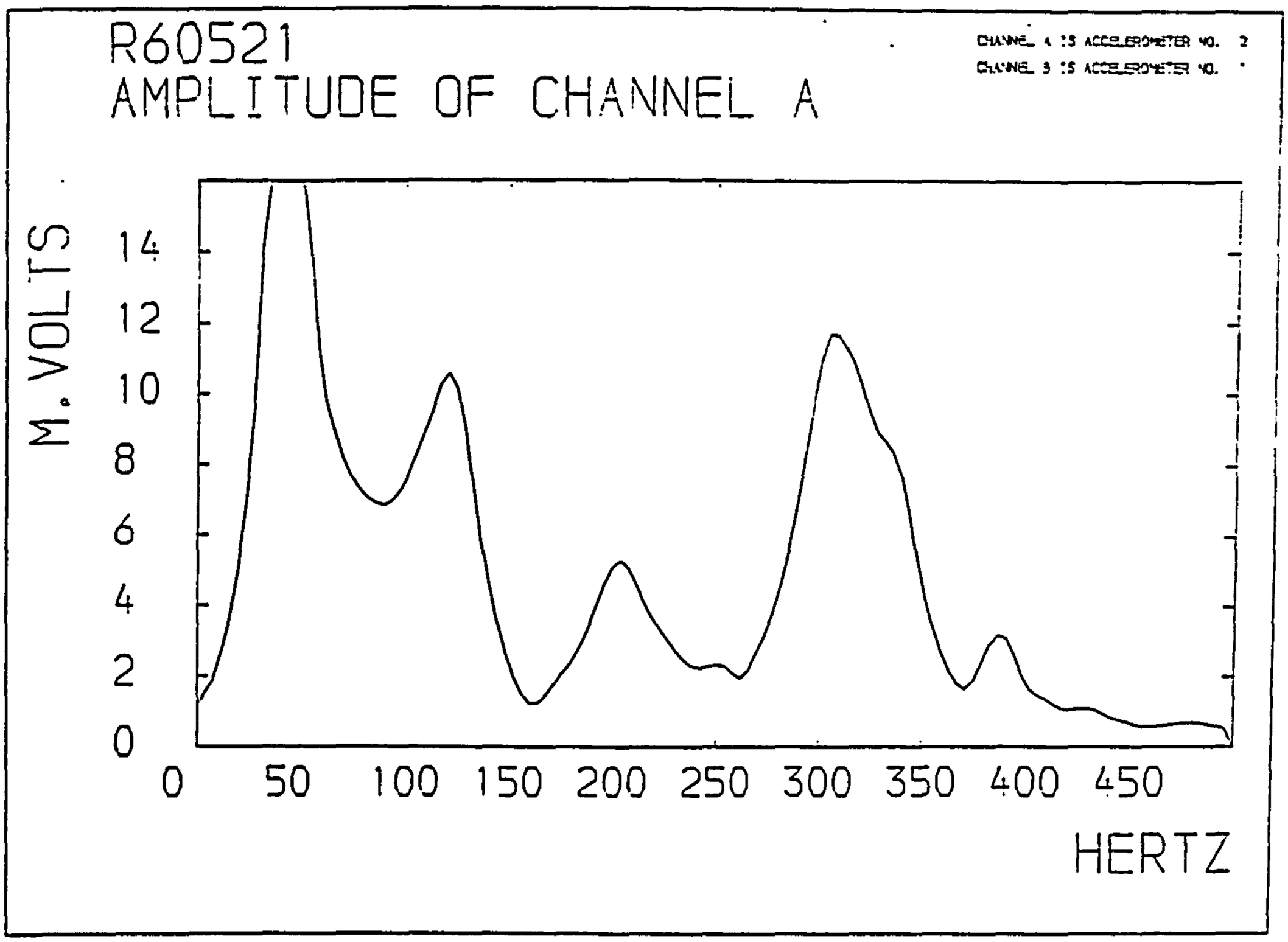

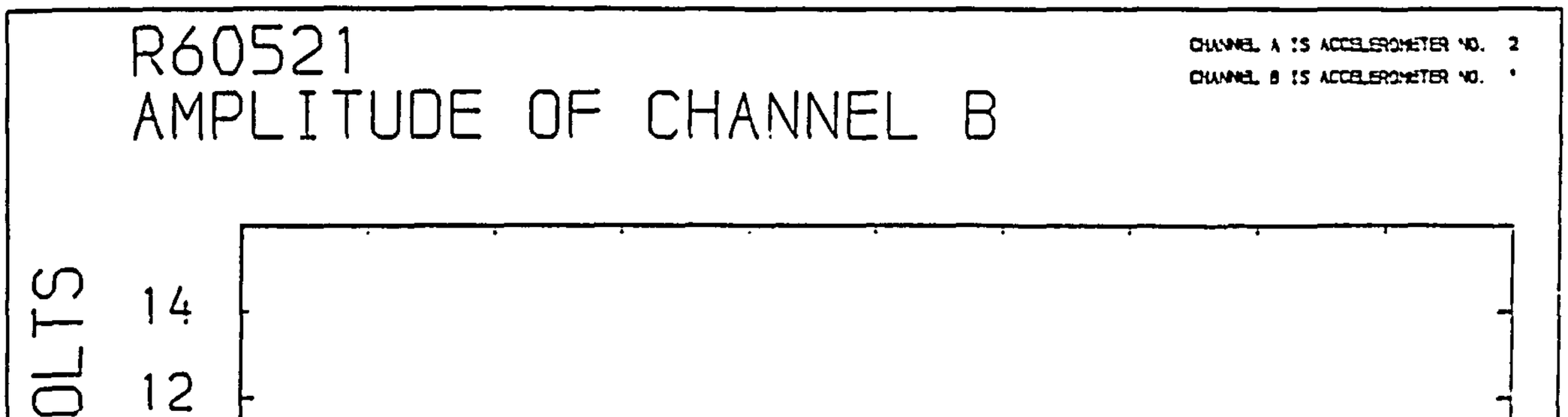

FIGURE 6.18 Examples of Frequency Response Produced by the Spectrum Analyzer

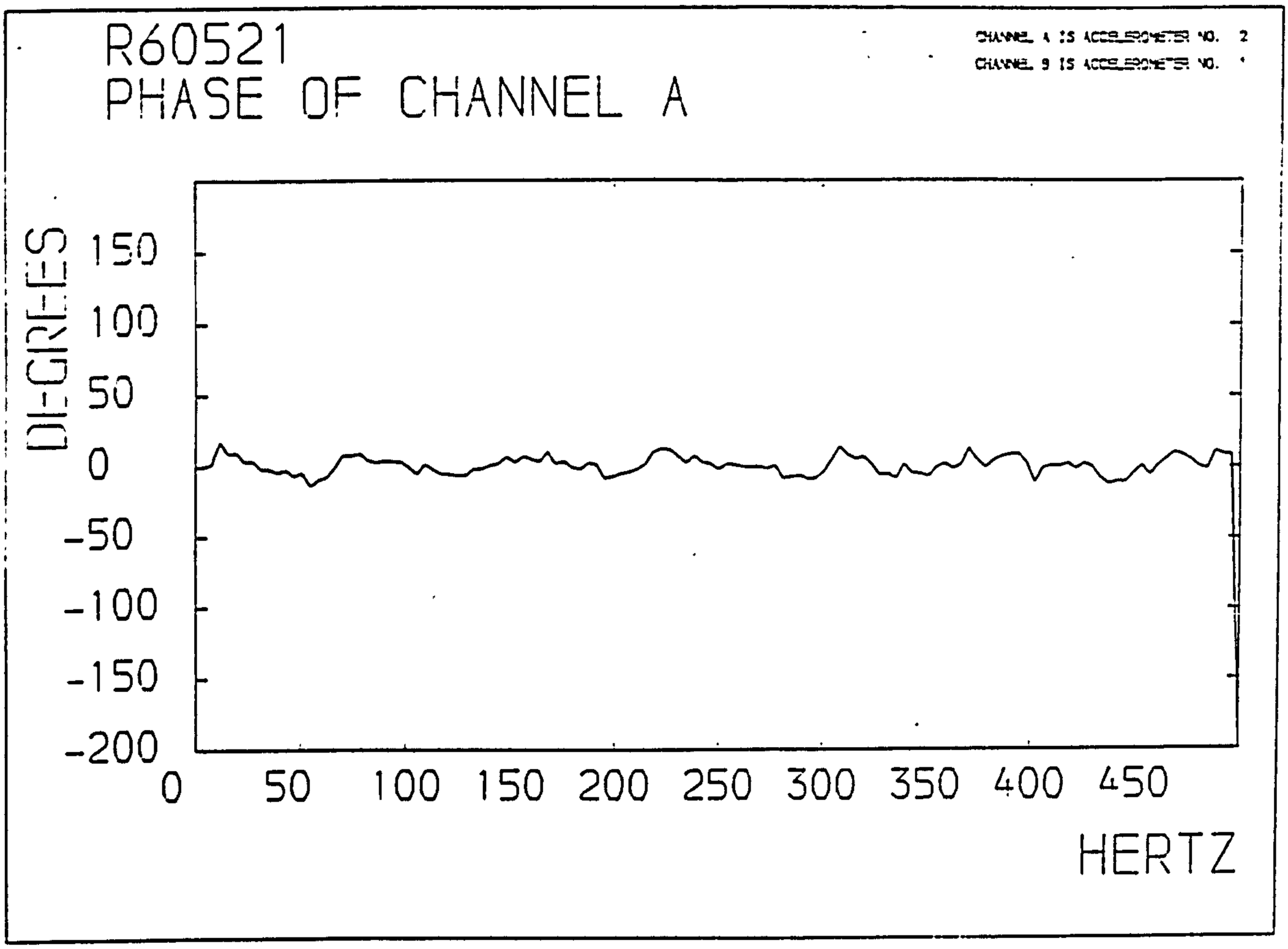

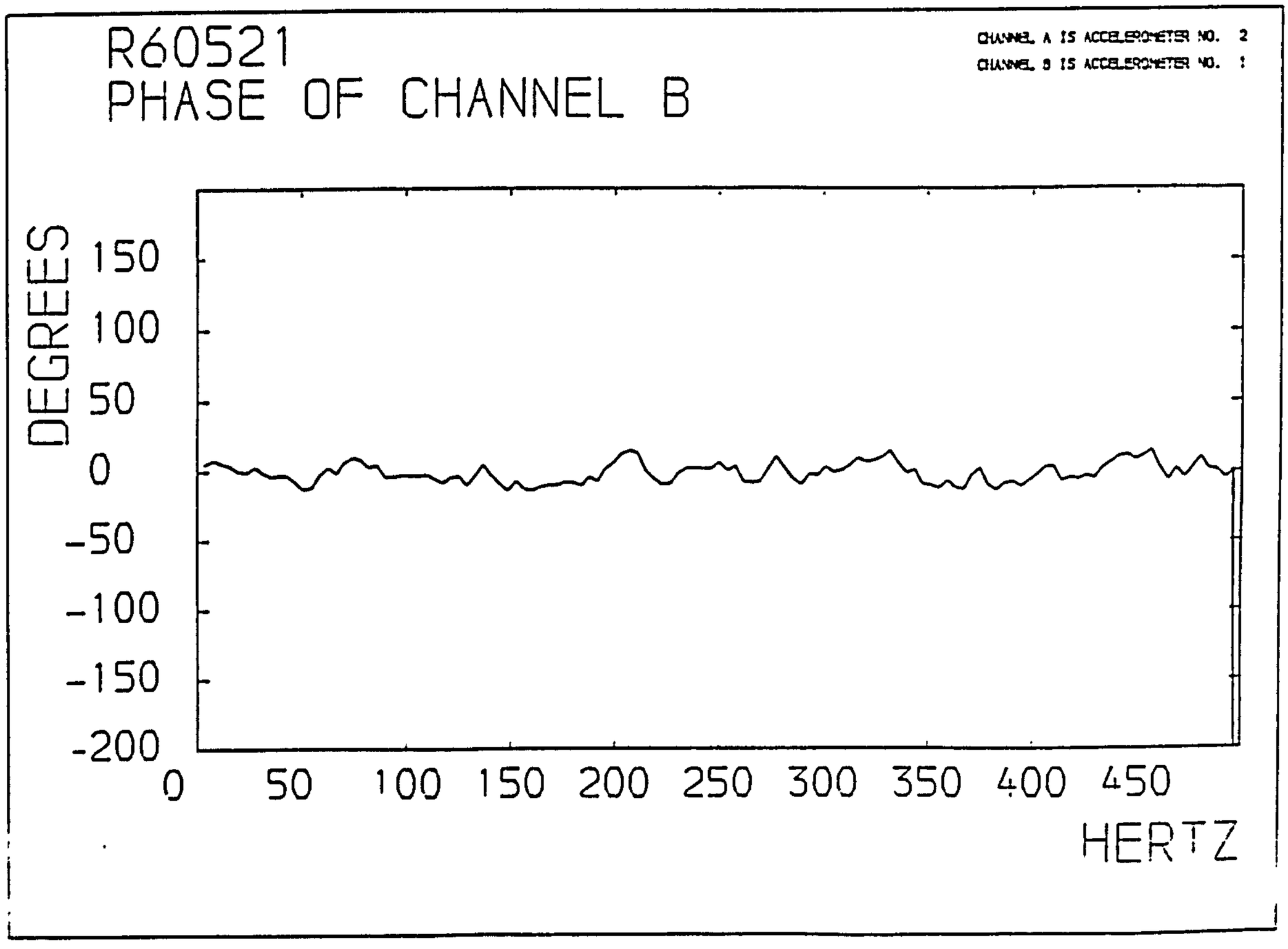

FIGURE 6.18 (cont)

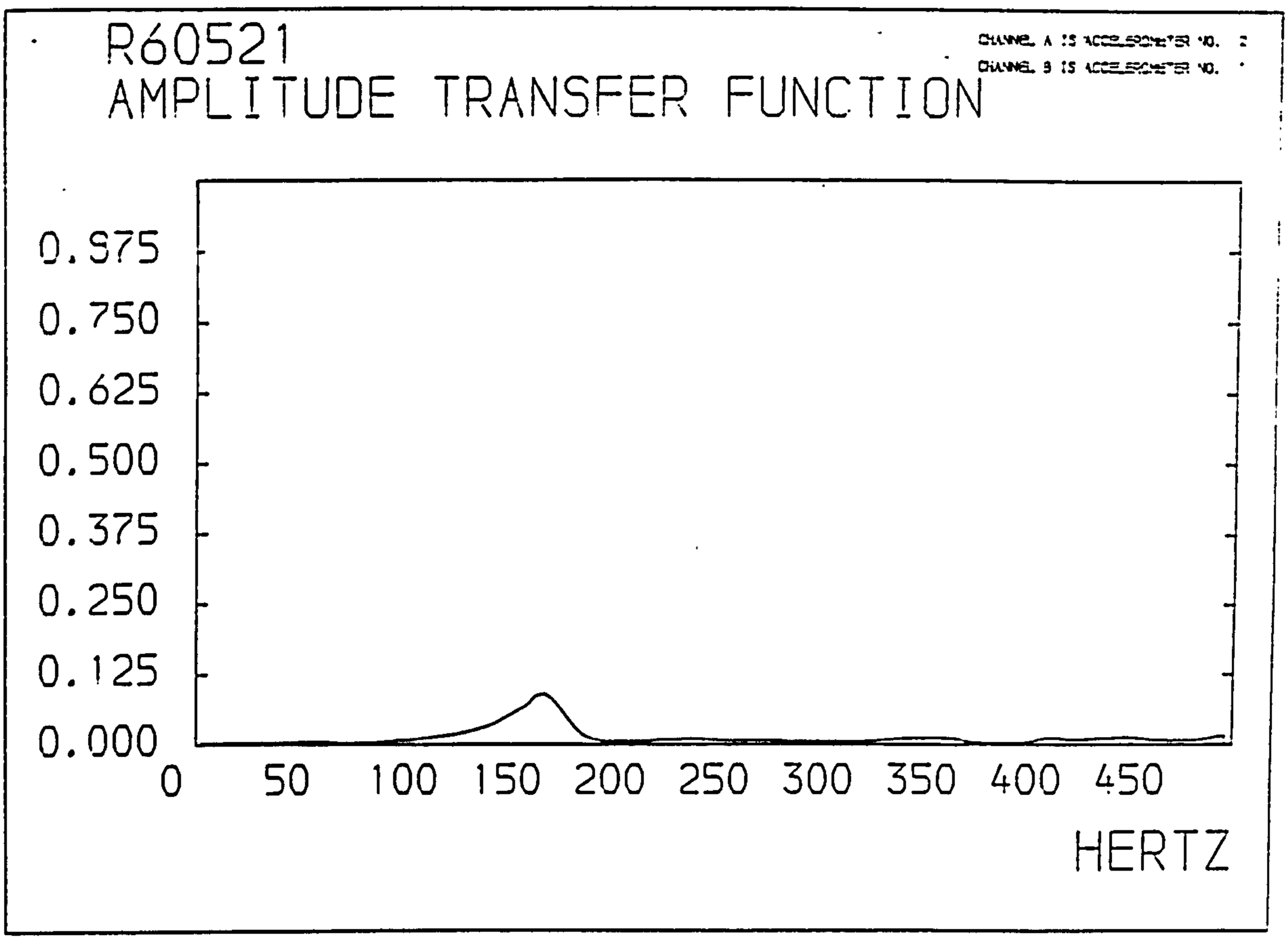

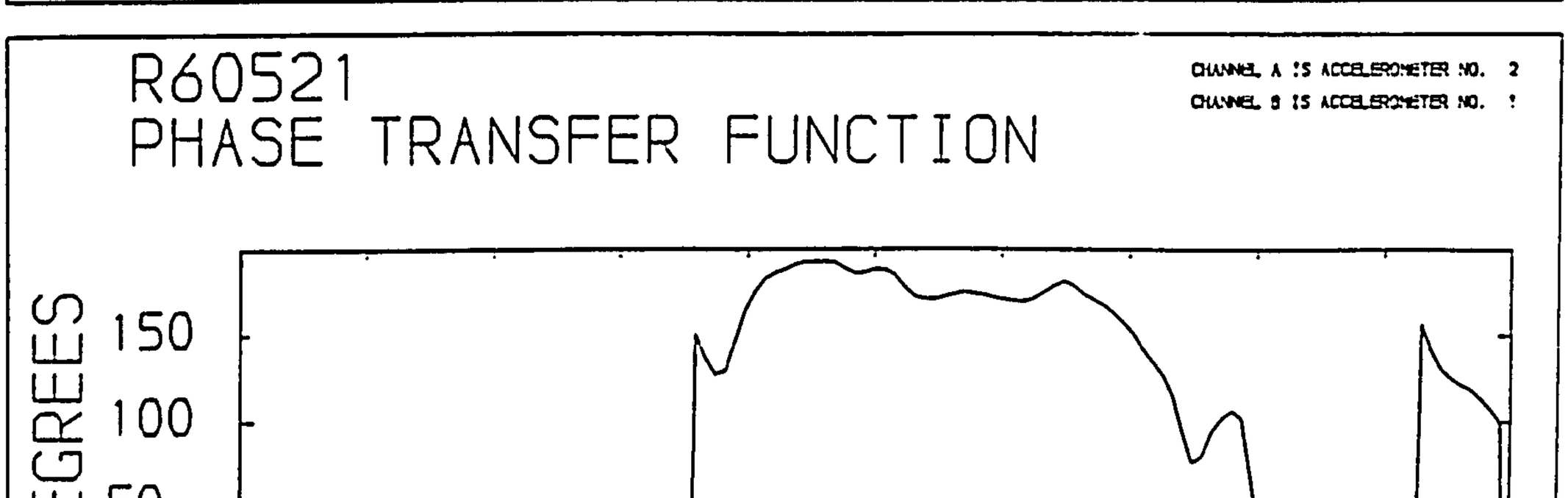

FIGURE 6.18 (cont)

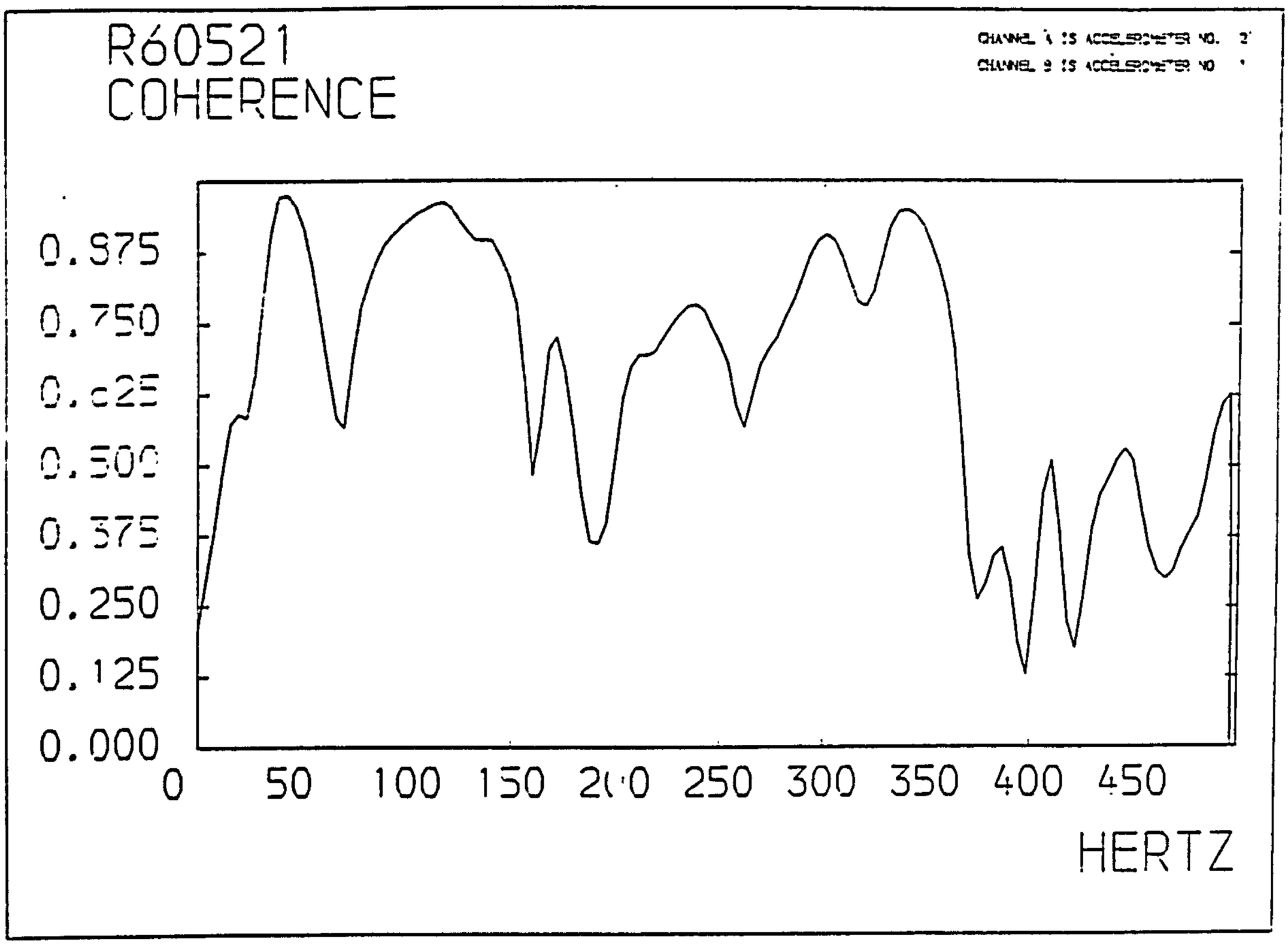

FIGURE 6.18 (cont)

```
**************************
*TITLE OF ANALYSIS IS*
*                        *
*R60521                  *
**************************
```

CHANNEL A IS ACCELEROMETER 2 DATE 24/7/85

CHANNEL B IS ACCELEROMETER 1

FREQUENCY	CHANNEL A		CHANNEL B		TRANSFER FUNCTION		COHERENCE
	AMPLITUDE	PHASE	AMPLITUDE	PHASE	AMPLITUDE	PHASE	
0	1.173	-1.809	.532	2.491	5E-03	3.273	.203
3.906	1.892	1.709	.704	7.964	5E-03	-2.2	.376
7.813	2.689	17.346	.876	5.618	5E-03	-4.936	.481
11.719	3.596	9.136	1.016	3.664	5E-03	-4.154	.574
15.625	4.91	9.527	1.501	.146	6E-03	-1.418	.59
19.531	6.849	3.664	2.361	-.636	6E-03	-.636	.583
23.438	9.663	3.664	3.033	3.273	6E-03	-.636	.658
27.344	14.12	-1.809	3.862	-.636	6E-03	-1.418	.791
31.25	15.996	-2.2	4.8	-3.764	6E-03	-3.373	.906
35.156	15.996	-4.545	5.457	-2.591	6E-03	-4.154	.972
39.063	15.996	-2.2	5.817	-3.373	6E-03	-5.718	.975
42.969	15.996	-6.891	5.692	-7.673	6E-03	-6.891	.958
46.875	15.996	-4.154	5.238	-12.754	7E-03	-10.409	.919
50.781	13.995	-13.536	4.644	-11.191	7E-03	-17.836	.85
54.688	11.149	-9.236	3.956	-2.591	7E-03	-28.391	.762
58.594	9.632	-7.282	3.252	2.882	7E-03	-40.509	.667
62.5	8.85	-1.027	2.424	-1.418	5E-03	-46.373	.583
66.406	8.178	7.964	1.736	6.4	4E-03	-36.209	.566
70.313	7.646	7.964	1.548	9.918	4E-03	-18.618	.689
74.219	7.287	9.527	1.611	7.964	5E-03	-11.191	.78
78.125	7.068	4.836	1.767	2.882	5E-03	-6.891	.825
82.031	6.911	2.882	1.955	4.446	6E-03	-4.936	.863
85.938	6.849	4.446	2.158	-4.154	7E-03	-4.936	.891
89.844	7.005	3.664	2.424	-3.764	8E-03	-6.891	.909
93.75	7.271	3.664	2.705	-2.591	9E-03	-7.673	.923
97.656	7.724	.146	3.096	-2.982	9E-03	-7.673	.934
101.563	8.334	-4.936	3.612	-2.982	.01	-6.891	.945
105.469	8.944	1.709	4.316	-2.2	.012	-6.891	.952
109.375	9.569	-1.809	5.238	-5.327	.013	-7.673	.96
113.281	10.304	-4.936	6.427	-8.064	.015	-7.673	.963
117.188	10.617	-5.327	7.552	-4.154	.017	-7.673	.954
121.094	10.211	-6.109	8.256	-2.982	.019	-9.236	.932
125	9.038	-6.109	8.287	-9.627	.022	-11.973	.913
128.906	7.396	-1.418	7.818	-3.373	.024	-16.273	.898
132.813	5.801	-1.027	7.146	4.836	.028	-22.527	.897
136.719	4.566	1.318	6.442	-2.2	.033	-28.391	.896
140.625	3.534	2.491	5.926	-8.064	.038	-34.254	.871
144.531	2.689	7.182	5.488	-13.536	.046	-41.682	.838
148.438	2.017	3.273	5.082	-6.891	.055	-49.5	.785
152.344	1.532	7.573	4.816	-12.364	.063	-63.964	.65
156.25	1.235	5.227	5.051	-13.536	.07	-96.8	.484
160.156	1.251	3.664	5.785	-10.8	.086	-136.673	.574
164.063	1.485	10.7	6.536	-9.627	.091	-160.909	.706
167.969	1.783	2.491	6.927	-9.627	.082	-178.109	.727
171.875	2.08	4.055	6.786	-7.673	.065	-194.527	.666
175.781	2.377	-.245	5.973	-7.673	.047	150.255	.564
179.688	2.768	-1.809	4.863	-10.018	.029	136.573	.449
183.594	3.268	2.882	3.659	-4.154	.017	127.191	.366
187.5	3.925	1.318	2.638	-5.891	.01	122.536	.352

FIGURE 6.19 Example of Spectrum Coordinates

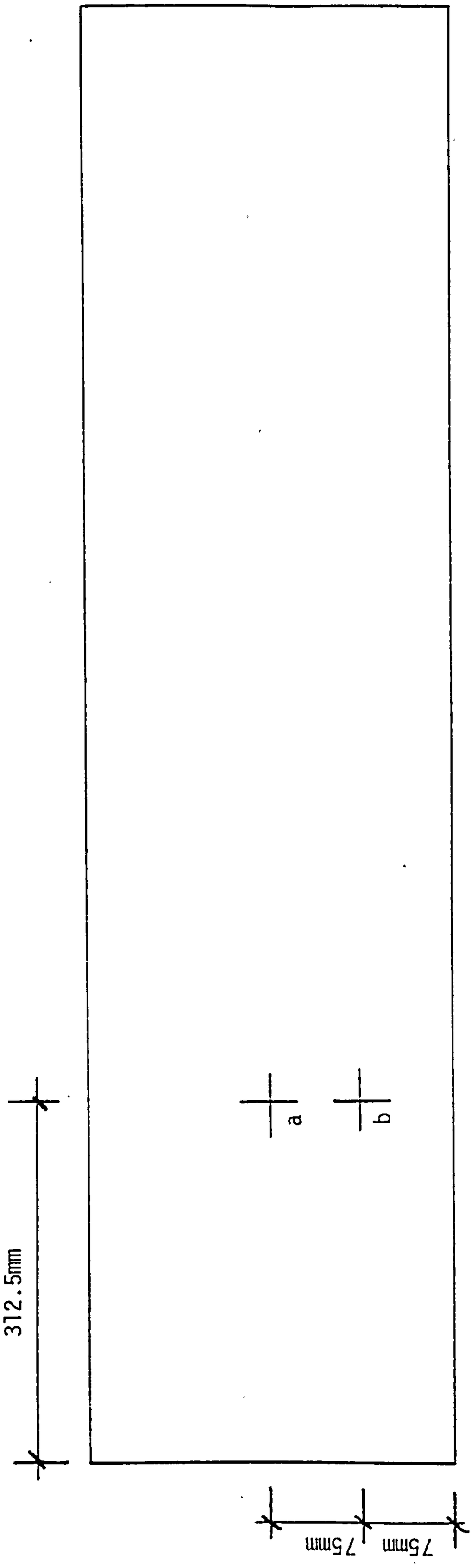

FIGURE 6.20 POSITIONs of RANDOM EXCITATION

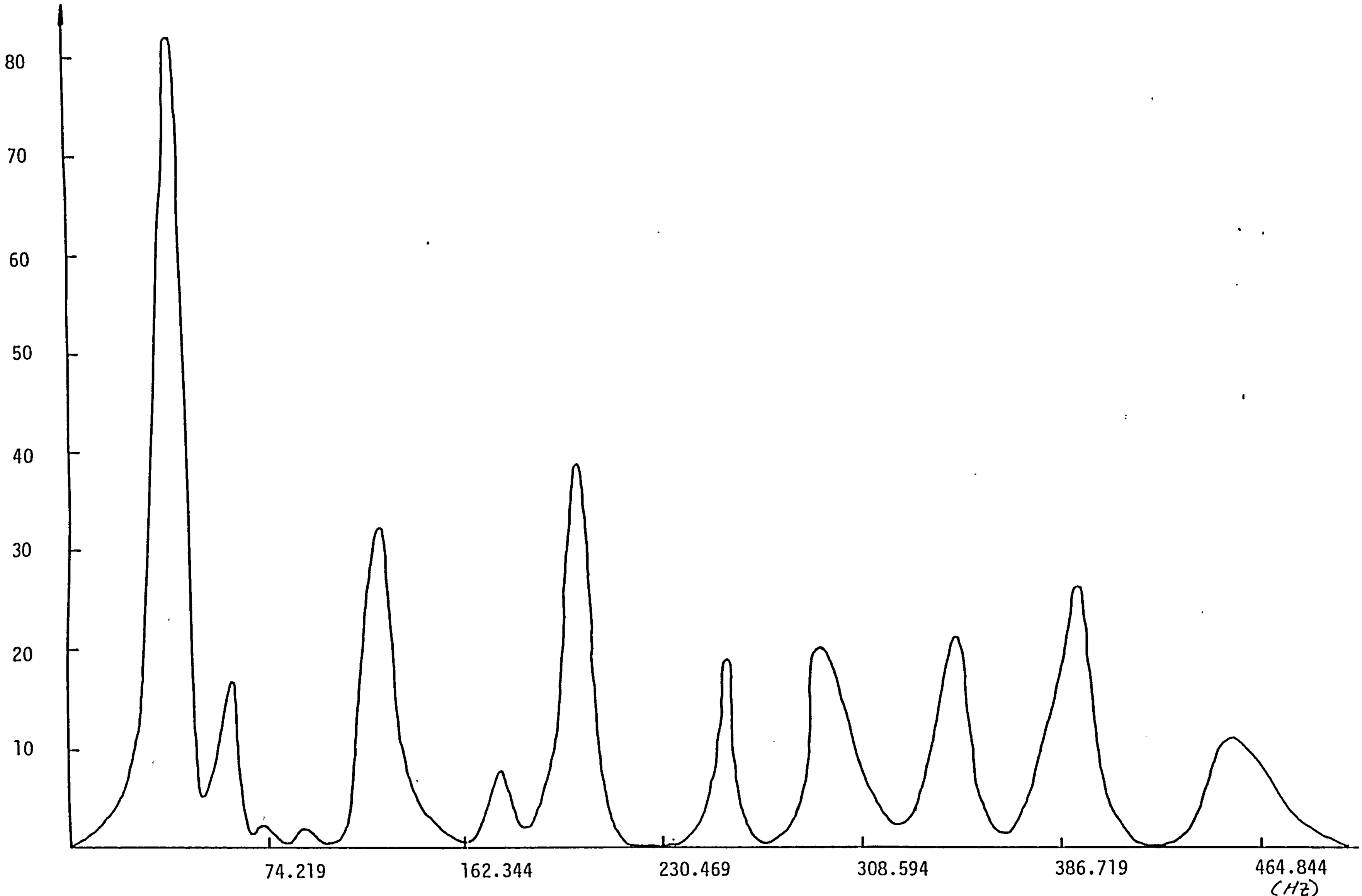

FIGURE 6.21 HISTOGRAM OF RESULTS FROM THE CENTRAL VIBRATION POSITION .

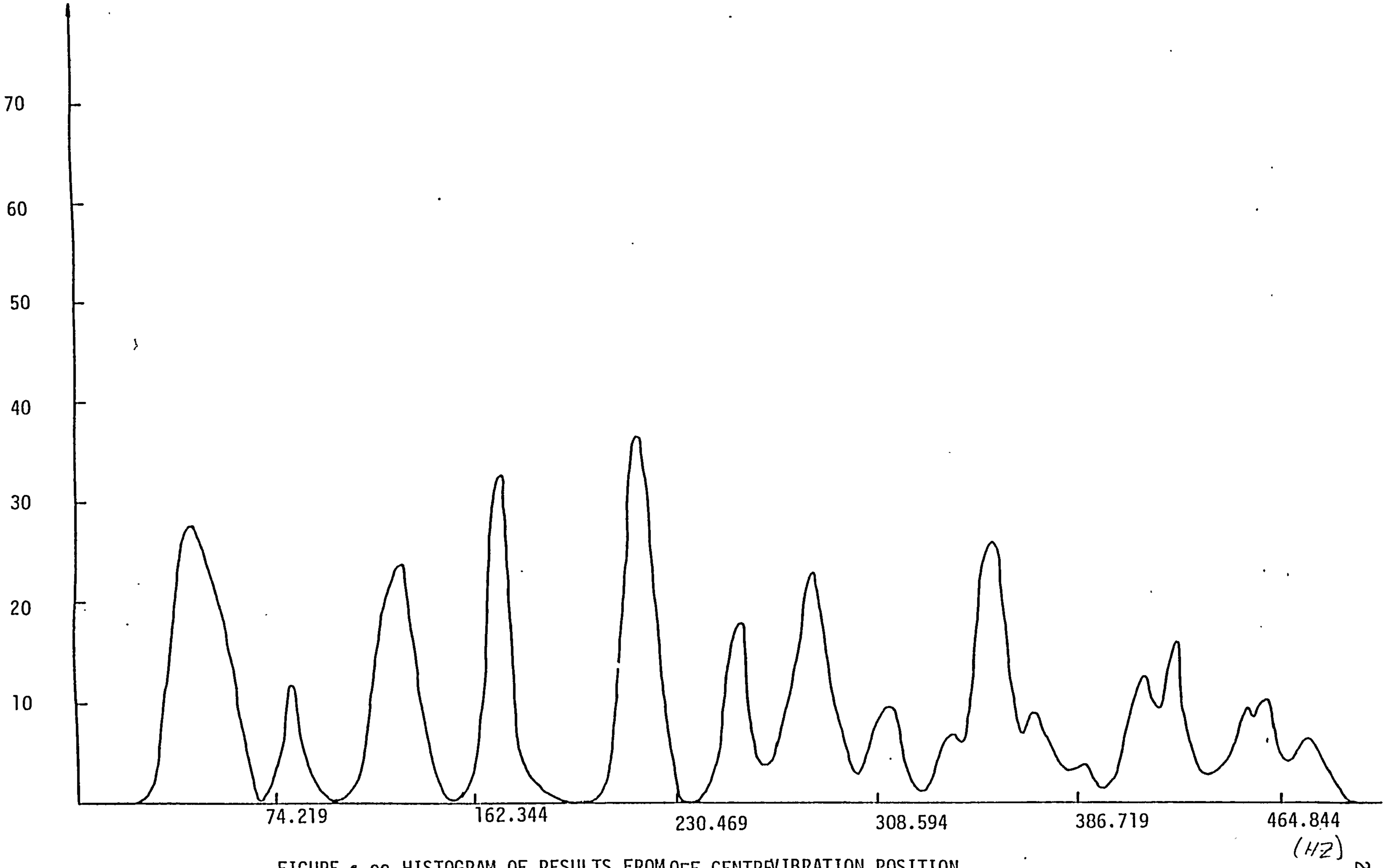

FIGURE 6.22 HISTOGRAM OF RESULTS FROM OFF CENTRE VIBRATION POSITION

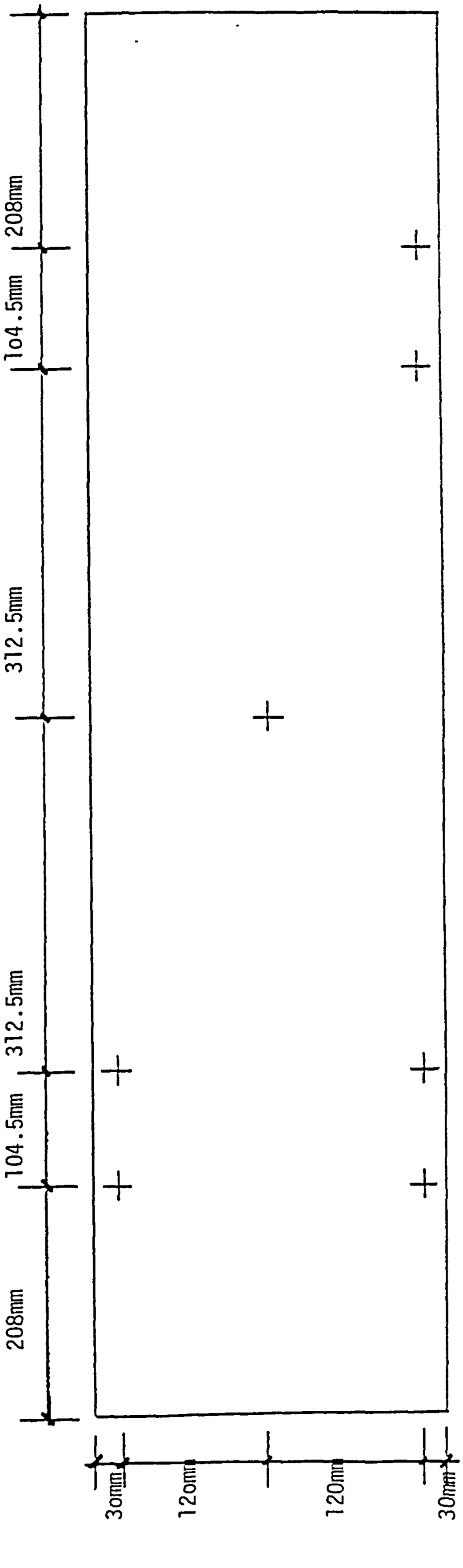

FIGURE 6.23 OPTIMUM ACCELEROMETER POSITIONS

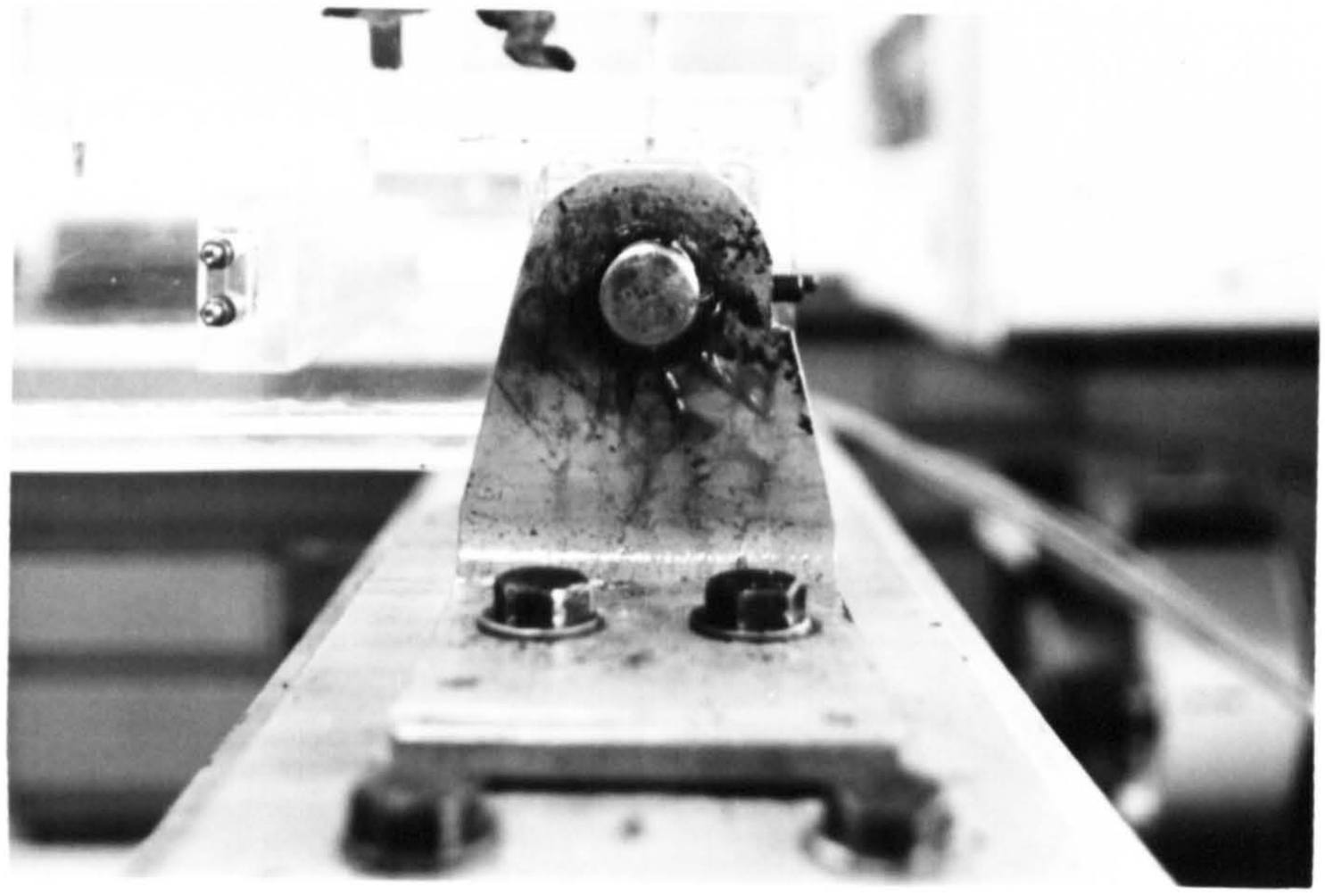

FIGURE 6.24 PINNED END BEARING

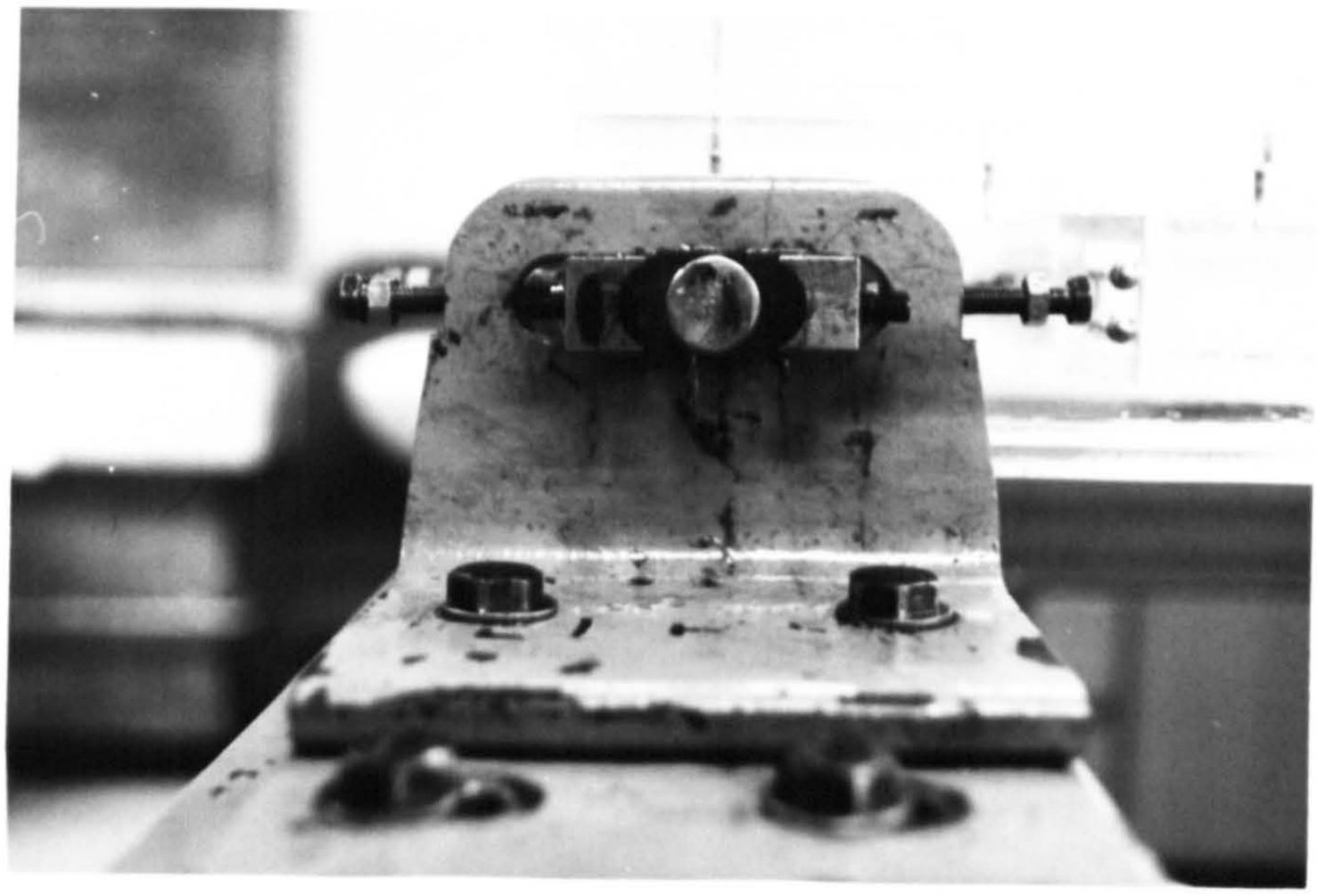

FIGURE 6.25 ROLLER END BEARING

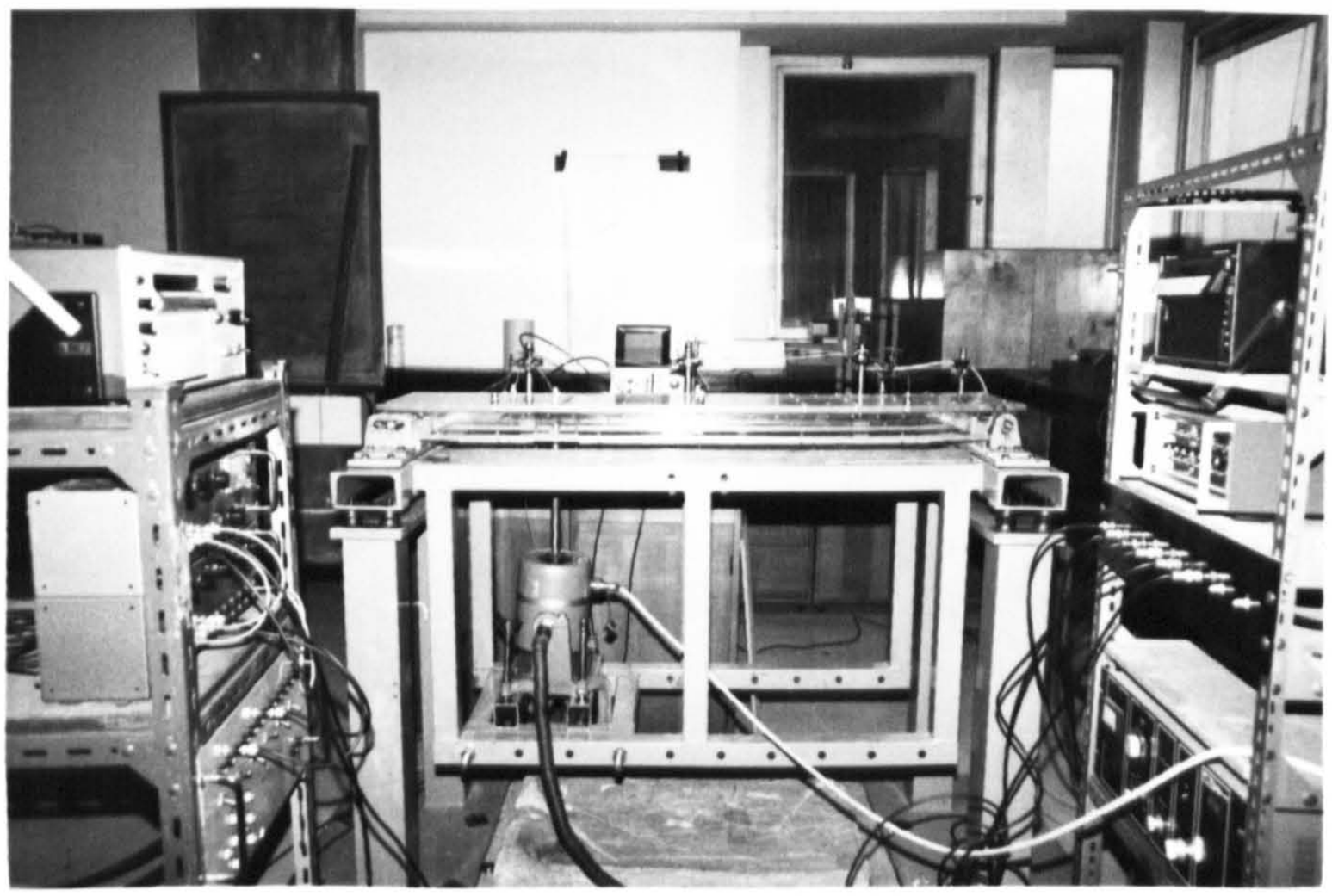

FIGURE 6.26 SINE WAVE APPARATUS

FIGURE 6.27 RANDOM WAVE APPARATUS

CONTENTS OF CHAPTER 7

CHAPTER 7 RESPONSE OF MODEL BRIDGE DUE TO STRUCTURAL CHANGES

7.1 Introduction

To test the hypothesis that the measurement of the direction and magnitude of changes in individual natural frequencies in a bridge structure can be used to predict the location, nature and magnitude of changes in structural form that have caused the shifts in the natural frequencies, a systematic laboratory study was carried out. The perspex model bridge described in chapter 6 formed the basis for this study and was monitored for dynamic response using the simple random excitation techniques, section 6.5.2, developed during the commissioning of the model and test rig.

In the earlier discussion in section 6.2.2. a very wide range of effects was identified which, through changes in stiffness and/or mass, will result in changes in dynamic response in a numerical model or in the real structure. In addition, practical monitoring of structures has indicated other changes in the configurations of structures which should not at first order level change stiffness or mass, but which do in fact result in appreciable changes in dynamic response, i.e. secord order changes. Thermal movements, for example associated with the annual temperature cycle have been correlated against appreciable cyclic changes in dynamic response by Structural Monitoring Limited (Ref.27). The choice of a laboratory study on a perspex model meant that not all of the real structural changes could be investigated. In addition, limitations on time meant that the investigation had to be restricted to only a few different effects chosen to span the range. Changes in the rotational and translational degrees of freedom at the model support points were chosen to study the effects of local changes in stiffness. Vertical differential movements of the support points were chosen to look at the changes in dynamic response associated with a second order change. The degree of shear connection between the plate desk and longitudinal stiffening beams was chosen to study the effect of an overall change in stiffness.

For each of these effects the magnitude of the change in structural form was quantified through static laboratory tests.

A comprehensive analytical study was carried out to correlate these changes in structural form with changes in natural frequency using the subspace iteration method.

Finally the correlation was investigated between the experimental and numerical modelling results in order to assess the potential of dynamic monitoring for measuring the structural integrity of bridge decks.

7.2 The Computer Model for Dynamic Analysis

The bridge model structure was modelled as a stiffened plate. The bridge deck was modelled with 112 hybrid plate bending elements, and the bridge supporting beams and cross beams were modelled with 59 eccentrically connected beam elements, giving a total number of 475 degrees of freedom. The model support points were modelled with four vertical springs of stiffness equal to $1x10^{30}N/mm^2$.

During the calibration of the calculated natural frequencies of the model bridge, it was found that the vibrator mechanism had to be included in the numerical model, since comparison was not achieved if the effect of the mechanism was neglected. The mechanism was modelled by using two small vertical springs of stiffness equal to $1x10^{3}N/mm^2$ at their respective locations. See Figure (7.1).

Using the computer model as described above the first 20 natural frequencies were calculated with the results given in Table 7.1; their corresponding mode shapes are given in Figure (7.2). The correlations between the computed and measured natural frequencies of the model bridge are given in Table 7.2. From this table it can be seen that correlation was satisfactory for the lower frequencies, but that very little correlation was found for the higher frequencies. Also for a number of the lower frequencies, i.e. modes 3,5,7,8,9, no correlation between the theoretical and experimental modes was found. Modes 3,5,7,8,9, were not predominant in the measured random vibration tests when the vibrator was connected at location (a) Figure (6.20).

The reason for these differences could be attributed to the method of vibration and/or the location of the vibrator, since the majority of the missing modes are associated with longitudinal bending, indicating that the vibration mechanism, which was placed at the quarter span prevented the structure from vibrating naturally in the higher longitudinal modes. It also can be seen that the 1st and 2nd torsional modes of vibration found experimentally were higher than the calculated modes, indicating that the vibration mechanism was affecting the overall stiffness of the model bridge.

7.3 The Model Bridge Changes

The aim of this section was to seek the evidence required to prove that small changes in structural form affect the structural natural frequencies. The changes applied to the model bridge fall into three categories, as mentioned before, with 5 changes associated with restraining the rotational and translational movement of the models boundary conditions, 6 changes associated with vertical differential displacement of the models boundary conditions, and 2 changes associated with loss of shear connection. In total thirteen different changes were introduced into the model bridge and Table 7.3 gives a complete list of these changes.

In order to assess what the above structural changes had on the global stiffness of the model bridge, simple static tests were carried out. These measurements were carried out after all the dynamic tests, with the isolation springs and vibration mechanism removed. Loads were applied as a central line load in increments of 50N up to 500N, then unloaded with the deflection measured at three locations across the model, see Figure 7.3. Hence changes in stiffness at an arbitrary point, i.e. the model's centre line, can be calculated from the load deflection curves, see Figure 7.4 for an example.

The original stiffness of the bridge was measured before and after all the changes in stiffness were applied to the model. The difference between each set of two successive stiffness measurement was approximately 3%. This difference could be attributed to errors in displacement measurement (measured to with $\pm$ 0.01mm) or more likely due to creep in the perspex model.

7.3.1 Changes in Rotation and Translation Constraints at the Support Points

i) Rotation in the pinned end was constrained : This was achieved by using the grub screws in the perspex bridge and in the support brackets, hence causing the bearings to be completely fixed at a single point, see Figure (6.6)

ii) Translation in the roller end was constrained : This was achieved by using the metal blocks and the black bolts in the supports brackets, hence preventing the bearing from translating, at a single point, see Figure (6.7).

iii) Rotation in the roller end was constrained : This was achieved by removing the black bolts in the metal blocks and by using the grub screws in the perspex bridge, hence rotation was prevented at a single point, see Figure (6.7).

iv) Rotation and translation in the roller end were both constrained by using a combination of (ii) and (iii) above.

v) The final change was to constrain all the model's bearings.

From the static measurement load deflection curves it was deduced that the following changes in stiffness occurred for each of the given structural change.

i) By fixing one of the model bridge roller bearings in rotation the stiffness is increased by 3.2%

ii) By fixing one of the model bridge roller bearings in translation the stiffness is increased by 11.7%

iii) By fixing both translation and rotation of one of the roller bearings stiffness increased by 11.9%

iv) By fixing the rotation of one of the pinned end the stiffness is increased by 3.5%

v) By fixing all the models bearings the stiffness is increased by 18.8%

The above results are given in Table (7.4).

7.3.2 Differential Displacement Changes

6 studies were carried out in this exercise, which was subdivided into two parts. The first part was to apply differential displacement to one of the pinned bearings, and the second part was to apply differential displacement to one of the roller bearings. These two parts were carried out to see what effects, if any, the bearings types had on the differential displacement. The differential displacement was achieved by placing different thickness of metal skims under each bearing hence causing an effective differential displacement of bearings. Three different levels of differential displacement were applied at each bearing type, i.e. displacements of 1mm, 2mm, 3mm. From the static measurement load deflection curves it was deduced that the following changes in stiffness occurred for the given structural changes :

i) Differential displacement of the roller end :

1mm differential displacement causes a decrease in stiffness of 3.4%
2mm differential displacement causes a decrease in stiffness of 4.4%
3mm differential displacement causes a decrease in stiffness of 5.5%

ii) Differential displacement of the pinned end.

1mm differential displacement caused a decrease in stiffness of 2.6%
2mm differential displacement caused a decrease in stiffness of 2.0%
3mm differential displacement caused a decrease in stiffness of 2.2%

The above results are given in Table 7.4.

One interesting point noted from this group of static measurements is that the structural change increased the torsional stiffness of the structure. In this case if the individual deflections are studied, i.e. dual gauges 1,2,3 Figure 7.3, and the changes in stiffness at each gauge is calculated, it is noted that the variation in stiffness of the two outer gauges was less than the total global variation, denoting an increase in torsional stiffness, Table 7.5, hence causing the hiccup in the changes in global stiffness for differential displacement at the pinned end bearing.

7.3.3 Loss of Shear Connection Changes

Two studies were carried out in this exercise by removing the screws connecting the perspex I-beams to the perspex deck. The first change was to remove every second screw connecting one of the longitudinal beams to the deck; the second change was to remove every second screw connecting both longitudinal beams to the deck.

From the static measurement load deflection curves it was deduced that 50% reduction in shear connection for one stiffening beam, reduced the overall stiffness by 2%, and the torsional stiffness was also noted to be reduced as expected. In the case of the reduction in shear connection for both stiffening beams, the overall stiffness was reduced by 7.9%. The above results are given in Table 7.4

7.3.4 Results

The effects which the structural changes had on the model bridge's measured natural frequencies are given in Table 7.6. For ease of study these results have also been plotted in the form of four graphs. In these graphs frequency is plotted against change in structural configuration, owing to the figures scales and the small variation in the natural frequencies due to a structural change, the curves may look horizontal, and the results are given in the following figures.

Figure 7.5 restraint in boundary conditions
Figure 7.6 differential displacement of a pinned support
Figure 7.7 differential displacement of a roller support
Figure 7.8 loss of shear connection between the stiffening beams and the bridge deck

Owing to the method of excitation and/or the method of frequency extraction the results given in Table 7.6 and Figures (7.5, 7.6, 7.7, 7.8) have omissions. For every experimental change a complete set of frequencies was not found.

7.4 The Model Bridge Computer Study

The model changes given above could not all be simulated correctly, since the computer model was a plate analysis, i.e. 2-dimensional model, with 3 degrees of freedoms per mode, i.e. Rx, Ry, z, whereas the model had 6 degrees of freedom, i.e. x,y,z,Rx,Ry,Rz. A study, as far as possible similar to that of the experimental changes was carried out as follows :

a. changes to rotational boundary conditions were simulated by introducing varying rotational stiffnesses at the supports.

b. differential displacement was simulated by varying the vertical support stiffness.

c. the effect of loss of shear connection was carried out as with the Westerhouse bridge study given in chapter 5.

The above changes in the computer model were split into six sections;

a) varying rotational stiffness of a pinned end; from being free to rotate to completely fixed, by adding a rotation spring and by incrementing the spring stiffness by a factor of $1x10^5 N/mm^2$ from zero stiffness to $1x10^{30} N/mm^2$

b) varying rotational stiffness of a roller end; from being free to rotate to completely fixed by adding a rotation spring and by incrementing the spring stiffness by a factor of $1x10^5 N/mm^2$ from zero stiffness to $1x10^{30} N/mm^2$

c) varying vertical stiffness of a pinned end from a spring of stiffness of $1x10^{30} N/mm^2$ to $1x10^5 N/mm^2$ by incrementing the stiffness by a factor of $1x10^5 N/mm^2$

d) varying vertical stiffness of a roller end from a spring of stiffness of $1x10^{30} N/mm^2$ to $1x10 N/mm^2$

e) fixing all boundary conditions

f) reducing shear connection along the interface between the plate and the stiffening beams. This was achieved by reducing the

eccenticity of every second beam element to zero as carried out for the Westerhouse bridge study given in Chapter 5.

Note : the pinned and roller ends were modelled separately because the finite element model included the stiffness of the vibrator mechanism.

Table 7.7 gives a complete list of the structural changes. The results from the above study are given in Table 7.8. This table is subdivided into five sections :

a. rotational stiffness of the pinned end
b. rotational stiffness of the roller end
c. vertical stiffness of the pinned end
d. vertical stiffness of the roller end
e. fixed all boundary conditions and the reductions in shear connection

To assess what effect the above computer changes had on stiffness, a static analysis of the dynamic model was carried out for each change. Stiffness is defined here as the central deflection when a transverse line load of magnitude unity acts at the centre of the span. The results of this static study are given in table 7.9.

7.5 Discussion of the Results

The discussion of the results will be divided into three sections :

7.5.1 Experimental Results

7.5.1.1 Restraints of the Boundary Conditions

From Table 7.6 and Figure 7.5 it can be seen that a large majority of the frequencies show random variation. The only frequencies which show any consistent change with the structural changes are the 1st, 2nd, 7rd and 10th natural frequencies. If the above frequencies are studied more closely, as given in Table 7.10, in general the following can be concluded :

i) The 1st and 10th natural frequencies vary accordingly to change in global stiffness

ii) The 7th natural frequency shows a general shift denoting the boundary conditions have been affected

iii) The 2nd natural frequency shows a general shift only when the rotational boundary conditions were affected.

7.5.1.2 Differential Displacement of the Pinned End

From Table 7.6 and Figure 7.6 it can be seen that a large majority of the frequencies show random variation. The only frequencies which show any consistent change with the structural changes are the 2nd, 4th, 5th, and 7th natural frequencies. If the above frequencies are studied more closely, as given in Table 7.11, in general the following can be concluded.

i) 4th, 5th, and 7th natural frequencies vary with changes in global stiffness

ii) 2nd natural frequency variation is consistent with the previous comments : as the differential displacement increases the model torsional stiffness increases, and this has been confirmed since with the 2nd natural frequency, the first torsional mode increases from a reduced value for small displacements, then increases as the displacement increases.

7.5.1.3 Differential Displacement of the Roller End

From Table 7.6 and Figure 7.7 the random effects of the results are again very pronounced with only one natural frequency, the 3rd mode showing any form of consistent change. If the above frequency is studied more closely, as given in Table 7.12 in general it can be seen that this natural frequency varies according to the change in global stiffness.

7.5.1.4 Shear Connection Changes

From Table 7.6 and Figure 7.8 it can be seen that the results are incomplete, but 5 of the natural frequencies show changes associated with the applied changed in stiffness (i.e. modes 1,2,6,7,10). If the above frequencies are studied more closely as given in Table 7.13. In general the following can be concluded :

i) The 1st natural frequency varies according to the changes in global stiffness

ii) The remaining four natural frequencies have had a greater effect on the shift in frequency for removal of shear connection in one beam, i.e. for reducing the torsional stiffness. It is interesting to note, from Table 7.2 that the affected frequencies are all associated with torsional or cross bending modes.

7.5.1.5 General Discussion

In general the results were disappointing but there were indications that at lower frequencies there was some consistent increase in natural frequency associated with an increase in stiffness. The results also support the proposition that different types of changes cause different effects in different natural frequencies,

e.g. Restraint of the boundary conditions affected 1,2,7,10 modes
Differential displacement of a pinned end affected 2,4,5,7 modes
Differential displacement of the roller end affected 3 modes
Shear connection affected 1,2,6,7,10 modes

The above examples do indicate that the method described in chapter 6 could well be a useful one for detecting structural changes in model bridges. Also the percentage changes in natural frequencies, were affected to different extents for different types of changes, and values of stiffness as follows, i.e.

i) Boundary conditions showed a maximum natural frequency increase of 13.2% in the 1st mode for a global increase in stiffness of 18.8% from the static measurements.

ii) Differential displacement of the pinned end showed a maximum natural frequency decrease of 8.7% in the 7th mode for a global decrease in stiffness of 2.6% from the static measurements

iii) Loss of shear connection showed a maximum natural frequency decrease of 8.1% in the 6th mode for a global decrease in stiffness of 7.9% from the static measurements.

Finally, it can be concluded from the results for the four types of structural changes in general, that as the structural stiffnesses increase the natural frequencies increase, and as the structural stiffnesses decrease the natural frequencies decrease.

The above results illustrate a problem that arose during each experiment and that is that a consistent number of natural frequencies was not found. This could be attributed to the method of vibration or possibly to the randomness of the frequency extraction method given in chapter 6. The reasons for the randomness of the results could be due to the fact that the spectral density of the accelerometer signals at higher frequencies, see Figure 6.18 were low, and of course points of resonance were deduced from these spectra density curves.

The above results have shown up a number of interesting points associated with the changes in natural frequencies caused by the changes in structural stiffness.

i) Boundary conditions : In general the shifts in natural frequencies were according to the shifts in stiffness, but with certain frequencies affected in different ways, i.e. in the 2nd natural frequency, the first torsional mode, was affected most when rotational stiffness of the bearing was increased.

ii) Differential Displacement of the pinned end : In this case the results showed two interesting points. The first was that the displacement caused a decrease in bending stiffness, and secondly the displacement caused an increase in torsional stiffness, denoting that twisting of the pinned bearing had occurred.

iii) Differential displacement of the roller end : In this case the results showed that in general the structural change has very little effect on the structural natural frequencies

iv) Reduction in shear connection : In this case the results showed that this structural change affects both torsional and cross bending modes of the structure. The effect is more pronounced when the effect is unsymmetrical.

So in general it may be concluded that :

i) If bending modes show an increase in stiffness then some form of bearing fixity has occurred.

ii) If this is a reduction of the torsional and cross bending modes then some form of loss of shear connection has occurred.

iii) If bending modes show a decrease with an associated trosional stiffness increase, i.e. a small decrease in torsional natural frequencies, then some form of differential displacement of pinned bearing has occurred.

7.5.2 Computer Dynamic Model Results

7.5.2.1 Rotational Stiffness Variation

As mentioned before rotational stiffnesses were introduced to both the pinned and roller bearing ends to see if the vibrator mechanism had any effect. It can be seen from Table 7.8 that the mechanism does affect the 2-D dynamic model. It also can be seen from Table 7.8 that changes in natural frequencies above the 6th mode are insignificant.

If the results from introducing a rotational stiffness are studied more closely as in table 7.14 it can be concluded

i) for both the pinned and roller ends when the stiffness of the springs increased above $1x10^{10}N/mm^2$ any further increase has no effect on the model's response.

ii) when bearing fixity has occurred, the second mode of vibration, i.e. the first torsional mode has the largest shift, i.e. 12.1% increase for a 25.1% increase in stiffness.

If the results from fixing all bearings are studied, Table 7.15, they show a much greater shift in natural frequencies, but in this case the first mode shows the greatest increase of 62.1% for an increase of stiffness of 105.6%

7.5.2.2 Vertical Stiffness Variation

As with the rotation stiffness the effect of the mechanism has had an effect. If the results are studied closely, as in Table 7.16 and Table 7.8 it can be concluded :

i) For both the pinned and roller ends the response of the model is not affected until the vertical springs stiffness is reduced to below $1x10^{10}N/mm^2$, as with the bearings study.

ii) The percentage change reduces to less than 1% for natural frequencies greater than the 6th mode.

iii) The reduction in vertical bearing stiffness has a more pronounced effect on the bending modes, i.e. modes 1,3,5 with much reduced effect on the torsional and cross bending modes, i.e. modes 2,4,6.

7.5.2.3 Reduction in Shear Connection

From Table 7.8 and Table 7.17 it can be seen, unlike the other studies, every natural frequency was affected. If Table 7.17 is studied, it can be seen that reduction in shear connection for one beam, has a greater effect on the bending modes, whereas when reduction is applied to both beams, the effect is greatest on the torsional and cross bending modes.

7.5.2.4 General Discussion

The above results have shown a number of interesting points associated with changes in natural frequencies caused by the changes applied to the numerical dynamic model. In general it may be concluded that :

i) If there is a shift in all frequencies and it is noted that the decrease is greatest in torsional modes, then some reduction in shear connection has occurred.

ii) If there is large decrease in bending modes associated with a smaller decrease in torsional modes, then there has been a reduction in bearings vertical stiffness

iii) If the shifts in frequencies are limited to the lower ones, i.e. 1st and 2nd, with the greatest effect on the torsional modes then some form of boundary fixity has occurred.

7.5.3 Comparison of the computed and measured natural frequencies

From the above discussion of results for the measured natural frequencies of the bridge model and the results of the bridge calculated natural frequencies, very little common variation was shown. Also from the static studies it can be seen that the variation in stiffness between the two methods of frequency calculation was large.

Comparison for each of the three types of structural change:

i) changes in boundary conditions

From the dynamic measurement studies it was concluded that if some form of bearing fixity has occurred, then the bending modes would show an increase in stiffness, whereas if bearing fixity occurs in the dynamic numerial model then the first two natural frequencies only show any considerable change with the first bending mode showing the greatest increase.

The above disagreement can be illustrated by the changes in the model's stiffness for different degrees of boundary fixity. e.g. if all boundary conditions are fixed then the model bridge shows an increase of stiffness of 18.8%, whereas the numerical dynamic model shows an increase in the first natural frequency of 105.6%. The large discrepancies could be due to the fact that the numerical model did not take into account any form of bearing friction, but this would not change the numerical models general conclusion of only affecting the first two modes of vibration.

One interesting point the static measurements showed was that fixing the translation bearing movement affected stiffness by 11.7% and this was far greater than that which occurred when fixing rotation, 3.5% for pinned bearings and 3.2% for roller bearings. This degree of freedom was not included in the dynamic numerical model

Another point that should be noted here is that the position of the boundary conditions in relationship to the models neutral axis is different in the two models. i.e. in the dynamic finite element model the boundary conditions are at the centre line of the plate elements and in the physical model the boundary conditions are at the centre line of the stiffening beams.

ii) changes in boundary conditions

From the dynamic measurements studies it was concluded that if some form of differential displacement has occurred at a fixed bearing then bending modes show a decrease with an associated small torsional decrease and if some form of bearing vertical stiffness has accurred then there is a large decrease in bending modes associated with smaller decrease in torsional modes.

The above two separate conclusions agree, but comparison cannot be made since the two natural frequencies which showed the greatest shift (i.e. modes 3,5) were not recorded during the original measurements of the unchanged model. These two modes were detected during the differential displacement measurements and they also show large shift compared to other changes when detected. Hence it could be stated that this type of structural change can be modelled in this way in a 2-D dynamic finite element idealisation but with the vertical stiffness varied between 1×10^{10} n/m^2 to zero for different levels of displacement.

iii) Changes in shear connections

From the dynamic measurements studies it was concluded that if some form of loss of shear connection has occurred then there is a reduction of the torsional and cross bending modes, and if a loss of shear connection occurs in the dynamic numerical model then there is a decrease in all frequencies, with greater shift in torsional modes.

Again the above two separate conclusions seem to agree, but again comparison cannot be made since the dynamic numerical model shows a reduction in stiffness of 34.7% whereas the model bridge showed a reduction in stiffness of 7.9%. If the numerical frequencies are scaled, then the same trend was shown with the measured frequency. This was checked by adjusting the eccentricity of the shear connections in the numerical model i.e. a reduction in eccentraty to produce a reduction in stiffness of 6.1%. The results are given in Table 7.18. These results show that lttle correlation was found.

This study gave hope that the method would work, but after further study i.e. on expanding the calculated natural frequencies data bank, little correlation was found, denoting that the physical structural change in the model bridge had been modelled incorrectly in the dynamic finite element model.

7.6 Conclusion

From the above discussions it is obvious that the results are very disappointing. The disappointing results can be attributed to a number of causes in both the natural frequencies response measurement studies and the calculation of the natural frequencies through the use of finite elements.

Response measurement studies : a complete set of natural frequencies for the unchanged model was not found. Also there was no consistency in the number of natural frequencies recorded for each structural change. The above two problems could possibly be resolved by a more extensive investigation into the number of different vibration mechanisms, and their location on the model bridge, eg. using a light vibration system, with a low stiffness, since the above problems were caused by the large stiffness of the system used.

Another problem which arose during this study was that the model bridge was too stiff. This was very noticeable in the model response spectra, Figure 6.18, since at higher frequencies it was very difficult to detect points of resonance hence natural frequencies. With the above in mind it

now seems that the applied structural changes did not alter the stiffness sufficiently to detect any shift in natural frequencies, since changes in higher modes of response were undetectable from the spectral curves. Owing to the simple form of the bridge model, and the results recorded, the following structural changes could possibly improve the situations.

a) progressive loss of shear connection from one end
b) completely removing a bearing
c) introducing diffferent materials for the bridge deck
d) cutting slots in the bridge deck.

The first two above possible improvements, were studied, to find what effect they would have on the models structural stiffness by carring out further static measurements tests.

It was found that if all the shear connections of one beam were removed from the centre line to one pinned end bearing a 4.5% reduction in overall stiffness occurred. The value is below the level recommended by Structural Monitoring Limited (Ref 11). In the case of removing a bearing, one roller bearing was removed, and the change in stiffness was seen to decrease by 77.5%. This value is very uncertain since it was noticed that the model was unstable with 3 supports. In general if different structural changes were applied to the model the situation would not improve, since the structure was too stiff, and this situation was not improved by the increase in tonsional stiffness caused by the vibrator mechanism. Hence a more flexible structure is required.

Finite element studies : The above numerical studies have shown the following deficiency in the dynamic numerical model.

i) The comparison between the finite element model and the measured natural frequencies, table 7.2 is satisfactory for the lower frequencies, but there is little correlation found for the higher frequencies.

ii) Since most of the changes were associated with boundary conditions, the changes could not be modelled correctly.

iii) Because of (ii) above the method described in section one of this thesis produced results which would introduce another level of uncertainty. The method given in section one was carried out so that additional information on the savings of computer time when restart analysis is used, could be determined.

Hence the computer model constructed was too unsophisticated for the model changes, but in this study a 2-D plate bending approach was followed, since this was the approach of Structral Monitoring Limited. It has been found that the structural changes applied to the above dynamic numerical model could not be modelled correctly i.e. translational degrees of freedom. A 3-D model could possibily be used, but by using such models, there would be an increase in computer cost by more than twofold. It was however noted that any structural change, if small, does not have much effect on natural frequencies above the 6^{th} mode and therefore by limiting the computer study to say 6 modes, computer costs would be contained. Another approach would be to use a mixed finite element formulation i.e. generally a 2-D model with points of interest i.e. the supports being modelled in 3-D.

In general the study carried out in this chapter has showen a number of points.

The measured frequencies showed a number of trends i.e.

i) If bending modes show an increase in stiffness then some form of bearing fixity has occurred.

ii) If there is a reduction of the torsional and cross bending modes them some form of loss of shear connection has occurred.

iii) If bending modes show a decrease with an associated torsional stiffness increase, i.e. a small decrease in torsional natural frequencies, then some form of differential displacement of pinned bearing has occurred.

The above trends denotes that the method shows signs of working, and hence merits further investigation.

The calculated frequencies showed a number of trends i.e.

i) If there is a shift in all frequencies and it is noted that the decrease is greatest in torsional modes, then some reduction in shear connection has accurred.

ii) If there is large decrease in bending modes associated with a smaller decrease in torsional modes, then there has been a reduction in bearings vertical stiffness.

iii) If the shifts in frequencies are limited to the lower ones i.e. 1^{st} and 2^{nd}, with the greatest effect on the torsional modes then some form of boundary fixity has accurred.

This study showed that this field needs much further investigation into the modelling of structural changes.

MODE NUMBER	FREQUENCY (HZ)
1	41.22
2	56.27
3	122.6
4	145.0
5	206.7
6	221.3
7	228.8
8	238.9
9	282.5
10	325.6
11	343.7
12	361.5
13	367.3
14	387.6
15	390.4
16	400.6
17	402.2
18	446.0
19	473.0
20	481.9

TABLE 7.1 BRIDGE FINITE ELEMENT MODEL
--------- NATURAL FREQUENCIES (HZ)

MODE	COMPUTER FREQUENCY	COMPUTER MODE SHAPE	MEASURED FREQUENCY	MEASURED MODE SHAPE
1	41.22	1st BENDING	41.2	1st BENDING
2	56.27	1st TORSION	60.7	1st TORSION
3	122.6	2nd BENDING	----	----
4	145.0	2nd TORSION	148.2	2nd TORSION
5	206.7	3rd BENDING	----	----
6	221.3	1st CROSS BEND.	221.6	1st CROSS BEND.
7	228.8	2nd CROSS BEND.	----	----
8	238.9	3rd TORSION	----	----
9	232.5	4th BENDING	279.5	----
10	325.6	4th TORSION	331.8	3rd TORSION
11	343.7	5th BENDING	----	----
12	361.5	3rd CROSS BEND.	----	----
13	367.3	4th CROSS BEND.	----	----
14	337.6	5th TORSION	----	----
15	390.4	5th CROSS BEND.	----	----
16	400.6	6th BENDING	----	----
17	402.2	6th TORSION	----	----
18	446.0	7th BENDING	----	----
19	473.0	7th TORSION	----	----
20	431.9	6th CROSS BEND.	----	----

TABLE 7.2 COMPARSION BETWEEN COMPUTED AND MEASURED RESPONSE

CHANGE NUMBER	CHANGE
1	PINNED END -FIX ROTATION
2	ROLLER END -FIX TRANSLATION
3	ROLLER END -FIX TRANSLATION AND ROTATION
4	ROLLER END -FIX ROTATION
5	FIX ALL BOUNDARY CONDITIONS
6	DIFFERENTIAL DISPLACEMENT OF ONE PINNED END BY 1mm
7	DIFFERENTIAL DISPLACEMENT OF ONE PINNED END BY 2mm
8	DIFFERENTIAL DISPLACEMENT OF ONE PINNED END BY 3mm
9	DIFFERENTIAL DISPLACEMENT OF ONE ROLLER END BY 1mm
10	DIFFERENTIAL DISPLACEMENT OF ONE ROLLER END BY 2mm
11	DIFFERENTIAL DISPLACEMENT OF ONE ROLLER END BY 3mm
12	REMOVE 50% OF SHEAR CONNECTORS OF ONE BEAM
13	REMOVE 50% OF SHEAR CONNECTORS OF BOTH BEAMS

TABLE 7.3 TABLE OF MODEL CHANGES

CHANGE NUMBER	CHANGE	CHANGE IN STIFFNESS
1	PINNED END -FIX ROTATION	3.5%
2	ROLLER END -FIX TRANSLATION	11.7%
3	ROLLER END -FIX TRANSLATION AND ROTATION	11.9%
4	ROLLER END -FIX ROTATION	3.2%
5	FIX ALL BOUNDARY CONDITIONS	18.8%
6	DIFFERENTIAL DISPLACEMENT OF ONE PINNED END BY 1mm	-2.6%
7	DIFFERENTIAL DISPLACEMENT OF ONE PINNED END BY 2mm	-2.0%
8	DIFFERENTIAL DISPLACEMENT OF ONE PINNED END BY 3mm	-2.2%
9	DIFFERENTIAL DISPLACEMENT OF ONE ROLLER END BY 1mm	-3.4%
10	DIFFERENTIAL DISPLACEMENT OF ONE ROLLER END BY 2mm	-4.4%
11	DIFFERENTIAL DISPLACEMENT OF ONE ROLLER END BY 3mm	-5.5%
12	REMOVE 50% OF SHEAR CONNECTORS OF ONE BEAM	-2.0%
13	REMOVE 50% OF SHEAR CONNECTORS OF BOTH BEAMS	-7.9%

-VE DENOTES DECREASE IN STIFFNESS

TABLE 7.4 TABLE OF THE MEASURED CHANGES IN STIFFNESS

DISPLACEMENT	DIAL GAUGE 1	DAIL GAUGE 2	DAIL GAUGE 3	AVERAGE
1mm	0.7%	-5.8%	-2.8%	-2.6%
2mm	0.2%	-3.2%	-2.9%	-2.0%
3mm	-0.1%	-3.2%	-0.4%	-2.2%

-VE DENOTES DECREASE IN STIFFNESS

TABLE 7.5 VARIATION OF STIFFNESS ACROSS BRIDGE DUE TO DIFFERENTAL DISPLACEMENT OF A PINNED BEARING

MODE NUMBER	ORIGNAL	PINNED FIX ROTAT. CHANGE 1	ROLLER FIX TRANS. CHANGE 2	ROLLER FIX TRANS. ROTAT. CHANGE 3	ROLLER FIX ROTAT. CHANGE 4	FIX ALL BOUND. COND. CHANGE 5	D. DISP PINNED 1mm CHANGE 6	D. DISP PINNED 2mm CHANGE 7	D. DISP PINNED 3mm CHANGE 8
1	41.22	39.66	42.78	42.78	42.00	46.69	40.44	42.78	42.78
2	60.75	56.06	59.97	56.06	55.28	62.31	56.06	57.63	60.75
3	----	120.1	119.3	120.9	119.3	126.3	123.2	123.2	126.3
4	148.2	144.3	148.2	----	148.2	----	----	134.1	133.4
5	----	139.6	173.2	180.2	171.6	181.8	176.3	174.0	174.8
6	221.6	209.9	226.3	227.1	211.5	210.7	208.4	207.6	211.5
7	279.5	250.6	252.1	256.8	252.1	257.6	255.2	258.4	256.8
8	291.2	305.2	----	----	----	----	----	----	270.9
9	308.4	311.5	306.0	309.1	306.0	311.5	313.1	311.5	309.9
10	331.8	341.2	340.4	346.6	334.1	353.7	341.2	345.1	347.4
11	----	386.7	386.5	387.3	385.7	----	393.5	393.5	395.1
12	416.2	411.5	414.6	423.2	415.4	414.6	413.1	424.8	430.2
13	467.7	431.0	433.4	----	----	450.6	434.9	459.9	452.9

TABLE 7.6 NATURAL FREQUENCIES OF THE MODEL BRIDGE WITH STRUCTURAL CHANGE (HZ)

MODE NUMBER	ORIGNAL	D. DISP ROLLER 1mm CHANGE 9	D. DISP ROLLER 2mm CHANGE 10	D. DISP ROLLER 3mm CHANGE 11	REMOVE 50% ONE BEAM CHANGE 12	REMOVE 50% TWO BEAM CHANGE 13
1	41.22	40.44	40.44	40.44	40.44	39.66
2	60.75	59.19	55.28	57.63	56.85	56.06
3	----	124.0	119.3	112.3	----	124.0
4	148.2	145.9	145.9	145.1	145.1	----
5	----	170.8	172.4	177.9	170.1	170.1
6	221.6	210.7	212.3	----	212.3	210.7
7	279.5	262.3	261.5	2o2.3	259.1	256.8
8	291.2	----	----	295.1	----	306.8
9	303.4	308.4	309.9	320.1	320.9	----
10	331.8	345.9	345.1	----	345.9	347.4
11	----	384.9	385.7	383.4	392.0	----
12	416.2	416.2	413.1	412.3	----	----
13	467.7	446.6	445.9	----	----	446.6

TABLE 7.6 (cont) NATURAL FREQENCIES OF THE MODEL BRIDGE WITH STRUCTURAL CHANGE (HZ)

DEFECT NUMBER	DEFECT	
1	INTRODUCE ROTATIONAL STIFFNESS OF AT ONE OF THE PINNED ENDS	1.0E05
2	ditto	1.0E10
3	ditto	1.0E15
4	ditto	1.0E20
5	ditto	1.0E25
6	ditto	1.0E30
7	INTRODUCE ROTATIONAL STIFFNESS OF AT ONE OF THE ROLLER ENDS	1.0E05
8	ditto	1.0E10
9	ditto	1.0E15
10	ditto	1.0E20
11	ditto	1.0E25
12	ditto	1.0E30
13	FIX ALL BOUNDARY CONDITIONS	
14	VERTICAL STIFFNESS OF ONE OF THE PINNED ENDS	1.0E05
15	ditto	1.0E10
16	ditto	1.0E15
17	ditto	1.0E20
18	ditto	1.0E25
19	ditto	1.0E30
20	VERTERAL STIFFNESS OF ONE OF THE ROLLER ENDS	1.0E05
21	ditto	1.0E10
22	ditto	1.0E15
23	ditto	1.0E20
24	ditto	1.0E25
25	ditto ditto	1.0E30
26	REDUCE SHEAR CONNECTORS IN ONE OF THE BEAMS	
27	REDUCE SHEAR CONNECTORS IN BOTH BEAMS	

TABLE 7.7 COMPUTER MODEL CHANGES

MODE NUMBER	ORIGINAL	COMPUTER CHANGE 1 (1.0E05)	COMPUTER CHANGE 2 (1.0E10)	COMPUTER CHANGE 3 (1.0E15)	COMPUTER CHANGE 4 (1.0E20)	COMPUTER CHANGE 5 (1.0E25)	COMPUTER CHANGE 6 (1.0E30)
1	41.22	42.80	45.69	45.69	45.69	45.69	45.69
2	56.27	57.69	63.07	63.08	63.08	63.08	63.08
3	122.6	123.6	126.7	126.7	126.7	126.7	126.7
4	145.0	146.0	150.2	150.2	150.2	150.2	150.2
5	206.7	207.3	209.5	209.5	209.5	209.5	209.5
6	221.3	221.3	221.4	221.4	221.4	221.4	221.4
7	228.8	228.8	228.8	228.8	228.8	228.8	228.8
8	238.9	239.4	241.6	241.6	241.6	241.6	241.6
9	282.5	282.8	284.2	284.2	284.2	284.2	284.2
10	325.6	325.9	327.0	327.0	327.0	327.0	327.0
11	343.7	343.8	344.6	344.6	344.6	344.6	344.6
12	361.5	361.8	363.0	363.0	363.0	363.0	363.0
13	367.3	367.3	367.5	367.5	367.5	367.5	367.5
14	387.6	387.7	387.8	387.8	387.8	387.8	387.8
15	390.4	390.7	391.9	391.9	391.9	391.9	391.9
16	400.6	400.6	400.8	400.8	400.8	400.8	400.8
17	402.2	402.3	402.9	402.9	402.9	402.9	402.9
18	446.0	446.0	446.1	446.1	446.1	446.1	446.1
19	473.0	473.0	473.3	473.3	473.3	473.3	473.3
20	481.9	481.9	481.9	481.9	481.9	481.9	481.9

TABLE 7.8 (a) RESULTS OF BRIDGE FINITE ELEMENT ANALYSIS (HZ)
ROTATIONAL STIFFNESS OF PINNED END VARIED

MODE NUMBER	ORIGINAL	COMPUTER CHANGE 7 (1.0E05)	COMPUTER CHANGE 8 (1.0E10)	COMPUTER CHANGE 9 (1.0E15)	COMPUTER CHANGE 10 (1.0E20)	COMPUTER CHANGE 11 (1.0E25)	COMPUTER CHANGE 12 (1.0E30)
1	41.22	42.88	45.84	45.64	45.84	45.84	45.84
2	56.27	57.78	63.50	63.50	63.50	63.50	63.50
3	122.6	123.6	126.7	126.7	126.7	126.7	126.7
4	145.0	146.0	150.2	150.2	150.2	150.2	150.2
5	206.7	207.3	209.4	209.4	209.4	209.4	209.4
6	221.3	221.3	221.4	221.4	221.4	221.4	221.4
7	228.8	228.8	228.8	228.8	228.8	228.8	228.8
8	238.9	239.4	241.5	241.5	241.5	241.5	241.5
9	282.5	282.8	284.1	284.1	284.1	284.1	284.1
10	325.6	325.9	326.9	326.9	326.9	326.9	326.9
11	343.7	343.8	344.5	344.5	344.5	344.5	344.5
12	361.5	361.8	363.1	363.1	363.1	363.1	363.1
13	367.3	367.3	367.5	367.5	367.5	367.5	367.5
14	387.6	387.7	387.8	387.8	387.8	387.8	387.8
15	390.4	390.7	391.9	391.9	391.9	391.9	391.9
16	400.6	400.6	400.8	400.8	400.8	400.8	400.8
17	402.2	402.3	402.9	402.9	402.9	402.9	402.9
18	446.0	446.0	446.1	446.1	446.1	446.1	446.1
19	473.0	473.0	473.3	473.3	473.3	473.3	473.3
20	481.9	481.9	481.9	481.9	481.9	481.9	481.9

TABLE 7.8 (b) RESULTS OF BRIDGE FINITE ELEMENT ANALYSIS (HZ)
ROTATIONAL STIFFNESS OF ROLLER END VARIED

MODE NUMBER	ORIGINAL	COMPUTER CHANGE 14 (1.0E05)	COMPUTER CHANGE 15 (1.0E10)	COMPUTER CHANGE 16 (1.0E15)	COMPUTER CHANGE 17 (1.0E20)	COMPUTER CHANGE 18 (1.0E25)	COMPUTER CHANGE 19 (1.0E30)
1	41.22	35.63	41.22	41.22	41.22	41.22	41.22
2	56.27	52.33	56.27	56.27	56.27	56.27	56.27
3	122.6	88.96	122.5	122.6	122.6	122.6	122.6
4	145.0	132.9	145.0	145.0	145.0	145.0	145.0
5	206.7	165.8	206.7	206.7	206.7	206.7	206.7
6	221.3	217.9	221.3	221.3	221.3	221.3	221.3
7	228.8	221.5	228.8	228.8	228.8	228.8	228.8
8	238.9	228.3	238.9	238.9	238.9	238.9	238.9
9	282.5	252.2	282.5	282.5	282.5	282.5	282.5
10	325.6	295.1	325.6	325.6	325.6	325.6	325.6
11	343.7	332.2	343.6	343.7	343.7	343.7	343.7
12	361.5	358.0	361.5	361.5	361.5	361.5	361.5
13	367.3	362.6	367.3	367.3	367.3	367.3	367.3
14	387.6	368.2	387.6	387.6	387.6	387.6	387.6
15	390.4	388.4	390.4	390.4	390.4	390.4	390.4
16	400.6	390.5	400.5	400.6	400.6	400.6	400.6
17	402.2	401.4	402.2	402.2	402.2	402.2	402.2
18	446.0	420.9	446.0	446.0	446.0	446.0	446.0
19	473.0	456.9	472.9	473.0	473.0	473.0	473.0
20	481.9	477.4	481.9	481.9	481.9	481.9	481.9

TABLE 7.8 (c) RESULTS OF BRIDGE FINITE ELEMENT ANALYSIS (HZ)
VERTICAL SPRINGS AT PINNED END VARIED

MODE NUMBER	ORIGINAL	COMPUTER CHANGE 20 (1.0E05)	COMPUTER CHANGE 21 (1.0E10)	COMPUTER CHANGE 22 (1.0E15)	COMPUTER CHANGE 23 (1.0E20)	COMPUTER CHANGE 24 (1.0E25)	COMPUTER CHANGE 25 (1.0E30)
1	41.22	36.99	41.22	41.22	41.22	41.22	41.22
2	56.27	52.65	56.27	56.27	56.27	56.27	56.27
3	122.6	85.15	122.5	122.6	122.6	122.6	122.6
4	145.0	132.5	145.0	145.0	145.0	145.0	145.0
5	206.7	164.2	206.7	206.7	206.7	206.7	206.7
6	221.3	217.9	221.3	221.3	221.3	221.3	221.3
7	228.8	221.5	228.8	228.8	228.8	228.8	228.8
8	238.9	228.8	238.9	238.9	238.9	238.9	238.9
9	282.5	252.4	282.5	282.5	282.5	282.5	282.5
10	325.6	295.2	325.6	325.6	325.6	325.6	325.6
11	343.7	332.3	343.6	343.7	343.7	343.7	343.7
12	361.5	358.0	361.5	361.5	361.5	361.5	361.5
13	367.3	362.6	367.3	367.3	367.3	367.3	367.3
14	387.6	368.2	387.6	387.6	387.6	387.6	387.6
15	390.4	383.4	390.4	390.4	390.4	390.4	390.4
16	400.6	390.5	400.5	400.6	400.6	400.6	400.6
17	402.2	401.4	402.2	402.2	402.2	402.2	402.2
18	446.0	420.9	446.0	446.0	446.0	446.0	446.0
19	473.0	456.9	472.9	473.0	473.0	473.0	473.0
20	481.9	477.4	481.9	481.9	481.9	481.9	481.9

TABLE 7.8 (d) RESULTS OF BRIDGE FINITE ELEMENT ANALYSIS (HZ)
VERTICAL SPRINGS AT ROLLER END VARIED

MODE NUMBER	ORIGINAL	COMPUTER CHANGE 13 FIXING ALL	COMPUTER CHANGE 26 50% ONE BEAM	COMPUTER CHANGE 27 50% TWO BEAM
1	41.22	66.80	36.09	32.66
2	56.27	77.61	51.27	43.88
3	122.6	141.3	107.4	100.9
	145.0	161.6	134.5	116.8
5	206.7	217.6	192.0	184.5
6	221.3	222.1	204.3	192.7
7	228.8	228.8	212.6	195.9
8	238.9	243.3	225.9	204.3
9	282.5	289.1	272.3	265.0
10	325.6	330.9	299.9	285.2
11	343.7	347.2	333.4	307.7
12	361.5	367.5	337.7	320.2
13	367.3	367.8	357.6	331.7
14	387.o	388.4	363.5	350.2
15	390.4	39o.2	365.3	384.9
16	400.6	401.9	390.1	388.9
17	402.2	404.5	395.8	391.1
18	446.0	446.3	440.9	424.5
19	473.0	474.6	443.2	432.6
20	481.9	482.0	462.8	440.7

TABLE 7.8 (a) RESULTS OF BRIDGE FINITE ELEMENT ANALYSIS (HZ)
OTHER CHANGE

CHANGE NUMBER	CHANGE		PERCENTAGE
1	ROTATIONAL STIFFNESS OF AT ONE OF THE PINNED ENDS	1.0E05	7.2%
2	ditto	1.0E10	25.1%
3	ditto	1.0E15	25.1%
4	ditto	1.0E20	25.1%
5	ditto	1.0E25	25.1%
6	ditto	1.0E30	25.1%
			25.1%
7	ROTATIONAL STIFFNESS OF AT ONE OF THE ROLLER ENDS	1.0E05	6.7%
8	ditto	1.0E10	23.9
9	ditto	1.0E15	23.9
10	ditto	1.0E20	23.9
11	ditto	1.0E25	23.9
12	ditto	1.0E30	23.9
13	FIX ALL BOUNDARY CONDITIONS		105.6%
14	VERTICAL STIFFNESS OF ONE OF THE PINNED ENDS	1.0E05	7.9%
15	ditto	1.0E10	0.0%
16	ditto	1.0E15	0.0%
17	ditto	1.0E20	0.0%
18	ditto	1.0E25	0.0%
19	ditto	1.0E30	0.0%
20	VERTERAL STIFFNESS OF ONE OF THE ROLLER ENDS	1.0E05	11.9%%
21	ditto	1.0E10	0.0%
22	ditto	1.0E15	0.0%
23	ditto	1.0E20	0.0%
24	ditto	1.0E25	0.0%
25	ditto	1.0E30	0.0%
	ditto		0.0%
26	REDUCE SHEAR CONNECTORS IN ONE OF THE BEAMS		19.3%
27	REDUCE SHEAR CONNECTORS IN BOTH BEAMS		34.7%

TABLE 7.9 EFFECTS ON STIFFNESS DUE TO STRUCTURE CHANGES
--------- IN THE MODEL BRIDGE FINITE ELEMENT MODEL

	MODE 1	MODE 2	MODE 7	MODE 10	INCREASE IN STIFFNESS
PINNED END FIX ROTATION	3.8%	7.7%	10.3%	2.9%	3.5%
ROLLER END FIX TRANSLATION	3.8%	1.3%	9.8%	2.7%	11.7%
ROLLER END FIX TRANS&ROTA.	1.9%	9.0%	9.8%	0.8%	3.2%
ROLLER END FIX ROTATION	3.8%	7.7%	8.1%	4.5%	11.9%
FIX ALL BOUNDARY	13.3%	2.6%	7.8%	6.7%	18.8%

TABLE 7.10 INCREASE IN CERTAIN MEASURED NATURAL FREQUENCIES FOR CHANGES IN BOUNDARY CONDITIONS

	MODE 2	MODE 4	MODE 5 *	MODE 7	DECREASE IN STIFFNESS
DISPLACEMENT 1mm	7.7%	---	-0.7%	8.7%	2.6%
DISPLACEMENT 2mm	5.1%	9.5%	0.6%	7.5%	2.0%
DISPLACEMENT 3mm	0.0%	9.9%	0.1%	8.1%	2.2%

* THESE PERCENTAGES ARE CALCULATED BY TAKING THE AVERAGES OF THE THREE RESULTS AS THE DATUM

TABLE 7.11 DECREASE IN CERTAIN MEASURED NATURAL FREQUENCIES FOR DIFFERENTIAL DISPLACEMENT OF A PINNED BEARING

	MODE 3 *	DECREASE IN STIFFNESS
DISPLACEMENT 1mm	4.6%	3.4%
DISPLACEMENT 2mm	0.6%	4.4%
DISPLACEMENT 3mm	-5.2%	5.5%

* THESE PERCENTAGES ARE CALCULATED BY TAKING THE AVERAGES OF THE THREE RESULTS AS THE DATUM

TABLE 7.12 DECREASE IN CERTAIN MEASURED NATURAL FREQUENCIES FOR DIFFERENTIAL DISPLACEMENT OF A ROLLER BEARING

	MODE 1	MODE 2	MODE 6	MODE 7	MODE 10	DECREASE IN STIFFNESS
50% REMOVED IN ONE BEAM	1.9%	6.4%	4.2%	7.3%	4.3%	2.0%
50% REMOVED IN BOTH	3.8%	7.7%	4.9%	8.1%	4.8%	7.9%

TABLE 7.13 DECREASE IN CERTAIN MEASURED NATURAL FREQUENCIES FOR LOSS OF SHEAR CONNECTION

	MODE 1	MODE 2	INCREASE IN STIFFNESS
PINNED ROTATIONAL STIFFNESS 1.0E10N/mm2	10.8%	12.1%	25.1%
PINNED ROTATIONAL STIFFNESS 1.0E5 N/mm2	3.8%	2.5%	7.2%
ROLLER ROTATIONAL STIFFNESS 1.0E10N/mm2	11.2%	12.9%	23.9%
ROLLER ROTATIONAL STIFFNESS 1.0E5 N/mm2	4.0%	2.7%	6.7%

TABLE 7.14 INCREASE IN CERTAIN CALCULATED NATURAL FREQUENCIES FOR FIXITY OF ROTATIONAL DEGREES OF FREEDOM

	MODE 1	MODE 2	MODE 3	INCREASE IN STIFFNESS
FIXING ALL BOUNDARY CONDITIONS	62.1%	37.9%	15.3%	105.6%

TABLE 7.15 INCREASE IN CERTAIN CALCULATED NATURAL FREQUENCIES FOR FIXITY OF ALL BOUNDARY DEGREES OF FREEDOM

	MODE 1	MODE 2	MODE 3	MODE 4	MODE 5	MODE 6	DECREASE IN STIFFNESS
VERTICAL STIFFNESS FOR PINNED BEARING 1.0E5N/mm2	13.6%	7.0%	27.4%	8.3%	19.8%	1.5%	7.9%
VERTICAL STIFFNESS FOR ROLLER BEARING 1.0E5N/mm2	10.3%	6.4%	30.5%	8.6%	20.5%	1.5%	11.99%

TABLE 7.16 DECREASE IN CERTAIN CALCULATED NATURAL FREQUENCIES FOR REDUCTION IN VERTICAL STIFFNESS OF THE BEARINGS

	MODE 1	MODE 2	MODE 3	MODE 4	MODE 5	MODE 6	MODE 7	DECREASE IN STIFFNESS
50% REDUCED IN ONE BEAM	12.4%	8.9%	12.4%	7.2%	7.1%	7.7%	7.1	19.3%
50% REDUCED IN BOTH	20.8%	22.1	17.7%	17.9%	10.7%	12.9%	14.4%	34.7%

TABLE 7.17 DECREASE IN CERTAIN CALCULATED NATURAL FREQUENCIES FOR REDUCTION IN SHEAR CONNECTION

	MODE 1	MODE 2	MODE 3	MODE 4	MODE 5	MODE 6	MODE 7	DECREASE IN STIFFNESS
ORIGNAL CALCULATED NATURAL FREQUENCIES (HZ)	41.22	56.27	122.6	145.0	206.7	221.3	228.3	----
50% REDUCTION IN BOTH BEAMS ECCENTRICITY=0.0% (HZ)	32.66	43.88	100.9	116.8	184.5	192.7	195.9	34.7%
PERCENTAGE CHANGE FOR ECCENTRICITY=0.0%	20.8%	22.1%	17.7%	19.6%	10.7	12.9%	14.4%	----
50% REDUCTION IN BOTH BEAMS ECCENTRICITY=12.5% (HZ)	40.0	54.6	119.9	141.7	204.3	219.2	226.0	6.1%
PERCENTAGE CHANCE WITH ECCENTRICITY=12.5%	2.9%	2.9%	2.1%	2.3%	1.1%	0.9%	1.2%	----
ORIGNAL MEASURED NATURAL FREQUENCIES (HZ)	41.22	60.75	----	148.2	----	221.6	279.5	----
50% REDUCTION IN BOTH BEAMS	39.66	56.06	124.0	----	170.1	210.7	256.8	7.9%
PERCENTAGE CHANGE	3.8%	7.7%	----	----	----	4.9%	8.1%	----

TABLE 7.18 FUTHER STUDIES ON LOSS OF SHEAR CONNECTIONS

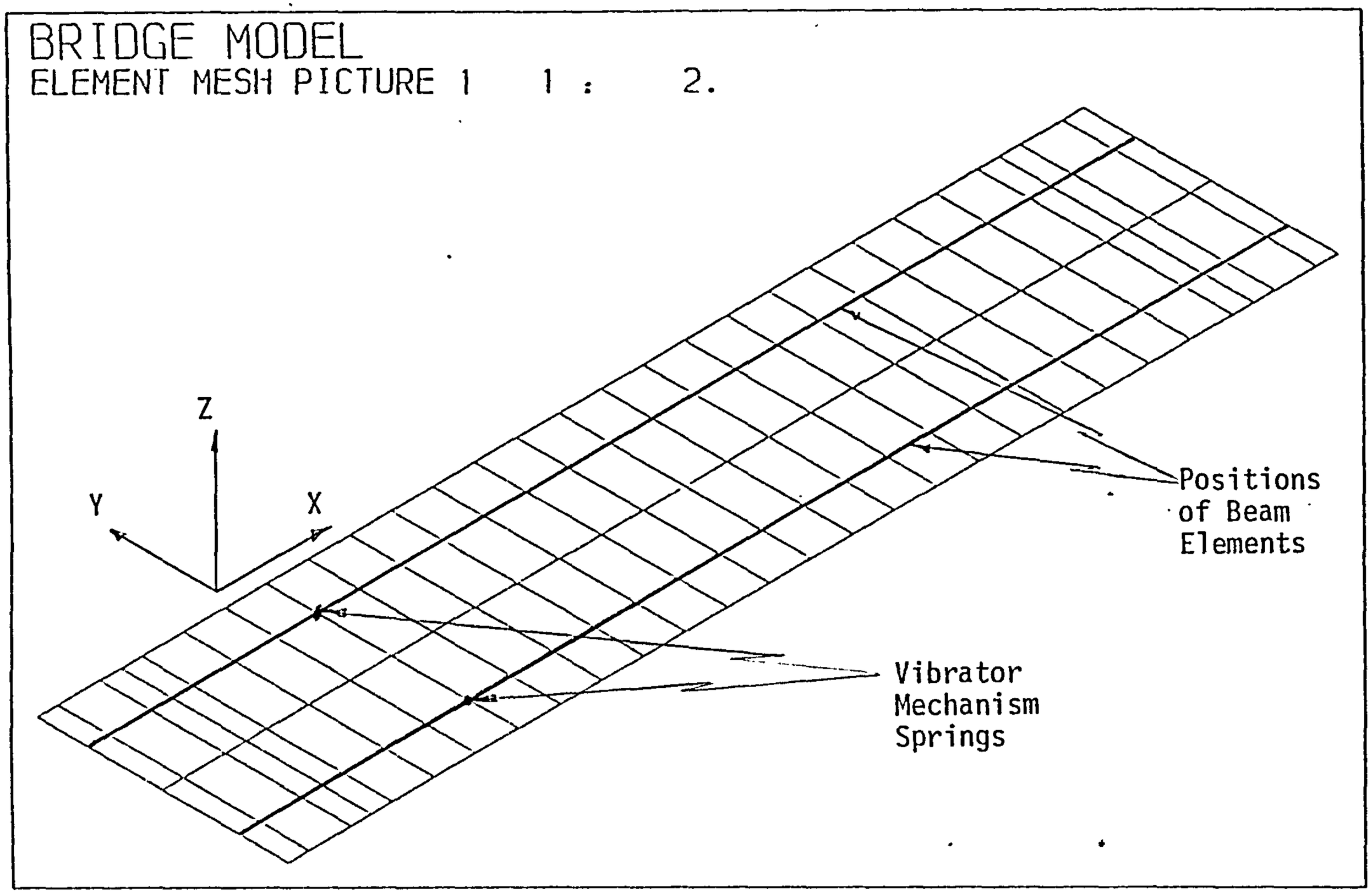

FIGURE 7.1 Element Mesh

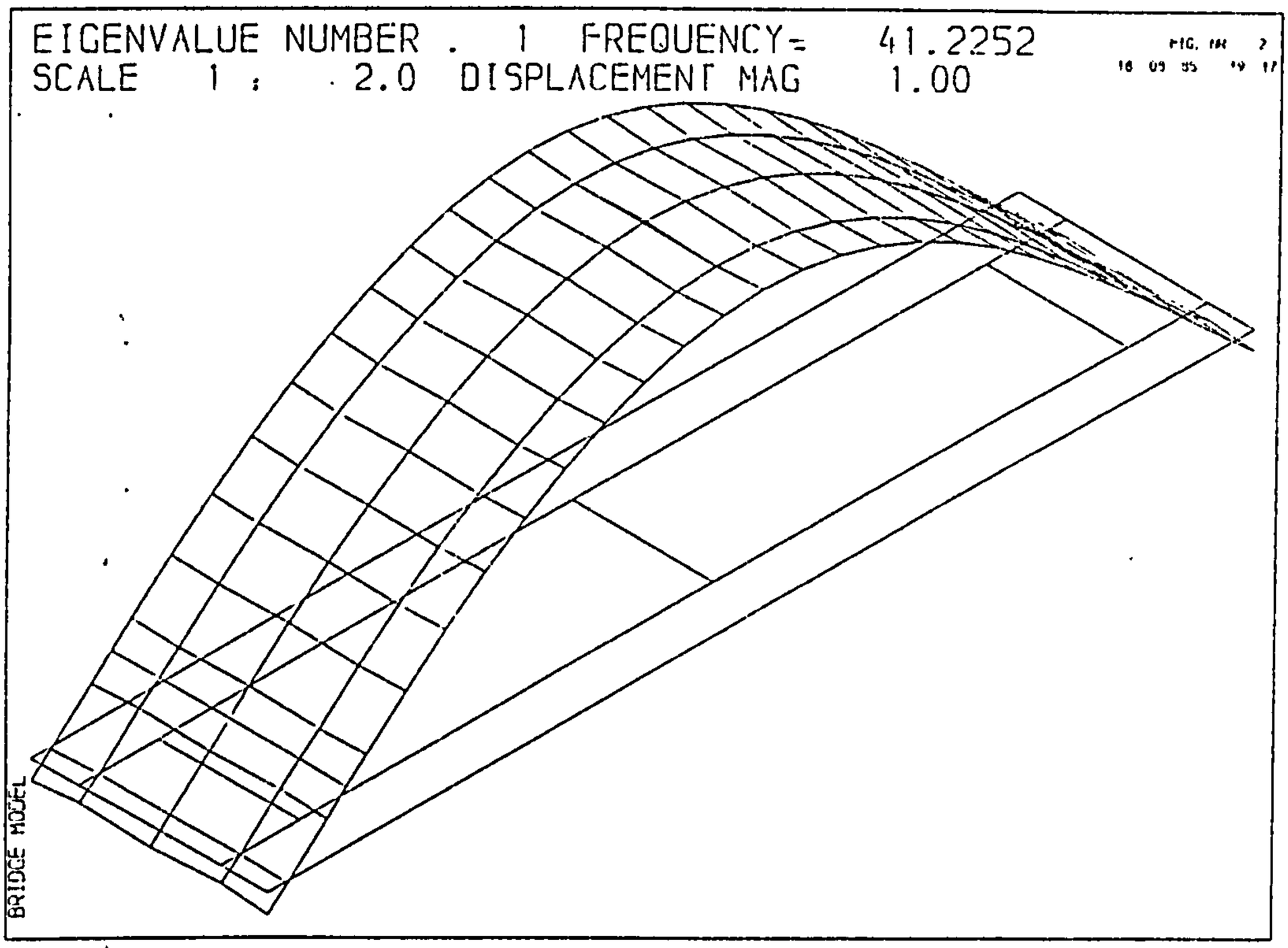

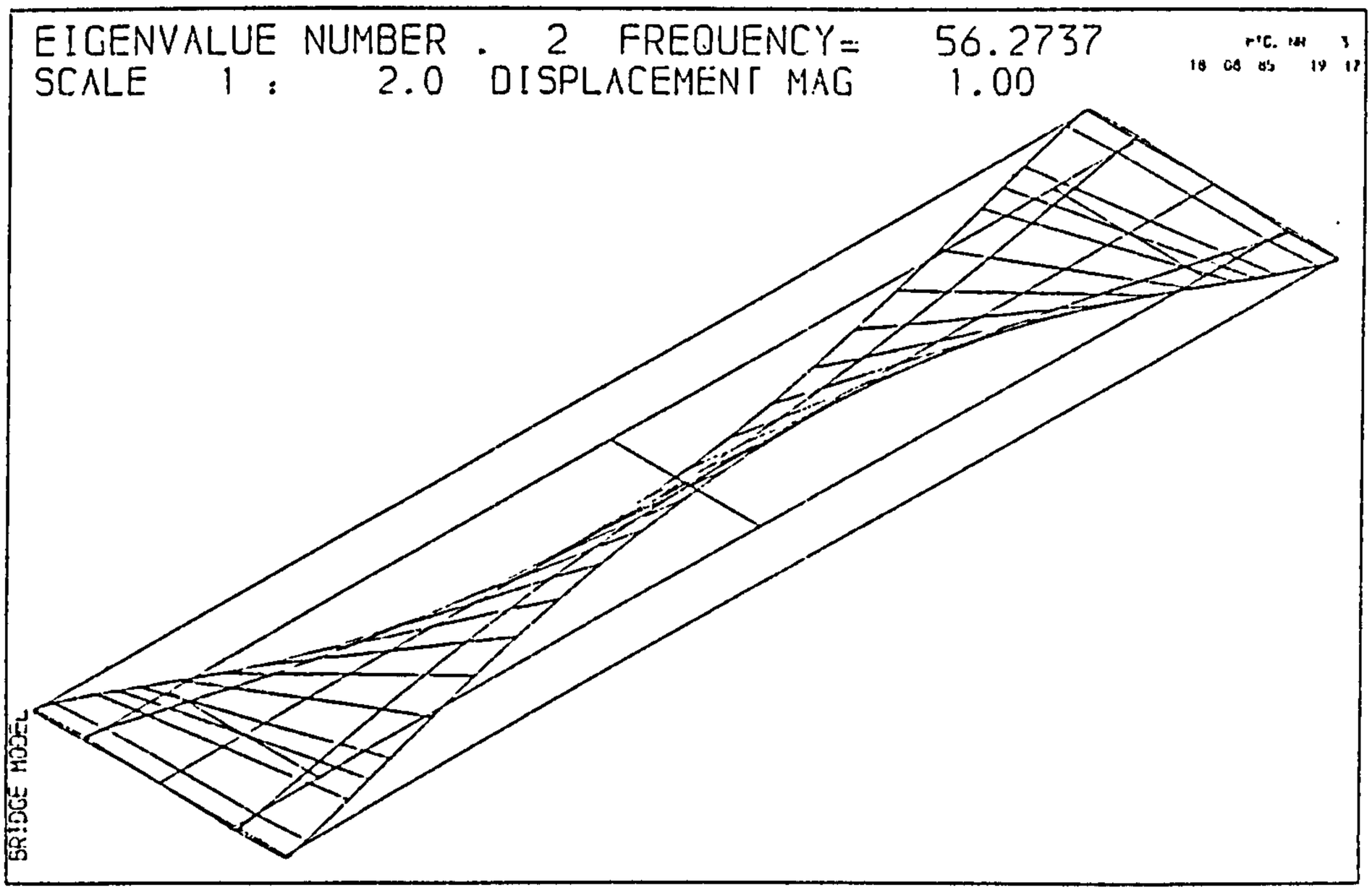

FIGURE 7.2 Mode Shapes

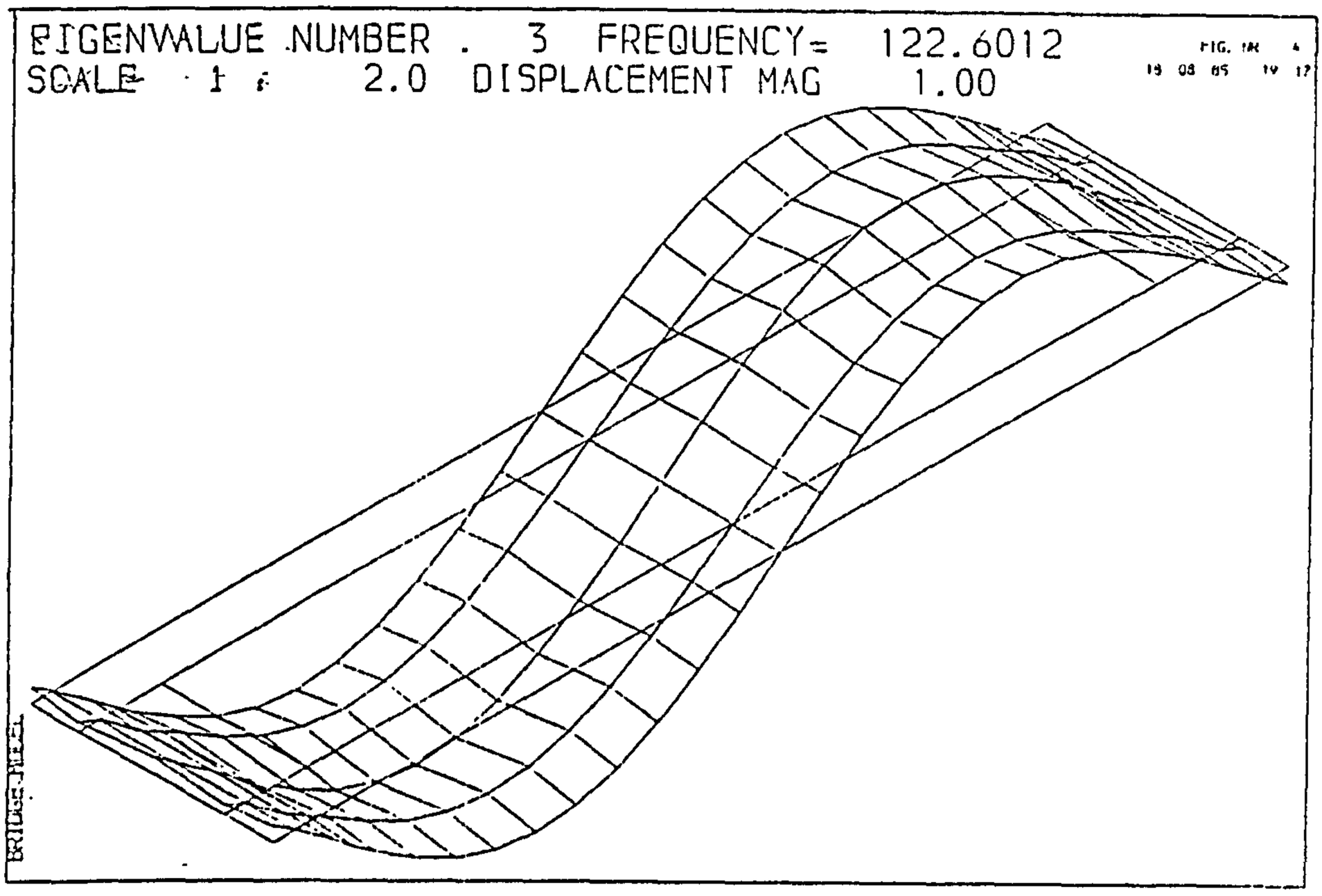

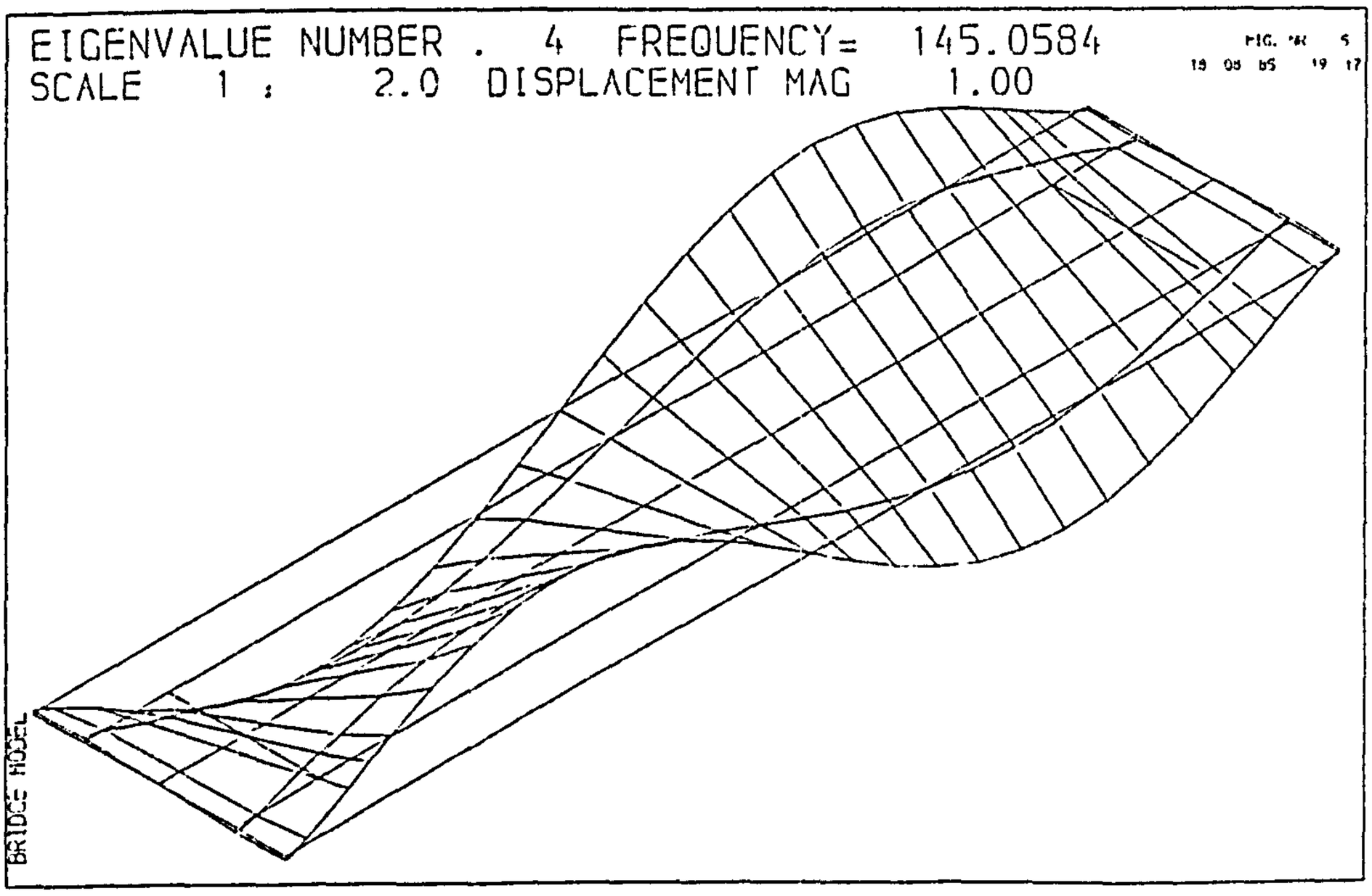

FIGURE 7.2 (cont)

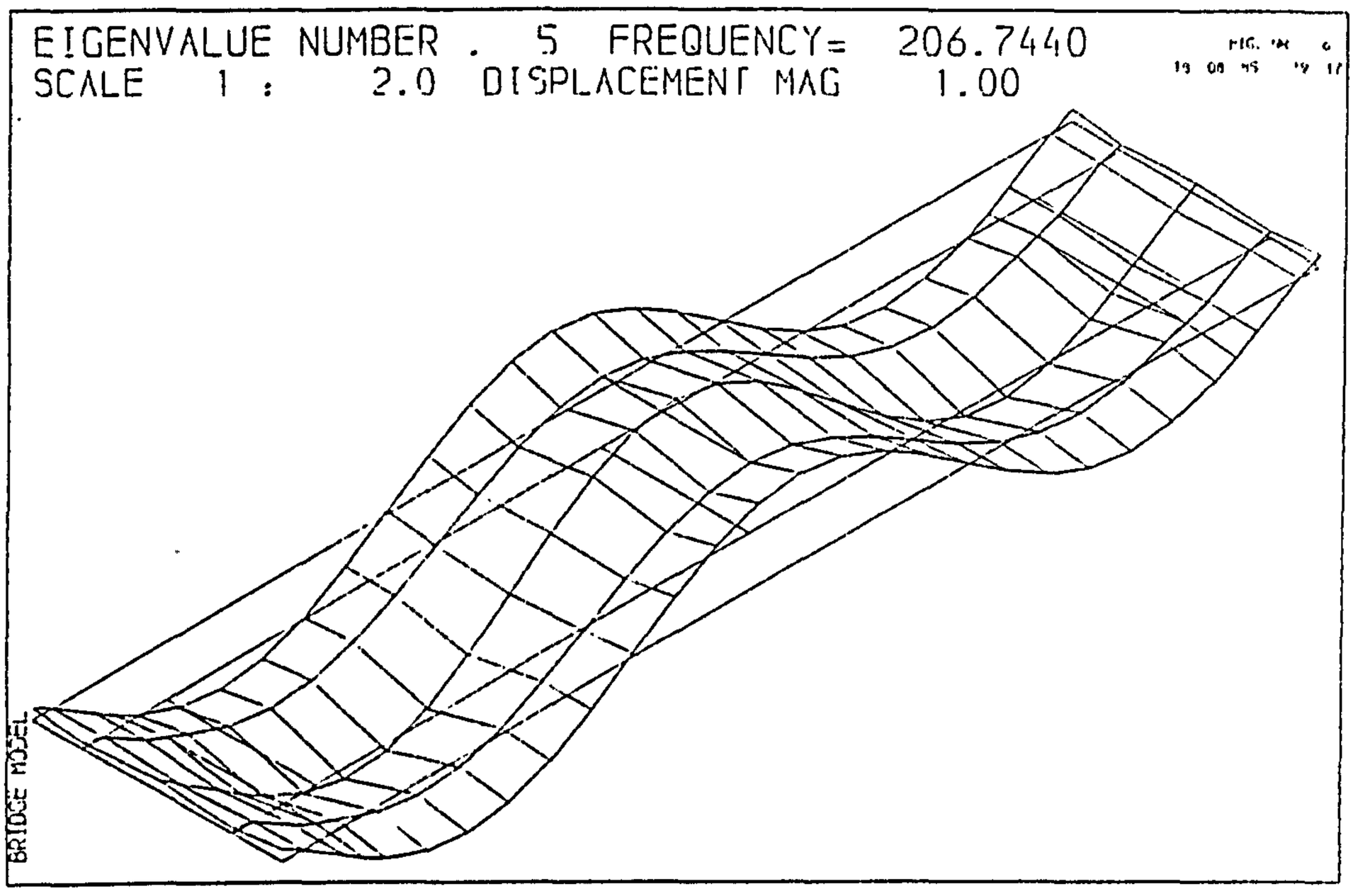

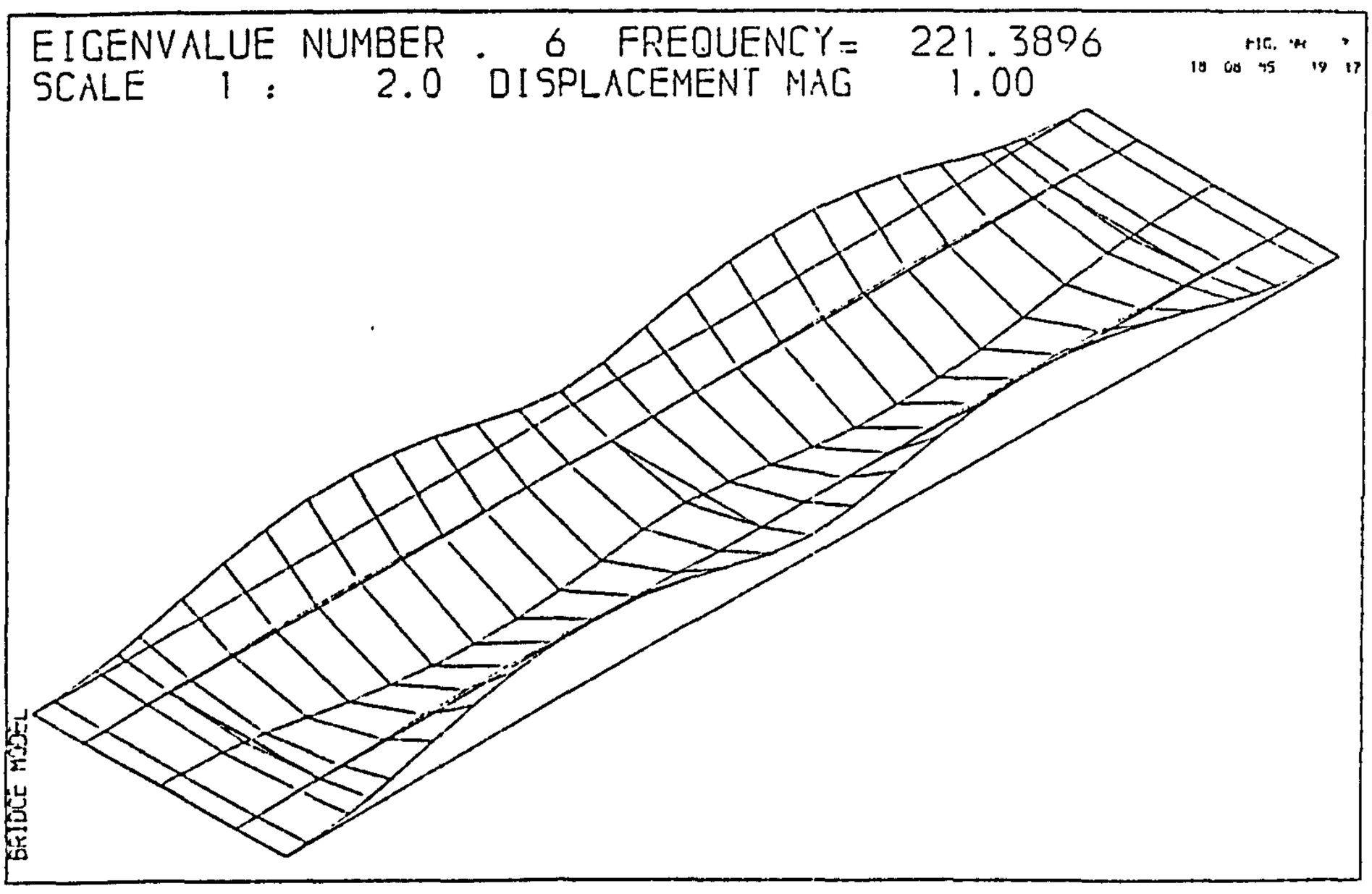

FIGURE 7.2 (cont)

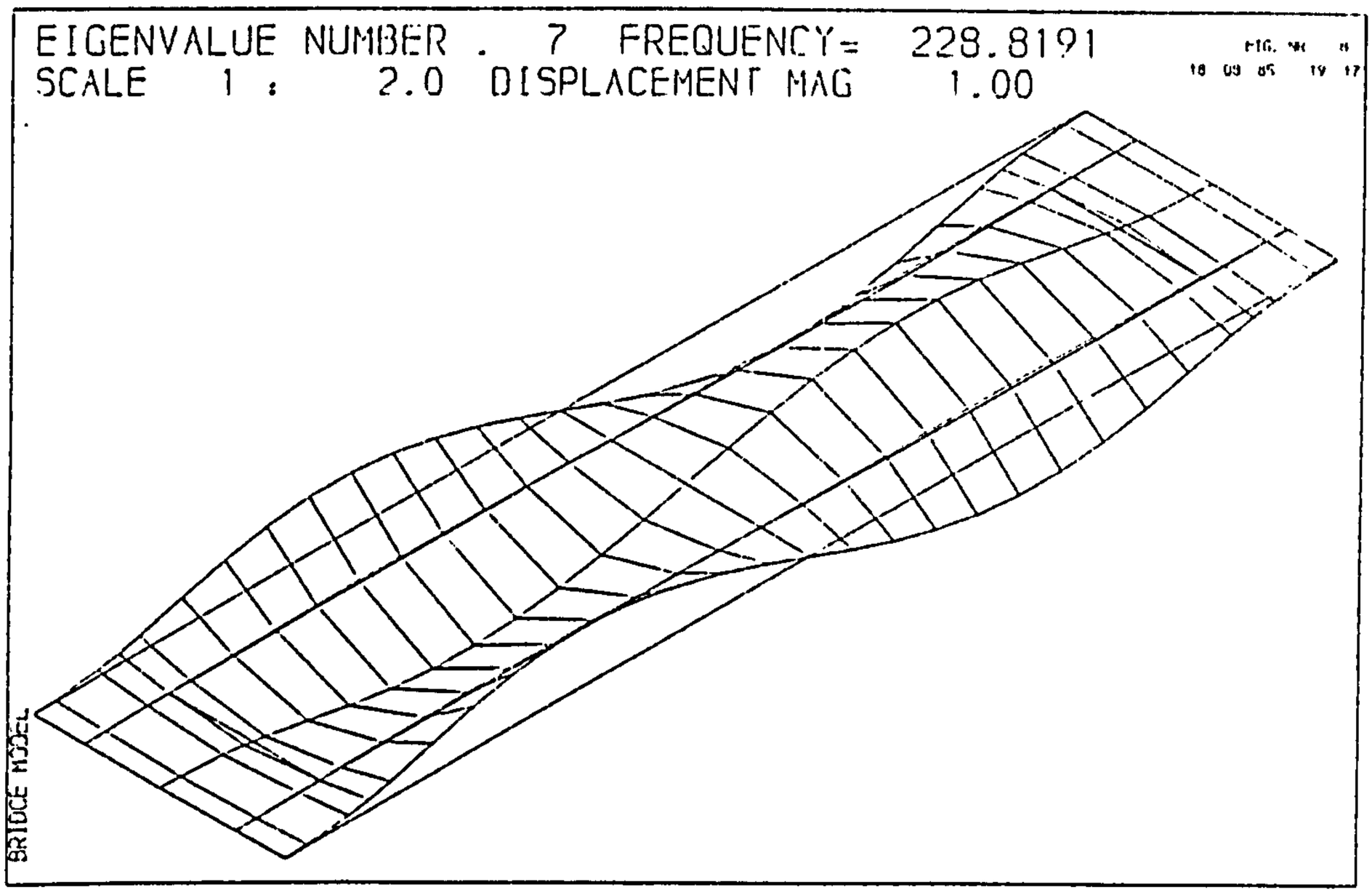

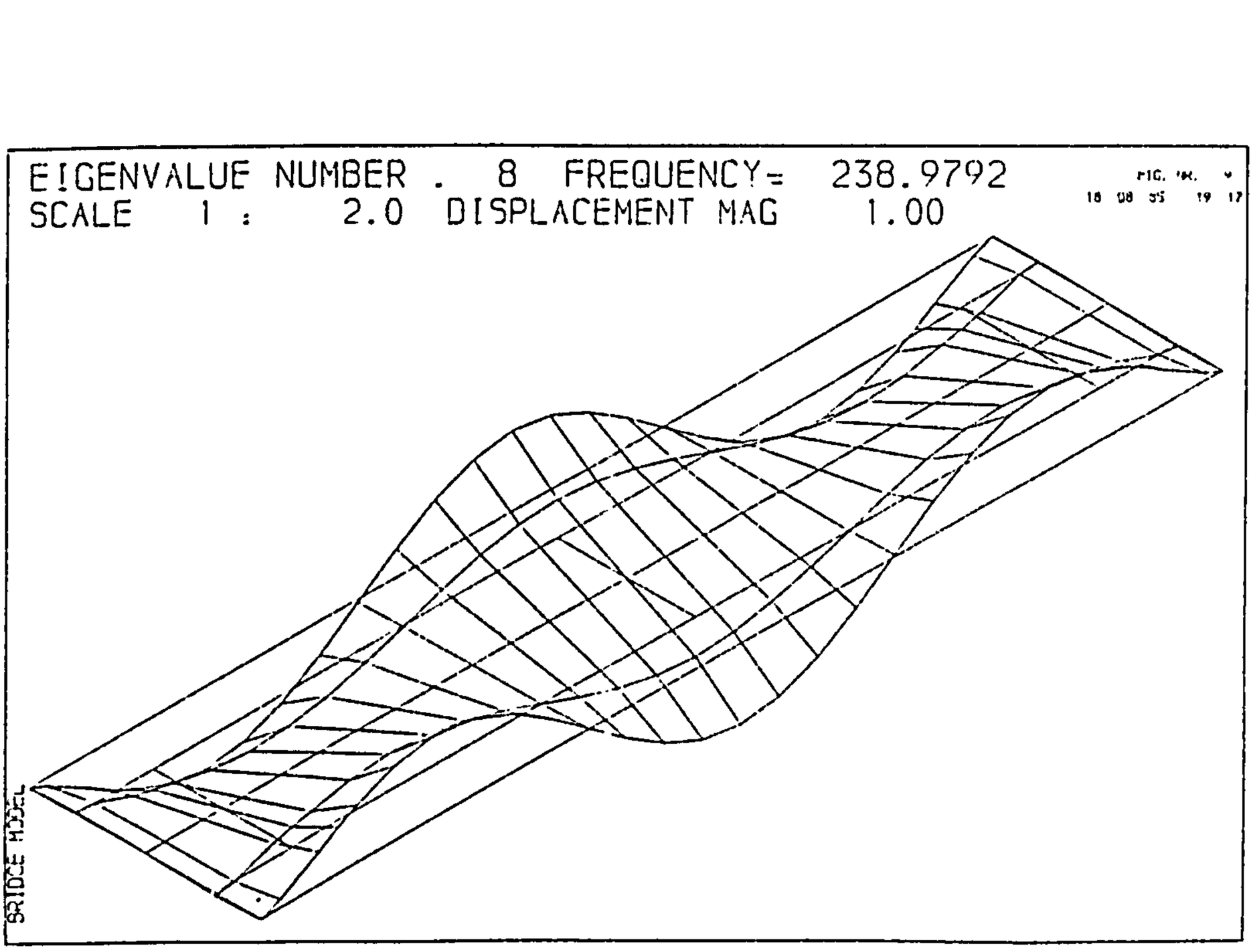

FIGURE 7.2 (cont)

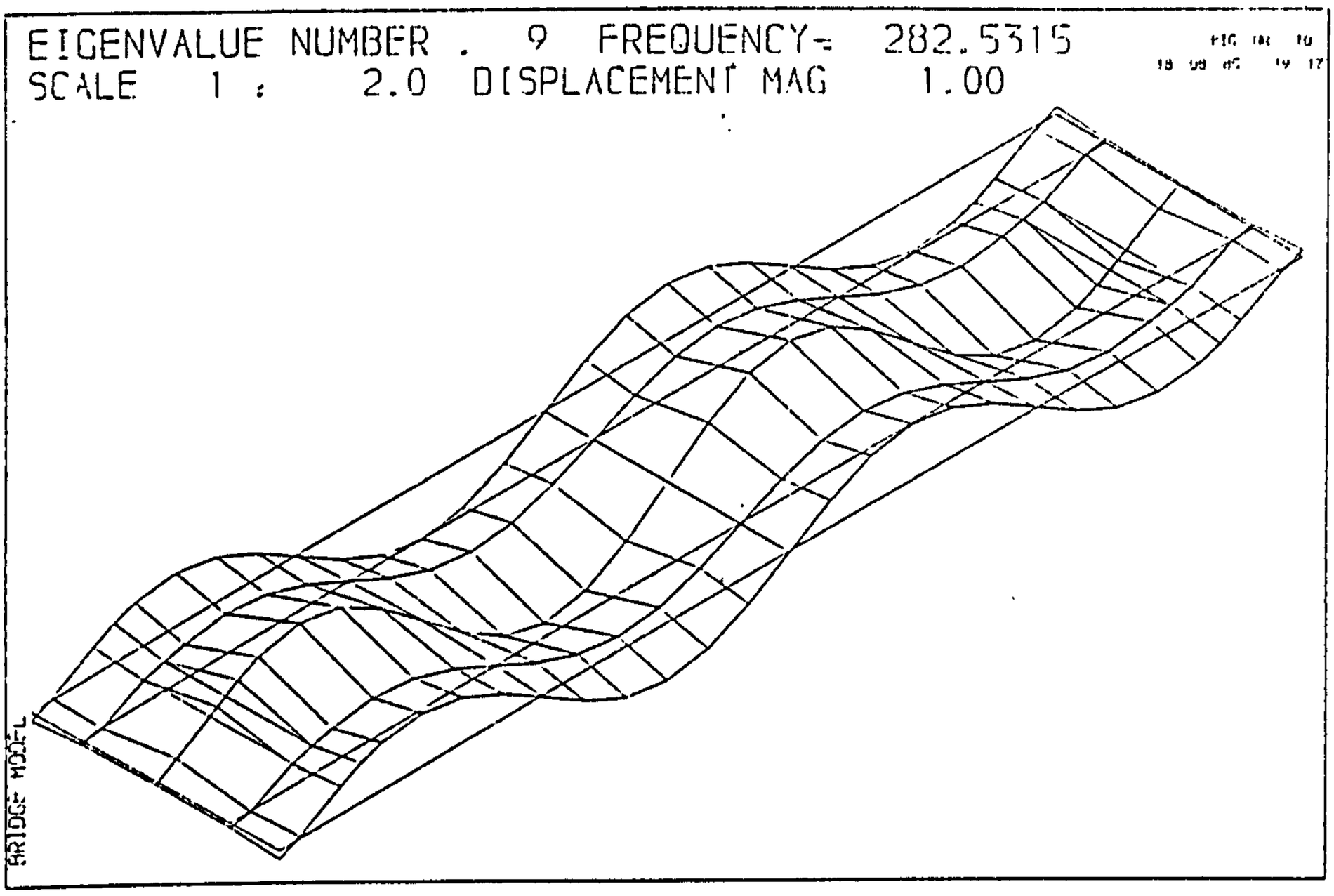

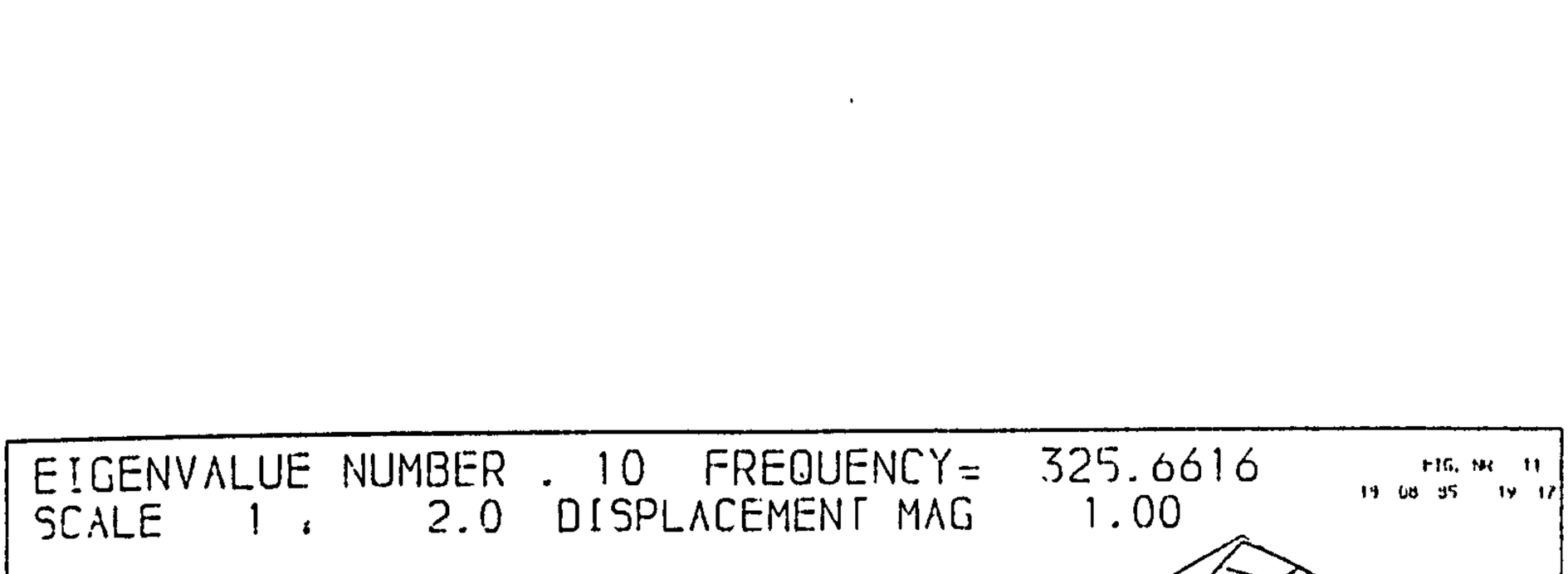

FIGURE 7.2 (cont)

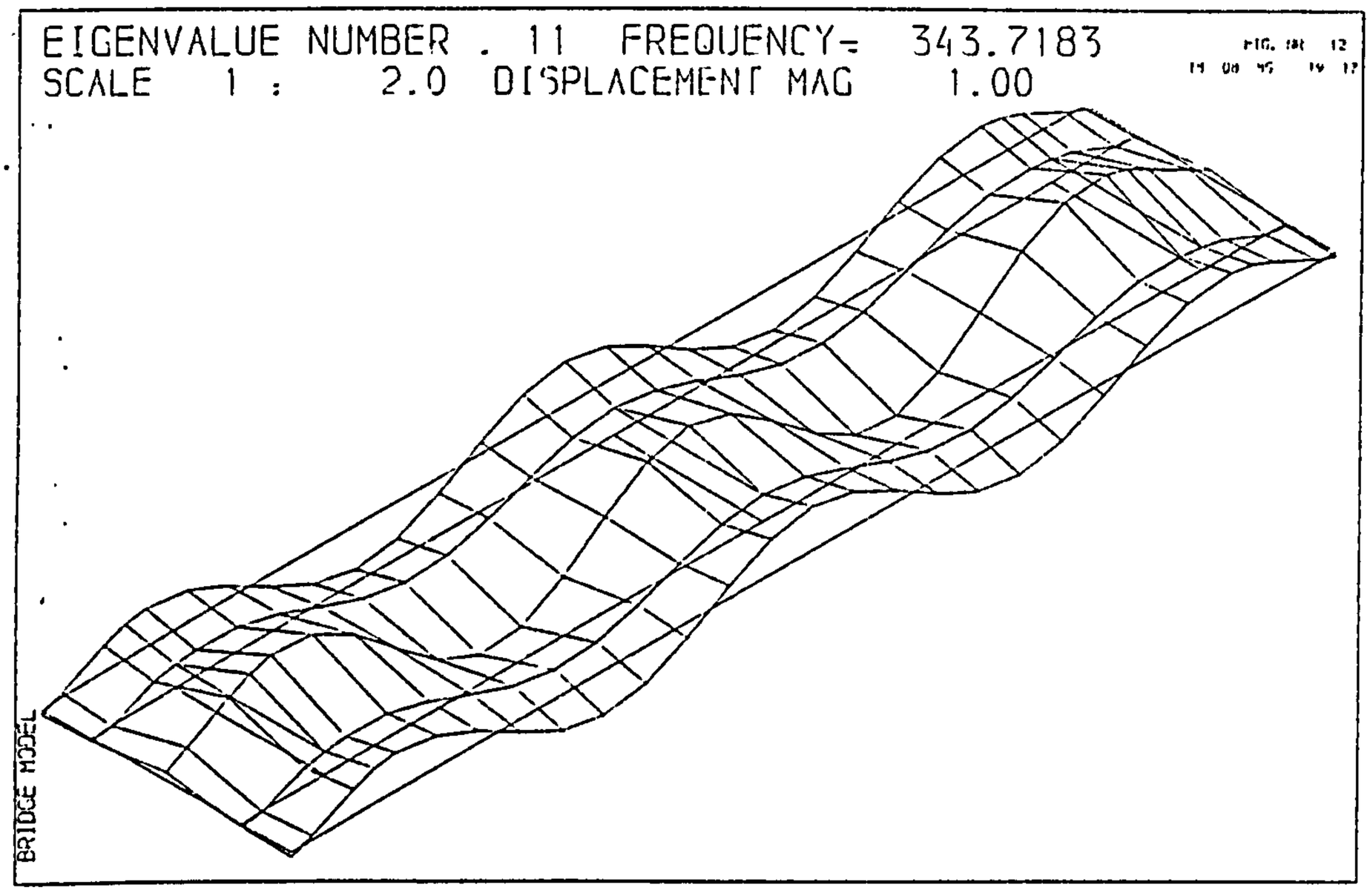

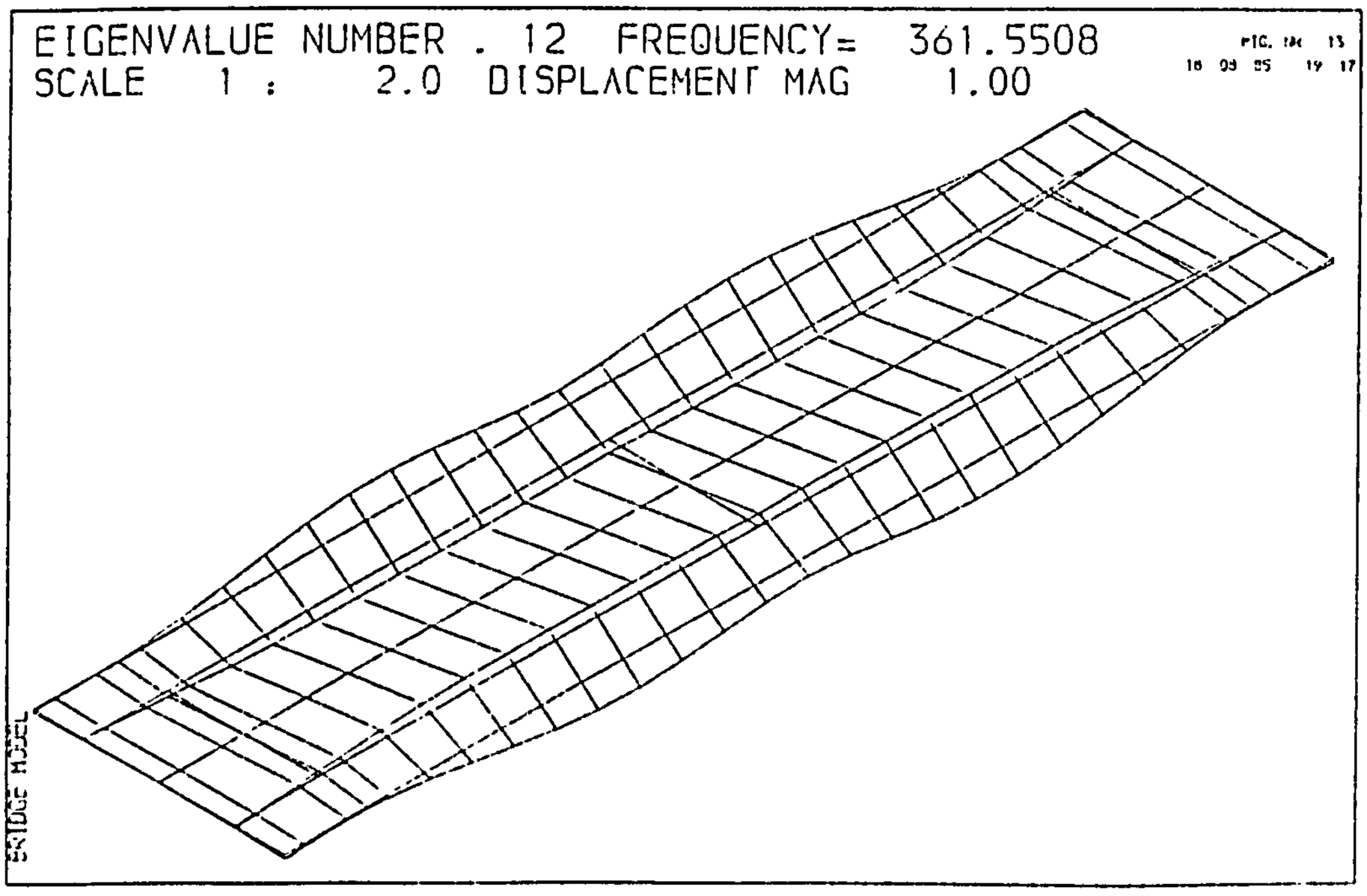

FIGURE 7.2 (cont)

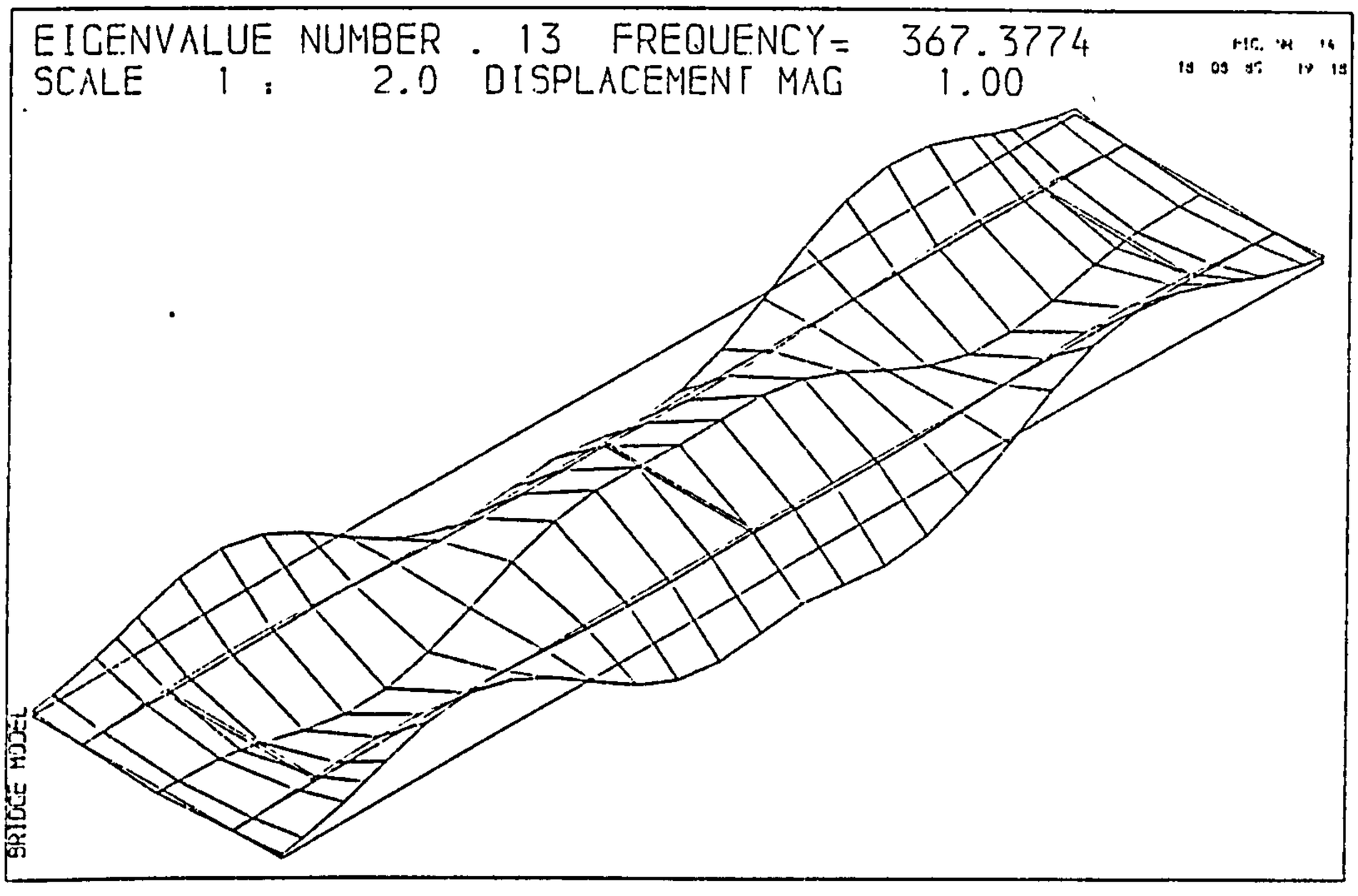

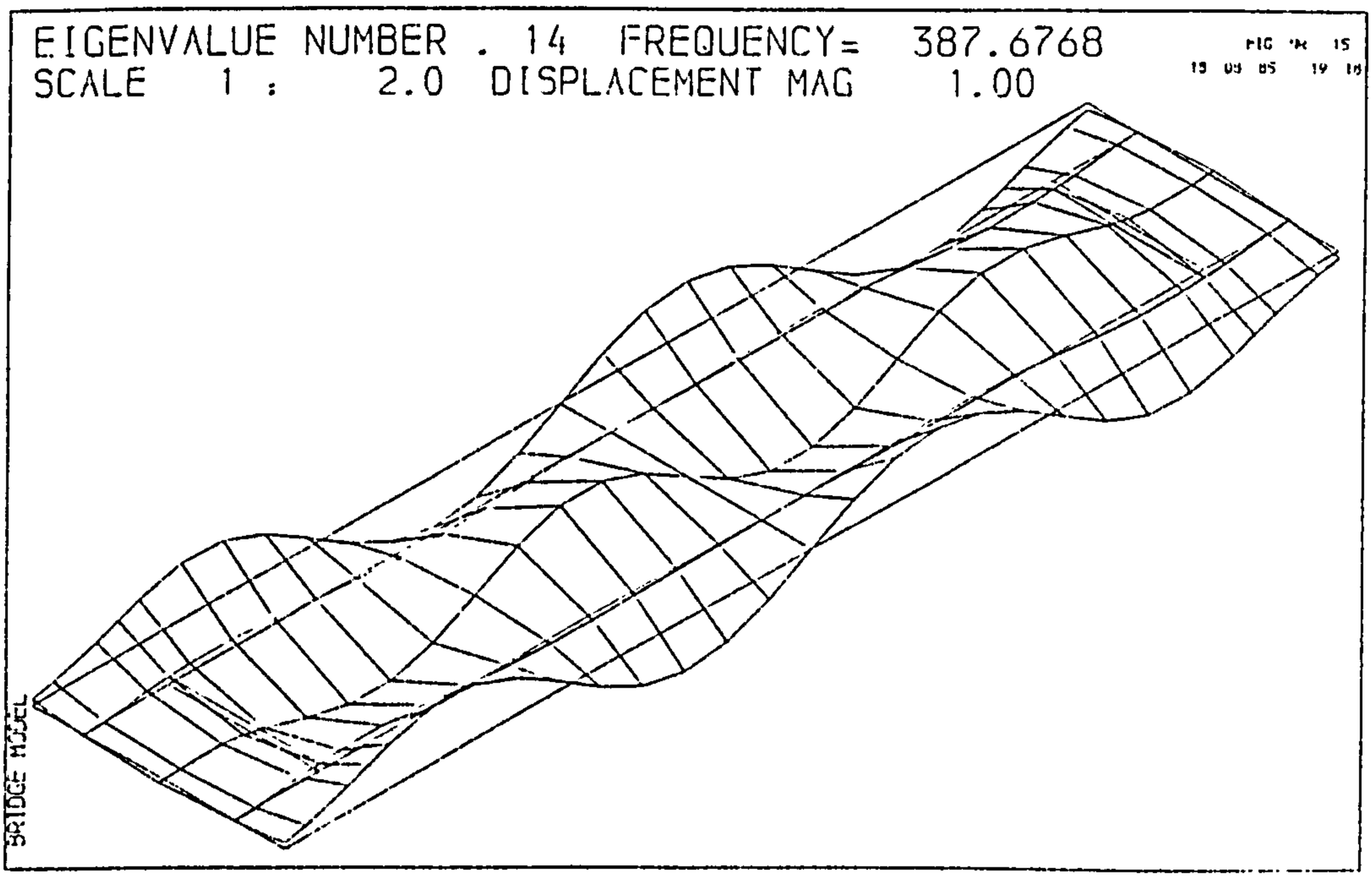

FIGURE 7.2 (cont)

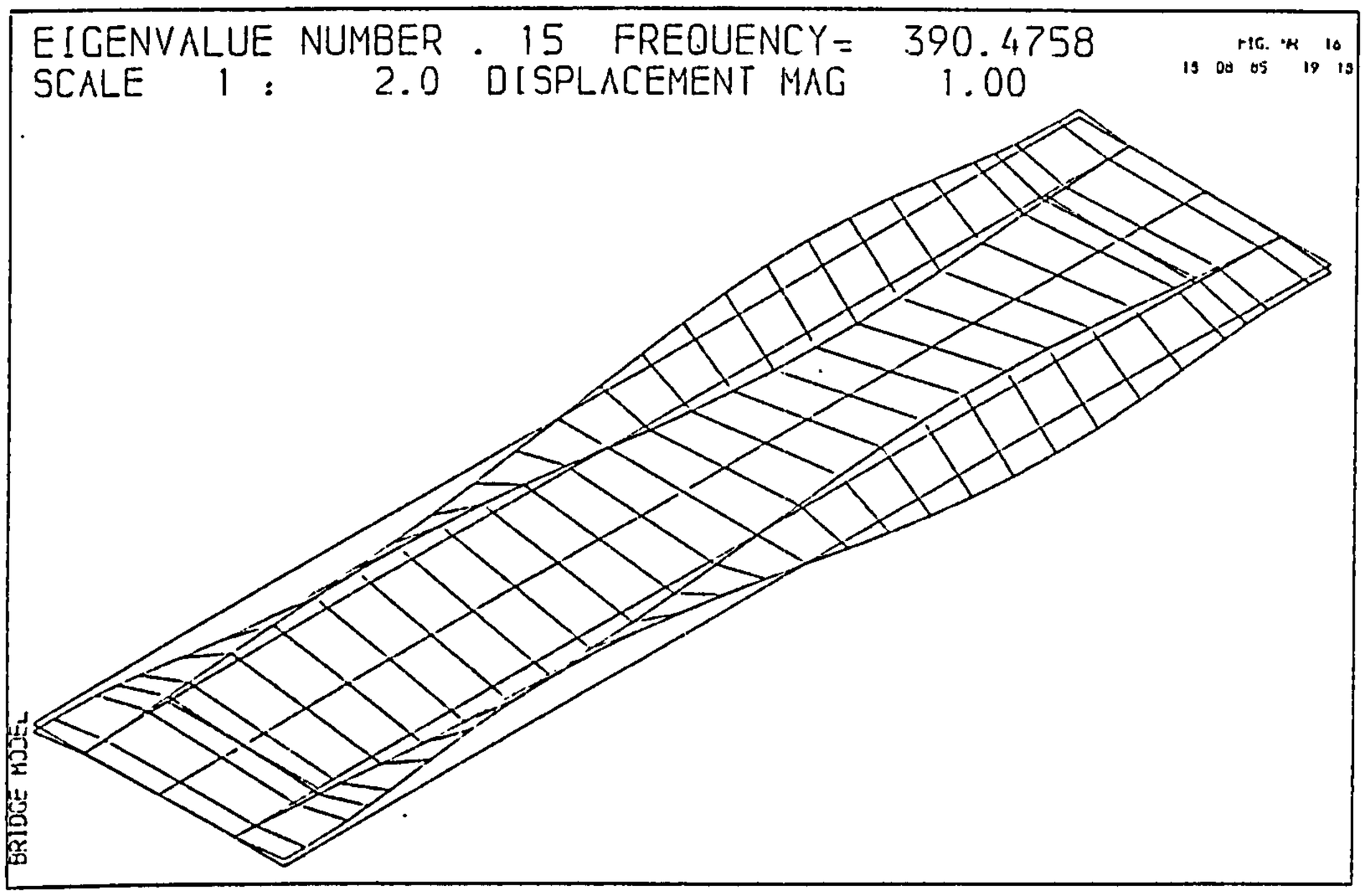

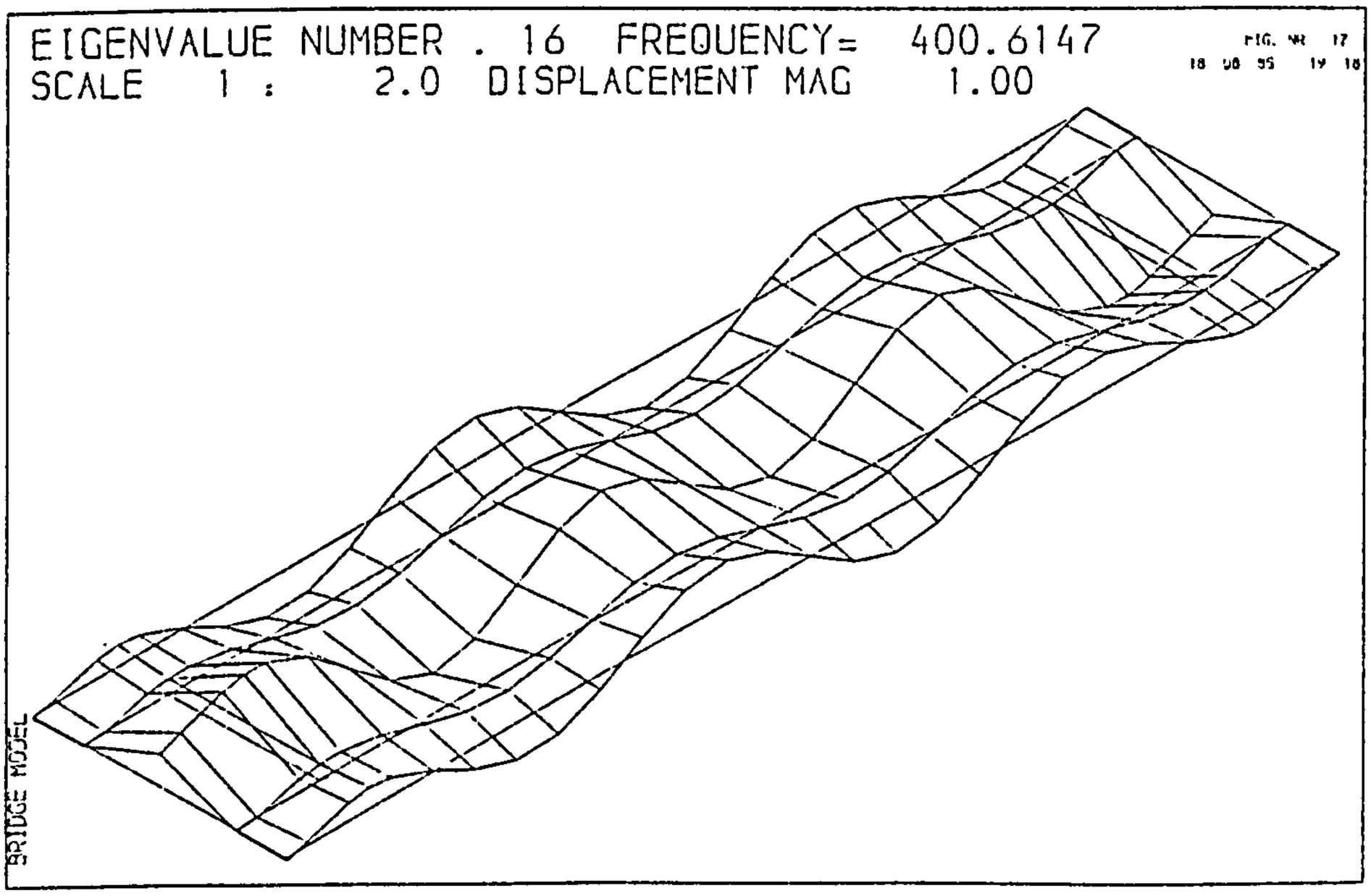

FIGURE 7.2 (cont)

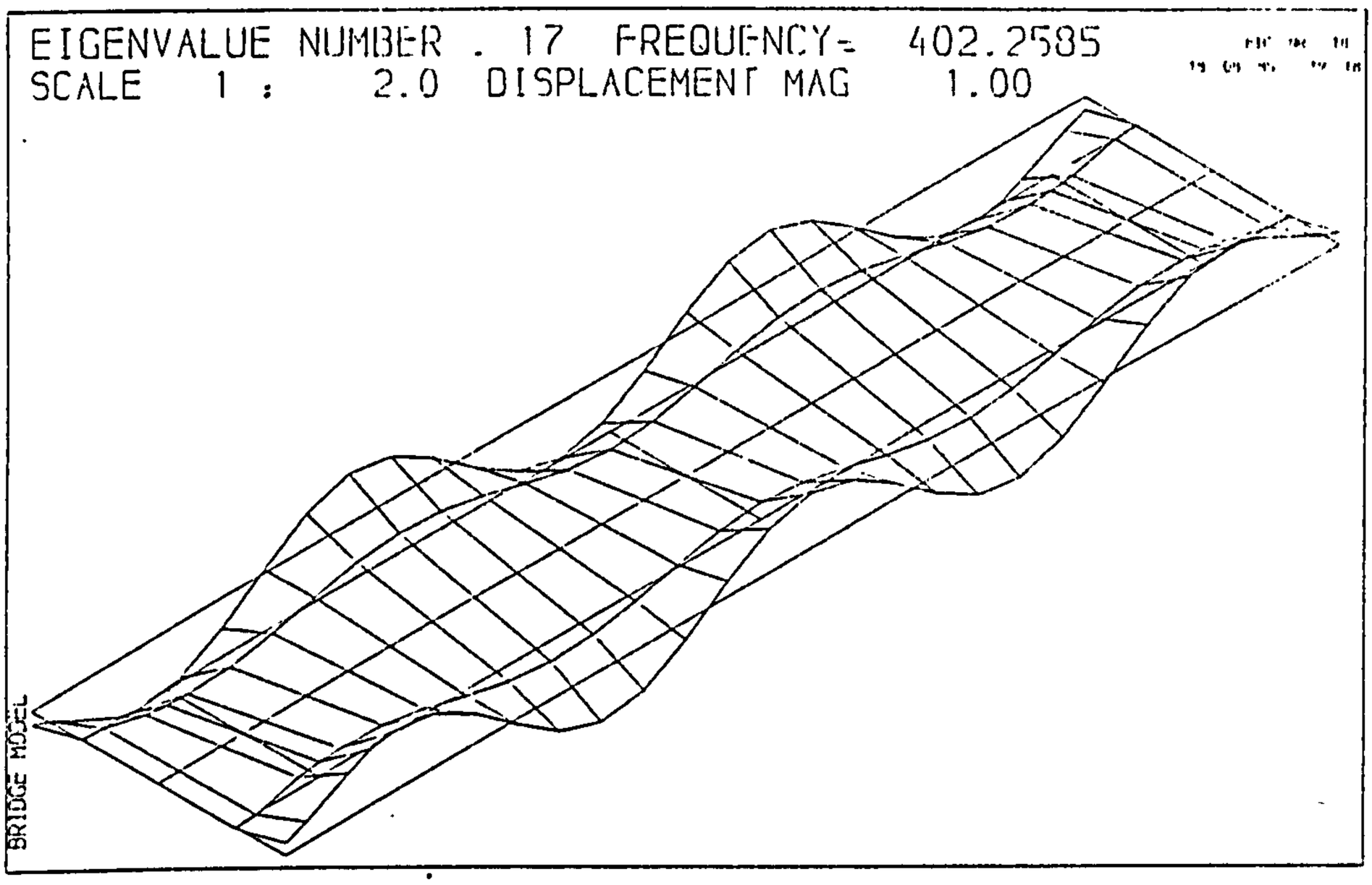

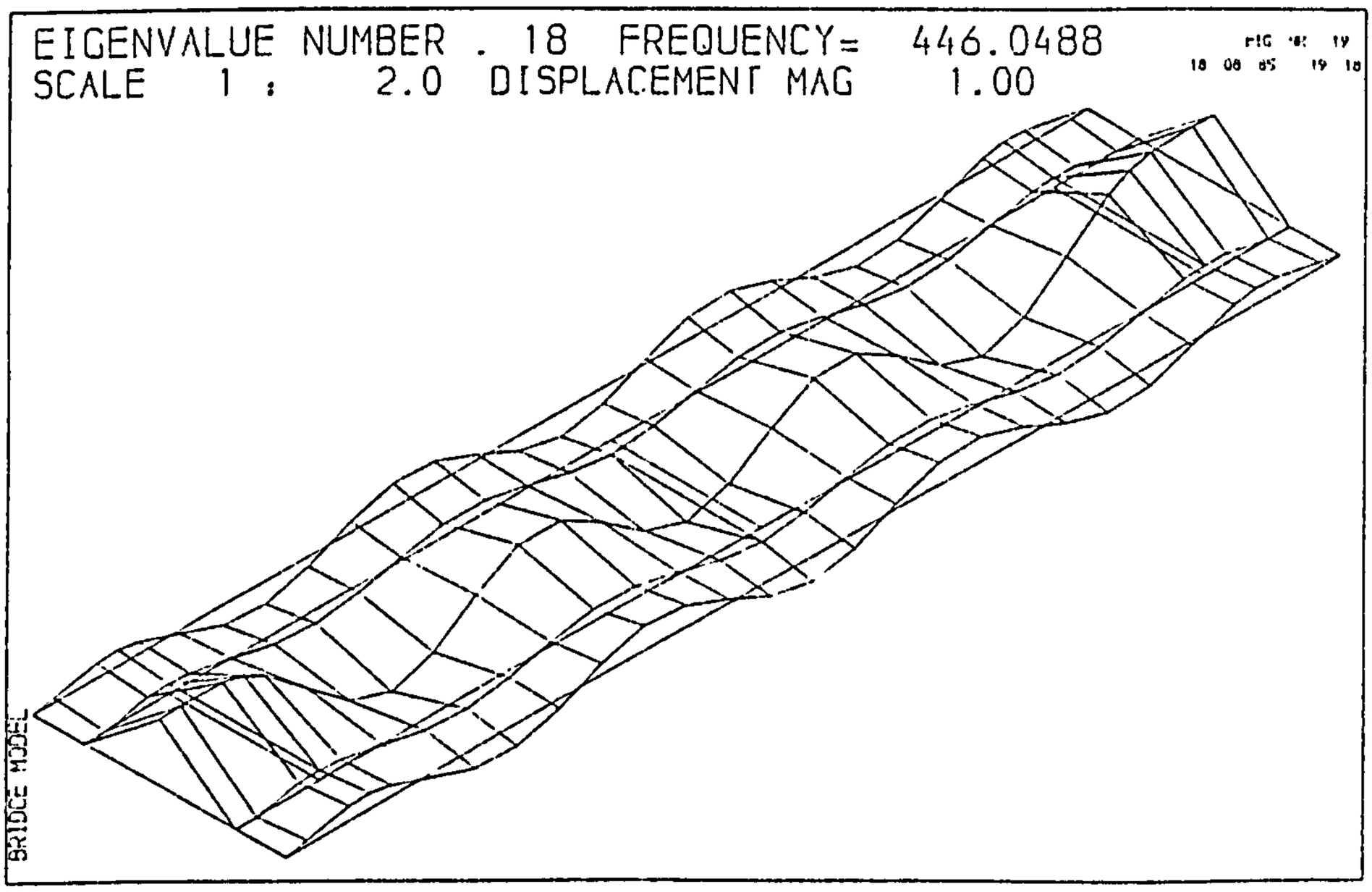

FIGURE 7.2 (cont)

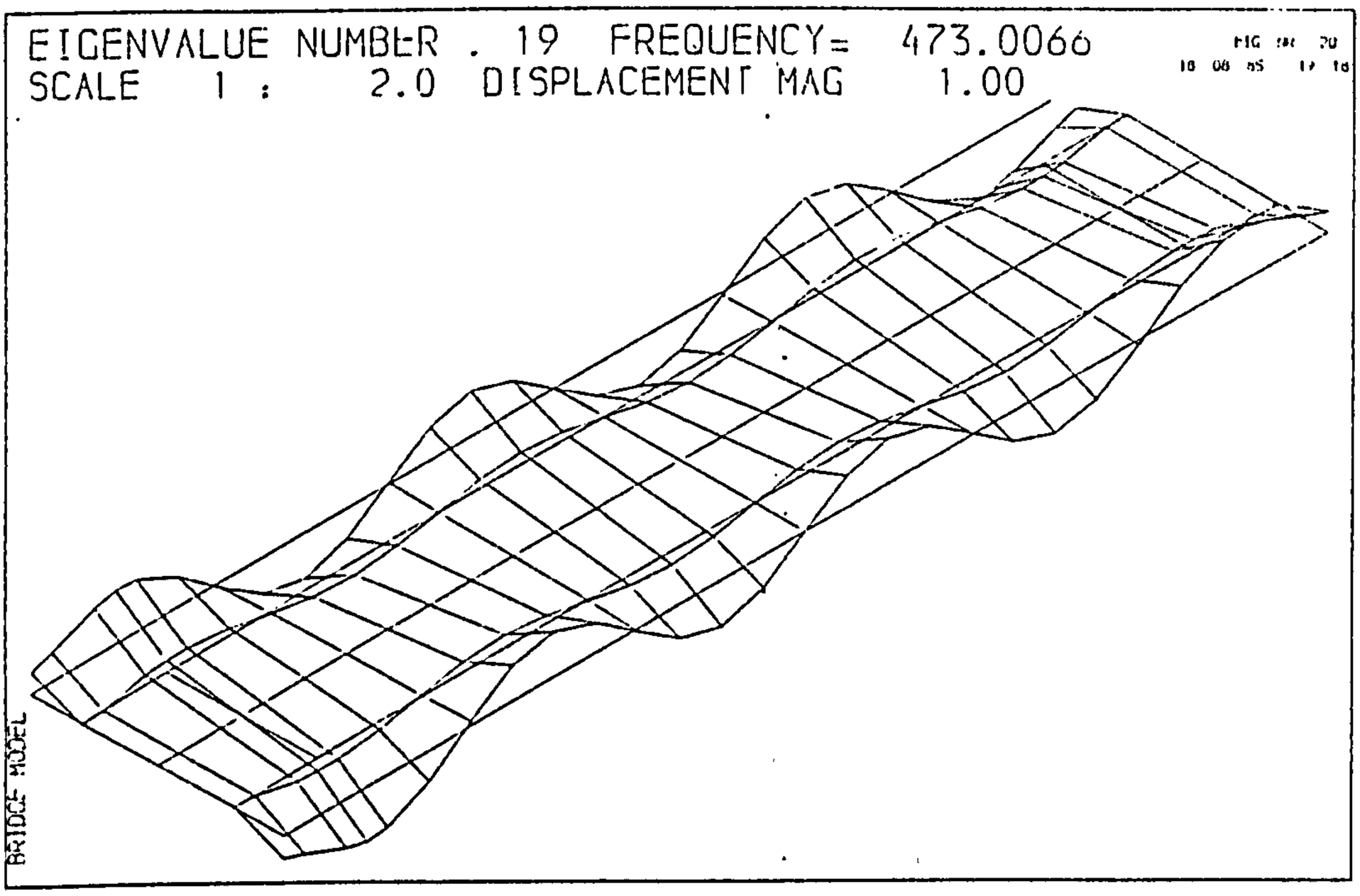

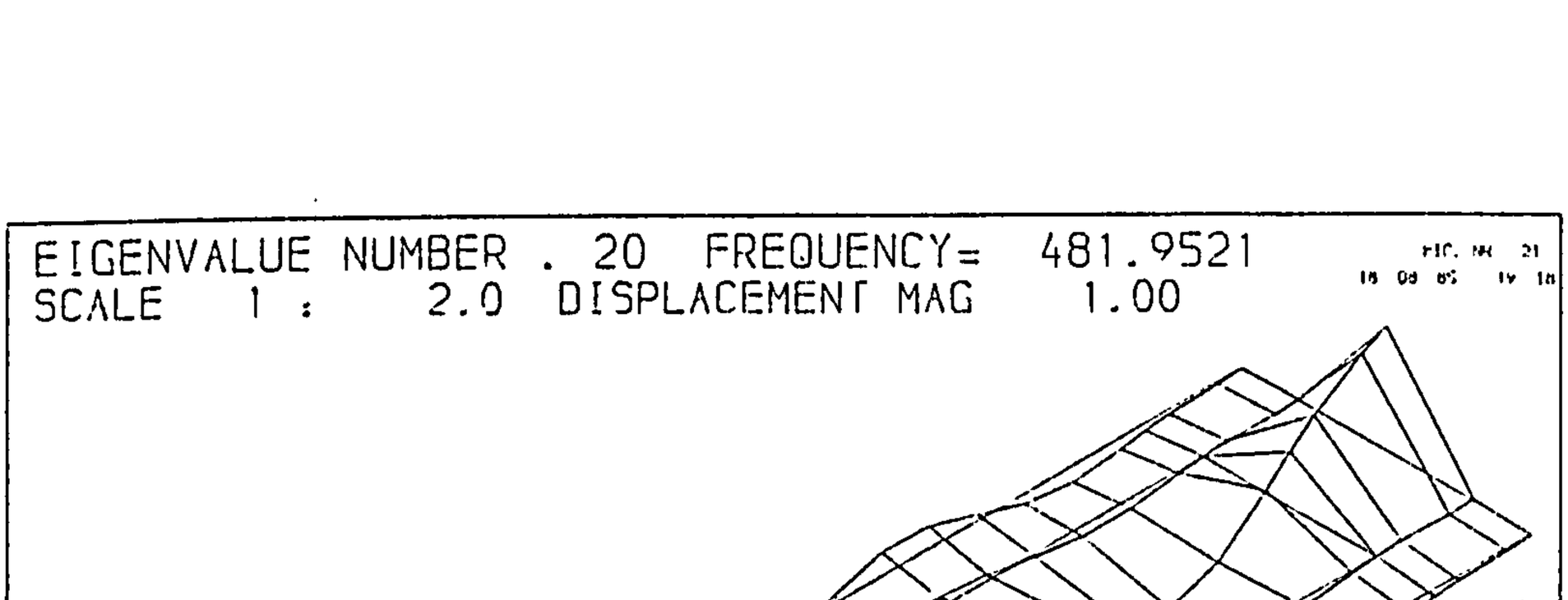

FIGURE 7.2 (cont)

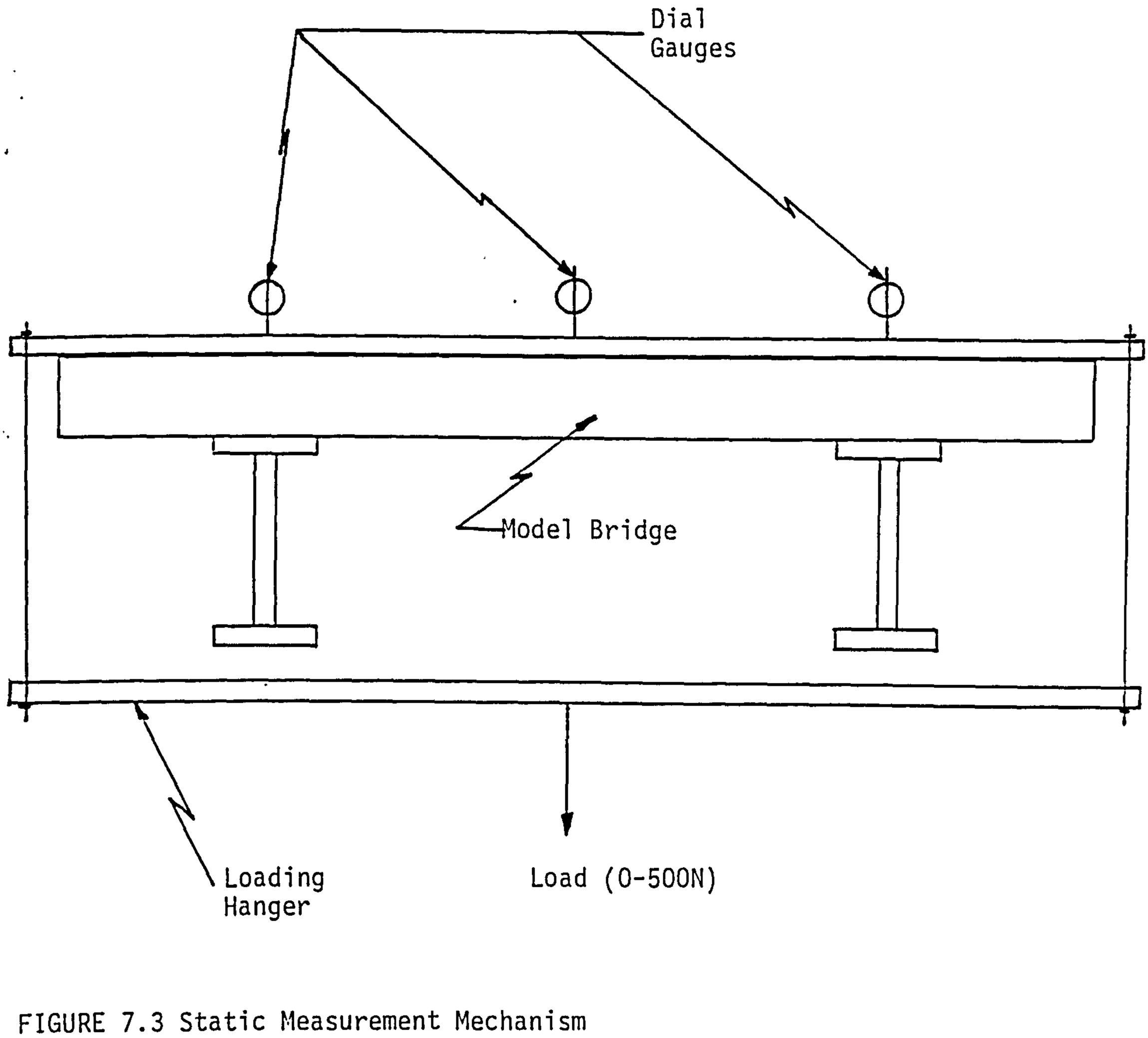

FIGURE 7.3 Static Measurement Mechanism

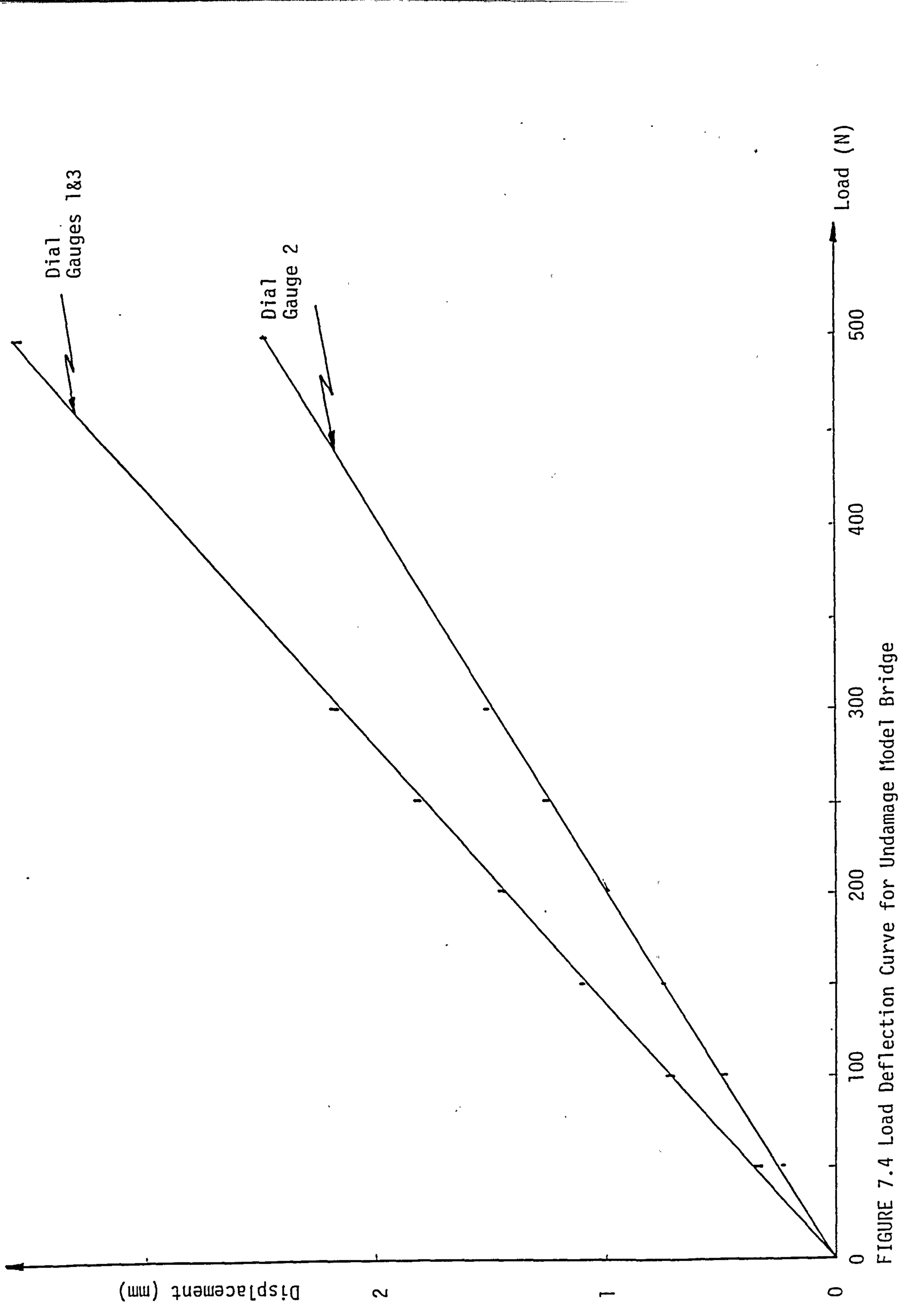

FIGURE 7.4 Load Deflection Curve for Undamage Model Bridge

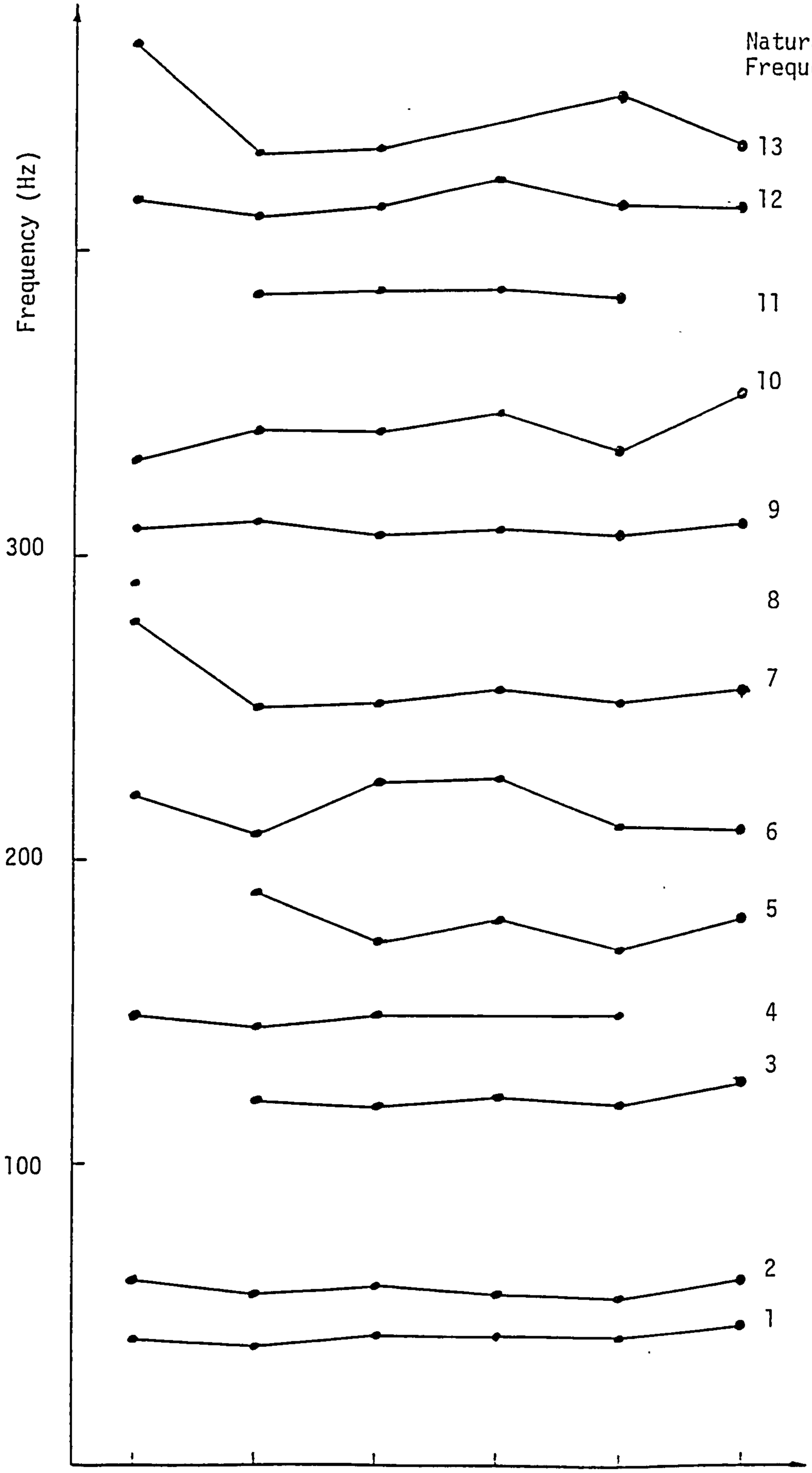

(1) orignal
(2) fix rotation of pinned end
(3) fix translation of roller end
(4) fix rotation and translation of roller end
(5) fix rotation of roller end
(6) fix all boundary conditions

FIGURE 7.5 Results of Bearing Changes

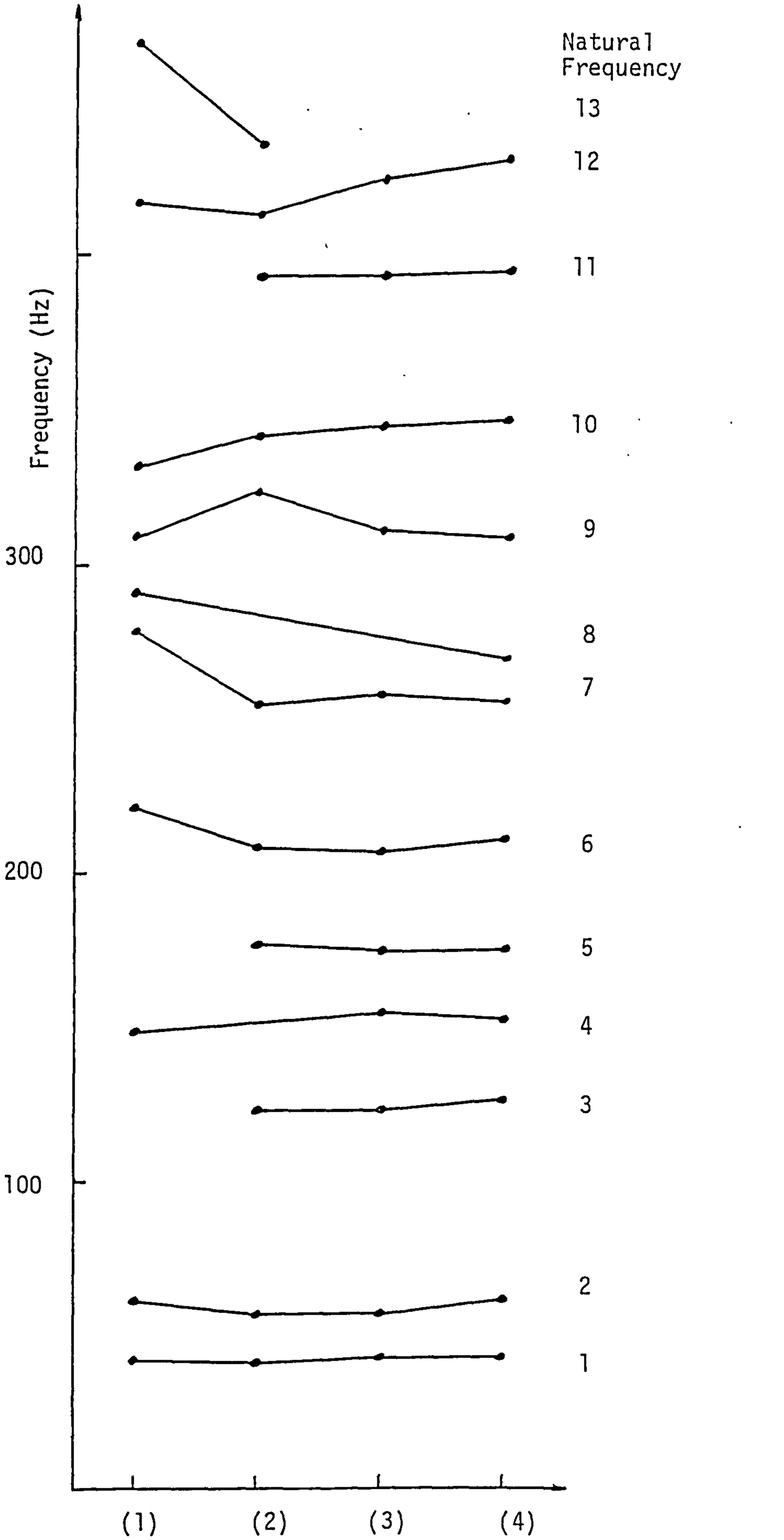

(1) orignal (3) d.disp. 2mm
(2) d.disp. 1mm (4) d.disp. 3mm

FIGURE 7.6 Diff. Displacement of one of the Pinned Bearings

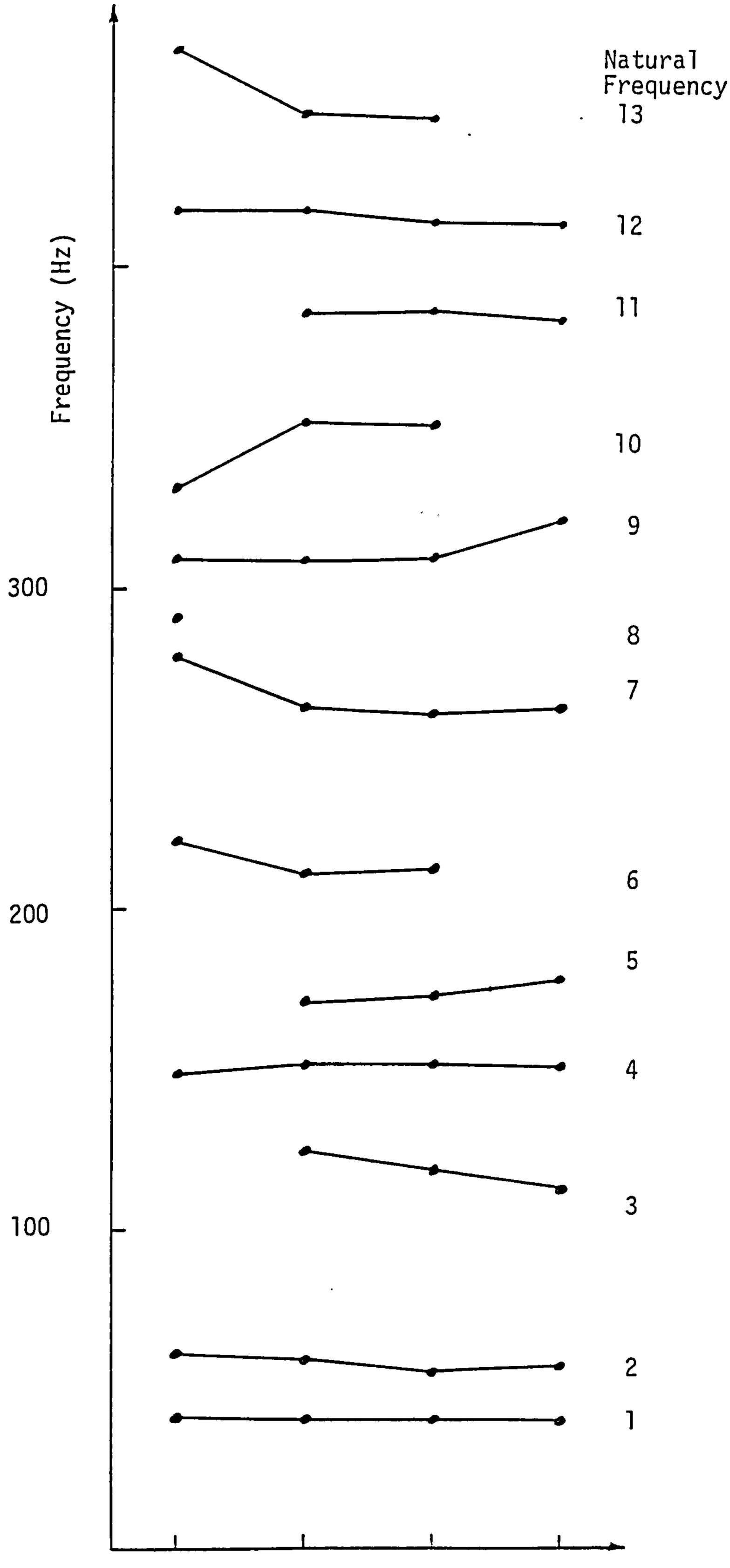

(1) orignal (3) d.disp. 2mm
(2) d.disp. 1mm (4) d.disp. 3mm

FIGURE 7.7 Diff. Displacement of one of the Roller Bearings

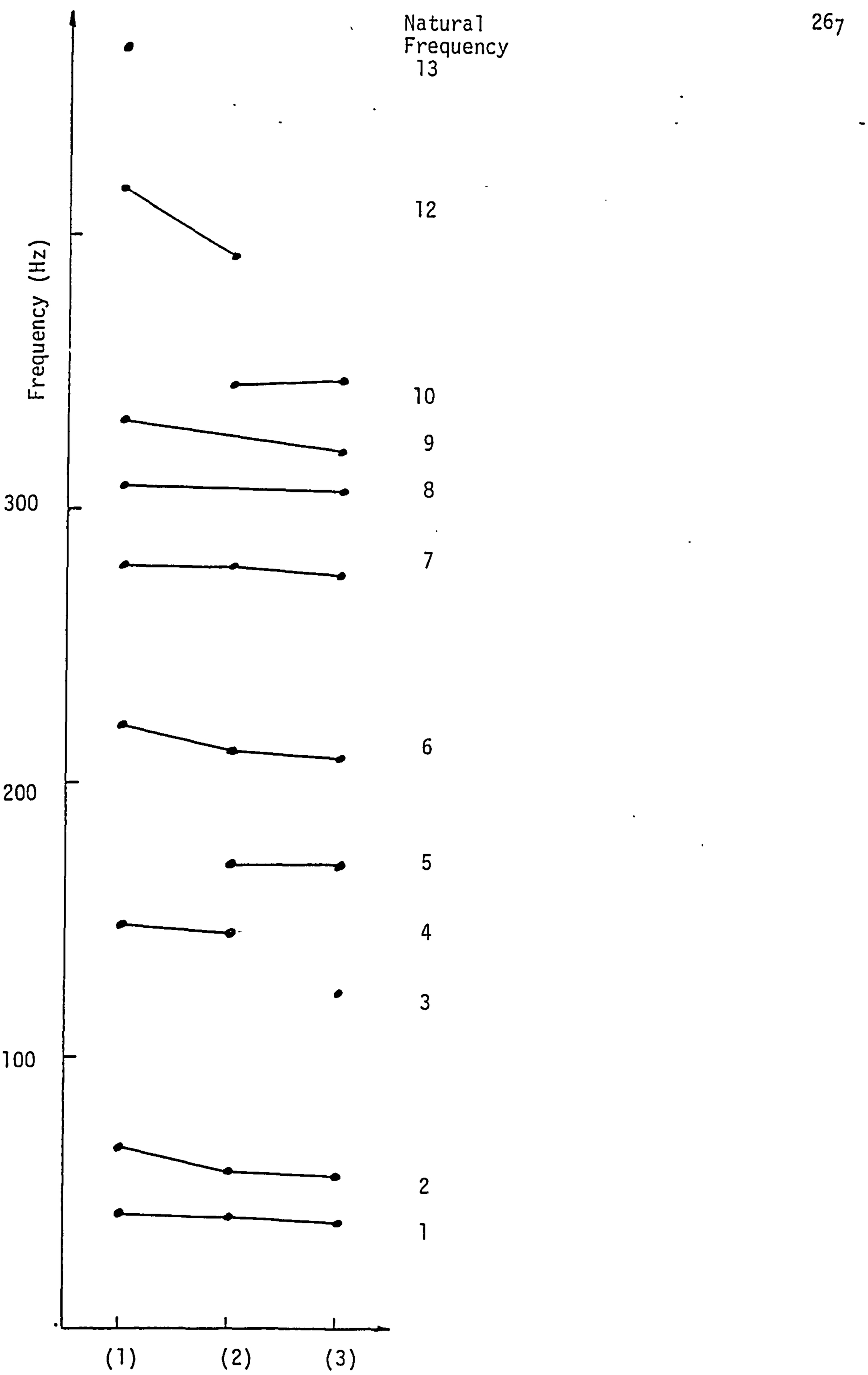

(1) orignal
(2) 50% shear connectors in one beam
(3) 50% shear connectors in both beams

FIGURE 7.8 Reduction in Shear Connection

CONTENTS OF CHAPTER 8

CHAPTER 8 CONCLUSION

As stated in the introduction to this thesis the aim of this research was to produce a simple and cheaper method of calculating and measuring the response of bridge decks to traffic flow over a period of time, to detect if any structural changes have occurred in the structural stiffness or mass.

The first objective, section one of this thesis, was to produce a simple and accurate method of solving the equations of motion of free vibration, the generalised eigenvalue problem, (i.e. equation 3.150). A number of methods were investigated based on the rate of change of the eigenvalue problem, and the reduced matrices produced by the subspace iteration method, and these methods are outlined in Chapter 3. One method proved to be very successful and is given by equations 4.2, 4.4 and the implementation of these equations into the finte element system FLASH is given in Section 4.5.

Five examples were used to test the methods stability and suitabilities to predict the change in natural frequency for a varied number of structural changes in stiffness and mass. The results of these studies are summarised by five figures, i.e. Figures 5.3, 5.5, 5.6, 5.9 and 5.10.

In general it was concluded that if a structural change in stiffness and/or mass was less than 40%, the method developed produced errors of less than 5%.

One important factor of the method described in section 4.5 is that only the structural changes in stiffness and/or mass are worked on, and the only data input required by the program are the structural changes. The above two points produce great savings in computer computations, and the results of the savings are summarized in Table 5.15

The second objective, section two of this thesis was to develop a simple, cheap and accurate method of measuring the natural frequencies of bridge decks, and to test the developed method capabilities against a model

bridge in which a number of different structural changes were applied. The first two of these objectives were achieved, I believe, and the method is based on using the simple fast fourier transform technique. The summary of the method developed is given in Chapter 6 Section 6.6.

The accuracy of the method could be in doubt because of the results of the studies of the physical structural changes applied to the model bridge as described in Cahpter 7. The reasons for this doubt could be:

i) There was no consistency in the number of natural frequencies recorded for each applied structural change.

ii) The magnitude of the structural changes was possibly too low.

One interesting point illustrated by the results, was that the method showed that different types of structural changes affected different modes of response by different accounts i.e. if differential displacement of a pinned end has occurred then the bending modes show a decrease with an associated small decrease in torsional stiffness modes.

8.1 Future Work

Before the method of vibration monitoring can be applied successfully in practice, more research has to be carried out. The further research could be:

i) To induce larger changes into the model bridge to the level recommended by Structral Monitoring Limited or to construct a larger model bridge structure in which larger strctural changes could be applied, i.e. a more flexible structure.

ii) To induce structural changes to a real bridge structure.

iii) To carry out a pilot study on a real bridge structure to see if any structural changes occur due to wear and tear.

iv) To carry out a detailel study into how to model small structural changes in finite dynamic models.

From the computer studies, if engineers are interested in determining the response of structures resulting from small changes in structural properties, this can only be achieved by resolving the complete equations of motion, and dynamic finite element analyses fall into three areas.

i) free vibration
ii) model methods of forced vibration
iii) direct integration schemes

The above problem has been resolved and is discussed in this thesis, but only at present for free vibration problems.

The solution to the second case, model methods of forced vibration, is first based on the calculation of the structural eigenvalues and eigenvectors. The eigenproblem is solved so that the "n" coupled equations of motion defining the structure can be uncoupled to "n" single equations of motion i.e. model superposition. Then the "n" single equations of motion are solved by the appropriate method, e.g. seismic analysis, steady state analysis and transient analysis, but the major part of the solution procedure is in calculating the structural eigenvalues and eigenvectors. Hence the method given in section 4.5 may be extended into the field of forced vibration without much complication.

One example of the forced vibration method in which this method would be useful is in the field of seismic (earthquake) transient analysis. That is, as the earthquake passes, parts of the structure become non-linear, i.e. changes in the structural stiffness occur, and hence the eigenvalues change so that the response of the structure can be calculated much more effectively.

REFERENCES

9. REFERENCES

1. ACM
   Transaction on Mathematical Software
   Vol 2, No 4 December 1976 PP 325 - 387

2. BAKER J.K.
   Vibration Isolation
   Engineering Design Guides 13
   Oxford University Press 1975

3. BATHE K.J.
   Finite Element Procedures in Engineering Analysis
   Prentice Hall 1982

4. BATHE K.J. and WILSON E.L.
   Solution Methods for Eigenvalue Problems in Structural Mechanics
   International Journal for Numerical Methods in Engineeering
   Vol 6 1973 PP 213 - 226

5. BATHE K.J. and WILSON E.L.
   Eigensolution of Large Structural Systems with Small Bandwidths.
   Journal of the Engineering Mechanics Division of A.S.C.E.
   June 1973 PP 467 - 479

6. BATHE K.J.
   Solution Methods for Large Generalised Eigenvalue Problems in Structural Engineering
   PhD Thesis 1971
   University of California

7. CAMPBELL R.B.

   The Extimation of Natural Frequencies and Damping Ratios of Offshore Structures
   PhD Thesis 1979
   M.I.T.

8. CHAUDHURI S.K. and SHORE S.
Dynamic Analysis of Horizontally curved I-Girder Bridge.
Journal of the Structural Division of A.S.C.E.
August 1977 PP 921 - 937

9. COUTE S.D. de BOOR C.
Elementary Numerical Analysis
McGraw-Hill 1972

10. DOUGLAS B.M. and REID W.H.
Dynamic Tests and System Identification of Bridges.
Journal of the Structural Division A.S.C.E.
October 1982 PP 2295 - 2312

11. DUGGEN D.M.
Personal Communication
Structural Monitoring Limited
Glasgow
June 1982

12. EDGERTON R.C. and BECROFT G.W.
Dynamics Stress in Continuous Plate Ginder Bridges.
Journal of the Structural Division A.S.C.E.
May 1956 Paper 973

13. EYRE R.
Dynamic Test on The Cleddon Bridge at Milford Haven.
T.R.R.L.
Suplementary Report 200UC

14. FLASH User Manual
WALDER U. and GREEN D.R.
Bern
Switzerland

15. FOX R.L. and KAPOOR M.P.
Rate of Change of Eigenvalues and Eigenvectors.
Journal of the A.I.A.A.
Vol 6 1968 PP 2426 - 2429

16. HEWLETT PACKARD 3582A
Spectrum Analyser
User Manual

17. KENLEY R.M. and DODDS C.J.
West Sole W.E. Platform : Detection of Damage by Structural Response Measurements.
Offshore Technology Conference
Houston 1980

18. LEONARD D.R.
Dynmaic Tests on Highway Bridges - Test Procedures and Equipment
T.R.R.L.
Laboratory Report 654.

19. LOLAND O.
A Vibration Method for Integrity Monitoring of Fixed Offshore Steel Platforms.
PhD Thesis 1978
University of Glasgow

20. MSC/NASTRAN
The Macneal-Schwendler Corporation
Los Angeles
U.S.A.

21. NEWLAND D.E.
An Introduction to Random Vibration and Spectral Analysis.
Longman 1984

22. NOBLE B.
Applied Linear Algebra
Prentice Hall 1969.

23. PRETLOVE A.J. and TURNER J.D.
Vibration in Older Bridges
Department of Engineering
University of Reading
February 1985

24. RAINER J.H. and PERNICA G.
Dynamic Testing of a Modern Concrete Bridge
Canada Journal of Civil Engineering
Vol 6 1979 PP 447 - 455

25. The Measurement and Analysis of the Dynamic Response of Southfield Bridge, Glenrothes
Structural Monitoring Limited
Report No 119 March 1979

26. Investigation of Vibration Methods for Monitoring the Integrity of Bridges. Stage 1 Report
Structural Monitoring Limited
Report No 205 September 1986

27. Investigation of Vibration Methods for Monitoring the Integrity of Bridges. Stage 2 Report
Structural Monitoring Limited
Report No 283 December 1982.

28. WALDER U.
FLASH - A Simple Tool for Complicated Problems.
Advances in Engineering Software
Vol 1 1979 PP 137 - 140

29. WALKER W.H. and VELETOS A.S.
Response of Simple Span Highway Bridges to Moving Vehicles
Bulletin 486
University of Illinois

30. WITTRICK W.H.
Rates of Changes of Eigenvalues with Reference to Buckling and Vibration Problems.
Journal of the Royal Aeronoatical Society
Vol 66 1962 PP 590 - 591

31. VELETSOS A.S. and HUANG T.
Analysis of Dynamic Response of Highway Bridges.
Journal of the Engineering Mechanics Division of A.S.C.E.
October 1970 PP 593 - 620

32. ZARGHAMEE M.S.
Optimum Frequency of Structure
Journal of the A.I.A.A.
Vol 6 1968 PP 749 - 750

APPENDIX

APPENDIX

A1 Theory of Frequency Extraction

In this section is given briefly methods of frequency extraction of random signals. These methods can be split into 3 types of analysis.

a) Fourier Transform

b) Fast Fourier Transform

c) Maximum Entropy Method

Each method will be given in order, and finally the method of windowing used in the fast fourier transform will be described.

A1.1 Fourier Transform

Any random signal x(t) can always be expressed as an infinite trigometric series (i.e. Fourier Series) of the form

$$x(t) = a_0 + a_1 \cos \frac{2\pi t}{T} + a_2 \cos \frac{4\pi t}{T} + \ldots\ldots$$
$$+ b_1 \sin \frac{2\pi t}{T} + b_2 \sin \frac{4\pi t}{T} + \ldots\ldots \qquad (1)$$

or in more compact notation

$$x(t) = a_0 + \sum_{k=1}^{\infty} \left(a_k \cos \frac{2\pi kt}{T} + b_k \sin \frac{2\pi kt}{T} \right. \qquad (2)$$

Where T is the period of the random signal.

a_0, a_k and b_k are constants and are known as FOURIER COEFFICIENTS and are given by

$$a_o = \frac{1}{T} \int_{-T/2}^{T/2} x(t)\ dt \qquad (3)$$

$$a_k = \frac{2}{T} \int_{-T/2}^{T/2} x(t) \cos \frac{2\pi kt}{T}\ dt \qquad (4)$$

$$b_k = \frac{2}{T} \int_{-T/2}^{T/2} x(t) \sin \frac{2\pi kt}{T}\ dt \qquad (5)$$

It can be show that if the t axis is adjusted so that $a_o = 0$

Hence equation (2) becomes

$$x(t) = \sum_{k=1}^{\infty} \left(a_k \cos \frac{2\pi kt}{T} + b_k \sin \frac{2\pi kt}{T}\right) \qquad (6)$$

Where the remaining coefficients a_k and b_k will be in general all different and their values may be illustrated graphically, see figure (A1).

The horizontal axis is chosen to represent frequency and the location of the k^{th} coefficient is

$$\omega_k = \frac{2\pi k}{T} \qquad (7)$$

which is the frequency of the k^{th} harmonic. The spacing between adjacent harmonics is

$$\Delta\omega = \frac{2\pi}{T} \qquad (8)$$

As the period T increases the frequency spacing decreases and becomes small, and will in fact reduce to zero. Hence x(t) can no longer be represented as a periodic function, so it can not be

analysed as discrete frequency components. But the same ideas can be applied, hence the FOURIER SERIES becomes a FOURIER INTEGRAL and the FOURIER COEFFICIENTS becomes continuous functions of frequencies called FOURIER TRANSFORMS.

Since the continous time series x(t) is not known, but only equally spaced samples are available, so the DISCRETE FOURIER TRANSFORMS (DFT) need to be applied. If using complex notation equations (4) and (5) can be combined, such that

$$x_k = a_k - i\, b_k \qquad (9)$$

Hence

$$x_k = \frac{1}{T} \int_0^T x(t)\, e^{-i\,\left(\frac{2\pi kt}{T}\right)} \, dt \qquad (10)$$

Suppose that this continuous time series is represented by the discrete series (x_r) r = 0. 1. 2.....(N-1)
where $t = r\Delta$ and $\Delta = T/N$. The integral in equation (10) may be replaced, approximately, by summation i.e.

$$x_k = \frac{1}{T} \sum_{r=0}^{N-1} x_r\, e^{-i\,\left(\frac{2\pi k}{T}\right)r\Delta}\, \Delta \qquad (11)$$

This amounts to assuming that the total area under the time series curve is given by the sum of each strip. Hence substituting

$T = N\Delta$ into (11) gives

$$x_k = \frac{1}{N} \sum_{r=0}^{N-1} x_r\, e^{-i\,\left(\frac{2\pi kr}{T}\right)} \qquad (12)$$

which may be regarded as an approximate formula for calculating the coefficients of the fourier series given in equation 1.

A1.2 The Fast Fourier Transform

The fast fourier transform (FFT) is a computer algorithm for calculating the discrete fourier transform (DFT). In the discrete transform N^2 computer operation are required to calculate the full sequence x_k but the FFT reduces the number of operations to $N \log_2 N$.

Hence the FFT offers an enormous reduction in computer operations and an increase in accuracy since fewer operations, produce fewer round-off errors.

The FFT works by partioning the full sequence (x_r) into a number of shorter sequences. Instead of calculating the DFT of the original sequence, only the DFT'S of the shorter sequences are calculated. The FFT then combines these together in an ingenious way to yield the full DFT of (x_r).

Suppose that (x_r) r = 0, 1, 2, ...(N-1) is the sequence shown in figure A2 where N is an even number and that this is partitioned into two shorter sequences (y_r) and (η) as shown in figure A2.

where $y_r = x_{2r}$

$$r = 0, 1, 2, \ldots\ldots (N/2 - 1) \qquad (13)$$

$\eta_r = x_{2r+1}$

The DFT'S of these two shorter sequencies are Y_k and Z_k where from equation (12)

$$Y_k = \frac{1}{N/2} \sum_{r=0}^{N/2 - 1} y_r \, e^{-i \frac{2\pi kr}{N/2}}$$

and (14)

$$Z_k = \frac{1}{N/2} \sum_{r=0}^{N/2 - 1} \eta_r \, e^{-i \frac{2\pi kr}{N/2}}$$

Now returning to the DFT of the original sequence (x_r) the summation is rearranged into separate sums similar to those accurring in (14).

First the old and even terms in (x_r) sequence are separated to obtain

$$X_k = \frac{1}{N} \sum_{r=0}^{N-1} X_r \, e^{-i \frac{2\pi rk}{N}} \qquad (12)$$

$$= \frac{1}{N} \left(\sum_{r=o}^{N/2-1} x_{2r} \, e^{-i \frac{2\pi (2r)k}{N}} + \sum_{r=o}^{N/2-1} x_{2r+1} \, e^{-i \frac{2\pi(2r+1)k}{N}} \right) \qquad (15)$$

Then substituting from (13)

$$X_k = \frac{1}{N} \left(\sum_{r=o}^{N/2-1} Y_r \, e^{-i \frac{2\pi rk}{N/2}} + e^{\frac{-i2\pi k}{N}} \sum_{r=o}^{N/2-1} \mathcal{Y}_r \, e^{\frac{-i2\pi rk}{N/2}} \right.$$

from which it can be seen that by comparing equations (16) with (13) gives

$$X_k = \frac{1}{2} \left(Y_k + e^{\frac{(2\pi k)}{N}} Z_k \right) \qquad (17)$$

for $k = 0, 1, 2, \ldots\ldots (N/2 - 1)$

The DFT of the original sequence can therefore be obtained directly from the DFT's of the two half-sequences Y_k and Z_k according to the above equation (17). This is the FFT method. If the original number of samples N is the sequence (x_r) is a power of 2 then the half-sequence (y_r) and $(\mathcal{Y}_r)$ may themselves be partitioned into quarter-sequences and so on, for more information see reference (21).

A1.3 The Maximum Entropy Method (MEM)

This method provides smooth, highly resolved response spectra from short time histories and was the method of frequency extraction used by Structural Monitoring Limited in their bridge deck studies. But the method is very complex to use, and involves large amounts of computer time. For discussion of the method see reference 7.

A1.4 Practical Application of FFT

Windowing : this phenomenom is a practical form of taking a length of random signal before analysis. There are a number of forms of windowing, and the Hewlett Packard 3582A spectrum analysis has three types of windowing function, which produce different results.

a. The FLAT TOP is optimized for minimum amplitude uncertainly. The frequency resolution is correspondingly by poorer than the other windowing functions.

b. The UNIFORM is the result of using no time domain window weighting. it is poorest in amplitude uncertainty, but is best in frequency certainty.

c. The HANNING is a traditional "window" function. It offers a compromise between the FLAT TOP and UNIFORM functions.

Since the Hewlett Packard spectrum analyser is a duel channel analyser, there are a number of functions which combine the two channels.

a. Transfer functions : this function decides the results of each FFT of the two channels to produce H_k.

$$\text{i.e. } H_k = \frac{Y_k}{X_k} \tag{18}$$

b. Coherence : For the duel channels, it represents the fraction of the system output power directly related to the imput.

When one analysis is carried out, the question arise as to how consequent windows are added together, and why. The method used in this research was to take the square root of the sum of the squares. A number of windows need to be combined to smooth out small inconsistencies in the random signals.

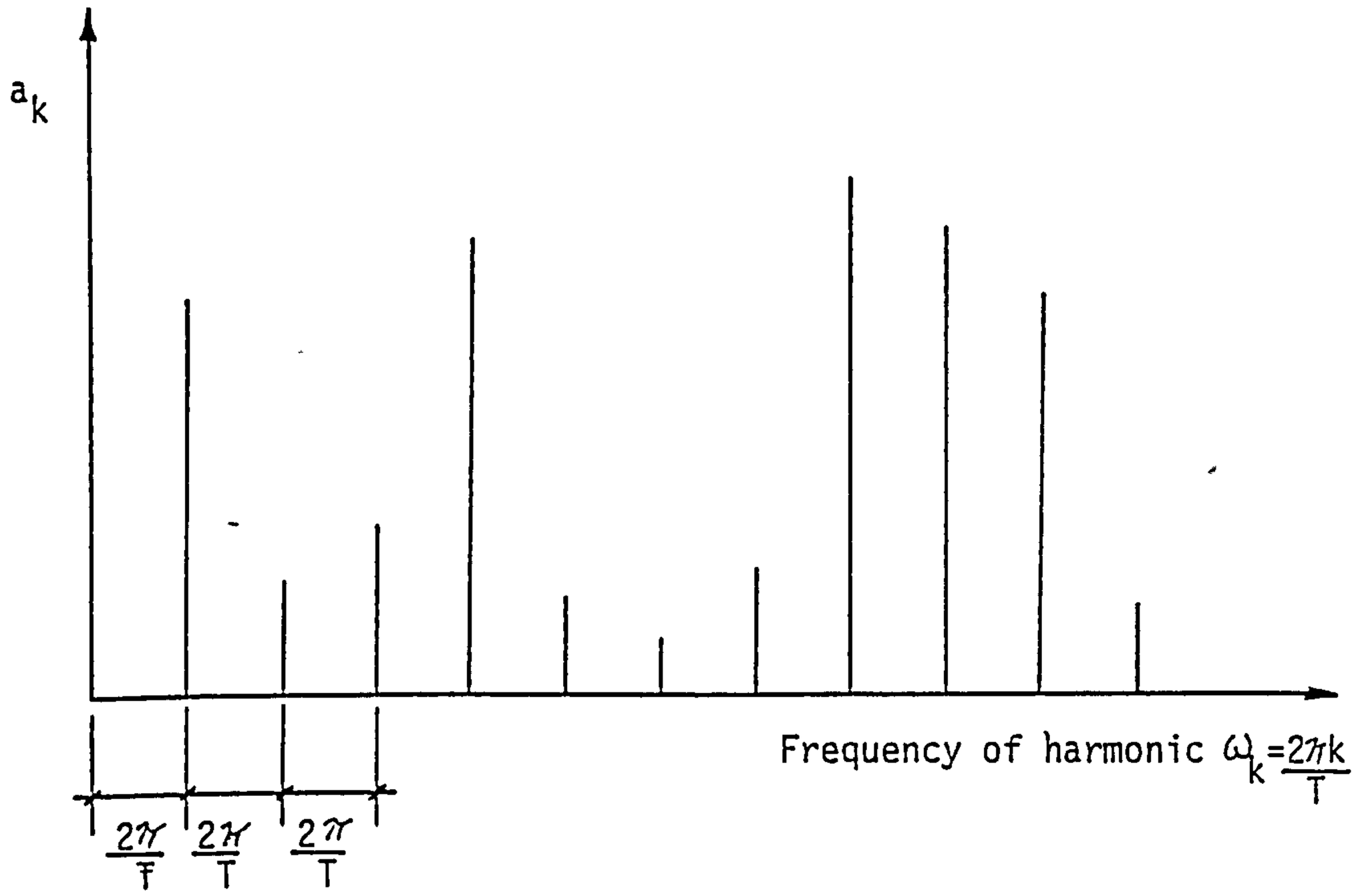

FIGURE A 1 GRAPHICAL REPRESENTATION OF FOURIER COEFFICIENTS

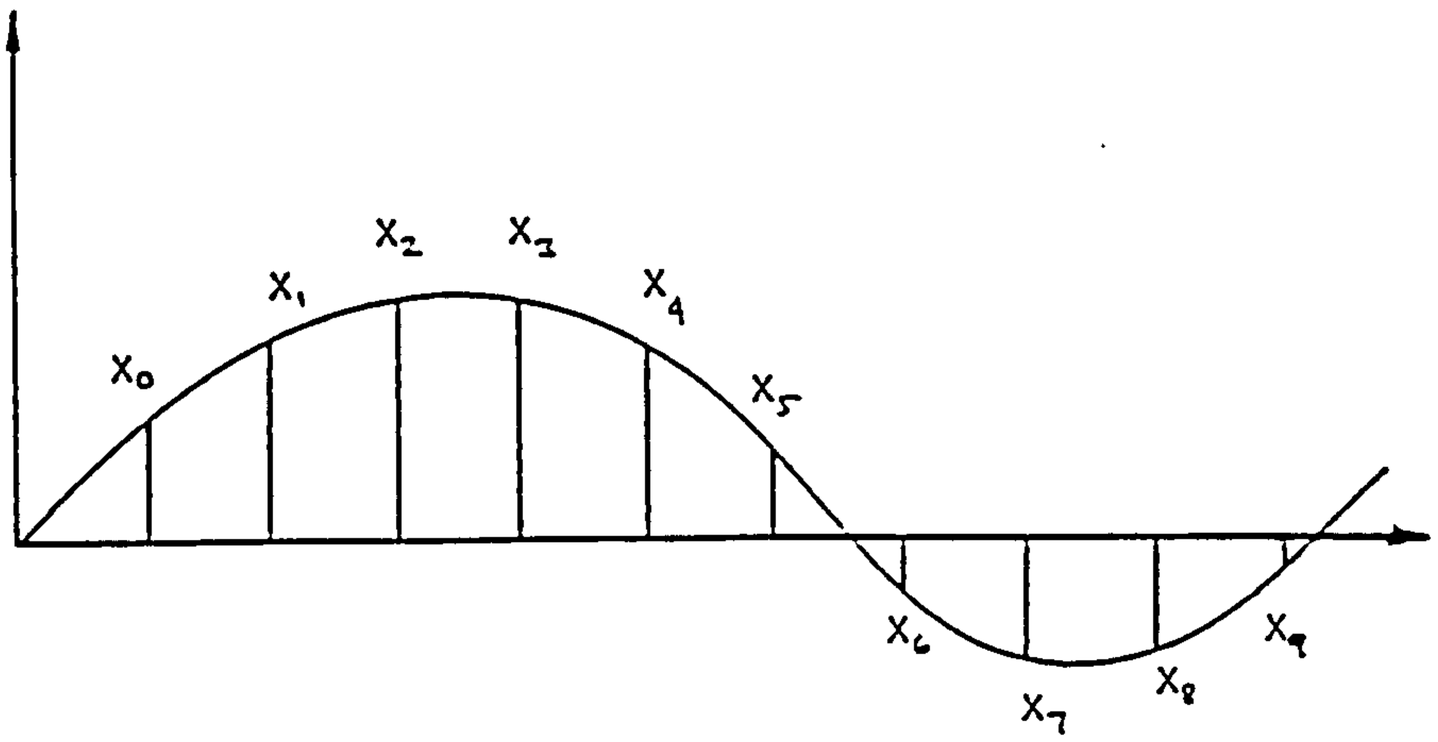

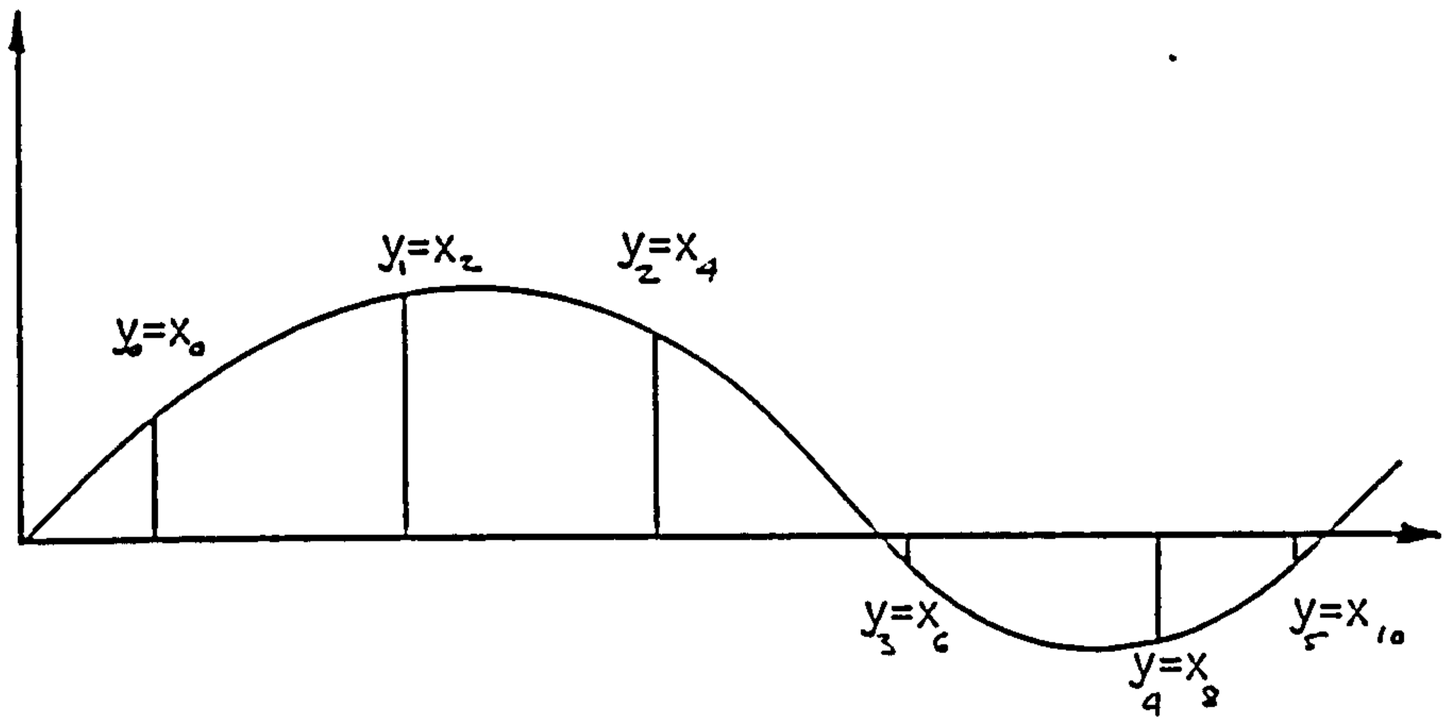

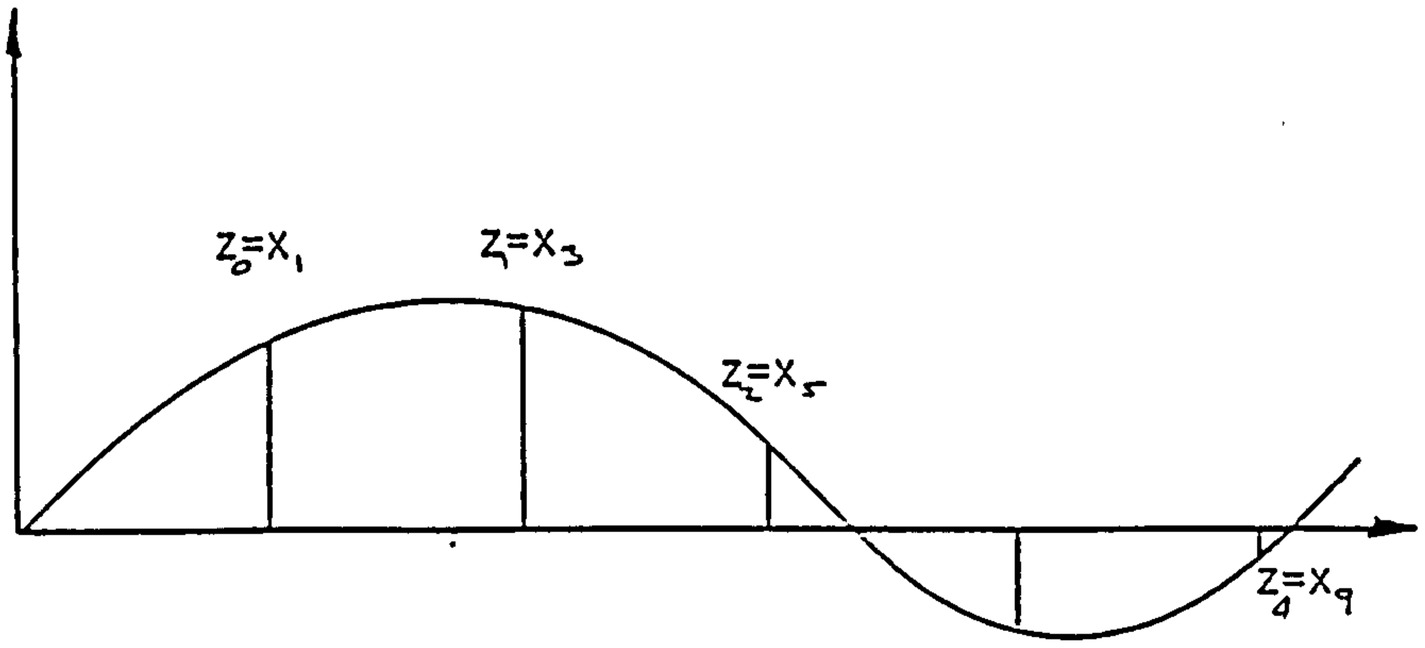

FIGURE A2 PARTITIONING THE SEQUENCES $\{x_r\}$ INTO TWO HALF SEQUENCES $\{y_r\}$ AND $\{z_r\}$

PUBLICATIONS

Proceedings

of

The Second International Conference

on

Civil and Structural Engineering Computing

Volume 2

Edited by
B. H. V. TOPPING

DYNAMIC REANALYSIS

J P A Burns, BSc(Eng),
Atkins Research and Development,
(formerly University of Glasgow) and
D R Green, BSc(Eng), MSc, PhD, CEng, MIStructE,
Department of Civil Engineering, Glasgow University

This paper will describe algorithms by which the dynamic reanalysis of structures can be carried out with a minimum preparation of data and at minimum computer costs. These techniques allow the designer to study, on an interactive basis, those parameters in a large structural idealisation which affect the dynamic response. The work has practical significance in monitoring structures through response to random excitation for changes in structural performance, and interactive design of structures where the influence of properties on the dyanamic response is required, i.e. dynamic sensitivity analysis.

The method is based on the Subspace Iteration Method developed by Bathe and Wilson in conjunction with work carried out by Fox and Kapoor and is a two stage process. (Refs. 1, 2).

The first stage of the method is to carry out a complete dynamic analysis of the structure using subspace iteration. The working matrices from this first analysis are saved to be operated on later by the second stage analysis associated with changes in the original structure. These changes can be for example, changes in boundary conditions, elements properties (stiffness or mass) and/or removing or including more elements. Since only the changes to the original system need be described, data definition and solution for this reanalysis is such that it can be carried out on an interactive basis.

This method of analysis has been incorporated into the general purpose civil engineering computer analysis program FLASH. Numerical results and examples will be presented to show the limits on changes in structural properties that are possible before a complete reanalysis of the structure is required and to illustrate the practical application of the technique.

INTRODUCTION

This paper describes alogorithms by which dynamic reanalysis of structures can be carried out with minimum preparation of data and at minimum computer costs. The method proposed is based on the subspace iteration method developed by Bathe and Wilson in conjunction with work carried out by Fox and Kapoor and is a two stage process (Refs. 1, 2).

PROBLEM DEFINITION

The equation of motion for any structural system can be written as:

$$M\ddot{u} = C\dot{u} + Ku = F \qquad (1)$$

in which M, C, F, are mass, damping and stiffness matrices of the system respectively, and u, $\dot{u}$, $\ddot{u}$ are the system vectors of displacement, velocity and acceleration respectively, and finally F is the applied structural forces.

If only the free vibration of the system are considered equation (1) can be written as:

$$M\ddot{u} + Ku = 0 \qquad (2)$$

The solution of the above differential equation is obtained by substituting

$$u = \phi \sin \omega (t - t_o) \qquad (3)$$

to produce the generalised eigenvalue problem:

$$K\phi = \omega^2 M\phi \qquad (4)$$

in which the eigenvalues (ω) gives the natural frequencies (f_i) and the corresponding eigenvectors (ϕ) gives the vibration mode shapes

PROBLEM SOLUTION

In order to solve equation (4) for the p lowest solutions it is written as:

$$K\Phi = M\Phi\ \Omega^2 \qquad (5)$$

where the columns in Φ are the M-orthonormalized eigenvectors ϕ_1, ϕ_2, ..., ϕ_p and Ω^2 is a diagonal matrix containing the eigenvalues ω_1^2, ω_2^2, ..., ω^2_p. There are a number of methods to solve equation (5) but the method which is normally used is subspace iteration (Ref. 1). The specific idea used in the solution is that the eigenvectors form an M-orthonormal basis of the p-dimensional least dominant subspace of the operations K and M.

In the solutions q linearly independent vectors are iterated simultaneously where $q < p$. In the k^{th} iteration the vectors span the q-dimensional subspace E_{k+1} and the "best" eigenvalues and

eigenvectors approximation are calculated using the Jacobi diagonalization method (Ref. 3).

If X_1 is defined as the starting iteration vectors, then the subspace iteration algorithm is defined as follows:

For k = 1, 2, ... iterating from E_k to E_{k+1}

$$K\bar{X}_{k+1} = MX_k \tag{6}$$

The projected matrices of K and M on E_{k+1} are found:

$$K\bar{X}_{k+1} = Y_k \tag{7}$$

$$K_{k+1} = \bar{X}^T_{k+1}\, Y_k \tag{8}$$

$$\bar{Y}_{k+1} = M\bar{X}_{k+1} \tag{9}$$

$$M_{k+1} = \bar{X}^T_{k+1}\, Y_{k+1} \tag{10}$$

The projected eigensystem (equation (8) and (9)) are solved using the Jacobi diagonalization method.

$$K_{k+1}\, Q_{k+1} = M_{k+1}\, Q_{k+1}\, \Omega^2_{k+1} \tag{11}$$

Hence

$$\Omega^2_{k+1} \to \Omega^2,\ X_{k+1} \to \Phi \text{ as } k \to \infty$$

provided the starting iteration vectors X_1 are not orthogonal to one of the required eigenvectors.

All the solution methods have one disadvantage in that for any reasonable sized structure the computer time and hence cost is large.

REANALYSIS

Design engineers often would like to carry out dynamic sensitivity analysis but this is very costly. One method of reanalysis implied by Fox and Kapoor is based on the rate of change of equation (4) (Ref.2). Rewriting equation (4) for i^{th} solution:

$$K\Phi_i - \lambda_i M\Phi_i = 0 \tag{14}$$

$$(K - \lambda_i M)\Phi_i = 0 \tag{15}$$

$$\text{If: } F_i = (K - \lambda_i M) \tag{16}$$

It follows that,

$$F\Phi_i = 0 \tag{17}$$

Premultiplication of equation (17) by Φ^T_i gives:

$$\Phi^T_i\, F\Phi_i = 0 \tag{18}$$

Differentiating equation (18) with respect to any disturbance δ_j yields:

$$\Phi^T_{i,j} F_i \Phi_i + \Phi^T_i F_{i,j} \Phi_i + \Phi^T_i F_i \Phi_{i,j} = 0 \tag{19}$$

The first and third terms of equation (19) are zero owing to the symmetry of F_i and equation (17) and hence:

$$\Phi^T_i\, F_{i,j}\, \Phi_i = 0 \tag{20}$$

If equation 16 is differentiated with respect to δ_j;

$$F_{i,j} = K_{,j} - \lambda_i M_{,j} - \lambda_{i,j} M \tag{21}$$

By combining equation (20) and (21) and using M-orthonormal of the eigenvectors gives:

$$\lambda_{i,j} = \Phi^T_i [K_{,j} - \lambda_i M_{,j}]\, \Phi_i \tag{22}$$

A method is proposed which involves the use of subspace iteration and equation (22) and is a two stage process. The first stage of the method is to carry out a complete dynamic analysis of the structure using subspace iteration. After the analysis vectors Y_i and X_i (from equation (6) - (10)) are saved to be operated on later in the second stage of the analysis.

The second stage is based on projecting the changed matrices $M_{,j}$ and $K_{,j}$ into the subspaces of M and K and solving these matrices using equation (22).

In mathematical form:

Rewriting equation (7)

$$KX = Y \tag{23}$$

where the columns in X are $X_1, X_2, \ldots X_p$

and Y are $Y_1, Y_2, \ldots Y_p$

If changes to stiffness matrix (δK) are induced, changes are caused in X, hence equation (22) becomes:

$$(K + \delta K)(X + \delta X) = Y \tag{24}$$

$$KX + \delta KX + K\delta X + \delta K\, \delta X = Y \tag{25}$$

Since KX = Y and neglecting second order terms equation (25) becomes:

$$K\delta X + \delta KX = 0 \tag{26}$$

$$\delta X = -K^{-1}\delta KX \tag{27}$$

$$\text{Hence, } \delta K_{REDUCE} = \delta X^T Y \tag{28}$$

Rewriting equation (9),

$$Y = MX \tag{29}$$

where the columns in Y are $Y_1, Y_2, \ldots Y_p$

and X are $X_1, X_2, \ldots Y_p$

If changes are induced in the mass matrix (δM)

changes are caused in Y also, hence equation (29) becomes:

$$Y + \delta Y = (M + \delta M)X \quad (30)$$

$$Y + \delta Y = MX + \delta MX \quad (31)$$

since Y = MX equation (31) becomes:

$$\delta Y = \delta MX \quad (32)$$

$$\text{Hence, } \delta M_{REDUCE} = X^T \delta Y \quad (33)$$

If a form of equation (22) is applied to equations (28) and (33) the following methods are produced.

a. Changes to stiffness matrix only.

i multiple δK by X; δKX (34)

ii solve $K\delta X = -\delta KX$ (35)

(decomposition of K has already been carried out in the full analysis)

iii calculate $\delta K_{REDUCE} = \delta X^T Y_{OLD}$ (36)

iv calculate the change in eigenvalues

$$\delta\lambda_i = Q_i^T \delta K_{REDUCE} Q_i \quad (37)$$

b. Changes to mass only

i calculate $\delta Y = \delta MX$ (38)

ii calculate $\delta M_{REDUCE} = X^T \delta Y$ (39)

iii calculate the change in eigenvalue

$$\delta\lambda_i = [Q_i^T \delta M_{REDUCE} Q_i]^* - \lambda_i \quad (40)$$

c. Changes to both stiffness and mass matrices. Steps (a) and (b) are carried out and the results from equations (37) and (40) are added together. This is done for numerical stability.

This method has the advantage over just equation (22) in that the projected matrices have all the properties of the eigenvalues under consideration, so changes in stiffness or mass with this method have a much more accurate effect on the eigenvalues, whereas equation (22) deals with the full matrices.

COMPUTER IMPLEMENTATION

This method has been incorporated into the general purpose civil engineering computer analysis program FLASH (Ref. 4). On the restart analysis the only data input is the changed structural properties; for example changes in boundary conditions, some or all element properties of stiffness or mass.

The only restriction of changes in the idealisation is that the orientation of the degrees of freedom should not change.

From these changes in idealisation, only the changes in the stiffness and mass matrices are generated in order to produce new Eigenvalues and hence natural frequencies.

To illustrate the application of the technique two numerical examples are given.

NUMERICAL EXAMPLES

Example 1: Skew Isotropic Slab

The slab given in figure 1 was analysed using 72 quadrilateral plate bending, hybrid finite elements with consistent mass formulation, with 3 degrees of freedom (U_Z, R_X, R_Y), giving a total number of degrees of freedom of 216. For this computer model the first ten natural frequencies were calculated using subspace iteration and are given in table 1.

A study of the effect of a 10% change in Young's modulus was carried out for 2, 8, 18, 32, 50, 72 elements. This grow of change was carried out from joint 1 and was analysed twice.

i under restart mode using the new method (NEW).

ii complete subspace iteration analysis (FULL)

and an error analysis was carried out as follows:

$$\% \text{ ERROR} = \frac{f_{i(FULL)} - f_{i(NEW)}}{f_{i(FULL)}} \quad (41)$$

with the envelope of the results given in figure 2. Figure 4 gives an example of the savings in data preparation.

Finally figure 3 shows the percentage computer time saving with respect to the number of changed elements.

Example 2: Beam Element Problem

The beam given in figure 5 was analysed using 12 shell beam element, with consistent mass formulation and 6 degrees of freedom (U_X, U_Y, U_Z, R_X, R_Y, R_Z) giving a total number of degrees of freedom of 72. For this computer model the first ten natural frequencies were calculated using subspace iteration and are given in table 2.

A study of the effects of one boundary condition was carried out, at joint 1. In the original analysis six springs of stiffness 1.0E10 NM were used to model the boundary conditions at joint 1, and the effect of continuously halving the springs stiffness on the beam's natural frequencies was studied. Since this is only a local effect only four of the natural frequencies were affected. As in example 1 an error analysis was carried out and the results are given in figure 6. Similar savings in data preparation to the previous example occur.

Since in this study only four degrees of freedom were effected, and the reanalysis time was "constant" and table 3 gives the percentage computer time savings.

CONCLUSION

This paper describes a method of carrying out dynamic reanalysis which can study overall effects on a structure (example 1) or just local effects (example 2) with great saving in computer time AND data preparation, since only the changed structural matrices are generated.

When localised changes are made in a structural idealisation the natural frequencies are affected in a localised way also. Example 2 shows that this localised response is correctly modelled and the method can be used in general for dynamic sensitivity analysis.

For example, in the solution of Inelastic Seismic Response Problems local changes occur in the stiffness matrix within each time increment. The dynamic sensitivity approach can be used here and would result in major reduction in solution time.

REFERENCES

1 Bathe, K.J. and Wilson, E.L., Large Eigenvalue Problems in Dynamic Analysis, Journal of the Engineering Mechanics Division of A.S.C.E., December 1972, 1471-1485.

2 Fox, R.L. and Kapoor, M.P., Rates of Change of Eigenvalues and Eigenvectors, A.I.A.A. Journal Vol. 6, No. 12, 1968, 2426-2429.

3 Bathe, K.J., Finite Element Procedures in Engineering Analysis, Prentice Hall 1982.

4. Walder, U. and Green, D.R., FLASH User Manual, Bern, Switzerland.

NUMBER	NATURAL FREQUENCY
1	0.836638
2	0.986545
3	2.371438
4	3.468227
5	4.547184
6	5.609784
7	7.550049
8	8.089236
9	10.090280
10	10.471880

TABLE 1. NATURAL FREQUENCIES FOR SKEW SLAB.

NUMBER	NATURAL FREQUENCY
1	3.749775
2	4.730255
3	6.431323
4	7.866933
5	9.302883
6	10.168750
7	12.652850
8	14.380870
9	16.524640
10	17.723680

TABLE 2. NATURAL FREQUENCY FOR BEAM ELEMENT PROBLEM.

OPERATION	% REDUCTION IN TIME
DATA INPUT	40.5
STIFFNESS MATRIX GENERATION	44.8
SOLUTION	84.8
TOTAL	78.7

TABLE 3. PERCENTAGE COMPUTER TIME SAVING FOR BEAM ELEMENT PROBLEM.

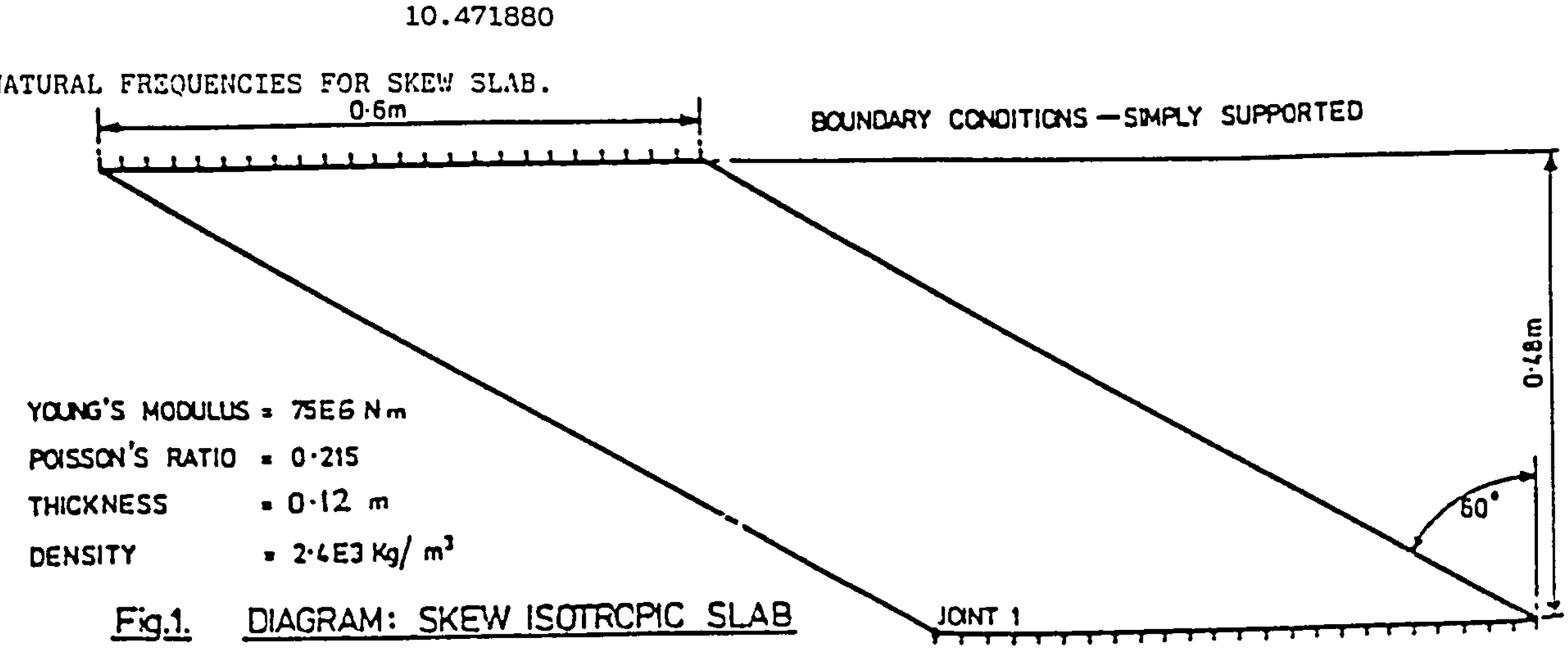

Fig.1. DIAGRAM: SKEW ISOTROPIC SLAB

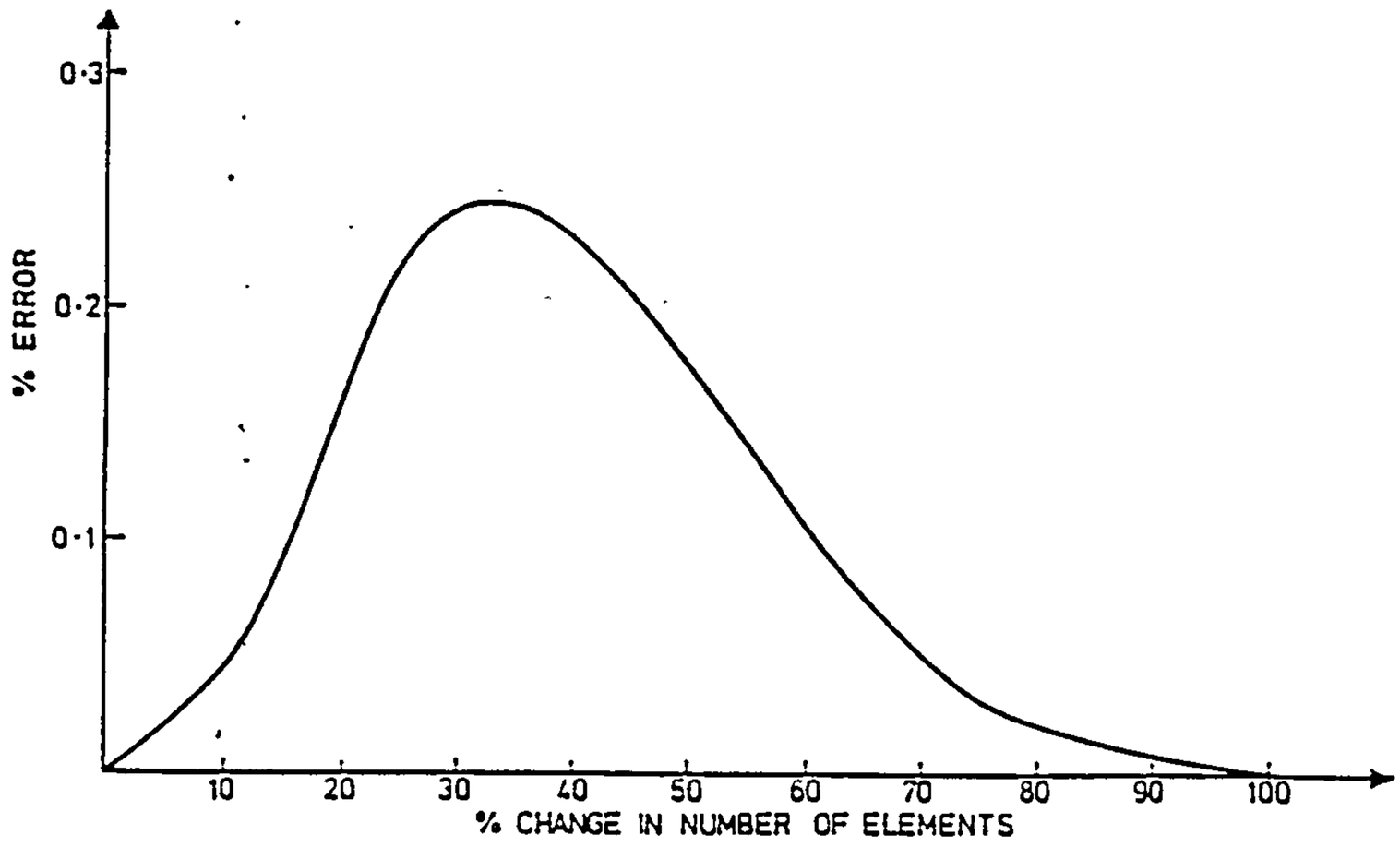

Fig.2. ENVELOPE OF ERRORS FOR A 10% CHANGE IN YOUNG'S MODULUS OF A SKEW SLAB

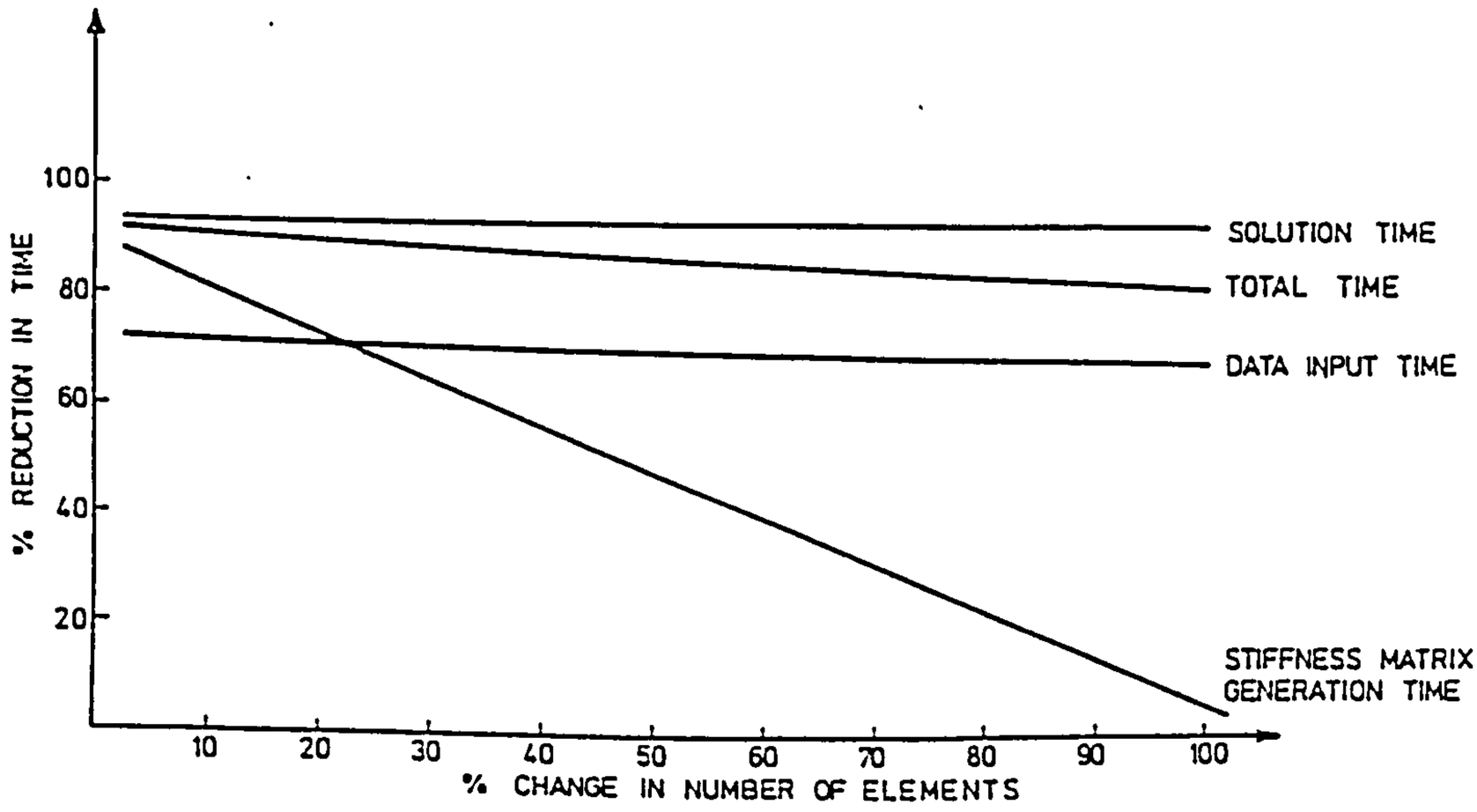

Fig.3. % SAVING IN COMPUTER TIME FOR SKEW SLAB

```
BEGIN
SKEW ISOTROPIC SCAB
PLATE 91 72 72 EIGENVALUES DYNAMIC 10
MATRIX 7 13 JOINT 1 1 7 COOD 0·0 PLUS 10·0 AND -6·928 4·0
*
ISOTROPIC 75·0E9  0·215  1·2 TYPE 3  TO 72
ISOTROPIC 67·5E9  0·215  1·2 TYPE 1  TO  2
MASS  2·4E3  TYPE  1 TO 72
*
MATRIX 12 6  ELEMENT 1   JOINT 2 9 8 1
*
TYPE   1  72 ELEMENT  1  TO 72
*
N F F  JOINT  1  TO 7
N F F  JOINT 85 TO 91
*
*
*
DYNAMIC  PRINT  10  RESTART
*
*
*
```

DATA INPUT FOR FULL ANALYSIS OF SKEW SLAB

Fg.4. EXAMPLE DATA INPUT FOR DYNAMIC REANALYSIS

```
RESTART
*
ISOTROPIC  75·0E8  0·215  1·2  TYPE  1 TO 2
*
*
*
*
*
*
*
*
*
*
```

DATA INPUT FOR RESTART ANALYSIS OF SKEW SLAB

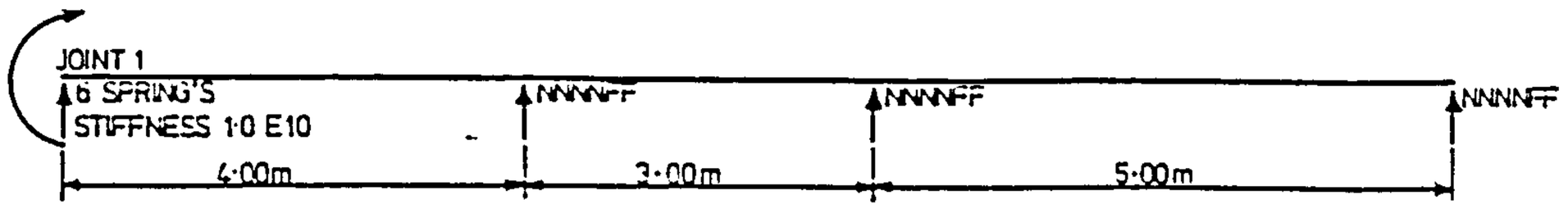

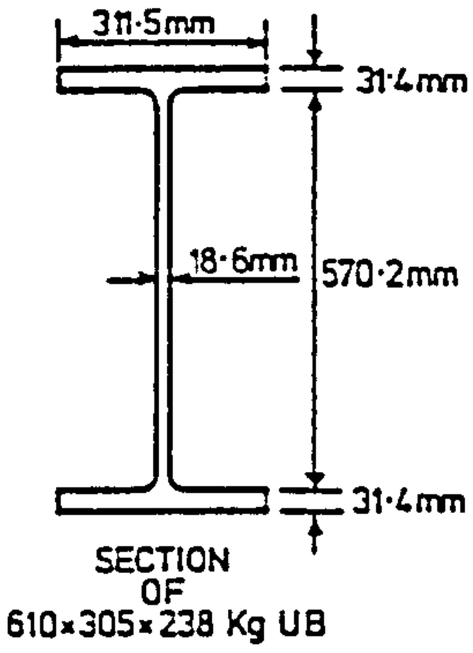

YOUNG'S MODULUS = 210E9 Nm
SHEAR MODULUS = 81E9 Nm
DENSITY = 77E3 Kg/m^3
BOUNDARY CONDITIONS

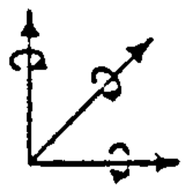

$V_x, V_y, V_t, R_x, R_y, R_t$
N DENOTES NOT FREE
F DENOTES FREE

Fig.5. DIAGRAM : BEAM ELEMENT PROBLEM

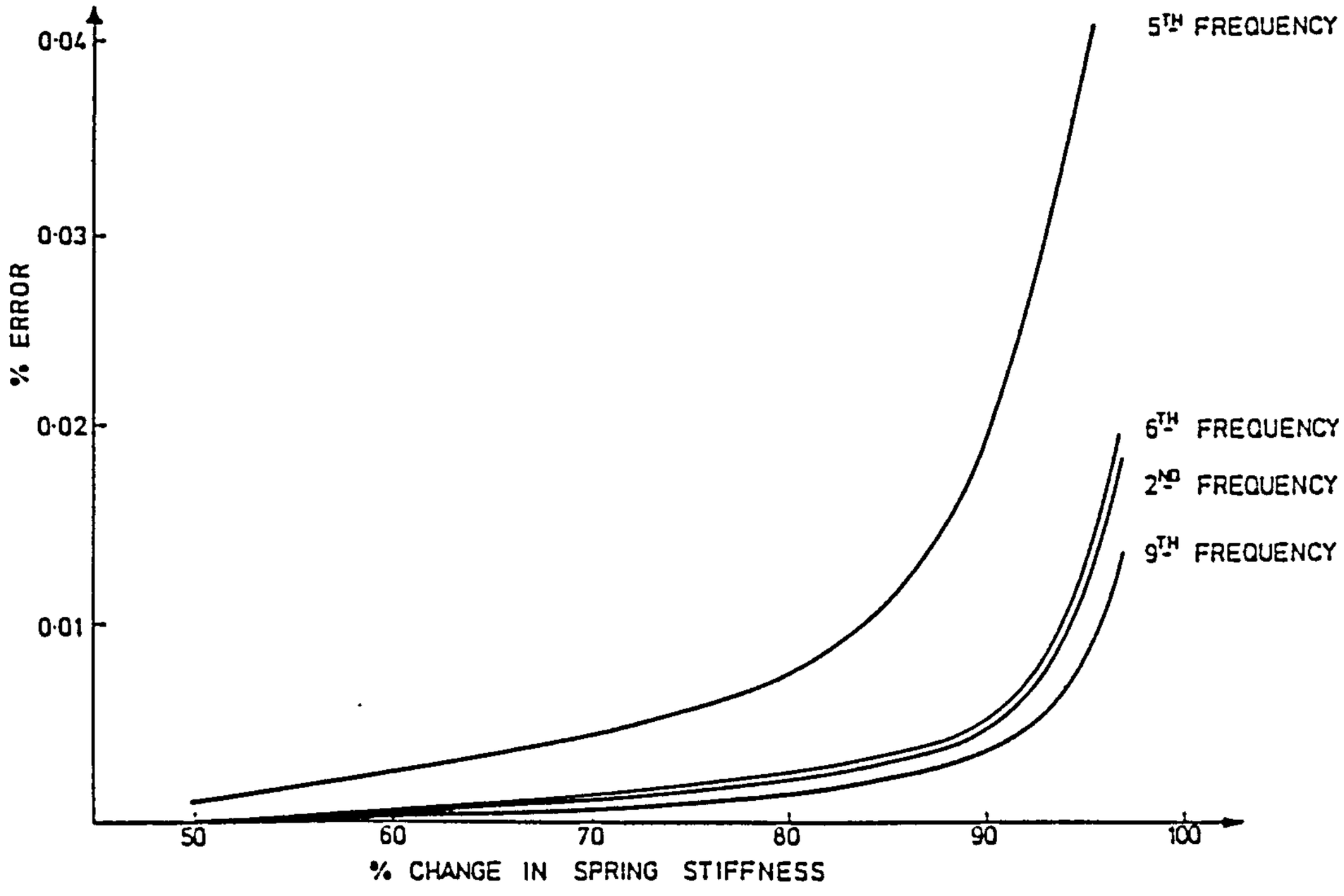

Fig. 6. ERRORS IN EIGENVALUES FOR CHANGE IN SPRING STIFFNESS IN JOINT 1 OF A BEAM